New Algebraic Methods
in Computational Geometry

Thorsten Theobald

Fakultät für Mathematik
Technische Universität München

New Algebraic Methods
in Computational Geometry

New Algebraic Methods
in Computational Geometry

Thorsten Theobald

Habilitationsschrift

2003

Fakultät für Mathematik
Technische Universität München

CONTENTS

1. INTRODUCTION

In its maturing stage, computational geometry has focused its attention mostly on linear objects. The motivation was sound: Why deal with curved shapes if we do not even understand polyhedral objects? In manufacturing, such a limitation is simply unacceptable. The time has come to bridge this gap.

From *Application challenges to computational geometry* ([30]).

The design of geometric algorithms can be seen as a reduction of the initial problems to sequences of subproblems on geometric, combinatorial, and algebraic properties of geometric objects [9, 45]. In the early ages of computational geometry, the algebraic aspects could often be neglected, since the degree of the problems under consideration was quite small. A famous "classical" example demonstrating the deep connections between algebraic methods and computational geometry is the field of motion planning (see [22, 119, 120]). Many current world-wide research efforts on *computational geometry of nonlinearly bounded bodies* indicate that algebraic methods will become increasingly important in computational geometry.

Algorithmic questions involving lines in $\mathbb{R}^3$ and $\mathbb{R}^n$ belong to the fundamental problems in computational geometry [26, 102, 136], coming from applications in computer graphics [104], robotics [122], visualization [106], and computer-aided geometric design (CAGD) [106]. These questions are immediately connected with nonlinear, algebraic problems, since the set of lines in real projective space $\mathbb{P}^3_{\mathbb{R}}$ is naturally associated with a certain quadric in $\mathbb{P}^5_{\mathbb{R}}$, the so-called Klein quadric.

In the last years, a variety of algorithmic questions involving lines in $\mathbb{R}^3$ and $\mathbb{R}^n$ have led to a challenging, both geometrically and algebraically rich class of algebraic-geometric core problems involving the

lines simultaneously tangent to given bodies in $\mathbb{R}^n$.

As an initial reference example, consider the problem of determining which bodies of a given scene in $\mathbb{R}^3$ cannot be seen from *any* viewpoint outside of the scene. Here, by "outside of the scene" we mean a viewpoint which is not contained in the convex hull of the bodies. From the geometric point of view, this leads to the problem of determining the *common tangent lines to four given bodies* in $\mathbb{R}^3$ (cf. Section 2.2). Besides several

visibility applications [21, 36, 41, 42, 43, 146], other algorithmic tasks leading to the same geometric core problem include computing smallest enclosing cylinders [3, 114], computing geometric permutations/stabbing lines [3, 103], controlling a laser beam in manufacturing [102], or placement problems in geometric modeling [40, 76].

However, already for the class of unit balls in $\mathbb{R}^3$ the questions of finiteness (under what conditions do there exist only finitely many real common tangents?) and the maximum number of real solutions show that the tangent problem is much more involved than its simple formulation suggests. In fact, the question on the *maximum number* of real common tangent lines to four unit spheres (in the finite case) was first formulated by David Larman [87]. Independently, this question – in the equivalent formulation of circular unit cylinders passing through four given points – was explicitly stated in [79]. For four general spheres, the question on the maximum number appears as an explicit open question in [30, Section 9]. Hence, it is not surprising that (in connection with the applications in [40]) concrete instances of the problem also served as hard three-dimensional geometric test problems for numerical polynomial solvers [144].

Real enumerative geometry. The tangent problem can be seen as a problem from *real enumerative geometry.* This discipline is concerned with questions of the following type: Given a class of geometric problems (say, given by a class of systems of polynomial equations) with a finite number of (a priori complex) solutions, what is the maximum number of real solutions?

One of the most famous classical results in enumerative geometry is the enumeration by Cayley and Salmon of the 27 (a priori complex) lines on a smooth cubic surface (see [71, 72]). According to another famous result, misstated by Steiner [135] and correctly proven first by Chasles (cf. [117]), there are 3264 (a priori complex) conics tangent to *five* given conics. For some rigorous modern treatises based on modern algebraic geometry see [56, 55, 81].

However, as pointed out in [55, p. 55], the question of how many solutions in a given enumerative setting can be *real* is still widely open. For an excellent recent survey we refer to [130]. The general difficulty of proving tight bounds of this kind may be seen by the following two aspects. For the conics tangent to five given conics the existence problem of 3264 *real* solutions had not been solved until few years ago ([110] and [55, §7.2]). Furthermore, as pointed out in [127], there are nearly no criteria or general techniques for proving the maximum number of real solutions.

Degeneracy of classes of polynomial equations. Besides the questions on the maximum number of (real) solutions which reflect the algebraic difficulty of a problem, efficient algorithmic approaches require to find *exact* characterizations of the configurations with infinitely many solutions, i.e., where the discrete and combinatorial nature of the problem gets lost. In contrast to other problems in computational geometry, characterizing these situations cannot be neglected (say, by applying perturbation techniques [46]), since the large algebraic degree involved makes it usually highly nontrivial to guarantee a correct perturbation.

1.1 Topics and results of this thesis.

In this thesis, we provide substantial contributions towards the clarification of the fundamental problems stated above. In the following, we give an outline of the results, and put them into appropriate contexts.

The main chapters are preceded by Chapter 2, which introduces relevant geometric concepts and connects the algorithmic applications to the geometric problems under investigation.

1.1.1 Common tangents to four spheres in $\mathbb{R}^3$

For the common tangents to four (not necessarily disjoint) spheres we show that in the case of finitely many solutions this number of common tangents is bounded by 12. For the case of *unit spheres* we provide a complete classification by showing the following theorem.

> *Four unit spheres in $\mathbb{R}^3$ whose centers are not collinear have at most 12 common tangent lines in $\mathbb{R}^3$. This bound is tight, i.e., there exists a configuration of four unit spheres in $\mathbb{R}^3$ with 12 distinct real common tangent lines.*

The fact that for this algebraic problem of degree 12 the cases with infinitely many common tangent lines can be characterized *exactly* is particularly remarkable. Moreover, our results solve the open questions in [30, 79, 87] mentioned before.

We complement this result by investigating the following question raised by David Cox:

> For which numbers $k \in \{0, \dots, 12\}$ does there exist a configuration with exactly k different common tangents in real space $\mathbb{R}^3$?

Additional motivation for studying this question comes from several quite different aspects. Firstly, any knowledge on the subset $K \subset \{0, \dots, 12\}$ of realizable numbers gives important information for the mentioned applications. When using numerical solvers of polynomial equations to find the numerical values of the tangents, the computations may become instable, especially for configurations of centers which are close to singular configurations (cf. Section 3.5). If not all numbers $k \in \{0, \dots, 12\}$ can be established in real space this offers the possibility of strong and valuable consistency checks within a program. If, however, all numbers can be realized then this proves the non-existence of such a control mechanism.

Secondly, the set of realizable numbers gives important insights into the algebraic, geometric, and combinatorial structure of the tangent problem. Observe that the tangent problem to four spheres could be seen as a purely geometric problem. In contrast to this, the proof of the theorem above is of algebraic nature and therefore does not fit well

together with additional purely geometric constraints (e.g., disjointness) on the spheres. Here, the hardness in the geometric construction of concrete configurations might be seen as an indication of the difficulty to establish a purely geometric proof.

Thirdly, exploring the realizable numbers allows to relate the tangent problem (which arose from recent applications) to some well-studied problems in classical and enumerative geometry (which mainly arose from their natural formulations). Concerning the 27 lines on a smooth cubic surface, the question of real solutions has already been studied long time ago ([113, 121], see also [111, p. 188]). In particular, for a cubic surface in $\mathbb{P}^3_{\mathbb{R}}$ only the numbers 3, 7, 15, and 27 can be established with *real* lines. Another famous example in geometry is Apollonius' problem which asks for the circles tangent to three given circles. For this problem, there exist configurations with $k \in \{0, 1, \dots, 6, 8\}$ real tangent circles but provably no configuration with 7 real tangent circles [101].

We show that the situation for the tangents to four unit spheres is different from these situations. Namely, we prove:

> For any number $k \in \{0, \dots, 12\}$ there exists a configuration of four
> unit spheres in $\mathbb{R}^3$ which have exactly k distinct common tangents
> in $\mathbb{R}^3$.

As an application of the results, we study the problem of finding the smallest circumscribing cylinder of a (not necessarily regular) tetrahedron in $\mathbb{R}^3$. Devillers, Mourrain, Preparata, and Trébuchet [37] demonstrated that using their state-of-the-art numerical polynomial solvers, various problems related to cylinders in $\mathbb{R}^3$ can be solved rather efficiently. In particular, they give a polynomial formulation for the smallest circumscribing cylinders of a tetrahedron in $\mathbb{R}^3$, whose Bézout number – the product of the degrees of the polynomial equations – is 60. However, these equations contain certain undesired solutions with multiplicity 4, and as a consequence of these multiplicities the computation times (using state-of-the-art numerical techniques) are about a factor 100 larger than those of similar problems in which all solutions occur with multiplicity 1.

In Section 3.4, we improve the results of [37] by providing a polynomial formulation for the locally extreme cylinders, whose Bézout bound is 36 and whose solutions generically have multiplicity one. We also present classes of tetrahedra for which the algebraic degrees in computing a smallest circumscribing cylinder can be considerably reduced.

We close Chapter 3 with a short discussion of dynamic visualization aspects of the tangent problem and their connection to homotopy-based solvers of polynomial equations.

1.1.2   *Common tangents to four quadrics in $\mathbb{P}^3$ and $\mathbb{R}^3$*

From the algebraic-geometric point of view, the tangent problem is of particular importance for the following reason. The formulation of the problem in terms of Plücker coordinates gives five quadratic equations in projective space $\mathbb{P}^5_{\mathbb{R}}$, whose common solutions in (complex space) $\mathbb{P}^5$ include a one-dimensional component at infinity (accounting for the "missing" $2^5 - 12 = 20$ solutions). Quite remarkably, as observed by P. Aluffi and W. Fulton [1], this excess component cannot be resolved by a single blow-up.

In Section 4.1, we solve the real enumerative question for quadratic surfaces in $\mathbb{P}^3$ (shortly, quadrics) by showing that 32 is the true upper bound of tangents to four quadrics, even over the reals. We present and analyze a class of configurations of four quadrics in $\mathbb{R}^3$ such that any configuration in this class leads to 32 distinct real common tangent lines.

In Section 4.2 we propose to use computer-algebraic methods to study intersection-theoretical phenomena such as this double blow-up. For this, we describe the ideal of the one-dimensional excess component. By extending the polynomial ring and adding suitable polynomials we simulate the blow-up in the computer algebra system SINGULAR and study the resulting ideal as well as the second blow-up.

1.1.3 Tangent problems to quadrics in n-dimensional space

In Chapter 5, we study the natural (real) enumerative generalizations of the tangent problem to n-dimensional space. Given $2n-2$ spheres (respectively quadrics) in n-dimensional space, what is the maximum number of (real) common tangent lines in the finite case? The number of $2n-2$ quadrics guarantees that in the generic case there is indeed a finite number of common tangent lines. The problem to find the common tangents to $2n-2$ given spheres in $\mathbb{R}^n$ arises, for example, in the computation of smallest enclosing cylinders in n-dimensional space (which is a fundamental problem in statistical analysis, see [24]).

Consider $2n-2$ spheres in $\mathbb{R}^n$ whose centers affinely span $\mathbb{R}^n$. We show that if the spheres have a finite number of complex common tangent lines, then that number is bounded by $3 \cdot 2^{n-1}$. Moreover, we show that there exists a configuration of unit spheres such that all these $3 \cdot 2^{n-1}$ tangents are real. We also discuss the case of $2n-2$ spheres whose centers have affine dimension less than n.

In Section 5.2, we consider the tangents to $2n-2$ quadrics in $\mathbb{P}^n$. Since this problem can be formulated as the complete intersection of $2n-2$ quadratic equations on the Grassmannian of lines in $\mathbb{P}^n$, the expected number of (complex) solutions is given by the product of the degrees of the equations with the degree of the Grassmannian,

$$d_n \; := \; 2^{2n-2} \cdot \frac{1}{n} \binom{2n-2}{n-1} \; .$$

As our main result of this section, we show: Given $2n-2$ general quadrics in $\mathbb{P}^n$ there are d_n complex lines that are simultaneously tangent to all $2n-2$ quadrics ($n \geq 2$), and there is a choice of quadrics in $\mathbb{R}^n$ for which all the lines are real and lie in affine space $\mathbb{R}^n$.

Our proof combines recent results in the real Schubert calculus with classical perturbation arguments adapted to the real numbers. With regard to the application mentioned above, Table 1.1 exhibits the amazingly large difference between the number of (real) tangent lines for spheres and the number of (real) tangent lines for general quadrics.

We also put the tangent problem to spheres into the perspective of common tangents to general quadrics. In particular, we discuss the problem of common tangents to $2n-2$ smooth quadrics in $\mathbb{P}^n$, and describe the excess component at infinity for the problem of spheres. In this setting, the upper bound on the number of tangents to spheres implies

n	3	4	5	6	7	8	9
$3 \cdot 2^{n-1}$	12	24	48	96	192	384	768
d_n	32	320	3584	43008	540672	7028736	93716480

Tab. 1.1: Maximum number of tangents to $2n-2$ spheres in $\mathbb{R}^n$ and to $2n-2$ quadrics in $\mathbb{P}^n$

that there will be at most $3 \cdot 2^{n-1}$ isolated common tangents to $2n-2$ quadrics in $\mathbb{P}^n$, when the quadrics all contain the same (smooth) quadric in a given hyperplane. In particular, the problem of the spheres can be seen as the case when the common quadric is at infinity and contains no real points.

In Section 5.3, as an application of the characterization of tangents to spheres, we give an efficient polynomial formulation for smallest circumscribing cylinders of a simplex in $\mathbb{R}^n$. Using this formulation we give a bound on the number of locally extreme cylinders based on the Bézout number. Since this bound is not tight, we provide better bounds for small dimensions; these bounds are based on mixed volume computations and Bernstein's Theorem. Moreover, we study in detail the locally extreme circumscribing cylinders of a regular simplex in $\mathbb{R}^n$. To exploit many symmetries in the analysis, we provide a formulation based on symmetric polynomials. Using elementary invariant theory, we show that the direction vector of every locally extreme circumscribing cylinder has at most three distinct values in its components. With this result we can illustrate our combinatorial results on the number of solutions for general simplices.

As a byproduct of our computational studies, we discovered a subtle but severe mistake in the paper [148] on the explicit determination of the smallest enclosing cylinder for a regular simplex in $\mathbb{R}^n$, thus completely invalidating the proof given there. In an appendix to Section 5.3, we give a description of that flaw, including some computer-algebraic calculations illustrating it.

1.1.4 Common transversals and tangents

In Chapter 6, we consider the lines which are simultaneously tangent to k spheres and $4-k$ lines in $\mathbb{R}^3$, $k \in \{0, \dots, 4\}$. From the algorithmic point of view, these problems immediately arise in the mentioned applications when the class of admissible bodies in the scene consists of both balls and polytopes (see Section 2.2.5). The case $k = 0$ asks for the common transversals to four given lines in $\mathbb{R}^3$. This geometric problem has been well-known for many years (see, e.g., [70, 75, 117]). In particular, if a configuration has only finitely many common transversals, then this number is bounded by 2; and it is well-known how to characterize the configurations with infinitely many common transversals.

We compute *tight* upper bounds for the number of real common tangents to k spheres and $4-k$ lines in the finite case, $k \in \{0, \dots, 4\}$. Table 1.2 summarizes our results. It shows the tight upper bounds for the maximum number of real solutions. The last column shows that in some cases, we are able to explicitly characterize the configurations with an

	tight upper bound # solutions	characterization of degenerate instances
4 lines	2 (well-known)	yes (well-known)
3 lines, 1 sphere	4	yes
2 lines, 2 spheres	8	yes
1 line, 3 spheres	12	–
4 unit spheres	12 (see Chapter 3)	yes (see Chapter 3)
4 spheres	12 (see Chapter 3)	–

Tab. 1.2: Lines tangent to k given spheres and transversal to $4-k$ given lines in $\mathbb{R}^3$

infinite number of real common tangents. In the entries with a "–" we do not know such a characterization.

The proofs of these results are of different flavors. For $k \in \{1, 2\}$, the upper bounds immediately follow from Bézout's Theorem. Whereas for $k = 1$ it is easy to give a construction matching this bound, for $k = 2$ we use a computation of intersection multiplicities based on standard bases in local rings to prove correctness of the construction. For $k = 3$, the Bézout bound in the Plücker formulation will be 16 instead of 12. In order to find a better bound for the number of solutions in $\mathbb{R}^3$, we prove that there are two solutions with multiplicity at least two in the plane at infinity.

The characterization of the degenerated situations in the case of three lines and one sphere is based on classical methods of geometry.

For the case of two lines and two spheres, we have to investigate the degenerated situations of an algebraic problem of degree 8. In order to establish this characterization, we develop a variety of symbolic methods and combine them with classical methods of classification of algebraic curves. First we deal with the more general problem where we replace the spheres in $\mathbb{R}^3$ by general quadrics in $\mathbb{P}^3$. In order to study the geometry of this problem, we fix two lines and a quadric in general position, and describe the set of (second) quadrics for which there are infinitely many common transversals/tangents in terms of an algebraic curve. It turns out that this set is an algebraic curve of degree 24 in the space $\mathbb{P}^9$ of quadrics. Factoring the ideal of this curve shows that it is remarkably reducible. Namely, the curve consists of 12 plane conics.

In the proof of this statement, we first investigate the ideal defining the algebraic curve of the set of (second) quadrics. Based on this, we prove the theorem with the aid of a computer calculation in the computer algebra system SINGULAR [62]. As will be explained in Section 6.2.3, the success of that computation depends crucially on the preceding analysis of the curve. Quite interestingly, there are real lines ℓ_1 and ℓ_2 and real quadrics Q such that all 12 components of the curve of second quadrics are real. In general, given real lines ℓ_1, ℓ_2, and a real quadric Q, not all of the 12 components are defined over the real numbers.

1.1.5   Algorithmic complexity of visibility computations with moving viewpoints

In Chapter 7, we change our viewpoint towards the following guiding question: In how far is the algebraic difficulty of visibility computations with moving viewpoints reflected by complexity-theoretical hardness results in the Turing machine model.

We analyze the *binary Turing machine complexity* of visibility computations in spaces of variable dimension. Here, an additional motivation of dealing with visibility computations in spaces of variable dimension comes from high-dimensional data visualization [139]. The classes of geometric bodies under consideration are that of balls, that of polytopes represented as the convex hull of finitely many points ("$\mathcal{V}$-polytopes"), and that of polytopes represented by an intersection of finitely many halfspaces ("$\mathcal{H}$-polytopes"). Roughly speaking, we show the following results that characterize the borderline between tractable and hard problems. If the dimension of the space is part of the input, then checking visibility of a given body B in the scene is $\mathbb{NP}$-hard for all three classes. In the case where the given body B degenerates to a single point, we can prove also membership in $\mathbb{NP}$ for the two classes of polytopes. If however, the dimension is fixed then the visibility problem becomes solvable in polynomial time for all three classes. (For precise statements of the results see Theorems 7.2 and 7.3.)

Moreover, we establish a link between these hardness results and the *view obstruction* or *lonely runner* conjecture from diophantine approximation [12, 34, 150]. For $x \in \mathbb{R}$ let $||x||_I$ denote the distance of x to a nearest integer. Then, for each positive integer n, let

$$\kappa(n) = \inf_{v_1,\dots,v_n \in \mathbb{N}} \sup_{\tau \in [0,1]} \min_{1 \leq i \leq n} ||\tau v_i||_I \,,$$

a measure for simultaneous homogeneous diophantine approximation. Wills [150] and later Cusick [34] conjectured that $\kappa(n) = \frac{1}{n+1}$. Although this conjecture has been investigated in a series of papers in the last 30 years (see the list of references in [27]), the exact value of $\kappa(n)$ is known only for $n \leq 5$. Our hardness results can be seen as a complexity-theoretical indication why the number-theoretical view obstruction problem is hard.

1.2   Publications in advance and viewpoint of this thesis.

Most of the results in this thesis have been published beforehand, partly in connection with various coauthors: see [19, 85, 90, 96, 131, 132, 140, 141, 142]. Rather than keeping the results of these papers separated, the material has been restructured in this thesis. The aim is to provide a comprehensive treatment of the results on that research. However, in order to allow a self-contained access to the three-dimensional problems (which are the most relevant ones for algorithmic purposes), the three-dimensional problems on spheres and quadrics are treated before the general n-dimensional problems.

The following list enumerates for each of the chapters of this thesis which papers are the essential sources of the results:

Chapter 2: [142].

Chapter 3: [19, 85, 90, 141].

Chapter 4: [132].

Chapter 5: [19, 131, 132].

Chapter 6: [96, 140].

Chapter 7: based on previously unpublished results obtained jointly with Peter Gritz-
mann.

1.3   Acknowledgments

Many persons have supported my work during the last years. I am grateful to all of them!

Specifically, I would like to thank Peter Gritzmann for offering me a position in his group, for supporting me in many aspects, and for having the ability to see many things in mathematics and science from an advanced viewpoint.

Thanks to all the persons with whom I had the pleasure to write a joint paper during the work on this thesis: René Brandenberg, I.G. Macdonald, Gábor Megyesi, János Pach, and Frank Sottile. In particular, additional thanks to Frank Sottile for introducing me to many techniques of computational algebraic geometry.

Thanks to Daniel Kotzor for his implementation of numerical methods within the scope of his Diplom thesis.

Thanks to David Cox and Hellmuth Stachel, who pointed out valuable references to me in an early stage of my work.

Thanks to Bernd Sturmfels for valuable discussions and for hosting a great and fruitful stay in Berkeley in the beginning of 2001.

Thanks to all the members of Peter Gritzmann's research group, not only for many kinds of individual support, but also for forming a very pleasant group: Andreas Alpers, Oliver Bastert, Franziska Berger, René Brandenberg, David Bremner, Andreas Brieden, Abhi Dattasharma, Achill Schürmann, Sven de Vries, as well as our system administrator Raymund Augustine and our secretary Klaudia Bachmeier.

Finally, thanks to Birgit.

2. BACKGROUND AND PRELIMINARIES

In order to keep this thesis self-contained within the different research communities involved, we present our geometric notions in Section 2.1. In Section 2.2, we introduce the algorithmic problems and the algorithmic framework relevant to our work. Finally, in Section 2.3, we review the well-known Plücker coordinates from line geometry and state some tangent conditions. These coordinates will be extensively used in Chapters 4 to 6.

2.1 Geometric preliminaries

2.1.1 Basic geometric notions

Dot product, scalar product, and norm. For $x, y \in \mathbb{C}^n$, let $x \cdot y := \sum_{i=1}^{n} x_i y_i$ denote their usual dot product. We write x^2 for $x \cdot x$. Within real space $\mathbb{R}^n$, the bilinear form $\mathbb{R}^n \times \mathbb{R}^n \to \mathbb{R}$, $(x, y) \mapsto x \cdot y$ is the Euclidean scalar product, and $|| \cdot || : \mathbb{R}^n \to \mathbb{R}$, $||x|| := (x \cdot x)^{1/2}$ is the Euclidean norm.

Projective spaces. For $n \geq 1$, let $\mathbb{P}^n$ denote n-dimensional complex projective space, and let $\mathbb{P}^n_{\mathbb{R}}$ denote n-dimensional real projective space.

Quadrics and spheres. Let $n \geq 1$, and let $Q \in \mathbb{C}^{n+1, n+1} \setminus \{0\}$, where $\mathbb{C}^{k,m}$ denotes the set of $k \times m$-matrices with complex entries. Then the set $\{x \in \mathbb{P}^n : x^T Q x = 0\}$ is a quadratic hypersurface in $\mathbb{P}^n$, shortly, a *quadric* in $\mathbb{P}^n$; without loss of generality we can assume that Q is symmetric. Throughout the presentation, we will often identify a quadric in $\mathbb{P}^n$ with the symmetric representation matrix Q. Quadrics which can be defined by representation matrices with *real* entries are called real quadrics.

A quadric defined by a representation matrix Q is *smooth* (i.e., the gradient of $x^T Q x$ is non-zero for any $(x_0, \ldots, x_n)^T \in \mathbb{P}^n$) if its representation matrix has rank $n+1$.

For $c \in \mathbb{R}^n$ and $r > 0$, the sphere in $\mathbb{R}^n$ with center c and radius r is denoted by $S(c, r)$. In $\mathbb{P}^n$, it is described by $(x_1 - c_1 x_0)^2 + \ldots + (x_n - c_n x_0)^2 = r^2 x_0^2$, and it is identified with the matrix

$$
\begin{pmatrix}
\sum_{i=1}^{n} c_i^2 - r^2 & -c_1 & -c_2 & \cdots & -c_n \\
-c_1 & 1 & 0 & \ldots & 0 \\
-c_2 & 0 & 1 & \ddots & \vdots \\
\vdots & \vdots & \ddots & \ddots & 0 \\
-c_n & 0 & \cdots & 0 & 1
\end{pmatrix} . \tag{2.1}
$$

Convexity. Let $n \in \mathbb{N}$. For a set $A \subset \mathbb{R}^n$, $\mathrm{conv}(A)$ denotes the convex hull of A. A *convex body* (or simply *body*) is a bounded, closed, and convex set which contains interior points. A *polytope* in $\mathbb{R}^n$ is the convex hull of finitely many points $v_1, \ldots, v_k \in \mathbb{R}^n$. A *simplex* in $\mathbb{R}^n$ is the convex hull of $n+1$ affinely independent points. In $\mathbb{R}^3$, a simplex is also called a *tetrahedron.* Let e_i denote the i-th standard unit vector in $\mathbb{R}^n$. Then for $c \in \mathbb{R}^n$ and $\rho_1, \ldots, \rho_n > 0$, $\mathrm{conv}(\{c \pm \rho_i e_i \ : \ 1 \leq i \leq n\})$ is called a *cross polytope* in $\mathbb{R}^n$. A *box* is a polytope of the form $\{x \in \mathbb{R}^n \ : \ \alpha_i \leq x_i \leq \beta_i\}$ with given $\alpha_i < \beta_i$, $1 \leq i \leq n$.

Segments and rays in $\mathbb{R}^n$. Let $x \neq y \in \mathbb{R}^n$, and let $w \in \mathbb{R}^n \setminus \{0\}$. Then $\mathrm{conv}\{x, y\}$ is the *segment* connecting x and y. A *ray issuing from x* is a set of the form $x + [0, \infty)w$.

2.1.2   Polynomial equations

Nonlinear geometric problems are naturally described in terms of polynomial equations. Throughout the text, we apply a number of techniques from computational algebraic geometry. For easily accessible, comprehensive treatments and the state of the art see [31, 32, 137]. In particular, let us recall the following version of Bézout's Theorem [32, p. 91], which will be used many times.

Theorem 2.1. (Bézout) *Let $n \geq 2$, and let $f_1, \ldots, f_n$ be homogeneous polynomials in $x_0, \ldots, x_n$ of degrees $d_1, \ldots, d_n > 0$. If $f_1, \ldots, f_n$ have a finite number of common zeroes in complex projective n-space $\mathbb{P}^n$ then the number of zeroes (counted with multiplicity) is $d_1 {\cdot} d_2 \cdots d_n$.*

The theorem does not only give a *theoretical* bound on the number of solutions. From the *practical* point of view, the computational costs of solving a system of polynomial equations are mainly dominated by the Bézout number (= product of the degrees) and the mixed volume (the latter one is discussed in Section 5.3.1).

2.2   Motivation and algorithmic background

As mentioned in the introduction, a variety of algorithmic applications has led to the algebraic core problems studied in the next chapters. Exemplarily, we describe three of these applications. The first one comes from ray-tracing with moving viewpoints and will also be our main visibility problem for the complexity-theoretical investigations in Chapter 7. Namely, we want to compute information on the viewpoint positions where the visibility topology of the scene changes. This includes tackling the problem of partial visibility, which will be introduced in Section 2.2.1. In Section 2.2.2 we introduce the problem of computing smallest enclosing cylinders. Then, in Section 2.2.3, we introduce the concept of envelopes in the design of computational-geometric data structures.

For all these problems and related problem classes, in dimension 2 the resulting geometric questions remain rather elementary (cf. [99, 105]), and the primary focus on these problems is on efficient algorithms and data structures. Therefore, exemplarily for the

treatment of two-dimensional problems of this kind, we present a sweep algorithm for the partial visibility problem in Section 2.2.4.

In Section 2.2.5, we show how the three-dimensional versions of these problems lead to the tangent problems to common bodies. In particular, for the smallest enclosing cylinder of a point set in $\mathbb{R}^3$, we study this reduction in full detail.

2.2.1   Partial visibility

We consider a scene in $\mathbb{R}^n$ consisting of $m + 1$ (not necessarily disjoint) convex bodies $B_0, B_1, \ldots, B_m$ from a class $\mathcal{X}$ in $\mathbb{R}^n$ ($\mathcal{X}$ might be the set of all balls or the set of all full-dimensional polytopes).

Let $v \in \mathbb{R}^n$ be the viewpoint of the scene. We call B_0 *partially visible from the viewpoint v (with respect to $B_1, \ldots, B_m$)* if there exists an $x \in B_0$ satisfying

$$\operatorname{conv}\{x, v\} \cap \operatorname{relint}(B_i) = \emptyset \quad \text{for all } 1 \le i \le m \,,$$

where $\operatorname{relint}(B_i)$ denotes the relative interior of the body B_i.

Concerning the variety of possible viewpoint areas, we will particularly concentrate on the most natural one: all viewpoints "outside of the scene" are possible. More precisely, if the body B_0 is partially visible from some viewpoint $v \in \mathbb{R}^n \setminus \operatorname{conv}(\bigcup_{i=0}^m B_i)$ then it is called *partially visible*; otherwise it is called *invisible*. A *visibility ray b for B_0* is a ray issuing from some point $x \in B_0$ with $b \cap \operatorname{relint}(B_i) = \emptyset$ for all $1 \le i \le m$. Hence, B_0 is partially visible if and only if there exists a visibility ray for B_0.

The main problem PARTIAL VISIBILITY with respect to a given body class $\mathcal{X}$ is defined as follows.

Problem PARTIAL VISIBILITY$_{\mathcal{X}}$:

Instance: m, n, bodies $B_0, B_1, \ldots, B_m \subset \mathbb{R}^n$ from the class $\mathcal{X}$.
Question: Decide whether B_0 is partially visible with respect to $B_1, \ldots, B_m$.

Bodies which are not partially visible can be immediately removed from the scene, which reduces the complexity of the visualization process. In case of dense crystals whose atoms are visualized as sufficiently large balls in $\mathbb{R}^3$, the reduction in complexity may be quite substantial.

Remark 2.2. The problem of partial visibility can be seen as one of the easiest visibility problem with moving viewpoints. Concerning the algebraic aspects treated in the next chapters, all the related visibility problems in [36, 41, 42, 43, 146] lead to the same algebraic questions.

2.2.2 Smallest enclosing cylinders

Let $n \in \mathbb{N}$. Given points $p_1, \ldots, p_m \in \mathbb{R}^n$, let $\mathcal{P} := \{p_1, \ldots, p_m\}$. For our purposes, we define a cylinder in $\mathbb{R}^n$ to be a set of the form

$$\mathrm{bd}(\ell + \rho \mathbb{B}^n),$$

where ℓ is a line in $\mathbb{R}^n$, $\mathbb{B}^n$ denotes the unit ball, $\rho > 0$, the addition denotes the Minkowski sum, and $\mathrm{bd}(\cdot)$ denotes the boundary of a set. We say that $\mathcal{P}$ *can be enclosed* in a cylinder $\mathcal{C}$ if $\mathcal{P}$ is contained in the convex hull of $\mathcal{C}$. Equivalently, we can speak of an enclosing cylinder of the polytope $\mathrm{conv}\{p_1, \ldots, p_m\}$. An enclosing cylinder of $\mathcal{P}$ of minimal radius is called a *smallest enclosing cylinder* of $\mathcal{P}$. One of the most natural examples of this class is the one for dimension 3, i.e., the smallest enclosing (circular) cylinder of a point set in $\mathbb{R}^3$.

In the notation of [17, 63], the radius ρ of a smallest enclosing cylinder of a polytope P is called the *outer $(n-1)$-radius* of P. This notion comes from the fact that it is the radius of an enclosing $(n-1)$-dimensional sphere in the optimal orthogonal projection of P onto an $(n-1)$-dimensional linear subspace.

The decision variant of the smallest enclosing cylinder problem asks whether there exists an enclosing cylinder of a given polytope P whose radius is not larger than a given value $r > 0$.

An enclosing cylinder $\mathcal{C}$ of a simplex P is called a *circumscribing* cylinder of P if all the vertices of P are contained in (the hypersurface) $\mathcal{C}$.

2.2.3 Envelopes

Let $\mathcal{B}$ be a collection of m convex bodies in $\mathbb{R}^3$. A line ℓ is called a *line transversal* of $\mathcal{B}$ if it intersects every member of $\mathcal{B}$. The set of line transversals of $\mathcal{B}$ can be represented as the region enclosed between an upper and a lower envelope as follows (see [2, 3, 26]). These representations are important in the design of data structures supporting ray shooting queries (i.e., seeking the first body, if any, met by a query ray) [2].

If we exclude lines parallel to the yz-plane, a line ℓ in $\mathbb{R}^3$ can be uniquely represented by its projections on the xy- and xz-planes: $y = \sigma_1 x + \sigma_2$, $z = \sigma_3 x + \sigma_4$. Hence, a line can be represented by the quadruple $(\sigma_1, \sigma_2, \sigma_3, \sigma_4) \in \mathbb{R}^4$.

Let B be a convex body in $\mathbb{R}^3$. For fixed $\sigma_1, \sigma_2, \sigma_3$, the set of lines $(\sigma_1, \sigma_2, \sigma_3, \sigma_4)$ that intersect B is obtained by translating a line in the z-direction between two extreme values $(\sigma_1, \sigma_2, \sigma_3, \phi_B^-(\sigma_1, \sigma_2, \sigma_3))$ and $(\sigma_1, \sigma_2, \sigma_3, \phi_B^+(\sigma_1, \sigma_2, \sigma_3))$, which represent lines tangent to B from below and from above, respectively. Hence, the set of line transversals to $\mathcal{B}$ can be represented as

$$\left\{ (\sigma_1, \sigma_2, \sigma_3, \sigma_4) \; : \; \max_{B \in \mathcal{B}} \phi_B^-(\sigma_1, \sigma_2, \sigma_3) \leq \sigma_4 \leq \min_{B \in \mathcal{B}} \phi_B^+(\sigma_1, \sigma_2, \sigma_3) \right\},$$

which is a region enclosed between a lower envelope and an upper envelope in $\mathbb{R}^4$. If the elements of $\mathcal{B}$ are balls or polytopes, then the set of line transversals defines a semialgebraic set in $\mathbb{R}^4$ (see [3]). Assuming general position, the vertices (= zero-dimensional faces) of the boundary of this region correspond to lines which are tangent to four of the bodies in $\mathcal{B}$ (cf. Section 2.2.5).

2.2.4 A sweep algorithm for the two-dimensional case

We present an efficient algorithm for solving the partial visibility problem for arbitrary convex bodies in $\mathbb{R}^2$. Here, we are not only interested in checking partial visibility of *one* of the bodies but also in computing *all* bodies which are not partially visible. In order to avoid several special cases we assume that the bodies are pairwise disjoint.

Let $\mathcal{B} := \{B_0, \ldots, B_m\}$ be a set of disjoint bodies in the plane. In the two-dimensional case, checking partial visibility of a body $B \in \mathcal{B}$ can be reduced to a finite number of geometric problems as follows (cf. the treatment of stabbing lines in [47]). Without loss of generality let $|\mathcal{B}| \geq 2$ and assume $B = B_0$. If there exists a visibility ray for B then we can continuously transform (i.e., rotate and translate) the visibility ray until we reach a situation where the underlying line is tangent to at least two of the bodies (one of them might be B_0 itself). Hence, it suffices to compute the set of all common tangent lines to all pairs of bodies in $\mathcal{B}$ and check whether one of these lines contains a visibility ray. For any pair of disjoint bodies, the number of common tangent lines is exactly 4 (which can be seen as a very special case of the results in [23, 89] on the number of common supporting hyperplanes in general dimension).

In order to handle any class of bodies in the plane algorithmically, we have to assume that we can perform the following operations on this class.

1. Compute the four common tangent lines to two bodies B_i, B_j.

2. Compute the at most two intersections of a ray or a line with a body B_i.

In the following, we assume that we have access to two oracles performing these operations. Obviously, for the class of discs, the class of polygons, and the class combining discs and polygons these oracles can be realized quite easily. In particular, if the maximum number of vertices of any polygon is bounded by a constant then both oracles can be implemented in constant time.

Definition 2.3. *A line is called* critical *if it is tangent to at least two bodies B_i, B_j with $0 \leq i \neq j \leq m$. A ray is called* critical *if it is contained in a critical line.*

Hence, the body B_0 is partially visible if and only if there exists a critical visibility ray for B_0. Consequently, it suffices to compute the set of critical lines and to check whether a critical line contains a visibility ray for B_0. Obviously, checking whether a given line contains a visibility ray for B_0 can be achieved with $O(m)$ calls to oracle 2.
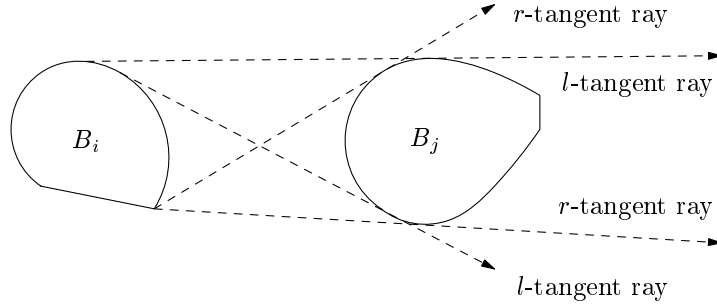
Fig. 2.1: r- and l-tangent rays from B_i to B_j

Theorem 2.4. *In dimension 2, the set of all partially visible bodies can be computed with $O(m^3)$ arithmetic steps, $O(m^2)$ calls to the first oracle and $O(m^3)$ calls to the second oracle.*

Proof. There are $4 \cdot \binom{m}{2}$ (not necessarily different) critical lines. For each critical line ℓ it can be computed with $O(m)$ arithmetic steps and $O(m)$ calls to the second oracle which bodies intersect with ℓ and which bodies are visible with regard to the line ℓ.   □

The algorithm of Theorem 2.4 computes the set of *all* partially visible bodies in cubic time. However, the straightforward idea to modify it to a quadratic time algorithm for checking partial visibility of one specific body does *not* work. The reason is that it is a priori not clear which of the $O(m^2)$ critical lines can be omitted. If we are only interested in partial visibility of one specific body, say B_0, we can do better by using the following plane sweep algorithm requiring $O(m^2 \log m)$ time and $O(m)$ space. (For extensive material on sweep techniques we refer to [9].)

We interpret the four common tangent lines of two bodies B_i and B_j as rays starting in some boundary point of B_i. As a consequence of the results in [23, 89], there are two tangent rays such that B_i is on the left side of these tangent rays ("*r*-tangent rays of B_i"); and there are two tangent rays such that B_i is on the right side of the tangent rays ("*l*-tangent rays of B_i"), see Figure 2.1.

For checking visibility of B_0 we first investigate the $2(m-1)$ (not necessarily different) *r*-tangent rays touching B_0 and some other body B_i, $1 \le i \le m$. For each *r*-tangent ray we consider the outer normal $u \in \mathbb{S}^1$ where $\mathbb{S}^1$ denotes the unit sphere in $\mathbb{R}^2$; with each of these normals $u \in \mathbb{S}^1$ we associate the corresponding angle $0 \le \alpha < 2\pi$ measured from the positive *x*-axis. As described in the following algorithm, we sweep the *r*-tangents according to increasing angles.

Sub-algorithm for sweeping the r-tangents of B_1 and B_i, $1 \le i \le m$:

1. Compute the set of *r*-tangents of B_0 and B_i, $1 \le i \le m$, and sort them by increasing angles.
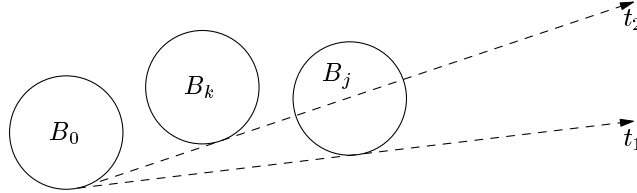
Fig. 2.2: Update step during the sweep

2. Compute the number of intersections of the first r-tangent with bodies B_i, $i \geq 1$.

3. Consider the r-tangents successively in the order of increasing angles. In each of these steps do:

   (a) Update the number of intersections with bodies B_i, $i \geq 1$.

   (b) If the number of intersections is 0, then B_0 is partially visible; STOP.

For the update step we use the following lemma.

Lemma 2.5. *Let t_1 and t_2 be r-tangent rays of B_0 with angles $0 \leq \alpha_1 < \alpha_2 < 2\pi$, and let C be some body with $t_1 \cap C \neq \emptyset$, $t_2 \cap C = \emptyset$. Then there exists an r-tangent ray to B_0 with angle $\alpha_0 \in [\alpha_1, \alpha_2)$ which is tangent to C.*

Proof. For any $\alpha \in [0, 2\pi)$ there exists some oriented tangent to B_0 with angle α (see, e.g., [14]) and therefore some r-tangent ray to B_0 with angle α. Let α_0 be the supremum of $\alpha \in [\alpha_1, \alpha_2)$ such that the tangent with angle α intersects with C. Since C is compact the tangent with angle α_0 is tangent to B_0 and C, i.e., the supremum is a maximum. $\square$

In each step of the sweep we update the number of intersections of the sweep ray with bodies B_i, $i \geq 1$, in the following way. Let us first consider the case where the new angle α_2 is strictly larger than the current angle α_1 and where the r-tangent rays with angle α_1 and α_2 are each tangent to exactly two bodies. Let the r-tangent ray with angle α_1 be tangent to B_0 and B_j, and let the r-tangent ray with angle α_2 be tangent to B_0 and B_k, $1 \leq j \neq k \leq m$. Then we only have to check whether the ray with angle α_2 intersects with B_j (i.e., if the sweep ray is just "entering" B_j) and if the ray with angle α_1 intersects with B_k (i.e., if the sweep ray is just "leaving" B_k); see Figure 2.2. Due to Lemma 2.5 any additional change would imply the existence of some r-tangent with angle $\alpha_0 \in (\alpha_1, \alpha_2)$. Consequently, the update step can be done in constant time. If there are several r-tangent rays with the same angle we can combine these update steps. The amortized costs for the update step are not larger than in the case of different angles. If during the sweep we reach a situation where the number of intersections is 0 then B_0 is partially visible and
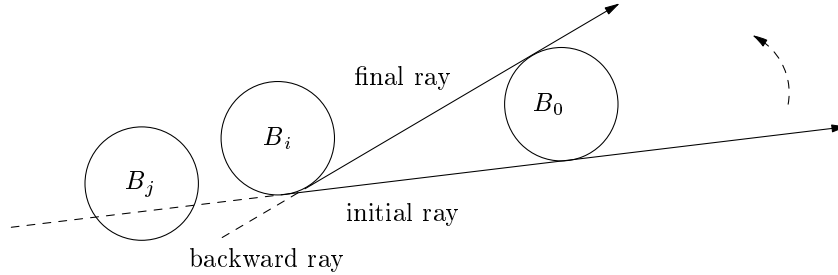
Fig. 2.3: Initial and final ray for sweeping the r-tangent rays of B_i, $i \geq 1$

we can stop immediately. After the inspection of the r-tangent rays of B_0 the l-tangent rays of B_0 are swept in the same way.

So far, we have inspected the r- and l-tangent rays of B_0. However, a visibility ray of B_0 is not necessarily tangent to B_0, and we also have to investigate the common tangents of bodies B_i, B_j with $1 \leq i \neq j \leq m$. More precisely, for every fixed $i \in \{1, \ldots, m\}$, we consider the critical rays which are tangent to B_i. Here, we start the sweep with that r-tangent ray from B_i to B_0 that has B_0 on the left side (see Figure 2.3). For this ray we count the number of intersections between B_i and B_0, and separately we count the number of intersections of the backward ray with other bodies. Now we sweep the r-tangent rays of B_i according to increasing angles and update the number of intersections between B_i and B_0 as well as the number of intersections of the backward ray. If we reach a situation where both numbers of intersections are simultaneously zero then B_0 is partially visible and we can stop immediately. In any case, the algorithm can stop if the r-tangent ray to B_i has B_0 on its right side; see the illustration in Figure 2.3. After sweeping the l-tangent rays of B_i the r-tangent rays of B_i are investigated in the same way.

The correctness of the whole algorithm follows from the fact that the sweep inspects all $O(m^2)$ critical visibility lines and that the update step is correct due to Lemma 2.5.

For sweeping the tangent rays of some given body B_i, $0 \leq i \leq m$, the time requirements are dominated by the time to sort the tangent rays according to increasing angles. We can conclude:

Theorem 2.6. *Let the dimension be $n = 2$. Then checking partial visibility of a body B_0 can be done with $O(m^2 \log m)$ arithmetic steps, $O(m^2)$ calls to the first oracle, and $O(m^2)$ calls to the second oracle, as well as $O(m)$ space.*

Similar algorithmic ideas can also be applied to the two-dimensional versions of other problems involving the interaction of lines with bodies.

Using much more sophisticated data structures, the logarithmic factor in time can be removed. Namely, with the concept of visibility complexes [4, 105], the partial visibility problem can be solved in time $O(m^2)$ with space requirements $O(m^2)$. For other recent results on visibility computations in $\mathbb{R}^2$ see also [4].

2.2.5 Algorithmic framework for three-dimensional problems

In the three-dimensional case we can essentially use the same framework as in the two-dimensional case. A line in real projective space $\mathbb{P}^3_{\mathbb{R}}$ can be regarded as a point on the (four-dimensional) Klein quadric in $\mathbb{P}^5_{\mathbb{R}}$ (cf. Section 2.3). Assuming that our bodies are given by algebraic inequalities (e.g., balls or polytopes), and assuming general position, the core problem (corresponding to the first oracle in Section 2.2.4) is to compute the common tangents to four bodies in $\mathbb{R}^3$ (cf. [3, 103]). However, in the three-dimensional case, there are also some special cases where we can transform a visibility ray only to a situation with less than four bodies, or where a configuration with four bodies has an infinite number of common tangents.

Let us consider the decision problem whether there exists an enclosing cylinder with radius r of a given point set. The following statement reduces that problem to a problem involving the common tangents to four spheres with radius r, including an exact characterization of all special cases which can occur.[1]

Theorem 2.7. *Let $\mathcal{P} = \{p_1, \ldots, p_m\}$ be a set of $m \geq 4$ points in $\mathbb{R}^3$, not all collinear. If $\mathcal{P}$ can be enclosed in a circular cylinder $\mathcal{C}$ of radius r, then there exists a circular cylinder $\mathcal{C}'$ of radius r enclosing all elements of $\mathcal{P}$ such that the surface $\mathcal{C}'$ passes through*

(i) at least four non-collinear points of $\mathcal{P}$, or

(ii) three non-collinear points of $\mathcal{P}$, and the axis ℓ of $\mathcal{C}'$ is contained in

    (a) the cylinder naturally defined by spheres of radius r centered at two of these points;

    (b) the double cone naturally defined by spheres of radius r centered at two of these points (and these spheres are disjoint);

    (c) or the set of lines which are tangent to the two spheres of radius r centered at two these points and which are contained in the plane equidistant from these points (and the spheres are non-disjoint).

Moreover, $\mathcal{C}$ can be transformed into $\mathcal{C}'$ by a continuous motion.

Figures 2.4 and 2.5 visualize the three geometric properties in the second possibility.

Since the second possibility in Theorem 2.7 characterizes the possible special cases, this lemma reduces our decision problem to the problem of finding the lines tangent to four given spheres with radius r in $\mathbb{R}^3$. Namely, it suffices to compute the circular cylinders of radius r passing through four given points (corresponding to case (i)) as well as the circular cylinders whose axes satisfy one of the conditions in (ii); the latter case gives a constant number of problems of smaller algebraic degree (since the positions of the axes are very restricted). Similarly, the theorem reduces the computation of a smallest

---

[1] We remark that a similar statement has already been used in [114], but the manuscript referenced there does not contain a complete proof.

(a) Cylinder   (b) Double cone with apex $(a/2, 0, 0)^T$
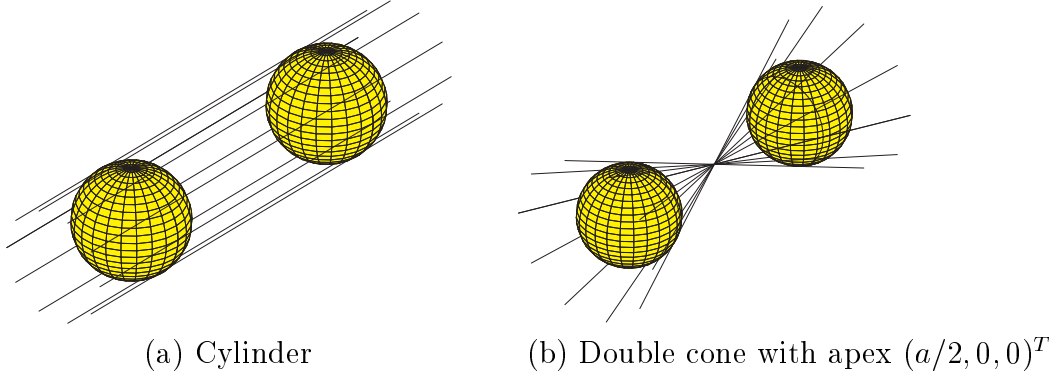
Fig. 2.4: Extreme situations of the set of hyperboloids for disjoint spheres

(a) Hyperboloid for $0 < x_h < 2r^2/a$ (b) Degenerated hyperboloid for $x_h = a/2$
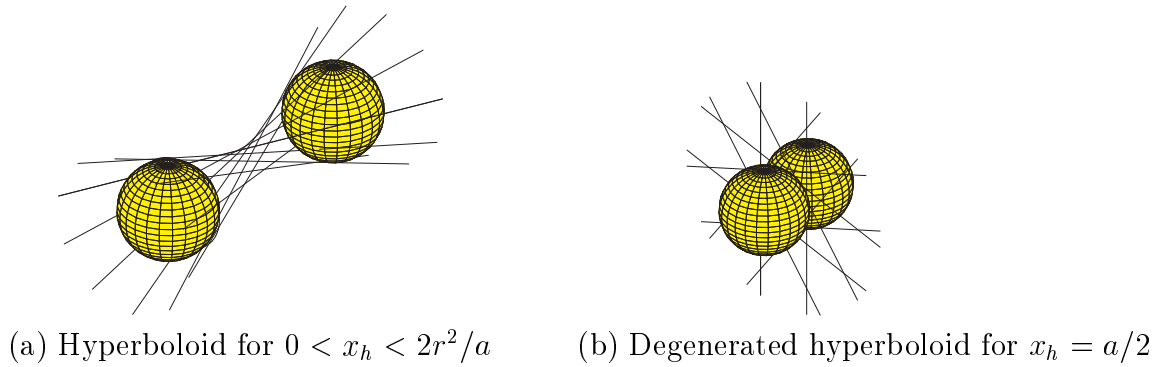
Fig. 2.5: The left figure shows a general situation for disjoint spheres; the right figure shows an extreme situation for non-disjoint spheres

enclosing cylinder of a tetrahedron in $\mathbb{R}^3$ to the computation of a smallest circumscribing cylinder of a tetrahedron.

Remark 2.8. Before we start with the proof, we remark that Theorem 2.7 and its different cases show a quite similar behaviour as the well known statement that the (unique) circumsphere of a simplex in $\mathbb{R}^n$ touches all its vertices, or one of its great $(n-1)$-circles is the circumsphere of one of the $(n-1)$-faces of the simplex (see [14, p. 54]).

In the proof we will apply the following geometric equivalence. A point $x \in \mathbb{R}^3$ is enclosed in a cylinder with axis ℓ if and only if ℓ is a transversal of the sphere with radius r centered at x (i.e., ℓ is a line intersecting the sphere).

Proof of Theorem 2.7. Let $\mathcal{C}$ be a cylinder with axis ℓ and radius r enclosing $\mathcal{P}$. Then, denoting by $S_i := S(p_i, r)$ the sphere with radius r centered at p_i, ℓ is a common transversal to $S_1, \dots, S_m$. By continuously translating and rotating ℓ, we can assume that ℓ is tangent

to two of the spheres, say S_1 and S_2. Further, by changing coordinates, we can assume that S_1 and S_2 have the form $S_1 = S((0, 0, 0)^T, r)$, $S_2 = S((a, 0, 0)^T, r)$ for some $a > 0$.

The set of lines tangent to two spheres of radius r constitutes a set of hyperboloids of one sheet (see, e.g., [33, 73]). Moreover, any of these hyperboloids touches the sphere S_1 on a circle lying in a hyperplane parallel to the yz-plane. Hence, the set of hyperboloids can be parametrized by the x-coordinate of this hyperplane which we denote by x_h.

If $S_1 \cap S_2 = \emptyset$ then the boundary values are $x_h = 0$ and $x_h = 2r^2/a$. These two extreme situations yield a cylinder and a double cone with apex $(a/2, 0, 0)^T$, respectively (see Figure 2.4). For $0 < x_h < 2r^2/a$ we obtain a hyperboloid of one sheet (see Figure 2.5(a)).

If $S_1 \cap S_2 \neq \emptyset$ then the boundary values are $x_h = 0$ and $x_h = a/2$. Here, for $0 < x_h < a/2$ we obtain hyperboloids of one sheet, too. For $x_h = a/2$ the hyperboloid degenerates to a set of tangents which are tangents to the circle with radius $r_c = \sqrt{4r^2 - a^2}$ in the hyperplane $x = a/2$ (see Figure 2.5(b)).

Let $x_{h,0}$ be the parameter value of the hyperboloid containing the line ℓ. The tangent to S_1 and S_2 is contained in the hyperboloid with some parameter value $x_{h,0}$. By decreasing the parameter x_h starting from $x_{h,0}$ the hyperboloid changes its shape towards the cylinder around S_1 and S_2. Let $x_{h,1}$ be the infimum of all $0 \leq x_h < x_{h,0}$ such that the hyperboloid does not contain a generating line tangent to some other sphere $S(p_i, r)$ for some $3 \leq i \leq m$. If $x_{h,1} = 0$, then by choosing any point of $\mathcal{P}$ not collinear to p_1 and p_2 we are in case (ii) (a).

If $x_{h,1} > 0$ then let p_3 be the corresponding point. Let $T(S_1, S_2, S_3)$ denote the set of lines simultaneously tangent to S_1, S_2, and S_3. Now let $x_{h,2}$ be the infimum of all $0 \leq x_h < x_{h,0}$ such that there exists a continuous function $\ell : (x_{h,2}, x_{h,1}) \to T(\{S_1, S_2, S_3\})$ with $\ell(x_h)$ lying on the hyperboloid with parameter x_h. Since the spheres are compact, the infimum is a minimum. If $x_{h,2} > 0$ then one of three hyperboloids involved by the three pairs of spheres must be one of the extreme hyperboloids in that situation and we are in cases (ii) (a), (b), or (c). If $x_{h,2} = 0$ then we distinguish between two possibilities. Either during this process we also reached a tangent to some other sphere $S(p_i, r)$ for some $4 \leq i \leq m$; in this case we are in case (i). Or during the transformation all the points $p_4, \ldots, p_m$ are enclosed in the cylinder with axis ℓ and radius r, but none of them is contained in it. Then we arrive at situation (ii) (a). $\square$

The crucial point in the algorithmic realization is that the main subproblem described in case (i) has finitely many solutions; to show this is the content of Section 3.2. Moreover, the special cases described in case (ii) can also be handled in a finite way.

Similar reductions can be done, e.g., in the case of the partial visibility problem if the class of admissible objects consists of unit balls. Hence, by our results of the later Section 3.2, we can solve this problem rigorously. If n denotes the number of unit balls, a first upper bound on the number of calls of the algebraic oracle is $O(n^5)$. Here, the algebraic oracle has to solve the corresponding polynomial equations of degree at most 12. Using the implementation techniques from [3, 103, 114] the exponent 5 can be decreased to a value below 4.

If the bodies are polytopes, then the common tangent lines to the bodies are common transversals to four given lines (stemming from the edges of the polytopes) in $\mathbb{R}^3$ (see [103]). Characterizing and computing the common transversals to four given lines in $\mathbb{R}^3$ is a classical problem in geometry (see, e.g., [75, §XIV.7]). For configurations of four lines with only finitely many common transversals, there are at most two solutions (which can be found by solving a quadratic equation); and it is well-known how to characterize the degenerate configurations with infinitely many common transversals.

However, in case the class of admissible objects consists of balls of general radii or of combinations of balls and polytopes, then we arrive soon at the situations where the geometry of the tangent problems is still open (see the discussions in Section 3.2.5 and in Chapter 6). Hence, we do not know how to do similar rigorous reductions of the algorithmic problems to a finite number of algebraic-geometric core problems, all having finitely many solutions. However, for a theoretical possibility to solve also these problems (based on real quantifier elimination) see Section 7.5.

2.3   Plücker coordinates

We review the well-known *Plücker coordinates* of lines in complex projective space $\mathbb{P}^n$. For a general reference, see [31, 74, 106]. Let $x = (x_0, x_1, \ldots, x_n)^T$ and $y = (y_0, y_1, \ldots, y_n)^T \in \mathbb{P}^n$ be two distinct points on a line ℓ. Then ℓ can be represented (not uniquely) by the $(n+1) \times 2$-matrix L whose two columns are x and y. Let $N := \binom{n+1}{2} - 1$. The Plücker vector $p = (p_{ij})_{1 \leq i < j \leq n} \in \mathbb{P}^N$ of the line ℓ is the vector of the determinants of the 2×2-submatrices of L, that is, $p_{ij} := x_i y_j - x_j y_i$. The set of all lines in $\mathbb{P}^n$ is called the *Grassmannian of lines in* $\mathbb{P}^n$ and is denoted by $\mathbb{G}_{1,n}$. The set of vectors in $\mathbb{P}^N$ satisfying the *Plücker relations*

$$p_{ij}p_{kl} - p_{ik}p_{jl} + p_{il}p_{jk} \;=\; 0 \qquad \text{for } 0 \leq i < j < k < l \leq n \tag{2.2}$$

is in 1-1-correspondence with $\mathbb{G}_{1,n}$. See, for example, [74, §VII.6], [54, §1.2.5], or (for dimension 3) [31, Theorem 11 in §8.6].

Remark 2.9. If $n = 3$ then (2.2) gives a single equation. In this case, the quadric in $\mathbb{P}^5$ defined by (2.2) is called *Klein quadric*.

Similarly, we describe $(n-2)$-planes in terms of *dual Plücker coordinates*. If an $(n-2)$-plane Λ is given as the intersection of the two hyperplanes $\sum_{i=0}^{n} u_i x_i$ and $\sum_{i=0}^{n} v_i x_i$, then the dual Plücker coordinates of Λ are defined by $q_{ij} := u_i v_j - u_j v_i$.

A line ℓ intersects an $(n-2)$-plane Λ in $\mathbb{P}^n$ if and only if the dot product of the Plücker vector p of ℓ and the dual Plücker vector q of Λ vanishes, i.e., if and only if

$$\sum_{0 \leq i < j \leq n} p_{ij} q_{ij} \;=\; 0 \tag{2.3}$$

(see, e.g., [74, Theorem VII.5.I]). Since this is a linear relation in the Plücker coordinates of the line ℓ, geometrically the set of lines intersecting a given $(n-2)$-plane is described by a hyperplane section of the Grassmannian in $\mathbb{P}^N$.

In dimension 3 this specializes as follows. For any line $\ell \subset \mathbb{P}^3$, the Plücker vector $(p_{01}, p_{02}, p_{03}, p_{12}, p_{13}, p_{23})^T$ coincides with the dual Plücker vector $(q_{23}, -q_{13}, q_{12}, q_{03}, -q_{02}, q_{01})^T$ in $\mathbb{P}^5$ [74, Theorem VII.3.I]. Hence, a line ℓ intersects a line ℓ' in $\mathbb{P}^3$ if and only if their Plücker vectors p and p' satisfy

$$p_{01}p'_{23} - p_{02}p'_{13} + p_{03}p'_{12} + p_{12}p'_{03} - p_{13}p'_{02} + p_{23}p'_{01} = 0 \, . \tag{2.4}$$

We use Plücker coordinates to characterize the lines tangent to a given quadric in $\mathbb{P}^n$. Recall the following algebraic characterization of tangency: The restriction of the quadratic form to the line ℓ is singular, in that either it has a double root, or it vanishes identically. When the quadric is smooth, this implies that the line is tangent to the quadric in the usual geometric sense.

Lemma 2.10. *Let L be an $(n+1) \times 2$-matrix representing the line $\ell \subset \mathbb{P}^n$. ℓ is tangent to a quadric Q in $\mathbb{P}^n$ if and only if the 2×2-matrix $L^T Q L$ is singular.*

Proof. If we denote the two columns of L by x and y, then the line ℓ consists of all points

$$\left\{ z = (z_0, \ldots, z_n)^T \; : \; z = \lambda x + \mu y, \, (\lambda, \mu)^T \in \mathbb{C}^2 \setminus \{(0,0)^T\} \right\} \, .$$

By the algebraic definition of tangency, ℓ is tangent to Q if and only if this line intersects the quadric exactly once (namely, with multiplicity 2), or if it is contained in the quadric. The homogeneous quadratic equation

$$(\lambda x + \mu y)^T Q (\lambda x + \mu y) = 0$$

can be made affine by setting $\mu = 1$. Since the discriminant of this affine quadratic equation in λ is

$$(2x^T Q y)^2 - 4(x^T Q x)(y^T Q y) = -4 \det(L^T Q L),$$

the statement follows immediately. $\qquad\square$

In order to transfer this condition to Plücker coordinates, we use the second exterior power of matrices

$$\wedge^2 \; : \; \mathbb{C}^{k,m} \;\; \rightarrow \;\; \mathbb{C}^{\binom{k}{2}, \binom{m}{2}}$$

(see [106, p. 145],[129]). The row and column indices of the resulting matrix are subsets of cardinality 2 of $\{1, \ldots, k\}$ and $\{1, \ldots, m\}$, respectively. For $I \subset \{1, \ldots, k\}$ and $J \subset \{1, \ldots, m\}$ with $|I| = |J| = 2$,

$$(\wedge^2 A)_{I,J} := \det A_{[I,J]},$$

where $A_{[I,J]}$ denotes the 2×2-submatrix of the given matrix A with row indices I and column indices J. Let ℓ be a line in $\mathbb{P}^n$ and L be an $(n+1) \times 2$-matrix representing ℓ. Interpreting the $\binom{n+1}{2} \times 1$-matrix $\wedge^2 L$ as a vector in $\mathbb{P}^N$, we observe $\wedge^2 L = p_\ell$, where p_ℓ is the Plücker vector of ℓ.

Lemma 2.11. *A line $\ell \subset \mathbb{P}^n$ is tangent to a quadric Q if and only if the Plücker vector p_ℓ of ℓ lies on the quadratic hypersurface in $\mathbb{P}^N$ defined by $\wedge^2 Q$, if and only if*

$$p_\ell^T \left(\wedge^2 Q \right) p_\ell \;=\; 0 \,. \tag{2.5}$$

Proof. Let L be a $(n+1) \times 2$-matrix whose two columns contain distinct points of ℓ. The Cauchy-Binet formula from multilinear algebra (see, e.g., [91]) implies

$$\begin{aligned}
\det(L^T Q L) &= (\wedge^2 L^T)(\wedge^2 Q)(\wedge^2 L) \\
&= (\wedge^2 L)^T (\wedge^2 Q)(\wedge^2 L) \,.
\end{aligned}$$

Now the claim follows from Lemma 2.10. $\square$

For an alternative deduction of this tangent condition see [129].

Explicitly, for a sphere with center $(c_1, c_2, c_3)^T \in \mathbb{R}^3$ and radius r the quadratic form $p_\ell^T \left(\wedge^2 Q \right) p_\ell$ is

$$\begin{pmatrix} p_{01} \\ p_{02} \\ p_{03} \\ p_{12} \\ p_{13} \\ p_{23} \end{pmatrix}^T \begin{pmatrix} c_2^2 + c_3^2 - r^2 & -c_1 c_2 & -c_1 c_3 & c_2 & c_3 & 0 \\ -c_1 c_2 & c_1^2 + c_3^2 - r^2 & -c_2 c_3 & -c_1 & 0 & c_3 \\ -c_1 c_3 & -c_2 c_3 & c_1^2 + c_2^2 - r^2 & 0 & -c_1 & -c_2 \\ c_2 & -c_1 & 0 & 1 & 0 & 0 \\ c_3 & 0 & -c_1 & 0 & 1 & 0 \\ 0 & c_3 & -c_2 & 0 & 0 & 1 \end{pmatrix} \begin{pmatrix} p_{01} \\ p_{02} \\ p_{03} \\ p_{12} \\ p_{13} \\ p_{23} \end{pmatrix} . \tag{2.6}$$

3. COMMON TANGENTS TO FOUR SPHERES IN $\mathbb{R}^3$

We discuss the lines which are simultaneously tangent to four (not necessarily disjoint) given spheres in $\mathbb{R}^3$.

In Section 3.1, we show that if four spheres in $\mathbb{R}^3$ with affinely independent centers have a finite number of common tangent lines in $\mathbb{C}^3$, then this number is bounded by 12. For reasons which will be discussed in detail in Chapter 4, rather than using Plücker coordinates we prefer an elementary description of the lines. Describing a line $\ell \subset \mathbb{C}^3$ by its direction vector $v \in \mathbb{P}^2$ and by a point p lying on the line with $p \cdot v = 0$ the common tangent lines to the four spheres can be characterized as the intersection of a cubic and a quartic curve in the projective plane corresponding to the three homogeneous variables v_1, v_2, and v_3.

In Section 3.2, we show the following result for unit spheres:

Theorem 3.1. *Four unit spheres in $\mathbb{R}^3$ whose centers are not collinear have at most 12 common tangent lines in $\mathbb{R}^3$. This bound is tight, i.e., there exists a configuration of four unit spheres in $\mathbb{R}^3$ with 12 distinct real common tangent lines.*

In Section 3.3, we study realization questions. In particular, David Cox had raised the question on the possible numbers of *real* solutions which can occur in the tangent problem. We complement Theorem 3.1 by answering this question as follows:

Theorem 3.2. *For any number $k \in \{0, \dots, 12\}$ there exists a configuration of four unit spheres in $\mathbb{R}^3$ which have exactly k distinct common tangents in $\mathbb{R}^3$.*

In Section 3.4, we discuss the optimization variant of the tangent problem. Given four affinely independent points $c_1, \dots, c_4 \in \mathbb{R}^3$, find the minimum radius r such that there exist a real common tangent line to the spheres $S(c_1, r), \dots, S(c_4, r)$. This problem is equivalent to finding the minimum circumscribing cylinder of a given (not necessarily regular) tetrahedron in $\mathbb{R}^3$.

In Section 3.5, we discuss some dynamic visualization aspects.

Before entering into the technical details, let us point out two other results in enumerative geometry, which are somewhat related to our tangent problem:

1. The number of spheres touching *four* given spheres in $\mathbb{R}^3$ is at most 16 in the generic case [77, 116]. (This can be regarded as the 3-dimensional version of Apollonius' problem).

2. The number of spheres tangent to four given skew lines in $\mathbb{R}^3$ is at most 8 (see [78]), and in [133] the configurations with infinitely many tangent spheres are characterized.

3.1   A cubic and a quartic equation

We represent a line in $\mathbb{C}^3$ by a point $p \in \mathbb{C}^3$ lying on the line and a direction vector $v \in \mathbb{P}^2$ of that line. (For notational convenience we typically work with a representative of the direction vector in $\mathbb{C}^3 \setminus \{0\}$.) If $v^2 \neq 0$ we can make p unique by requiring that $p \cdot v = 0$.

By definition, a line $\ell = (p, v)$ is tangent to the sphere with center $c \in \mathbb{R}^3$ and radius r if and only if it is tangent to the quadratic hypersurface $(x - c)^2 = r^2$, i.e., if and only if the quadratic equation $(p + \mu v - c)^2 = r^2$ in μ has a solution of multiplicity two. When ℓ is real then this is equivalent to the metric property that ℓ has Euclidean distance r from c (see Figure 3.1).

The tangent condition on ℓ gives the equation

$$\frac{(v \cdot (p - c))^2}{v^2} - (p - c)^2 + r^2 = 0\,.$$

For $v^2 \neq 0$ this is equivalent to

$$v^2 p^2 - 2v^2 p \cdot c + v^2 c^2 - (v \cdot c)^2 - r^2 v^2 = 0\,, \tag{3.1}$$

and, using Lagrange's identity,

$$v^2 p^2 - 2v^2 p \cdot c + (c \times v)^2 - r^2 v^2 = 0\,. \tag{3.2}$$

Here, the notion $\times$ of the vector product is also used for complex vectors.

Let $c_1, \dots, c_4 \in \mathbb{R}^3$ be affinely independent, let $r_1, \dots, r_4 > 0$, and let T be the tetrahedron with vertices $c_1, \dots, c_4$. Without loss of generality we can choose c_4 to be the origin and set $r := r_4$. Then the remaining centers span $\mathbb{R}^3$. Subtracting the equation for the sphere centered at the origin from the equations for the spheres $1, 2, 3$ gives the

$$\ell = \{p + \mu v \ : \ \mu \in \mathbb{R}\}$$
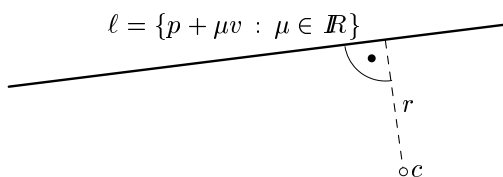
Fig. 3.1: Distance of the line ℓ from c in the real case

system

$$
\begin{aligned}
p \cdot v &= 0 \,, \\
p^2 &= r^2 \,, \quad \text{and} \\
2v^2 p \cdot c_i &= (c_i \times v)^2 - v^2(r_i^2 - r^2) \,, \qquad 1 \le i \le 3 \,.
\end{aligned}
\tag{3.3}
$$

Remark 3.3. Note that this system of equations does not have a solution with $v^2 = 0$. Namely, if we had $v^2 = 0$ then $v \cdot c_i = 0$ for all $i \in \{1, 2, 3\}$. Since the centers span $\mathbb{R}^3$, this would imply $v = 0$, contradicting $v \in \mathbb{P}^2$. This validates our assumption that $v^2 \ne 0$ prior to (3.1).

By assumption, c_1, c_2, and c_3 are linearly independent. Hence, the matrix $M := (c_1, c_2, c_3)^T$ is invertible, and we can solve the equations in the bottom line of (3.3) for p:

$$
p = \frac{1}{2v^2} M^{-1} \begin{pmatrix} (c_1 \times v)^2 - v^2(r_1^2 - r^2) \\ (c_2 \times v)^2 - v^2(r_2^2 - r^2) \\ (c_3 \times v)^2 - v^2(r_3^2 - r^2) \end{pmatrix} .
\tag{3.4}
$$

Now substitute this expression for p into the the first and second equation of the system (3.3) and then clear the denominators. This gives two homogeneous equations in the coordinate v, namely a cubic and a quartic. By Bézout's Theorem, this means that if the system has only finitely many complex solutions, then the number of solutions is bounded by $3 \cdot 4 = 12$.

Remark 3.4. In [76] the common (complex) tangents to four spheres have been formulated by polynomial equations with Bézout number 24. Thus our polynomial formulation improves that result. Moreover, by the results in Section 3.2.2, our formulation is optimal, even over the reals.

3.2 An exact characterization of the finiteness problem for unit spheres

In this section we consider unit spheres and prove Theorem 3.1. In detail, in Section 3.2.1, we treat the case of affinely independent centers. We start from the characterization of the common tangents from Section 3.1 in terms of the a cubic and a quartic curve in $\mathbb{P}^2$. If all spheres have the same radius then the cubic curve describes the lines equidistant to four given points in $\mathbb{R}^3$, and it is discussed in [15, 112]. Thus our main task is to relate the cubic to the quartic equation. If the cubic curve is *irreducible*, a detailed geometric inspection ensures that the cubic and the quartic cannot have a common component; hence, the desired result is implied by Bézout's Theorem. In case of a *reducible* cubic, we use the results from [112] to find suitable parametrizations of the quadratic or linear factors. Substituting the parametrization into the radius condition gives a univariate polynomial equation whose leading coefficient can be explicitly analyzed.

In Section 3.2.2, we show that 12 tangents can indeed be established in real space, and we exhibit a whole class of these configurations based on $c_1, \ldots, c_4$ constituting an equifacial tetrahedron.

Finally, Section 3.2.3 contains the proof for the affinely dependent case. In this case, we give a direct argument using the ellipses passing through the *four* centers, whose shorter half-axis is fixed.

3.2.1   Affinely independent centers

If all four spheres have the same radius r, then (3.4) simplifies to

$$p = \frac{1}{2v^2} M^{-1} \begin{pmatrix} (c_1 \times v)^2 \\ (c_2 \times v)^2 \\ (c_3 \times v)^2 \end{pmatrix} . \tag{3.5}$$

Note that this expression is independent of r. By Cramer's rule,

$$M^{-1} = \frac{1}{6V}(c_2 \times c_3, c_3 \times c_1, c_1 \times c_2) , \tag{3.6}$$

where $V := \det(c_1, c_2, c_3)/6$ denotes the oriented volume of T. Introducing the normal vectors

$$n_1 := (c_2 \times c_3)/2, \quad n_2 := (c_3 \times c_1)/2, \quad n_3 := (c_1 \times c_2)/2, \tag{3.7}$$

and substituting (3.5) into $p \cdot v = 0$, we can eliminate p and obtain a homogeneous cubic condition for the direction vector v:

$$\sum_{i=1}^{3} (c_i \times v)^2 n_i \cdot v = 0 . \tag{3.8}$$

In order to simplify this equation, we express v in terms of the three centers c_1, c_2, c_3, i.e.,

$$v = \sum_{j=1}^{3} t_j c_j \tag{3.9}$$

with homogeneous coordinates t_1, t_2, t_3. This yields

$$n_i \cdot v = n_i \cdot \sum_{j=1}^{3} t_j c_j = t_i n_i \cdot c_i .$$

As the scalar triple product $n_i \cdot c_i$ is invariant for $1 \le i \le 3$, equation (3.8) simplifies to

$$\sum_{i=1}^{3} t_i (c_i \times v)^2 = 0 . \tag{3.10}$$

Let A_i be the area of the face of T which is opposite to c_i, $1 \le i \le 4$. By using $A_1 = ||n_1||$, $A_2 = ||n_2||$, $A_3 = ||n_3||$, $A_4 = ||(c_1 - c_2) \times (c_3 - c_2)||/2$, and setting $F := (A_1^2 + A_2^2 + A_3^2 - A_4^2)/2 = -(n_1 \cdot n_2 + n_2 \cdot n_3 + n_3 \cdot n_1)$, the expansion of this sum yields

$$A_1^2 t_2 t_3 (t_2 + t_3) + A_2^2 t_3 t_1 (t_3 + t_1) + A_3^2 t_1 t_2 (t_1 + t_2) + 2F t_1 t_2 t_3 = 0 \,. \tag{3.11}$$

In Section 3.2.4 we give an alternative deduction of that cubic curve based on a classical construct in projective geometry, the pedal surface of a tetrahedron.

We conclude that the set of lines tangent to the spheres $S(c_i, r)$ for *some* radius r can be characterized by the homogeneous cubic equation (3.11) in t_1, t_2, t_3. In addition, for a *fixed* radius r, equation (3.5) in conjunction with $p^2 = r^2$ leads to a homogeneous equation of degree 4. Hence, unless the cubic curve $\mathcal{C}$ and the quartic curve $\mathcal{Q}$ in projective plane $\mathbb{P}^2$ have a common component, Bézout's Theorem implies there are 12 (possibly complex) solutions including multiplicities.

The irreducible case

Assume first that $\mathcal{C}$ is irreducible (over $\mathbb{C}$). Then $\mathcal{C}$ and $\mathcal{Q}$ have a common component if and only if $\mathcal{C} \subset \mathcal{Q}$. Now observe that any solution of (3.11) uniquely defines a radius r via (3.5). Hence, if $\mathcal{C} \subset \mathcal{Q}$ then the radius is constant for all elements in $\mathcal{C}$. Since we know six points on $\mathcal{C}$, namely the six edge directions, it suffices to prove the following lemma.

Lemma 3.5. *If all six edge directions give the same radius, then $\mathcal{C}$ is reducible.*

Proof. Consider two directions, parallel to two skew edges of T, say $v := c_1 - c_4$ and $v' := c_3 - c_2$. Using (3.5) and (3.6), we can compute the corresponding radii r_v and $r_{v'}$. We obtain

$$r_v = \frac{2 A_2 A_3 ||n_1 + n_2||}{3 V c_1^2} \,,$$

$$r_{v'} = \frac{||(c_1 \times (c_3 - c_2))^2 (c_2 \times c_3) + 4 A_1^2 (c_3 \times c_1) + 4 A_1^2 (c_1 \times c_2)||}{12 V (c_3 - c_2)^2} \,.$$

Applying the relation $A_4 = ||(c_1 - c_2) \times (c_3 - c_2)||/2$, the latter expression can be compactly written as

$$r_{v'} = \frac{2 A_1 A_4 ||n_1 + n_2||}{3 V (c_3 - c_2)^2} \,.$$

Now $r_v = r_{v'}$ implies

$$c_1^2 A_1 A_4 = (c_3 - c_2)^2 A_2 A_3 \,. \tag{3.12}$$

Let $a_{ij} = ||c_i - c_j||$, $i \ne j$. Further, let R_i denote the circumradius of the face opposite to c_i, $1 \le i \le 4$. In view of the well-known triangle formula "$R = (abc)/4A$", we have

$R_1 = a_{23}a_{24}a_{34}/4A_1$ and three analogous equations for R_2, R_3, and R_4. Hence, (3.12) becomes

$$R_1 R_4 = R_2 R_3 \,. \tag{3.13}$$

By our assumptions, the radii corresponding to the directions $c_2 - c_4$ and $c_3 - c_1$ as well as the radii corresponding to the directions $c_3 - c_4$ and $c_2 - c_1$ coincide. Thus, we obtain

$$R_2 R_4 = R_1 R_3 \,, \qquad R_3 R_4 = R_1 R_2 \,, \tag{3.14}$$

and hence $R_1 = R_2 = R_3 = R_4$. Therefore, the four faces of the tetrahedron are equidistant from the center of the sphere through $c_1, \dots, c_4$. In other words, the *in-center* of T coincides with its *circumcenter*. Hence, the circumcenter of a face is the point at which the inscribed sphere of T touches that face. In particular, it lies inside the face, which implies that every face of T has only *acute* angles.

Let α_{ij} denote the angle at c_i in the face opposite to c_j. By the Law of Sines ([33, p. 13]), $a_{23} = 2R_1 \sin\alpha_{41} = 2R_4 \sin\alpha_{14}$, so that

$$\sin\alpha_{ij} = \sin\alpha_{ji} \,, \qquad 1 \le i \ne j \le 4 \,.$$

Altogether, any pair of faces have a common edge, identical acute angles opposite to this edge, and the same circumradius. Consequently, the two faces are congruent and have the same area, i.e., $A_1 = A_2 = A_3 = A_4$. However, if all four faces have the same area, the cubic $\mathcal{C}$ is *reducible*; this will be discussed in detail below. $\qquad\square$

The reducible cases

Now let $\mathcal{C}$ be reducible over $\mathbb{C}$. We distinguish between the case $A_1 = A_2 = A_3 = A_4$ and the case that not all of A_1, A_2, A_3, A_4 are equal.

The case of an equifacial tetrahedron

If $A_1 = A_2 = A_3 = A_4$ then the tetrahedron with vertices $c_1, \dots, c_4$ defines a (not necessarily regular) equifacial tetrahedron. The cubic equation (3.11) decomposes into the union of three lines,

$$(t_1 + t_2)(t_2 + t_3)(t_3 + t_1) = 0 \,. \tag{3.15}$$

We consider the line $t_1 + t_2 = 0$, the other two cases are symmetric. In $\mathbb{P}^2$, the line $t_1 + t_2 = 0$ can be parametrized by

$$(t_1, t_2, t_3)^T = (\mu, -\mu, \lambda)^T \in \mathbb{P}^2 \,, \qquad [\lambda, \mu] \in \mathbb{P}^1 \,. \tag{3.16}$$

For convenience of notation, we dehomogenize by setting $\mu = 1$ and write $\lambda = \infty$ for the point $[\lambda, \mu] = [1, 0] \in \mathbb{P}^1$. Thus our parametrization is

$$t_1 = 1, \quad t_2 = -1, \quad t_3 = \lambda, \qquad \lambda \in \mathbb{C} \cup \{\infty\} \,. \tag{3.17}$$

Substituting these expressions into the square of (3.5) yields a polynomial equation $P_4(\lambda) = 0$ of degree at most 4 in λ. We show that the polynomial P_4 cannot degenerate to zero; hence, the equation has at most 4 solutions. For a polynomial q in the variable λ, let $\mathrm{Coeff}_{\lambda,k}(q)$, denote the coefficient of λ^k in the polynomial q. In the following computations no higher power in λ than the inspected one can occur. Since in (3.17) the degree of t_3 is larger than the degree of t_2, we obtain

$$\mathrm{Coeff}_{\lambda,2}\left((c_1 \times v)^2\right) = 4A_2^2, \quad \mathrm{Coeff}_{\lambda,2}\left((c_2 \times v)^2\right) = 4A_1^2, \quad \mathrm{Coeff}_{\lambda,2}\left((c_3 \times v)^2\right) = 0\,.$$

Hence, (3.6) implies

$$\mathrm{Coeff}_{\lambda,4}\left(\left(M^{-1}((c_1 \times v)^2, (c_2 \times v)^2, (c_3 \times v)^2)^T\right)^2\right) = \left(\frac{4A_1A_2\|n_1 + n_2\|}{3V}\right)^2\,.$$

Since $\mathrm{Coeff}_{\lambda,2}(v^2) = c_3^2$, the coefficient of degree 4 in P_4 vanishes if and only if

$$\frac{2A_1A_2\|n_1 + n_2\|}{3V} = rc_3^2\,. \tag{3.18}$$

Let $r_0 > 0$ be the radius defined by this equation. For $0 < r \neq r_0$, the leading coefficient of P_4 does not vanish, and P_4 has exactly 4 zeroes in $\mathbb{C}$ counted with multiplicity.

For $r = r_0$, the polynomial P_4 is of degree at most 3. However, it cannot degenerate to the zero polynomial, since the polynomials for $r \neq r_0$ have (possibly complex) zeroes. In particular, at any of these zeroes λ the polynomial P_4 for $r = r_0$ does not evaluate to 0. Hence, for $r = r_0$ there are at most 3 solutions in $\mathbb{C}$. Additionally, in this case we have to consider the solution $\lambda = \infty$. More precisely, r_0 can be interpreted as follows. For $\lambda = \infty$ within the parametrization, the resulting radius r_∞ is computed – in the same way as r_0 – by using the leading coefficients. This implies $r_\infty = r_0$.

Altogether, for any given radius $r > 0$, there are at most $3 \cdot 4 = 12$ common tangents in $\mathbb{C}^3$ to the four spheres $S(c_i, r)$.

The remaining reducible cases

Now consider the case that not all of the faces have the same area. The homogeneous cubic equation (3.11) defines a cubic curve $\mathcal{C}$ in projective plane $\mathbb{P}^2$. Based on a discussion of the real algebraic curve defined by (3.11), we will parametrize the components of $\mathcal{C}$. As already mentioned, the directions of the six tetrahedron edges give points on $\mathcal{C}$. In particular, let $X_{ij} := c_i - c_j$, $1 \leq i < j \leq 4$.

Following [112], we characterize the relationships between those six points on $\mathcal{C}$. Due to (3.9) the t-coordinates of $X_{14}, X_{24}, X_{34}, X_{12}, X_{13}, X_{23}$ are $(1, 0, 0)^T$, $(0, 1, 0)^T$, $(0, 0, 1)^T$, $(1, -1, 0)^T$, $(1, 0, -1)^T$, and $(0, 1, -1)^T$, respectively.

For any of the four tetrahedron faces, the set of directions parallel to that face defines a line in $\mathbb{P}^2_{\mathbb{R}}$. Of course, this remains true even after applying the linear variable transformations.

(a) Complete quadrilateral   (b) Configuration of the points X_{ij}
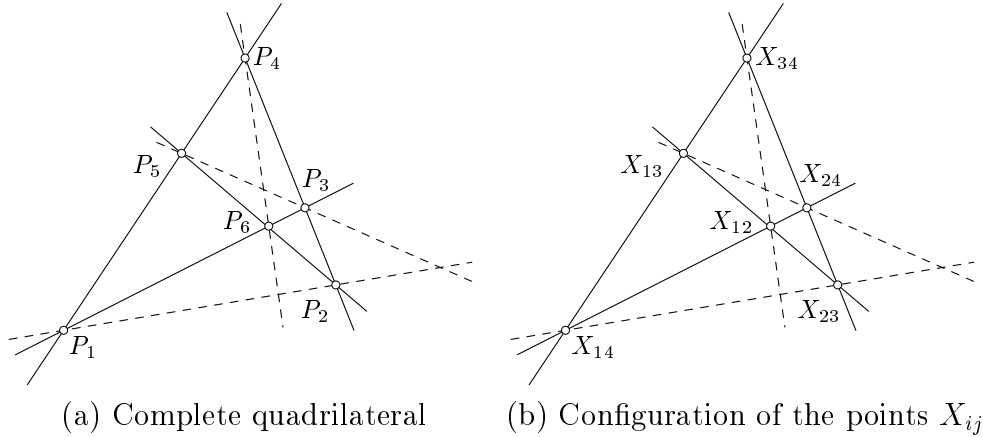
Fig. 3.2: A complete quadrilateral consists of 4 lines and 6 vertices $P_1, \ldots, P_6$; the three diago-
nals are drawn by dashed lines. Figure (b) shows a complete quadrilateral stemming
from the reducible case.

In order to characterize this configuration of four lines, the following notation will be
useful. A complete quadrilateral in real projective plane consists of four lines in general
position and the six points in which the lines intersect [33], see Figure 3.2(a); here, general
position means that no three lines have a common point of intersection.

Since there does not exist a vector which is parallel to more than two faces, the four
lines define a complete quadrilateral. One line contains the set of points $\{X_{12}, X_{23}, X_{34}\}$,
another one contains $\{X_{12}, X_{24}, X_{14}\}$, the third one contains $\{X_{13}, X_{34}, X_{24}\}$, and the
fourth one contains $\{X_{23}, X_{34}, X_{24}\}$. In particular, the points X_{ij} are the 6 vertices of the
complete quadrilateral. Figure 3.2(b) illustrates this configuration.

Since the cubic $\mathcal{C}$ is reducible (over $\mathbb{C}$), it can be decomposed into a line and a (not
necessarily irreducible) conic section. An irreducible conic section intersects with any
given line in at most two points; this implies that an irreducible conic section does not
contain three collinear points. Hence, one of the factors of $\mathcal{C}$ is a line l that contains at
least two of the six points X_{ij}.

Whenever some direction vector v of a real common tangent is parallel to a face of the
tetrahedron, v can only take the direction of an edge; otherwise, the tangent cannot have
the same distance from all three vertices of that face. For this reason, l cannot contain
two points from the same line of the complete quadrilateral. Hence, l must be one of the
three diagonals of the complete quadrilateral. Any of these diagonals contains two points
X_{ij}, X_{kl} which do not have any common index.

Without loss of generality we can assume that l contains X_{13} and X_{24}. First we show
that this implies $A_1 = A_3$ and $A_2 = A_4$. Since the t-coordinates of X_{13} and X_{24} are
$(1, 0, -1)^T$ and $(0, 1, 0)^T$, l is given by $t_1 + t_3 = 0$. The coefficient τ of t_2^2 in the remain-
ing conic section must be non-zero, because the coefficient of $t_1 t_2^2$ in (3.11) is non-zero.

Comparing the coefficients of $t_1 t_2^2$ and $t_3 t_2^2$ in (3.11) with the corresponding coefficients in the decomposed representation yields $\tau = A_1^2 = A_3^2$; hence $A_1 = A_3$. Furthermore, let τ_1 and τ_2 denote the coefficients of $t_1 t_2$ and $t_2 t_3$ in the remaining conic section, respectively. Comparing the coefficients of $t_1^2 t_2$ yields $\tau_1 = A_3^2 = A_1^2$. In the same way, with regard to $t_2 t_3^2$ and $t_1 t_2 t_3$ we obtain $\tau_1 = A_1^2$, and $2F = 2A_1^2$, whence (by definition of F): $A_2 = A_4$. Hence, the remaining conic section results to

$$A_1^2 (t_1 t_2 + t_2^2 + t_2 t_3) + A_2^2 t_1 t_3 = 0 \,. \tag{3.19}$$

Since, by assumption, not all of the faces have the same area, we have $A_1 \neq A_2$. Furthermore, it can be verified that for $A_1 \neq A_2$ the conic section (3.19) is irreducible.

Parametrizing the line l can be done like in the case $A_1 = A_2 = A_3 = A_4$. In particular, the line l gives at most 4 common tangents.

In order to parametrize (3.19), we intersect the conic with a suitable pencil of lines. First observe that X_{14} is a regular point on the conic with tangent $A_1^2 t_2 + A_2^2 t_3 = 0$. Then consider the pencil of lines

$$\lambda A_1^2 t_2 - (A_1^2 t_2 + A_2^2 t_3) = 0, \qquad \lambda \in \mathbb{C} \cup \{\infty\}$$

with apex X_{14}. In particular, solving for t_3 gives $t_3 = A_1^2 (\lambda - 1) t_2 / A_2^2$. The parameter value $\lambda = 0$ gives the tangent in X_{14}; the parameter value $\lambda = \infty$ yields $t_2 = 0$, which is the line through X_{14} and X_{34}. Replacing t_3 in (3.19) via the pencil equation and eliminating the linear factor t_2 caused by the apex $(1, 0, 0)^T$ yields $(A_1^2 (\lambda - 1) + A_2^2) t_2 + A_2^2 \lambda t_1 = 0$. This gives the parametrization

$$(t_1, t_2, t_3)^T = (-A_1^2 (\lambda - 1) - A_2^2, A_2^2 \lambda, A_1^2 (\lambda - 1) \lambda)^T \,, \qquad \lambda \in \mathbb{C} \cup \{\infty\} \,. \tag{3.20}$$

Consequently,

$$\mathrm{Coeff}_{\lambda^4}((c_1 \times v)^2) = 4 A_1^4 A_2^2, \quad \mathrm{Coeff}_{\lambda^4}((c_2 \times v)^2) = 4 A_1^6, \quad \mathrm{Coeff}_{\lambda^4}((c_3 \times v)^2) = 0 \,.$$

Here, the radius r_0 where the leading coefficient vanishes is the same one as in (3.18) and refers to the situation $\lambda = \infty$. Hence, the conic section gives at most 8 common tangents. Altogether, we obtain at most $4 + 8 = 12$ common tangents in this reducible case.

3.2.2 A configuration with 12 common tangents

The easiest example of a construction with 12 real tangents stems from a regular tetrahedron configuration of $c_1, \dots, c_4$. Since in Section 3.2.3 we will relate the affinely dependent configurations to the limit case of affinely independent configurations, we exhibit a more general class of configurations with 12 real tangents.

Namely, consider an equifacial tetrahedron, as in Section 3.2.1. It is well-known that the vertices of such a tetrahedron T can be regarded as four pairwise non-adjacent vertices of a rectangular box (see, e.g., [86]). Hence, there exists a representation $c_1 = (\lambda_1, \lambda_2, \lambda_3)^T$, $c_2 = (\lambda_1, -\lambda_2, -\lambda_3)^T$, $c_3 = (-\lambda_1, \lambda_2, -\lambda_3)^T$, $c_4 = (-\lambda_1, -\lambda_2, \lambda_3)^T$ with $\lambda_1, \lambda_2, \lambda_3 > 0$.

Assuming without loss of generality $v^2 = 1$, (3.1) gives

$$c_i \cdot v + 2c_i \cdot p = \sum_{j=1}^{3} \lambda_j^2 + p^2 - r^2, \quad 1 \leq i \leq 4 . \tag{3.21}$$

Subtracting these equations pairwise gives

$$4(\lambda_2 p_2 + \lambda_3 p_3) = -4(\lambda_1 \lambda_3 v_1 v_3 + \lambda_1 \lambda_2 v_1 v_2)$$

(for indices 1, 2) and analogous equations, so that

$$\lambda_1 p_1 = -\lambda_2 \lambda_3 v_2 v_3 , \quad \lambda_2 p_2 = -\lambda_1 \lambda_3 v_1 v_3 , \quad \lambda_3 p_3 = -\lambda_1 \lambda_2 v_1 v_2 .$$

Since $p \cdot v = 0$, this yields $v_1 v_2 v_3 = 0$. By assuming without loss of generality $v_1 = 0$, we obtain

$$p = \left(-\frac{\lambda_2 \lambda_3}{\lambda_1} v_2 v_3, 0, 0 \right) .$$

So (3.21) becomes

$$\lambda_2^2 v_2^2 + \lambda_3^2 v_3^2 = \sum_{j=1}^{3} \lambda_j^2 + \left(-\frac{\lambda_2 \lambda_3}{\lambda_1} v_2 v_3 \right)^2 - r^2 ,$$

which, by using $v_2^2 + v_3^2 = 1$, gives

$$\lambda_2^2 \lambda_3^2 v_2^4 + (\lambda_1^2 \lambda_2^2 - \lambda_1^2 \lambda_3^2 - \lambda_2^2 \lambda_3^2) v_2^2 + \lambda_1^2 (r^2 - \lambda_1^2 - \lambda_2^2) = 0 . \tag{3.22}$$

There are two distinct real solutions for v_2^2 if and only if

$$\lambda_1^2 \lambda_2^2 + \lambda_1^2 \lambda_3^2 + \lambda_2^2 \lambda_3^2 > 2\lambda_1 \lambda_2 \lambda_3 r . \tag{3.23}$$

Since the volume V of T is $8\lambda_1 \lambda_2 \lambda_3/3$ and the area A of a face is $2\sqrt{\lambda_1^2 \lambda_2^2 + \lambda_1^2 \lambda_3^2 + \lambda_2^2 \lambda_3^2}$, (3.23) becomes $A^2/4 > 3Vr/4$. In case of reality, both solutions for v_2^2 are positive if and only if

$$r^2 > \lambda_1^2 + \lambda_2^2 \tag{3.24}$$

and

$$\lambda_1^2 \lambda_3^2 + \lambda_2^2 \lambda_3^2 > \lambda_1^2 \lambda_2^2 . \tag{3.25}$$

Hence, there will be 12 distinct real common tangents to $S(c_1, r)$, ..., $S(c_4, r)$ if and only if r satisfies (3.23) and the three inequalities such as (3.24), and if in addition the

tetrahedron T satisfies the three inequalities such as (3.25). Since $2\sqrt{\lambda_1^2 + \lambda_2^2}$ is the length of one of the edges, it follows that we require

$$\frac{e}{2} < r < \frac{A^2}{3V}\,,$$

where e is the length of the longest edge; also, expressing (3.25) by using the area A gives

$$A^2 > 8\lambda_1^2\lambda_2^2\,.$$

Applying the formula "$A = \frac{1}{2}ab\sin\gamma$" on the left side and the Laws of Cosines on the right side establishes a relation among the angles α, β, and γ of the face triangle:

$$\tan\beta\tan\gamma > 2\,.$$

Since $\tan\alpha\tan\beta\tan\gamma = \tan\alpha + \tan\beta + \tan\gamma$ in a triangle and since all three angles are acute, we can conclude:

Lemma 3.6. *Let $c_1,\ldots,c_4$ constitute an equifacial tetrahedron, and let $r > 0$. Then there are exactly 12 distinct real common tangents to $S(c_1,r),\ldots,S(c_4,r)$ if and only if*

a)
$$\frac{e}{2} < r < \frac{A^2}{3V}\,,$$

   where e is the length of the longest edge, A is the area of a face, and V is the volume of the tetrahedron; and

b) *the angles in one (and hence in all) of the face triangles satisfy*

$$\tan\beta + \tan\gamma > \tan\alpha\,, \tag{3.26}$$

   where α is the largest of the three angles.

Figure 3.3 depicts the configuration $c_1 = (4,4,4)^T$, $c_2 = (4,-4,-4)^T$, $c_3 = (-4,4,-4)^T$, $c_4 = (-4,-4,4)^T$ and radius $\sqrt{33}$, which gives 12 tangents by Lemma 3.6.

3.2.3 Affinely dependent centers

Let $c_1,\ldots,c_4$ be non-collinear points in the xy-plane. As introduced in Section 2.2.2, a circular cylinder in $\mathbb{R}^3$ with radius r is a set of the form $\mathrm{bd}(\ell + r\mathbb{B}^3)$. We work in real space and look for circular cylinders C with radius r passing through $c_1,\ldots,c_4$. Unless the axis of C is parallel to the xy-plane, the intersection of C with the xy-plane is an ellipse with smaller half-axis r. We can assume that none of the given points is contained in the convex hull of the other points; otherwise, three points are collinear (giving at most two distinct circular cylinders) or there is no circular cylinder.
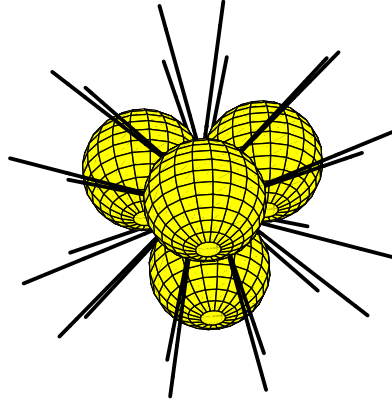
Fig. 3.3: Construction with 12 tangents. Note that the four spheres slightly intersect with each
        other.

An axis parallel to the xy-plane is only possible if the quadrangle formed by $c_1, \ldots, c_4$
is a trapezoid. Since such an axis can be located above or below the xy-plane, and since a
parallelogram has two pairs of parallel edges, we obtain at most 4 circular cylinders with
axis parallel to the xy-plane. If $c_1, \ldots, c_4$ constitute a trapezoid but not a parallelogram,
this number reduces to 2.

Now any ellipse with smaller half-axis r passing through $c_1, \ldots, c_4$ defines two circular
cylinders with radius r, whose intersection with the xy-plane gives the ellipse; in case of
a circle these two cylinders coincide.

Consider a general ellipse

$$E : ax^2 + 2hxy + by^2 + 2gx + 2fy + d = 0 \,,$$

in other form

$$a(x - x_0)^2 + 2h(x - x_0)(y - y_0) + b(y - y_0)^2 + d' = 0 \,. \tag{3.27}$$

Comparing the coefficients of the two forms yields

$$\begin{pmatrix} a & h \\ h & b \end{pmatrix} \begin{pmatrix} x_0 \\ y_0 \end{pmatrix} = \begin{pmatrix} -g \\ -f \end{pmatrix} \,.$$

With the standard invariants of conic section classification

$$I_1 = \operatorname{tr} \begin{pmatrix} a & h \\ h & b \end{pmatrix} = a + b \,,$$

$$I_2 = \det \begin{pmatrix} a & h \\ h & b \end{pmatrix} = ab - h^2 \,,$$

$$I_3 = \det \begin{pmatrix} a & h & g \\ h & b & f \\ g & f & d \end{pmatrix} \,,$$

and the notation $F := gh - af$, $G := fh - bg$, we obtain $x_0 = G/I_2$, $y_0 = F/I_2$. In particular, since E is an ellipse, we have $I_3 \neq 0$, $I_2 > 0$, and $I_1 I_3 < 0$. Consequently, the absolute term d' in (3.27) results to

$$
\begin{aligned}
d' &= \frac{1}{I_2^2} \begin{pmatrix} G & F & I_2 \end{pmatrix} \begin{pmatrix} a & h & g \\ h & b & f \\ g & f & d \end{pmatrix} \begin{pmatrix} G \\ F \\ I_2 \end{pmatrix} \\
&= \frac{1}{I_2} \left(gG + fF + dI_2 \right) \\
&= \frac{I_3}{I_2} \, .
\end{aligned}
$$

E has smaller half-axis r if and only if both eigenvalues of the matrix

$$
-\frac{I_2}{I_3} \begin{pmatrix} a & h \\ h & b \end{pmatrix}
$$

are positive and the larger one is $1/r^2$, i.e., if the largest solution of the quadratic equation in λ

$$
I_3^2 \lambda^2 + I_1 I_2 I_3 \lambda + I_2^3 = 0
$$

is $1/r^2$ and both solutions are positive.

It is well-known that the set of ellipses passing through four given points are members of the pencil of conics $S_1 + \mu S_2$, with S_1, S_2 equations of two arbitrary conics passing through the four points (see, e.g., [109]). Let $I_1(\mu)$, $I_2(\mu)$, $I_3(\mu)$ be the invariants of $S(\mu) := S_1 + \mu S_2$, so that $I_i(\mu)$ is a polynomial in μ of degree i. Any ellipse $S(\mu)$ with smaller half-axis r passing through $c_1, \ldots, c_4$ must necessarily satisfy the condition

$$
\frac{I_3(\mu)^2}{r^4} + \frac{I_1(\mu) I_2(\mu) I_3(\mu)}{r^2} + I_2(\mu)^3 = 0 \, . \tag{3.28}
$$

Equation (3.28) is of order 6 in μ. The two cases for r where the coefficient of degree 6 vanishes stem from our affine notation of a pencil and refer to the case $\mu = \infty$.

Altogether, there are at most 12 circular cylinders with smaller half-axis r passing through $c_1, \ldots, c_4$, whose axis is not parallel to the xy-plane. It remains to show that this number can be decreased in the case of parallelograms and trapezoids.

For the parallelogram case, suppose that the parallelogram is given by the two pairs of parallel lines $y = \gamma$, $y = -\gamma$, and $y = \alpha x + \beta$, $y = \alpha x - \beta$ for some constants $\alpha, \beta, \gamma > 0$. As generators S_1, S_2 of the pencil of conics through the four vertices, we can choose the two degenerated conics given by the two pairs of lines

$$
\begin{aligned}
S_1 &: (y - \gamma)(y + \gamma) = 0 \, , \\
S_2 &: (y - \alpha x - \beta)(y - \alpha x + \beta) = 0 \, .
\end{aligned}
$$

Since both the center of S_1 and the center of S_2 is $(x_0, y_0) = (0,0)^T$, each ellipse in the pencil $S_1 + \mu S_2$ has center $(0,0)^T$. Hence, any ellipse $S(\mu)$ in the pencil is of the form

$$ax^2 + 2hxy + by^2 + 1 = 0 \, .$$

Since

$$I_3(\mu) = \det \begin{pmatrix} a_1 + \mu a_2 & h_1 + \mu h_2 & 0 \\ h_1 + \mu h_2 & b_1 + \mu b_2 & 0 \\ 0 & 0 & 1 + \mu \end{pmatrix} = I_2(\mu)(1 + \mu) \, ,$$

Equation (3.28) becomes

$$I_2(\mu)^2 \left((1 + \mu)^2 r^4 + I_1(\mu)(1 + \mu)r^2 + I_2(\mu) \right) = 0 \, .$$

Consequently, since $I_2(\mu) \neq 0$ for any ellipse in the pencil, we obtain a quadratic condition in μ.

For the trapezoid case, suppose that two vertices are located on the line $y = 0$ and that two vertices are located on the line $y = 2\alpha$ with $\alpha > 0$. Then S_2 can be chosen as the degenerated conic consisting of two parallel lines

$$S_2 : y(y - 2\alpha) = 0 \, .$$

The representation matrix of the ellipse $S_1 + \mu S_2$ is of the form

$$\begin{pmatrix} a_1 & h_1 & f_1 \\ h_1 & b_1 + \mu & g_1 - \alpha\mu \\ f_1 & g_1 - \alpha\mu & d_1 \end{pmatrix} \, .$$

Therefore $I_2(\mu)$ is only linear in μ, and $I_3(\mu)$ is only quadratic in μ. Hence, equation (3.28) is only of degree 4 in μ. We can conclude:

Corollary 3.7. *Let* $c_1, \ldots, c_4$ *be affinely dependent, and let* $r > 0$. *If* $c_1, \ldots, c_4$ *form a trapezoid, then there are at most 10 common tangents to* $S(c_1, r), \ldots, S(c_4, r)$. *If* $c_1, \ldots, c_4$ *form a parallelogram, then there are at most 8 common tangents to* $S(c_1, r), \ldots, S(c_4, r)$.

Concerning constructions with many real tangents in the affinely dependent case, we give a construction with 8 real tangents. Let $c_1, \ldots, c_4$ constitute a square with edge length e. For $e/2 < r < \sqrt{2}e/2$ two neighboring spheres intersect with each other, but a sphere does not intersect with its opposite partner. Hence, the opposite pairs of the intersection circles are disjoint, and they lie on the vertical planes bisecting opposite edges of the square. The four common tangents to such a pair of intersection circles are common tangents to the four spheres which altogether gives 8 common tangents.

We remark that the upper bound of 12 is not tight in the affinely dependent case. In fact, our proof replaces the condition "$1/r^2$ is the largest eigenvalue and both eigenvalues

are positive" by the weaker condition "$1/r^2$ is an eigenvalue". Meanwhile, Megyesi has shown that the number of real tangents to four unit spheres with coplanar centers is bounded by 8 ([93]). Quite interestingly, that proof does not decrease the algebraic degree of the problem. Instead, based on an an explicit analysis it shows that the set of conic sections under investigation always contains some hyperbolas.

Finally, we want to explain what happens to some of the tangents when trying to approach a rectangle configuration (with at most 8 common tangents) as a limit case of affinely independent centers. Let $c_1, \ldots, c_4$ constitute a rectangle in the xy-plane. By lifting two opposite of the four centers appropriately, we can establish a configuration with 12 tangents by Lemma 3.6. By reducing the height of the resulting box with base rectangle in the xy-plane, we can interpret the rectangle as limit case of this flattening process. Now Lemma 3.6 explains where some of the 12 tangents get lost in this limit process. Namely, flattening of the box implies that the triangular faces of the tetrahedron tend towards rectangular triangles. However, then $\tan\alpha$ in (3.26) tends to infinity, and (3.26) is violated at some stage of this process. Intuitively, this means that some of the tangents get lost even before the limit case is reached.

3.2.4   Relations to classical projective geometry

In this section, we provide an alternative characterization of the cubic equation (3.11) based on the pedal surface of a tetrahedron from classical projective geometry. Throughout this section, we work in real space.

Note that the numbers in (3.9) can be interpreted as barycentric coordinates of the direction vector v in the projective space relative to c_1, c_2, c_3 (cf. [33]). If we allow c_4 to be an arbitrary vector again, the representation in barycentric coordinates is

$$v = \sum_{j=1}^{4} t_j c_j \, . \tag{3.29}$$

Then the equation of Π_∞, the plane at infinity in three-dimensional real projective space $\mathbb{P}^3_\mathbb{R}$, is

$$t_1 + t_2 + t_3 + t_4 = 0 \tag{3.30}$$

(cf. [33]). The locus of all points x with the property that the feet of the perpendiculars from x on the planes supporting the faces of the tetrahedron T lie in a plane, is a cubic surface Σ ([111, Exer. 17 on p. 118]). At the end of this section, we provide a proof of this statement. Namely, Σ is given by

$$A_1^2 t_2 t_3 t_4 + A_2^2 t_1 t_3 t_4 + A_3^2 t_1 t_2 t_4 + A_4^2 t_1 t_2 t_3 = 0 \, , \tag{3.31}$$

or, in a nicer (but slightly imprecise) form

$$\frac{A_1^2}{t_1} + \frac{A_2^2}{t_2} + \frac{A_3^2}{t_3} + \frac{A_4^2}{t_4} = 0 \, . \tag{3.32}$$

Obviously, all six lines defined by the edges $c_i c_j$, $1 \leq i \neq j \leq 4$, belong to Σ. Consider now any circular cylinder C circumscribing T and let $x(C)$ denote the point at infinity of the axis of C. We claim that $x(C) \in \Sigma$, i.e., its barycentric coordinates satisfy (3.31). By the Wallace-Simson Theorem, the feet of the perpendiculars from c_4 on the planes $c_1 c_2 x(C)$, $c_1 c_3 x(C)$, $c_2 c_3 x(C)$ are collinear ([33, Exer. 11 on p. 16], [68]). Consequently, the feet of the perpendiculars from c_4 on the four planes supporting the faces of the tetrahedron $c_1 c_2 c_3 x(C)$ lie in a plane. But then $x(C)$ is in the same relation to the tetrahedron $c_1 c_2 c_3 c_4$, i.e., $x(C) \in \Sigma$ (see [6, p. 25]).

By solving (3.30) for t_4 and substituting this expression into (3.31), we obtain a cubic equation in t_1, t_2, t_3. It can be easily checked that for $c_4 = 0$ this equation is equivalent to (3.11).

The pedal surface of a tetrahedron. We close this section by providing a proof for the pedal surface of a tetrahedron. Let $c_1, \ldots, c_4 \in \mathbb{R}^3$ be the vertices of a tetrahedron T, let N_i denote the unit outer normal vector of the face opposite to c_i, and let A_i denote the area of that face. An elementary computation (using (3.7), $n_4 := ((c_1 - c_2) \times (c_3 - c_2))/2$ and a suitable orientation) shows

$$A_1 N_1 + A_2 N_2 + A_3 N_3 + A_4 N_4 = 0 \,. \tag{3.33}$$

We would like to write up the equation of the so-called *pedal surface* Σ of the tetrahedron, i.e., the locus of the points x such that the feet of the perpendiculars from x to the planes supporting the faces of the tetrahedron lie in a plane.

Let $w_i \in \mathbb{R}^3$ be the vector connecting x to the foot of the perpendicular from x to the plane supporting the face opposite to c_i. The feet of these perpendiculars (i.e., the endpoints of these vectors) are coplanar if and only if the determinant of the 4×4-matrix with i-th row $(w_i, 1)$ vanishes. The latter condition is equivalent to

$$(w_2\, w_3\, w_4) - (w_1\, w_3\, w_4) + (w_1\, w_2\, w_4) - (w_1\, w_2\, w_3) = 0 \,,$$

where $(a\, b\, c) = (a \times b) \cdot c$ is the scalar triple product. If b_i is defined by $v_i = b_i N_i$, then the equation becomes

$$\frac{(N_2\, N_3\, N_4)}{b_1} - \frac{(N_1\, N_3\, N_4)}{b_2} + \frac{(N_1\, N_2\, N_4)}{b_3} - \frac{(N_1\, N_2\, N_3)}{b_4} = 0 \,. \tag{3.34}$$

It follows from (3.33) by taking scalar products with $N_2 \times N_3$ that

$$A_1 (N_1\, N_2\, N_3) + A_4 (N_2\, N_3\, N_4) = 0 \,,$$

and from the analogous relations we obtain that for some $b \in \mathbb{R}$,

$$(N_2\, N_3\, N_4) = b A_1 \,, \quad (N_1\, N_3\, N_4) = -b A_2 \,, \quad (N_1\, N_2\, N_4) = b A_3 \,, \quad (N_1\, N_2\, N_3) = -b A_4 \,.$$

Comparing this with (3.34) yields

$$\frac{A_1}{b_1} + \frac{A_2}{b_2} + \frac{A_3}{b_3} + \frac{A_4}{b_4} = 0 \,. \tag{3.35}$$

Let $t_1, \ldots, t_4$ denote the projective barycentric coordinates of x relative to $c_1, \ldots, c_4$. Notice that t_i is proportional to $c_i A_i$ (cf. [33]). Therefore, x satisfies the required property if and only if

$$\frac{A_1^2}{t_1} + \frac{A_2^2}{t_2} + \frac{A_3^2}{t_3} + \frac{A_4^2}{t_4} = 0 \,, \tag{3.36}$$

as desired.

3.2.5 Open questions

Concerning the geometry of the tangent problem, there are two main open questions. Firstly, under which conditions do four spheres of *arbitrary* radii do have infinitely many real common tangent lines? There are some obvious situations with infinitely many real common tangent lines: whenever the four centers are collinear and the four spheres are inscribed in the same hyperboloid of one sheet. We conjecture that there does not exist any configuration with four spheres of arbitrary radii, non-collinear centers, and infinitely many real common tangent lines. For the special case of affinely dependent centers, this has recently been proven by Megyesi [95].

Secondly, in our construction with 12 real common tangent lines the unit spheres are intersecting each other. Hence, the natural question arises, which is still open: What is the maximum number of real common tangent lines to four disjoint unit spheres (cf. the treatment of realization questions in the next section)?

3.3 Realization questions

In this section, we prove Theorem 3.2 stated at the beginning of this chapter. For any $k \in \{0, \ldots, 12\}$ we give geometric constructions leading to this number of common tangents (of course, some values of k are trivial). For some of the constructions, the number of different real tangent lines can be computed by combining careful geometric investigations with symmetry arguments. However, for some constructions, a purely geometric correctness proof seems to be out of reach. In these cases the algebraic framework developed in Section 3.1 and 3.2 helps to establish a rigorous proof. This leads to nice and effective interactions between the geometry and the algebra of the problem.

Before giving an outline of the paper, we remark that the cases with 0, 1, 2, or ∞ tangents are trivial. For the unit spheres centered in $c_1 = (0, 0, 0)^T$, $c_2 = (2, 0, 0)^T$, $c_3 = (4, 0, 0)^T$, $c_4 = (6, t, 0)^T$, the values $t = 0$, $t = 1$, $t = 2$, and $t = 3$ lead to ∞, 2, 1, and 0 distinct real tangents, respectively. Constructions of four (non-disjoint) spheres with 12 and 8 tangents have already been given in Sections 3.2.2 and 3.2.3, respectively.

The constructions for the remaining numbers are presented in the following order. In Section 3.3.1, we analyze constructions where the centers are the vertices of a regular tetrahedron. Besides the constructions with 12 real tangents known from Section 3.2.2

this also yields constructions with 3 and 6 tangents. Based on this analysis, Section 3.3.2 deals with constructions where three centers form an equilateral triangle; this gives constructions with 3, 6, 9, and 7 tangents. Parallelogram configurations of the four centers are discussed in Section 3.3.3; in particular, this yields constructions with 4, 5, and 8 tangents. In Section 3.3.4 gives constructions with 10 and 11 tangents. In Section 3.3.5, we close the discussion of realization questions with a short discussion of the relation between the algebra and the geometry of the tangent problem.

3.3.1   The case of a regular tetrahedron

In Section 3.2.2, we have given a specific configuration with 12 real tangents, where the four centers constitute the vertices of a regular tetrahedron. The following complete classification of a regular tetrahedron configuration will be used within the constructions in the next sections. As before, let $c_1, \ldots, c_4$ be the centers of the four spheres in $\mathbb{R}^3$. By appropriate scaling, the four spheres of radius r can be transformed into unit spheres.

Lemma 3.8. *Let $c_1, \ldots, c_4$ be the vertices of a regular tetrahedron with edge length 1.*

(a) *For $1/2 < r < 3\sqrt{2}/8$ there exist exactly 12 distinct real common tangents to the spheres $S(c_1, r), \ldots, S(c_4, r)$.*

(b) *For $r = 1/2$ and $r = 3\sqrt{2}/8$ there exist exactly 3 and 6 distinct real common tangents, respectively.*

(c) *For $r < 1/2$ or $r > 3\sqrt{2}/8$ there do not exist any real common tangents.*

Proof. Let $c_4 = (0, 0, 0)^T$, $c_1 = (1, 0, 0)^T$, $c_2 = (1/2, \sqrt{3}/2, 0)^T$, $c_3 = (1/2, \sqrt{3}/6, \sqrt{6}/3)^T$ be the vertices of a regular tetrahedron with edge length 1. In this situation, the cubic (3.11) is reducible and can be decomposed into

$$(t_1 + t_2)(t_2 + t_3)(t_3 + t_1) = 0 , \tag{3.37}$$

where t_1, t_2, t_3 are the homogeneous coordinates of the direction vector v in the basis c_1, c_2, c_3. By symmetry of this equation it suffices to consider the factor $t_1 + t_2 = 0$. Over the reals, this linear equation can be parametrized by $(t_1, t_2, t_3)^T = (1, -1, \lambda)^T$, $-\infty < \lambda \leq \infty$. Here, the case $\lambda = \infty$ refers to the homogeneous vector $t = (0, 0, 1)^T$. Using (3.5) and $p^2 = r^2$, $r^2(\lambda)$ can be expressed by

$$r^2(\lambda) = \frac{9\lambda^4 + 14\lambda^2 + 9\lambda}{32(\lambda^2 + 1)^2}$$

with nominator of degree 4 and strictly positive denominator. The function graph of $r(\lambda)$ is depicted in Figure 3.4. Elementary calculus yields

$$\left[r^2(\lambda)\right]' = \frac{\lambda(\lambda^2 - 1)}{4(\lambda^2 + 1)}$$
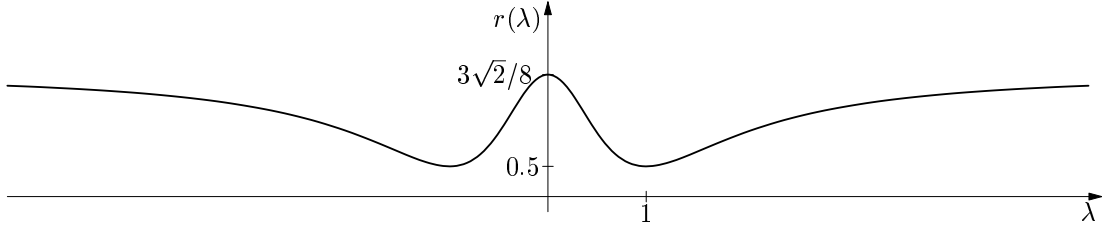
Fig. 3.4: The function $r(\lambda) = \left(\frac{9\lambda^4 + 14\lambda^2 + 9}{32(\lambda^2+1)^2}\right)^{1/2}$

with strictly positive denominator. Hence,

$$
\begin{aligned}
\min r(\lambda) &= r(1) = r(-1) = 1/2\,, \\
\max r(\lambda) &= r(0) = \lim_{\lambda \to -\infty} r(\lambda) = \lim_{\lambda \to \infty} r(\lambda) = 3\sqrt{2}/8 \approx 0.5303\,.
\end{aligned}
$$

Note that the difference between $\min r(\lambda)$ and $\max r(\lambda)$ is rather small. The extreme values and the strict monotony of $r^2(\lambda)$ between these values show: for $1/2 < r < 3\sqrt{2}/8$ there are four different real solutions of λ and hence four different real tangents. Considering all three factors of (3.37), there are exactly 12 different tangents altogether.

   In case $r = 1/2$ these 12 tangents collapse to 3 tangents. The direction vectors in t-coordinates are $(1, 1, -1)^T$, $(1, -1, 1)^T$, and $(-1, 1, 1)^T$, respectively. In case $r = 3\sqrt{2}/8$ the 12 tangents collapse to 6 tangents; the direction vectors are the direction vectors of the 6 tetrahedron edges. $\qquad\square$

   Figure 3.5 shows a regular tetrahedron configuration with edge length 1 and radius $r = 53/100$. Since a tangent to $S(c_1, r), \ldots, S(c_4, r)$ can also be interpreted as axis of a circular cylinder with radius r circumscribing the tetrahedron with vertices $c_1, \ldots, c_4$, the following statement can be deduced immediately (cf. the treatment of optimization aspects in Section 3.4).

Corollary 3.9. *Let T be a regular tetrahedron with edge length $a > 0$. Then the smallest and largest circular cylinder circumscribing T have radius $a/2$ and $3\sqrt{2}a/8$, respectively.*

Remark 3.10. The lower bound $a/2$ in Corollary 3.9 can also be deduced from the fact that a minimal circular cylinder *enclosing* a regular tetrahedron with edge length a has radius $a/2$ [147].

3.3.2   Equilateral triangle constructions

In this section, we give configurations with 3, 6, 7, and 9 tangents. We start from a regular tetrahedron configuration with edge length 1. However, in order to stress symmetries, we now use the coordinates $c_1 = (\sqrt{3}/3, 0, 0)^T$, $c_2 = (-\sqrt{3}/6, 1/2, 0)^T$,
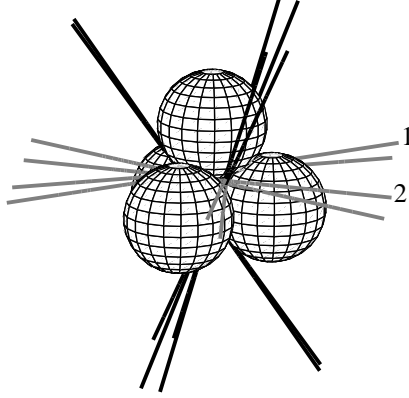
Fig. 3.5: Construction of four (non-disjoint) spheres with 12 common tangents. Here, if the coordinates of $c_1, \dots, c_4$ are those of Section 3.3.2 then there are exactly 6 tangents which touch all spheres with positive z-coordinate. These tangents are drawn in grey color.

$c_3 = (-\sqrt{3}/6, -1/2, 0)^T$, $c_4 = (0, 0, \sqrt{6}/3)^T$. Further, let $1/2 < r < 3\sqrt{2}/8$. Figure 3.6(a) shows the parallel projection of this configuration on the xy-plane. Note that $c_1, \dots, c_3$ form an equilateral triangle in the xy-plane with center in the origin. By Lemma 3.8, the spheres $S(c_i, r)$, $1 \le i \le 4$, have 12 real common tangents.

In this configuration with 12 real tangents, 6 of the tangents touch all four spheres with positive z-coordinate, and 6 tangents touch exactly two spheres with negative z-coordinates (see Figure 3.5). We call these tangents the upper and the lower tangents, respectively.

Now observe what happens when replacing the z-coordinate in c_4 by increasing values $t > \sqrt{6}/3$. The geometry of this process implies: the z-coordinate $v_3/\|v\|$ of the unit direction vector increases, until eventually – for some value $t = t_9$ – the tangent touches two of the spheres $S(c_1, r)$, $S(c_2, r)$, $S(c_3, r)$ at the same point (see Figure 3.6(a) for an illustration of the xy-projection). In the latter situation, the 6 upper tangents collapse to 3 tangents. Figure 3.6 depicts the section of this constellation through the xz-plane. One of these 3 remaining upper tangents touches $S(c_2, r)$ and $S(c_3, r)$ in the same point, namely on the circle where $S(c_2, r)$ and $S(c_3, r)$ intersect; this circle of intersection is located in the plane $y = 0$. By symmetry of the equilateral triangle, the other 4 upper tangents collapse to 2 tangents in the same way. Since for $t = t_9$ the lower tangents neither have vanished nor collapsed (see below), the four spheres have exactly 9 different common tangents.

In order to compute t_9, let $c_s = (-\sqrt{3}/6, 0, 0)^T$ and $r_s = \sqrt{r^2 - 1/4}$ denote the center and the radius of the circle of intersection. Then, setting $b = \|c_s - c_1\|$ and $z_9 = ((\sqrt{3}/2)^2 - (r - r_s)^2)^{1/2}$, a straightforward geometric computation yields the two

(a) Projection on the xy-plane (b) Section through the xz-plane
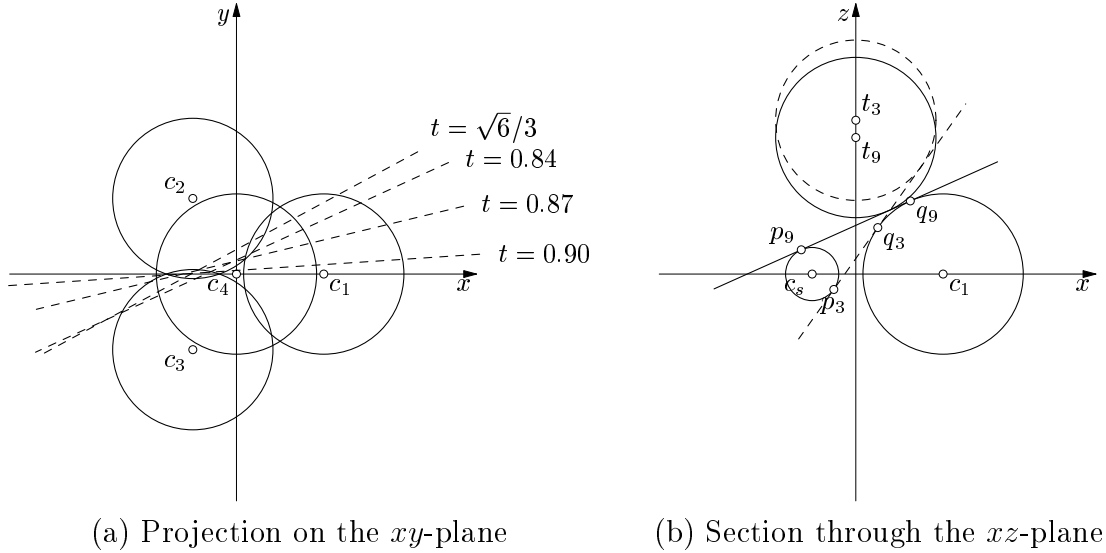
Fig. 3.6: Different views of the constructions with 3, 6, and 9 tangents. The common radius of the spheres is 0.53.

points on the tangent p_9, q_9,

$$p_9 = (-\sqrt{3}/6 - r_s(r - r_s)/b, 0, r_s z_9/b)^T, \qquad q_9 = (\sqrt{3}/3 - r(r - r_s)/b, 0, r z_9/b)^T.$$

p_9 is located on the circle of intersection, and q_9 is located on $S(c_3, r)$ (see Figure 3.6(b)). Now the tangent condition for the sphere $S((0, 0, t_9)^T, r)$ implies a quadratic equation for t_9. The larger one of the two solutions gives the desired value of t_9.

For values $t > t_9$ there exist at most 6 real tangents. Analogous to the critical case with 9 tangents there exists some value t_3 where the 6 lower tangents collapse to 3 tangents. The dashed lines in Figure 3.6(b) show the section of this situation through the xz-plane. The tangent in the xz-plane is given by the two points

$$p_3 = (-\sqrt{3}/6 + r_s(r + r_s)/b, 0, -r_s z_3/b)^T, \qquad q_3 = (\sqrt{3}/3 - r(r + r_s)/b, 0, r z_3/b)^T,$$

where $z_3 = ((\sqrt{3}/2)^2 - (r + r_s)^2)^{1/2}$. For values $t > t_3$ there does not exist any common tangent to the four spheres.

In particular, for any given r satisfying $1/2 < r < 3\sqrt{2}/8$ the two values t_3 and t_9 can be computed exactly. However, since the resulting expressions are quite long, we only give some numerical values to illustrate the relationships in size. Table 3.1 contains some values of r together with the resulting numerical values of t_3 and t_9. Figure 3.7 illustrates the construction.

For a construction with 7 tangents, we start from the above configuration with 9 tangents. In this configuration, the remaining 3 upper tangents are critical in the sense

r	t_9	t_3
0.51	0.8463	0.8478
0.52	0.8760	0.9293
0.53	0.9028	1.0172

Tab. 3.1: Some values of the radius r and the resulting coordinates t_9 and t_3 leading to 9 and 3 distinct real common tangents, respectively.
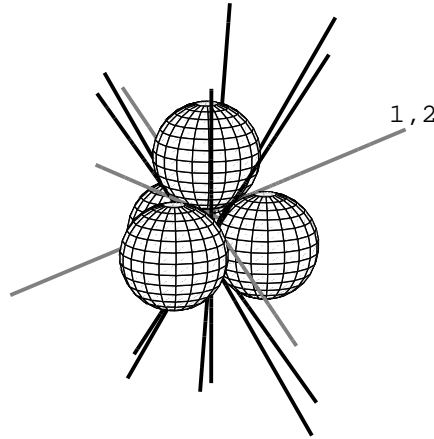
Fig. 3.7: In this construction with 9 real tangents, the remaining 3 upper tangents are drawn in grey color. The tangent labeled by 1,2 stems from the tangents labeled by 1 and 2 in Figure 3.5.

that for any additional increment of the z-value of c_4 these tangents vanish. Now we move the fourth center $(0, 0, t_9)^T$ along the line $(0, 0, t_9)^T + \lambda(q_9 - p_9)$, $\lambda \in \mathbb{R}$. For any $\lambda > 0$, the line through p_9 and q_9 is still tangent to the four spheres. However, the other two upper tangents from the situation $\lambda = 0$ immediately vanish for $\lambda > 0$. Hence, there exists some $\varepsilon > 0$ such that any configuration with $0 < \lambda < \varepsilon$ leads to exactly 7 common tangents. As an example, for $r = 0.53$ we can choose $0 < \lambda < 1/10$.

3.3.3 Parallelogram constructions

In order to give constructions with 4, 5, and 8 tangents, we start from the following situation depending on some parameter $a \in \mathbb{R}$. Let $c_1 = (-a - 1, -1, 0)^T$, $c_2 = (-a + 1, -1, 0)^T$, $c_3 = (a - 1, 1, 0^T)$, $c_4 = (a + 1, 1, 0)^T$ define a parallelogram in the xy-plane, and let $r = 1$. By Corollary 3.7, a parallelogram configuration gives at most 8 real common tangents.

As illustrated in Figure 3.8(a), the special case $a = 0$ yields a square. Obviously, these four spheres have two common tangents, namely the lines $x = z = 0$ and $y = z = 0$.
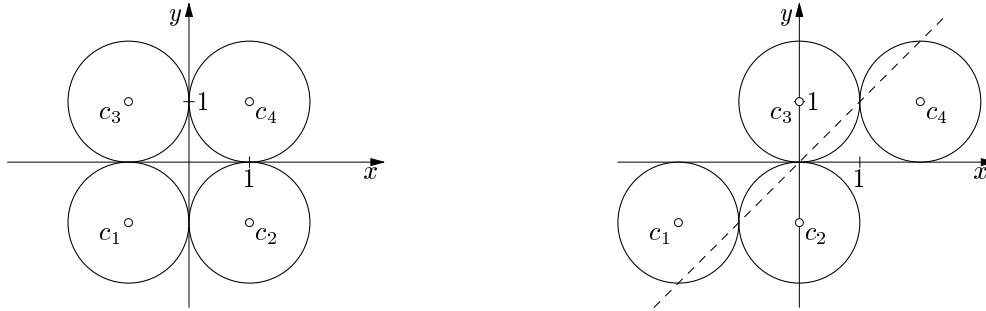
(a) $a = 0$ gives 2 real common tangents.

(b) $a = 1$ gives 3 real common tangents.

Fig. 3.8: Initial configurations for constructions with 5 and 8 real tangents. In the right figure the dotted line shows the two tangents with z-coordinate $\sqrt{2}$ and $-\sqrt{2}$, respectively.

Now observe what happens for parameter values $0 < a < 1$. For $0 < a < 1$, there exist exactly 5 tangents. As before, one of the tangents is the line defined by $y = z = 0$. However, the tangent $x = z = 0$ from the case $a = 0$ splits for $a > 0$ into four tangents. More precisely, for $0 < a < \infty$ there are two tangents parallel to the xy-plane (see the dotted line in Figure 3.8(b)); these two tangents are symmetric with respect to the xy-plane.

For $0 < a < 1$, there exist two tangents passing through the origin. These two tangents are symmetric with respect to the xz-plane, too. Here, we have to compute the lines which pass through the origin and which are tangent to $S(c_3, 1)$ and $S(c_4, 1)$. For $0 < a < 1$, there exist two lines with this property. By symmetry, these lines are also tangent to $S(c_1, 1)$ and $S(c_2, 1)$. For $a = 1$, these two lines collapse to the line $y = z = 0$. Obviously, if $0 < a < 1$ then multiplying the y-coordinates of all four centers by a factor μ slightly larger than 1 yields a configuration with 4 instead of 5 distinct common tangents.

Now we turn towards a construction with 8 tangents. For $0 < a \leq 1/2$, we multiply the y-coordinates of all four centers by some $0 < \mu \leq 1$ such that $\|c_1 - c_3\| = \|c_2 - c_4\| = 2$. Geometrically, the upper spheres "roll" on top of the lower spheres (see Figure 3.9(a)). Elementary geometry yields $\mu = \sqrt{1 - a^2}/2$. Compared to the situation $a = 0$, for $0 < a < 1/2$ the tangent $y = z = 0$ is split into 4 tangents in the same way as in the transition from 2 to 5 tangents.

In particular, since $5^2 + 12^2 = 13^2$, the choice $a = 5/13$ yields the rational coordinates $c_1 = (-18, -12, 0)^T/13$, $c_2 = (8, -12, 0)^T/13$, $c_3 = (-8, -12, 0)^T/13$, $c_4 = (18, -12, 0)^T/13$. This configuration is depicted in Figure 3.9(b). For $a = 1/2$ the 4 tangents passing through the origin collapse to 2 tangents; hence, this yields another configuration with 6 real tangents.

Note that in the configuration with 8 tangents there are 4 points which belong to more than one sphere. However, the radius can be slightly decreased without altering the num-
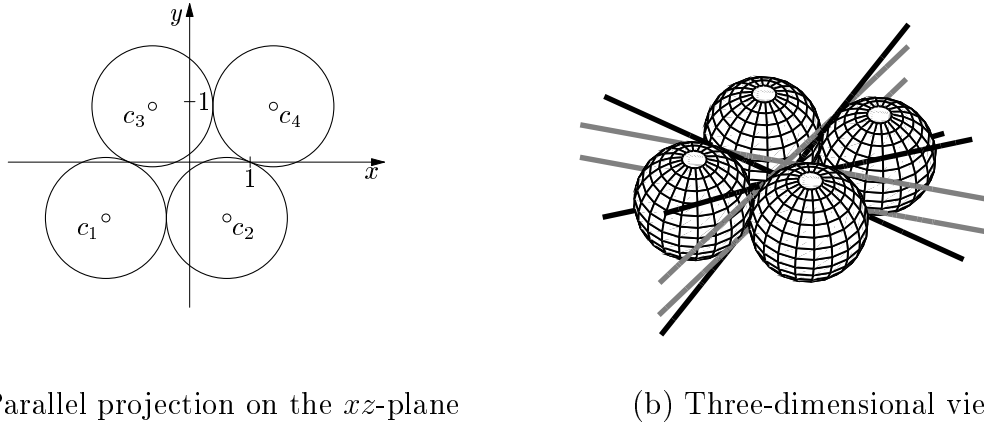
(a) Parallel projection on the xz-plane   (b) Three-dimensional view

Fig. 3.9: Construction with 8 tangents. In the right picture, tangents which are parallel to the xy-plane are drawn in grey color.

ber of common tangents. After rescaling these disjoint spheres we obtain a configuration of 4 *disjoint* unit spheres with 8 common tangents.

3.3.4   Constructions with 10 and 11 real tangents

In order to give constructions with 10 and 11 distinct real tangents, we start from the initial regular tetrahedron in Section 3.3.2 (see Figure 3.6(a)). However, for notational convenience, we exchange the centers c_3 and c_4. By Lemma 3.8, the radius $r = 3\sqrt{2}/8$ leads to 6 common tangents, whose directions are the directions of the six tetrahedron edges. Figure 3.10 shows the projection of this situation in the direction of the edge c_2c_4. Note that the lower left disc in this figure refers to the spheres $S(c_2, r)$ and $S(c_4, r)$.

In this situation, we move the spheres $S(c_2, r)$ and $S(c_4, r)$ slightly in opposite directions along the edge connecting their centers. This movement does not change the position of the tangent with direction c_2c_4. However, the movement will give some "freedom" to any of the five other tangents, and hence any of these edges will split into two edges. Intuitively, this situation leads to 11 tangents; by increasing the radius slightly the tangent with direction c_2c_3 vanishes.

To formalize this idea, we consider the four centers $c_1 = (\sqrt{3}/3, 0, 0)^T$, $c_2 = (-\sqrt{3}/6, 1/2 + a, 0)^T$, $c_3 = (0, 0, \sqrt{6}/3)^T$, $c_4 = (-\sqrt{3}/6, -1/2 - a, 0)^T$ for some $a > 0$. In order to apply the algebraic framework from Section 3.3.1, we translate all centers by $-c_4$; this translation moves c_4 into the origin. Since the two faces $c_1c_2c_3$ and $c_1c_3c_4$ have the same area, and the two faces $c_1c_2c_4$ and $c_2c_3c_4$ have the same area, we have $A_1 = A_3$ and $A_2 = A_4$. As already seen in (3.19), the cubic (3.11) specializes to

$$(A_2^2 t_1 + A_1^2 t_3)(A_1^2(t_1 t_2 + t_2^2 + t_2 t_3) + A_2^2 t_1 t_3) = 0 \,.$$

In particular, the cubic is reducible. Using (3.20), the set of all real tangents to the four
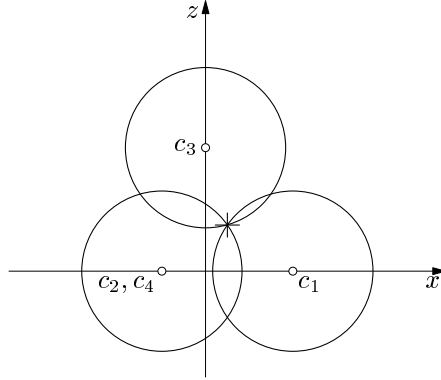
Fig. 3.10: Parallel projection of $S(c_1, r), \ldots, S(c_4, r)$ in the xz-plane with $r = 3\sqrt{2}/8$. This is the projection along the edge with direction $c_2 c_4$. The position of the common tangent in this direction is marked by the cross.

spheres $S(c_i, r)$ for *some* radius $r > 0$ can be parametrized by the line

$$(t_1, t_2, t_3)^T = (A_1^2, A_2^2 \lambda, -A_1^2)^T, \qquad -\infty < \lambda \leq \infty \tag{3.38}$$

and the conic section

$$(t_1, t_2, t_3)^T = (-A_1^2(\lambda - 1) - A_2^2, A_2^2 \lambda, A_1^2(\lambda - 1)\lambda)^T, \qquad -\infty < \lambda \leq \infty. \tag{3.39}$$

For a given radius, the linear function gives at most 4 common tangents and the conic section gives at most 8 common tangents. Analogous to Section 3.3.1, for both parametrizations the square of the radius function $r(\lambda)$ is a rational function in λ.

A suitable choice of a which will have the desired properties and which leads to rational values of A_1^2, A_2^2 is $a = (\sqrt{112/100} - 1)/2$. Then $A_1^2 = 78/400$, $A_2^2 = 84/400$, and the parametrization of the linear factor yields

$$r^2(\lambda) = \frac{169(1764\lambda^4 + 2492\lambda^2 + 1521)}{32(175\lambda^2 + 169)^2}.$$

The graph of $r(\lambda)$ is shown in Figure 3.11. The derivative of $r^2(\lambda)$ is

$$\left[r^2(\lambda)\right]' = \frac{1183\lambda(11438\lambda^2 - 7943)}{8(169\lambda^2 + 175)^3}$$

with nominator of degree 3 and strictly positive denominator. In particular, $r(0) = 3\sqrt{2}/8 \approx 0.5303$ is a local maximum, and

$$\lim_{\lambda \to -\infty} r(\lambda) = \lim_{\lambda \to \infty} r(\lambda) = \sqrt{\frac{169 \cdot 1764}{32 \cdot 175^2}} > 0.54.$$
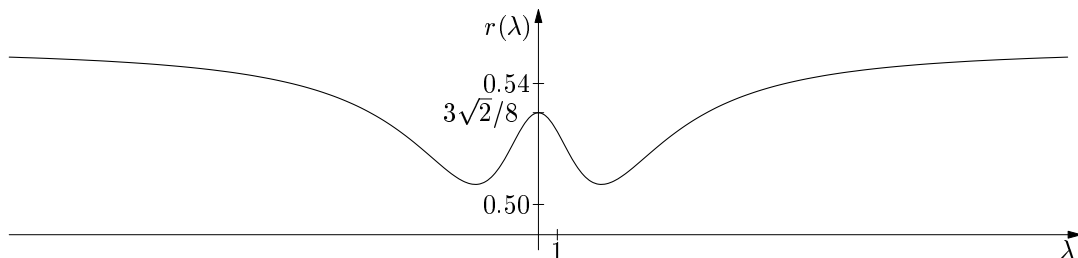
Fig. 3.11: In the parametrization of the linear factor, the square of the radius function $r(\lambda)$ is a rational function in λ.
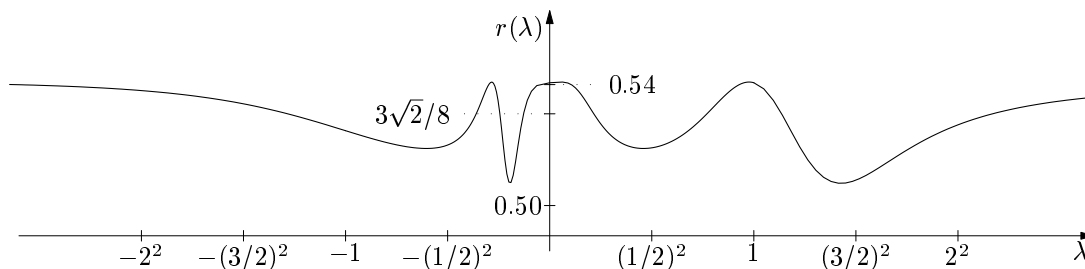
Fig. 3.12: $r(\lambda)$ for the parametrization of the conic section. For better illustration of the region near $\lambda = 0$ the λ-axis is scaled quadratically.

Consequently, there exist exactly three different real values of λ with $r(\lambda) = 3\sqrt{2}/8$; and for slightly larger radii r than $3\sqrt{2}/8$, say $r_1 < r \leq r_2$ with $r_1 := 3\sqrt{2}/8$, $r_2 := 0.54$, we only obtain two such real values of λ.

It remains to show: for a given radius $r \in [r_1, r_2]$, the parametrization of the conic section contains exactly 8 real values of λ with $r(\lambda) = r$. Figure 3.12 illustrates the function graph of $r(\lambda)$. By (3.39), the λ-values $-\infty$, $-A_2^2/A_1^2 + 1$, 0, 1, ∞ represent the t-vectors $(0,0,1)^T$, $(0,1,-1)^T$, $(1,0,0)^T$, $(1,-1,0)^T$, and $(0,0,1)^T$, respectively. For all these λ-values we obtain $r(\lambda) = 3\sqrt{1378}/206 > 0.54$. These 5 values decompose the real axis into 4 intervals. If any of these intervals contains some value λ with $r(\lambda) < 3\sqrt{2}/8$, then for a given $r \in [r_1, r_2]$, there are at least 8 solutions with $r(\lambda) = r$. We can choose, e.g., the following values of λ: $-3/10$, $-5/100$, $2/10$, and 2. For any of these 4 values we obtain $r(\lambda) < 0.52$ which implies the desired result. Since there cannot be more than 8 solutions, there are exactly 8 real solutions.

Finally, it can be easily checked that for $A_2 > A_1$ the line (3.38) and the conic section (3.39) do not have real intersection points; so the tangents stemming from the line and the tangents stemming from the conic section are indeed different. This completes the proof of the constructions with 10 and 11 tangents.

3.3.5 Discussion and open questions

In this section, we have shown that for any $k \in \{0, \ldots, 12\}$ there exists a configuration with four unit spheres and exactly k distinct real common tangents. Although we have motivated every construction by purely geometric arguments, the rigorous proofs of some constructions (in particular 10, 11 tangents) heavily depend on the algebraic framework of the problem as developed in Sections 3.1 and 3.2. We interpret this observation as an indication why a purely geometric proof of the upper bound of 12 real common tangents (Theorem 3.1) should be quite hard to establish.

Furthermore, observe that all constructions with more than 8 tangents are based on non-disjoint sphere configurations. Already in Section 3.2.5 we have stated the open question on the maximum number of distinct real tangents for disjoint unit spheres. The difficulty in treating this question is the same one as above. Namely, it seems to be difficult to exploit the condition of disjointness in the algebraic setting; but we do not know how to handle these situations from a purely geometric point of view.

Finally, the following open problem plays an important role in the interplay between the algebra and the geometry of the tangent problem. For some famous problems in enumerative geometry (flexes and bitangents of plane curves, lines on cubic surfaces, conics tangent to five given conics), the resulting Galois groups in the generic case are non-solvable [69]. This situation reflects the difficulty of purely geometric methods to handle these problems. Using the computer algebra system GAP [115] for the handling of groups, we have checked for some specific instances of tangents to four unit spheres that the resulting Galois groups are non-solvable. It is an open problem to provide a non-computer-algebraic proof of this non-solvability for generic instances.

3.4 Computing smallest circumscribing cylinders of a tetrahedron in $\mathbb{R}^3$

We study the optimization aspect of the tangent problem. Given affinely independent centers $c_1, \ldots, c_4 \in \mathbb{R}^3$, finding the minimal radius $r > 0$ such that the spheres $S(c_1, r), \ldots, S(c_4, r)$ have a real common tangent is equivalent to finding the minimal radius of a circular cylinder circumscribing the tetrahedron with vertices $c_1, \ldots, c_4$. In Section 2.2.5, we have seen that this problem is tightly connected to the computation of a smallest enclosing cylinder for general polytopes in $\mathbb{R}^3$.

As mentioned in Section 2.1.2, the computational costs of solving a system of polynomial equations are dominated by the Bézout number and the mixed volume (the latter will become relevant in the n-dimensional case treated in Section 5.3). Hence, it is an essential task to find the right algebraic formulations.

In Section 3.4.1, we apply our framework of Sections 3.1 and 3.2 to provide a formulation for the smallest circumscribing cylinder of a tetrahedron with Bézout number 36.

Based on this formulation, we can investigate tetrahedron classes for which the degrees can be further reduced. This is done in Section 3.4.2.

3.4.1   General tetrahedra in $\mathbb{R}^3$

In the proof of [37, Theorem 6], a polynomial formulation is given to compute a smallest enclosing cylinder of a tetrahedron in $\mathbb{R}^3$. This formulation describes the problem by three equations in the direction vector $v = (v_1, v_2, v_3)^T$ of the line, one of them normalizing the direction vector v by

$$v_1^2 + v_2^2 + v_3^2 \; = \; 1 \,. \tag{3.40}$$

The equations are of degree 10, 3, and 2, respectively, thus giving a Bézout number of 60. However, as pointed out in that paper, some of the solutions to that system are artificially introduced by the formulation and occur with higher multiplicity, and there are only 18 really different solutions. Even more severely, in the experiments in that paper (using SYNAPS, a state-of-the-art software for numerical polynomial computations), the numerical treatment of these multiple solutions needs much time, roughly a factor 100 compared to similar systems without multiple solutions.

Here, we present an approach, which reflects the true algebraic bound of 18. Namely, we give a polynomial formulation with Bézout bound 36 in which every solution generically has multiplicity one. The additional factor 2 just results from the fact that due to the normalization condition (3.40) every solution v also implies that $-v$ is a solution as well.

Our framework is based on Sections 3.1 and 3.2. Here, we are interested in real lines. As before, a line in $\mathbb{R}^3$ is represented by a direction vector $v \in \mathbb{R}^3 \setminus \{0\}$ and a point $p \in \mathbb{R}^3$ lying on the line with $p \cdot v = 0$. Moreover, we assume $v^2 = 1$.

Let $c_1, \dots, c_4$ be the affinely independent vertices of the given tetrahedron, and assume $c_4 = 0$. Further let $M := (c_1, c_2, c_3)^T$. After substituting (3.5) into $p \cdot v = 0$, we set $v^2 = 1$ in the resulting denominator; this gives the homogeneous cubic equation which we denote by $g_1(v_1, v_2, v_3) = 0$. Hence, we arrive at the following polynomial optimization formulation in terms of the variables v_1, v_2, and v_3 to compute the square of the radius of the minimal circumscribing cylinder.

$$\begin{aligned}
\min & \left(\tfrac{1}{2} M^{-1} \begin{pmatrix} v^2 p_1^2 - (v \cdot p_1)^2 \\ v^2 p_2^2 - (v \cdot p_2)^2 \\ v^2 p_3^2 - (v \cdot p_3)^2 \end{pmatrix} \right)^2 \\
\text{s.t.} \quad g_1(v_1, v_2, v_3) & = 0 \,, \\
g_2(v_1, v_2, v_3) := v^2 - 1 & = 0 \,.
\end{aligned} \tag{3.41}$$

Rather than using $v^2 = 1$ to further simplify the objective function, we prefer to keep the homogeneous form, so that the objective function is a homogeneous polynomial of degree 4. We denote this polynomial by f.

By the considerations in Section 3.2, the edge directions of the base tetrahedron are admissible solutions; thus the set of admissible solutions is nonempty.

Using Lagrange multipliers λ_1 and λ_2, a necessary local optimality condition is

$$\text{grad } f = \lambda_1 \text{grad } g_1 + \lambda_2 \text{grad } g_2 \,. \tag{3.42}$$

By thinking of an additional factor λ_0 before grad f and considering (3.42) as a system of linear equations in λ_0, λ_1, λ_2, we see that if (3.42) is satisfied for some vector v then the determinant

$$\det \begin{pmatrix} -\frac{\partial f}{\partial v_1} & \frac{\partial g_1}{\partial v_1} & \frac{\partial g_2}{\partial v_1} \\ -\frac{\partial f}{\partial v_2} & \frac{\partial g_1}{\partial v_2} & \frac{\partial g_2}{\partial v_2} \\ -\frac{\partial f}{\partial v_3} & \frac{\partial g_1}{\partial v_3} & \frac{\partial g_2}{\partial v_3} \end{pmatrix} \tag{3.43}$$

vanishes.

Lemma 3.11. *(a) For any normalized direction vector $(v_1, v_2, v_3)^T \in \mathbb{R}^3$ of the axis of a locally extreme circumscribing cylinder, the determinant (3.43) vanishes. If there are only finitely many locally extreme, normalized direction vectors then that number is bounded by 36.*

(b) For a generic tetrahedron the number of solutions is indeed finite, and all solutions have multiplicity one.

Proof. Let v be the direction vector of an axis of a locally extreme circumscribing cylinder. Then v satisfies the first constraint of (3.41), and the determinant (3.43) vanishes. Since these are homogeneous equations of degree 3 and 6, respectively, Bézout's Theorem implies that in connection with $v^2 = 1$ we obtain at most 36 isolated solutions.

For the second statement it suffices to check that for one specific tetrahedron there are only finitely many solutions and that all solutions are pairwise distinct. $\qquad\square$

3.4.2 Special tetrahedron classes in $\mathbb{R}^3$

We investigate conditions under which the degree of the resulting equations decreases. Moreover, we show that for the equifacial tetrahedron, the minimal circumscribing radius can be computed quite easily.

In Section 3.2.1, we have seen that the polynomial g_1 in the cubic equation factors into a linear polynomial and an irreducible quadratic polynomial if and only if the four faces of the tetrahedron T can be partitioned into two pairs of faces $\{F_1, F_2\}$, $\{F_3, F_4\}$ with $\mathrm{area}(F_1) = \mathrm{area}(F_2) \neq \mathrm{area}(F_3) = \mathrm{area}(F_4)$. Moreover, g_1 factors into three linear terms if and only if the areas of all four faces of T are equal.

First let us consider the case where g_1 decomposes into a linear polynomial and an irreducible quadratic polynomial. By optimizing separately over the linear and the quadratic constraint, the degrees of our equations are smaller than for the general case. Namely, analogously to the derivation in Section 3.4.1, for the quadratic constraint we obtain a Bézout bound of

$$(3 + 1 + 1) \cdot 2 \cdot 2 = 20 \,,$$

and for the linear constraint we obtain

$$(3 + 0 + 1) \cdot 1 \cdot 2 = 8 \,.$$

Thus, we can conclude:

Lemma 3.12. *If the four faces of the tetrahedron can be partitioned into two pairs of faces* $\{F_1, F_2\}$, $\{F_3, F_4\}$ *with* $area(F_1) = area(F_2) \neq area(F_3) = area(F_4)$ *then there are at most 28 isolated local extrema for the minimal circumscribing cylinder. They can be computed from two polynomial systems with Bézout numbers 20 and 8, respectively.*

Equifacial simplices. As described in Section 3.2.2, for an equifacial tetrahedron the cubic polynomial g_1 factors into three linear terms. Hence, we obtain at most $3 \cdot 8 = 24$ local extrema. Somewhat surprisingly, it is even possible to compute smallest circumscribing cylinder of an equifacial tetrahedron essentially without any algebraic computation. We follow the notation and reasoning in Section 3.2.2. Thus we assume that the vertices of an equifacial tetrahedron have the form $c_1 = (\lambda_1, \lambda_2, \lambda_3)^T$, $c_2 = (\lambda_1, -\lambda_2, -\lambda_3)^T$, $c_3 = (-\lambda_1, \lambda_2, -\lambda_3)^T$, $c_4 = (-\lambda_1, -\lambda_2, \lambda_3)^T$ with $\lambda_1, \lambda_2, \lambda_3 > 0$. For any radius $r > 0$, the direction vector of any common tangent to the four spheres $S(c_1, r), \dots, S(c_4, r)$ satisfies $v_1 v_2 v_3 = 0$. Considering without loss of generality the case $v_1 = 0$, (3.22) yields

$$r^2 \;=\; -\frac{\lambda_2^2 \lambda_3^2}{\lambda_1^2} v_2^4 - \left(\lambda_2^2 - \lambda_3^2 - \frac{\lambda_2^2 \lambda_3^2}{\lambda_1^2} \right) v_2^2 + \lambda_1^2 + \lambda_2^2 \,. \tag{3.44}$$

Thus, by computing the derivative of this expression $r^2 = r^2(v_2)$ and taking into account the three cases $v_i = 0$, we can reduce the computation of the minimal circumscribing cylinder to solving three univariate equations of degree 3. However, we can still do better. Substitute $z_2 := v_2^2$, and let ρ be the expression for r^2 in terms of z_2,

$$\rho(z_2) \;=\; -\frac{\lambda_2^2 \lambda_3^2}{\lambda_1^2} z_2^2 - \left(\lambda_2^2 - \lambda_3^2 - \frac{\lambda_2^2 \lambda_3^2}{\lambda_1^2} \right) z_2 + \lambda_1^2 + \lambda_2^2 \,.$$

Since the second derivative of that quadratic function is negative, $\rho(z_2)$ is a concave function. Hence, within the interval $z_2 \in [0, 1]$, the minimum is attained at one of the boundary values $z_2 \in \{0, 1\}$. Consequently, two of the components of $(v_1, v_2, v_3)^T$ must be zero and therefore v is perpendicular to two opposite edges. Since the latter geometric characterization is independent of our specific choice of coordinates, we can conclude:

Theorem 3.13. *If all four faces of the tetrahedron T have the same area then the axis of a minimum circumscribing cylinder is perpendicular to two opposite edges.*

Hence, for an equifacial tetrahedron it suffices to investigate the cross products of the three pairs of opposite edges (equipped with an orientation), and we do not need to solve a system of polynomial equations at all.

In order to illustrate how these three solutions relate to the 18 solutions of the general approach above, we consider the regular tetrahedron in $\mathbb{R}^3$. In the general approach, as already pointed out in [37], the six edge directions $c_i c_j$ ($1 \leq i < j \leq 4$) all have multiplicity 1, and each of the three directions in Theorem 3.13, $c_1 c_2 \times c_3 c_4$, $c_1 c_3 \times c_2 c_4$, $c_1 c_4 \times c_2 c_3$, have multiplicity 4.

3.5 Dynamic visualization aspects

As illustrated within the constructions in Section 3.3, many properties and constructions of the tangent problem can best be understood in terms of *dynamic* configurations. For a dynamic visualization of our algebraic problem of degree 12, we do not only have to solve a single system, but instead have to solve several systems per second. In this section, we briefly describe a prototype of a homotopy-based visualization tool, which demonstrates that visualization of algebraic-geometric problems of this degree in real time is indeed possible. For a demonstration video of these visualizations see the video review tape of the Symposium on Computational Geometry 2002 [85].

General framework. In the last years, homotopy continuation techniques techniques have been very fruitfully applied to build state-of-the-art numerical solvers of polynomial equations (see [32, 143]). The goal is to find all solutions of a zero-dimensional system of polynomial equations

$$f_1(x_1, \ldots, x_n) = \ldots = f_n(x_1, \ldots, x_n) = 0 \,,$$

abbreviated $f(x) = 0$. The idea of the homotopy technique is to start from a second system $g(x) = 0$ whose solutions are known a priori. Then we consider the family of systems of equations

$$0 = h(x, \lambda) := (1 - \lambda)g(x) + \lambda f(x)$$

for $0 \le \lambda \le 1$. By successively increasing λ in small steps from 0 to 1 we can use either Newton's method to find the solutions for the next step, or solvers of ordinary differential equations. The latter approach is based on the equation

$$J(x(\lambda), \lambda)\frac{dx(\lambda)}{d\lambda} = -\frac{\partial h}{\partial \lambda}(x(\lambda), \lambda), \quad J(x, \lambda) := \left(\frac{\partial h_i}{\partial x_j}(x, \lambda)\right),$$

which is implied by the Implicit Function Theorem.

Homotopy methods for the tangents to spheres. If the starting system $g(x) = 0$ of a homotopy solver has more solutions than the system $f(x) = 0$, some paths necessarily diverge as $\lambda \to 1$. Therefore a main concern in the design of homotopy solvers is to find an appropriate starting system of polynomials $g(x)$, which is expected to have the same number of zeroes as $f(x)$. By Bernstein's Theorem, this means that the starting polynomials $g(x)$ should have the same Newton polytope as $f(x)$ (see, e.g., [32, 137]).

For two reasons, homotopy techniques seem to be particularly suitable for visualizing configurations of the tangents to spheres. Firstly, for the given polynomial formulation the Bézout number agrees with the number of expected zeroes. Secondly, as exhibited in Section 3.3, geometric understanding of configurations suggests also to inspect topologically neighboring configurations. For two-dimensional geometric problems, the latter issue is treated comprehensively in dynamic geometry software such as CINDERELLA [108].

Implementation aspects. The homotopy-based visualization of dynamic tangent configurations has been prototypically implemented in Visual C++. The input to the program is a description of the dynamic configurations. For computing and visualizing the tangents of the initial configurations, the homotopy method starts from a standard starting system. For the subsequent configurations, it starts from the preceding configuration. Both Newton's method and numerical methods for solving the differential equation are implemented.

The 3D graphics have been implemented using the OPEN GL-based COIN 3D graphics library. This library provides an application programming interface based on the widely distributed OPEN INVENTOR graphics library.

Frontiers of the implementation. Despite an automatic adaption of the step size, numerical problems of course arise whenever we reach too close to a configuration in which the Jacobian matrix J is singular. If this configuration is only an intermediate configuration on a homotopy path, this can be avoided by choosing a long way round the singularity. However, if the singular configuration is our destination, then this strategy obviously does not work. Experimental data on the numerical behavior can be found in the Diplom thesis of D. Kotzor [84].

4. COMMON TANGENTS TO FOUR QUADRICS IN $\mathbb{P}^3$ AND $\mathbb{R}^3$

In this chapter, we study the problem of common tangents to four quadrics in $\mathbb{P}^3$ and relate it to the sphere problem discussed in Chapter 3.

Using Plücker coordinates, each of the tangent conditions gives a quadratic equation in $\mathbb{P}^5$. In connection with the single Plücker relation (2.2), we obtain five quadratic equations in $\mathbb{P}^5$. By Bézout's Theorem, if this system has only finitely complex solutions, then this number is bounded by 32. The discrepancy between this upper bound and the number of 12 for spheres is caused by the fact that for spheres, the common zeroes of the Plücker formulation in $\mathbb{P}^5$ include a one-dimensional excess component at infinity (accounting for the "missing" $2^5 - 12 = 20$ solutions [1]). This observation can also be seen as the main argument why we used an elementary description of lines in Chapter 3.

In Section 4.1, we solve the real enumerative question for quadrics by showing that 32 is the true upper bound for quadrics, even over the real numbers.

In Section 4.2, we propose some computer-algebraic methods to relate the enumerative geometry problem for general quadrics to the enumerative geometry problem for spheres. In order to resolve the one-dimensional component of solutions at infinity, the algebraic-geometric technique of blow-ups can be used. In most examples coming from geometry, a single blow-up suffices to resolve an excess component. However, for the tangent problem after one blow-up the excess component is still not resolved, and a second blow-up is necessary. Thus the tangent problem is an outstanding example of a natural geometric problem whose analysis requires a double blow-up. The aim of this section is to use computer-algebraic methods to show the necessity of a second blow-up.

4.1 Real lines

Recall from Section 2.1.1 that we call a quadratic hypersurface real if it can be described by a quadratic form with real coefficients. Here, we show the following result.

Theorem 4.1. *There exists a configuration of four real quadrics in $\mathbb{P}^3$ with 32 distinct real common tangent lines.*

Before going into the technical details, let us illustrate the geometric idea underlying our construction. We start from the well-known fact that four lines in $\mathbb{P}^3$ have at most two or infinitely many common transversals (see, e.g., [75, §XIV.7]). In order to demonstrate the geometry behind this number of two, consider a tetrahedron $\Delta \in \mathbb{R}^3$, where we fix two opposite edges e_1 and e_2. Let $\ell_1, \ldots, \ell_4$ be the lines underlying the other four edges. These

four lines intersect pairwise in the vertices of Δ. Hence, the two common transversals are the lines underlying the two edges e_1 and e_2. See Figure 4.1.
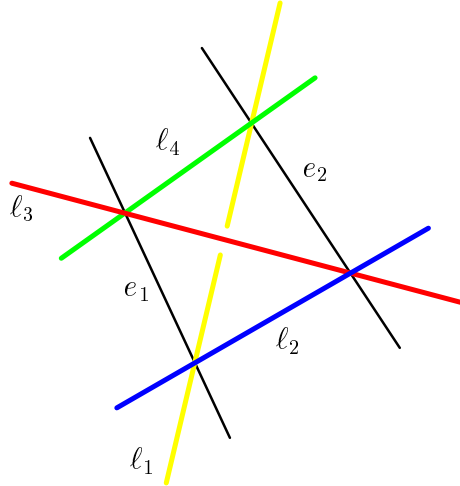
Fig. 4.1: Tetrahedron configuration of four lines in $\mathbb{R}^3$ with two real tangents.

Consider the lines $\ell_1, \ldots, \ell_4$ as (degenerate) infinite circular cylinders with radius $r = 0$. If we increase the radius slightly, then the cylinders intersect pairwise in the regions (combinatorially) given by the four vertices of Δ. Intuitively, after this perturbation process, the common tangents roughly have the direction of e_1 and e_2. However, due to the intersection of the cylinders every of these intersection points defines four combinatorial types. Therefore, there are $4 \cdot 4$ tangents close to the direction of e_1 and $4 \cdot 4$ tangents close to the direction of e_2. Figure 4.2 illustrates this situation for the case of a regular tetrahedron.

While this demonstration of Theorem 4.1 is visually appealing and is easily verified numerically, its proof requires more work. Namely, perturbing the given lines into cylinders transforms a problem of degree 2 into one of degree 32. In order to make this idea precise, we describe a family of projective configurations each of which is equivalent to that of Figure 4.1. Exploiting symmetries, we are able to determine configurations in the family having all common transversals real. This provides a constructive proof of Theorem 4.1.

We realize the tetrahedral configuration of Figure 4.1 in projective 3-space, using the coordinates $(x_0, x_1, x_2, x_3)^T$ for $\mathbb{P}^3$. For the lines $\ell_1, \ldots, \ell_4$, we we give a description in terms of equations, as well as a parametrization using the coordinates $[s, t]$ for $\mathbb{P}^1$.

$$
\begin{aligned}
\ell_1 &: \quad x_0 = x_3 = 0 \,, \quad i.e., \ (0, s, t, 0)^T \,, \\
\ell_2 &: \quad x_1 = x_0 = 0 \,, \quad i.e., \ (0, 0, s, t)^T \,, \\
\ell_3 &: \quad x_1 = x_2 = 0 \,, \quad i.e., \ (t, 0, 0, s)^T \,, \\
\ell_4 &: \quad x_2 = x_3 = 0 \,, \quad i.e., \ (s, t, 0, 0)^T \,.
\end{aligned}
\tag{4.1}
$$

Then the lines underlying e_1 and e_2 are $(s, 0, t, 0)^T$ and $(0, s, t, 0)^T$, respectively.
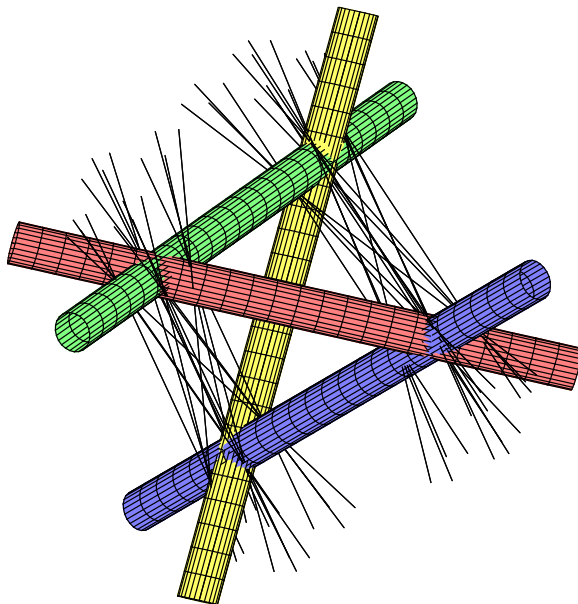
Fig. 4.2: Configuration of 4 quadrics with 32 real tangents.

Now, for some parameters $\alpha, \beta \in \mathbb{R}$, consider the four quadrics

$$
\begin{aligned}
Q_1 &: & x_1^2 + x_2^2 - \alpha(x_3^2 + x_0^2) &= 0 \,, \\
Q_2 &: & x_2^2 + x_3^2 - \alpha(x_0^2 + x_1^2) &= 0 \,, \\
Q_3 &: & x_3^2 + x_0^2 - \beta(x_1^2 + x_2^2) &= 0 \,, \\
Q_4 &: & x_0^2 + x_1^2 - \beta(x_2^2 + x_3^2) &= 0 \,.
\end{aligned}
$$

For $\alpha = \beta = 0$, these quadrics become the corresponding lines, and for small $\alpha, \beta > 0$, these quadrics are deformations of the lines. Recall that the signature of a quadric denotes the number of positive eigenvalues of its representation matrix minus the number of negative eigenvalues. Since for $\alpha, \beta > 0$ each quadric Q_i has rank 4 and signature 0, we see that all four quadrics are ruled surfaces.

Theorem 4.2. *Let $(\alpha, \beta) \in \mathbb{R}^2$ satisfy*

$$
\alpha\beta(1 - \alpha\beta)(1 + \beta)(1 + \alpha)\big((1 - \alpha)^2(1 - \beta)^2 - 16\alpha\beta\big) \ \neq \ 0 \,.
$$

Then there are 32 distinct (possibly complex) common tangent lines to $Q_1, \ldots, Q_4$. Moreover, if $0 < \alpha, \beta < 3 - 2\sqrt{2}$, then all these 32 distinct tangent lines are real.

Proof. We work in the Plücker coordinates for the space of lines in $\mathbb{P}^3$. Since the quadrics only contain monomials of the form x_i^2, the four tangent equations (2.5) of $Q_1, \ldots, Q_4$

only contain monomials of the form p_{ij}^2. More precisely, the four tangent equations give the following system of linear equations in $p_{01}^2, \ldots, p_{23}^2$:

$$
\begin{pmatrix}
-\alpha & -\alpha & \alpha^2 & 1 & -\alpha & -\alpha \\
\alpha^2 & -\alpha & -\alpha & -\alpha & -\alpha & 1 \\
-\beta & -\beta & 1 & \beta^2 & -\beta & -\beta \\
1 & -\beta & -\beta & -\beta & -\beta & \beta^2
\end{pmatrix}
\begin{pmatrix}
p_{01}^2 \\
p_{02}^2 \\
p_{03}^2 \\
p_{12}^2 \\
p_{13}^2 \\
p_{23}^2
\end{pmatrix}
= 0 \,.
$$

We permute the variables into the order $(p_{02}, p_{13}, p_{03}, p_{12}, p_{01}, p_{23})$. Then, for α, β satisfying

$$
\alpha\beta(1 - \alpha\beta)(1 + \beta)(1 + \alpha) \;\neq\; 0\,, \tag{4.2}
$$

Gaussian elimination yields the following system:

$$
\begin{pmatrix}
-\beta & -\beta & (1 - \alpha)(1 - \beta) & 0 & 0 & 0 \\
0 & 0 & \alpha & -\beta & 0 & 0 \\
0 & 0 & 0 & -\beta & \alpha & 0 \\
0 & 0 & 0 & 0 & \alpha & -\beta
\end{pmatrix}
\begin{pmatrix}
p_{02}^2 \\
p_{13}^2 \\
p_{03}^2 \\
p_{12}^2 \\
p_{01}^2 \\
p_{23}^2
\end{pmatrix}
= 0 \,.
$$

Hence, in connection with the single Plücker equation (2.2), we have the following system of equations:

$$
-\beta p_{02}^2 - \beta p_{13}^2 + (1 - \alpha)(1 - \beta)p_{03}^2 \;=\; 0\,, \tag{4.3}
$$

$$
p_{01}p_{23} - p_{02}p_{13} + p_{03}p_{12} \;=\; 0\,, \tag{4.4}
$$

$$
\alpha p_{01}^2 \;=\; \alpha p_{03}^2 \;=\; \beta p_{12}^2 \;=\; \beta p_{23}^2 \,. \tag{4.5}
$$

We analyze this system for α, β satisfying (4.2) by considering the following three disjoint cases.

Case 1: $p_{02} = 0$.
Since $p_{13} = 0$ would imply that all components are zero and hence contradict $(p_{01}, \ldots, p_{23})^T \in \mathbb{P}^5$, we can assume $p_{13} = 1$. Then (4.3) and (4.5) imply

$$
\alpha p_{01}^2 \;=\; \alpha p_{03}^2 \;=\; \beta p_{12}^2 \;=\; \beta p_{23}^2 \;=\; \frac{\alpha\beta}{(1 - \alpha)(1 - \beta)} \neq 0 \,.
$$

Since (4.4) implies $\mathrm{sgn}(p_{01}p_{23}) = -\mathrm{sgn}(p_{03}p_{12})$, only 8 of the $2^4 = 16$ sign combinations for $p_{01}, p_{03}, p_{12}, p_{23}$ are possible. More precisely, the 8 (possibly complex) solutions for $p_{01}, p_{03}, p_{12}, p_{23}$ are

$$
(p_{01}, p_{03}, p_{12}, p_{23})^T = \frac{1}{\sqrt{(1 - \alpha)(1 - \beta)}} \left(\gamma_{01}\beta, \gamma_{03}\beta, \gamma_{12}\alpha, -\mathrm{sgn}(\gamma_{01}\gamma_{03}\gamma_{12})\alpha\right)^T \tag{4.6}
$$

with $\gamma_{01}, \gamma_{03}, \gamma_{12} \in \{-1, 1\}$. Hence, for $\alpha, \beta \in \mathbb{R}^2$ satisfying (4.2), this case gives 8 distinct common tangents.

Case 2: $p_{13} = 0$.
This case is symmetric to case 1. Setting $p_{13} = 1$, the resulting 8 solutions for the variables $p_{01}, p_{03}, p_{12}, p_{23}$ are the same ones as in (4.6).

Case 3: $p_{02}p_{13} \neq 0$.
Without loss of generality, we can assume $p_{02} = 1$. Solving (4.4) for p_{13} and substituting this expression into (4.3) yields

$$-\beta - \beta p_{01}^2 p_{23}^2 - \beta p_{03}^2 p_{12}^2 - 2\beta p_{01}p_{03}p_{12}p_{23} + (1-\alpha)(1-\beta)p_{03}^2 \;=\; 0 \,.$$

We next use (4.5) to write this in terms of p_{01}. This is straightforward for the squared terms, but for the other terms, we observe that, by (4.5), $p_{01}p_{23} = \pm p_{03}p_{12}$ and since $p_{02}p_{13} \neq 0$, the Plücker equation (4.4) implies these have the same sign. This gives the quartic equation in p_{01}

$$-\beta + (1-\alpha)(1-\beta)p_{01}^2 - 4\alpha p_{01}^4 \;=\; 0 \,.$$

Considering this equation as a quadratic equation in p_{01}^2, the discriminant is

$$(1-\alpha)^2(1-\beta)^2 - 16\alpha\beta \,. \tag{4.7}$$

Hence, for $\alpha, \beta \in \mathbb{R}^2$ satisfying (4.2), and for which this discriminant does not vanish, there are two different solutions for p_{01}^2. For each of these two solutions for p_{01}^2, there are 8 distinct solutions for $p_{01}, p_{03}, p_{12}, p_{23}$, namely

$$(p_{01}, p_{03}, p_{12}, p_{23})^T \;=\; \sqrt{p_{01}^2}\,(\gamma_{01}, \gamma_{03}, \gamma_{12}, \mathrm{sgn}(\gamma_{01}\gamma_{03}\gamma_{12}))^T \tag{4.8}$$

with $\gamma_{01}, \gamma_{03}, \gamma_{12} \in \{-1, 1\}$. Since p_{13} is uniquely determined by p_{01}, p_{02}, p_{03}, p_{12}, case 3 gives 16 distinct common tangents.

With this solution, we can easily determine when all solutions are real. First, suppose that $\alpha = \beta$. Then the discriminant (4.7) becomes $(\alpha^2 - 6\alpha + 1)(\alpha + 1)^2$, and its smallest positive root is $\alpha_0 := 3 - 2\sqrt{2} \approx 0.17157$. In particular, for $0 < \alpha < \alpha_0$, the discriminant in case 3 is positive and both solutions for p_{01}^2 are positive. Thus, for $0 < \beta = \alpha < \alpha_0$, the solutions of all three cases are distinct and real. Next, fix $0 < \alpha < \alpha_0$ and suppose that $0 < \beta < \alpha$. Then the discriminant (4.7) is positive. To see this, note that for fixed $0 < \alpha < \alpha_0$, the discriminant (4.7) is decreasing in β for $0 < \beta < \alpha$ and positive when $\beta = \alpha$. This concludes the proof of Theorem 4.2. $\qquad\Box$

Figure 4.3 illustrates the construction and the 32 tangents for $\alpha = 1/10$ and $\beta = 1/20$.
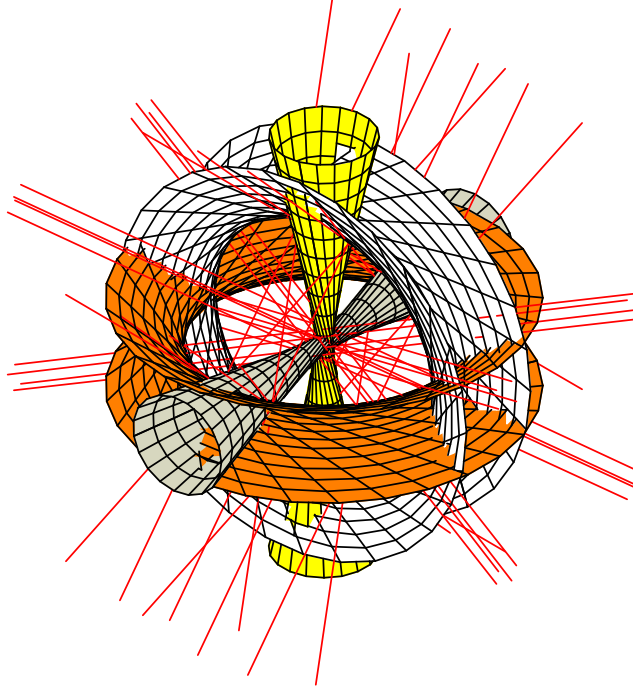
Fig. 4.3: The configuration of quadrics from Theorem 4.2.

4.2   Computer-algebraic aspects

Let four spheres in $\mathbb{R}^3$ be given by centers $c_1, \ldots, c_4 \in \mathbb{R}^3$ and radii $r_1, \ldots, r_4 > 0$. By (2.6), each of the tangent conditions gives a quadratic equation in Plücker coordinates, and additionally we have to consider the single Plücker equation (2.2). So we obtain a system with Bézout number $2^5 = 32$ in the projective space $\mathbb{P}^5$ of Plücker coordinates p_{ij}, $0 \leq i < j \leq 3$.

Besides the isolated solutions there is an excess component of tangents located in the plane at infinity. Namely, any vector $p \in \mathbb{P}^5$ which satisfies

$$p_{01} = p_{02} = p_{03} = p_{12}^2 + p_{13}^2 + p_{23}^2 = 0 \tag{4.9}$$

both fulfils the algebraic tangent condition given by (2.6) and the Plücker condition (2.2). Due to the conditions $p_{01} = p_{02} = p_{03} = 0$, the geometric lines described by the Plücker vectors in this variety are located in the plane at infinity.

A fundamental technique in algebraic geometry is to resolve singularities of a variety by means of a blow-up. Here, we use this technique to remove the excess component of our variety of tangents. Intuitively, we can think of lifting our variety into a space of larger dimension, there having the freedom to add further information which then allows to distinguish the points we do not want to count.

(a) Plane curve (b) After the blow-up
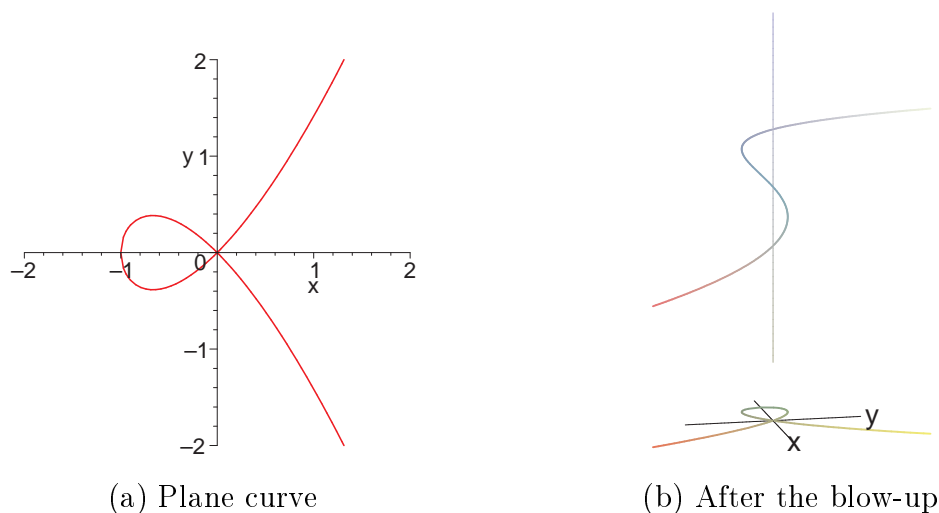
Fig. 4.4: The nodal cubic.

In most examples coming from geometry, a single blow-up suffices to resolve an excess component. However, for the tangent problem to spheres it has originally been observed by P. Aluffi and W. Fulton [1] that after one blow-up the excess component is still not resolved and that a second blow-up is necessary.

4.2.1 Algebraic-geometric background

Before providing the computer-algebraic details, let us shortly review the geometric idea of the blow-up technique (see [55, 71]). For an illustration, consider the nodal cubic curve in $\mathbb{R}^2$ defined by $y^2 = x^2(x + 1)$ (see Figure 4.4(a)). The origin is a singular point of the curve. In order to determine the exact multiplicity of the origin, we resolve the singularity by means of a blow-up. Namely, we embed the two-dimensional curve C appropriately into $\mathbb{R}^2 \times \mathbb{P}^1_{\mathbb{R}}$. For each point $(x, y) \in \mathbb{R}^2$ we encode its tangent direction x/y in the third component. Formally, we consider the curve in $\mathbb{R}^2 \times \mathbb{P}^1_{\mathbb{R}}$ defined by the two equations in the variables $(x, y, [t_0, t_1])$,

$$y^2 = x^2(x + 1), \qquad t_0 x = t_1 y. \tag{4.10}$$

The latter equation expresses that the tangent direction x/y coincides with t_1/t_0. The illustration in Figure 4.4(b) shows that this curve consists of two branches: on the one hand we have the branch $E := (0, 0) \times \mathbb{P}^1_{\mathbb{R}}$, called the *exceptional divisor*, and on the other hand we have the "stretched" curve $\tilde{C}$ which we wanted to achieve. Figure 4.4(b) illustrates that $\tilde{C}$ does not contain a singular point anymore.

The concept can be generalized to resolve not only single singular points but also common components (see [55, 71]). Our excess component E is given by (4.9) in $\mathbb{P}^5$. The

underlying theory requires to start from an affine space. Therefore we set $p_{23} = 1$ (since we want to analyze the excess component, we choose a variable here which does not affect the existence of our excess component itself).

The ideal I_E generated by the polynomials in (4.9) is a radical ideal, i.e., whenever I_E contains some positive power of a polynomial f then it also contains f itself. For that reason we can blow up $\mathbb{R}^n$ *along the subvariety* E (see [125, p. 111]). (In case I_E is not radical, this leads to the more general notion of a blow-up *along the subscheme* defined by an ideal I_E.)

4.2.2   *Simulating the double blow-up*

Using the computer-algebra system SINGULAR [62], we can simulate the blow-up as follows. First we define a polynomial ring R in the variables $p_{01}, p_{02}, p_{03}, p_{12}, p_{13}$ over a field with characteristic zero (i.e., the base field is $\mathbb{Q}$). Moreover, we choose a degree reverse lexicographical ordering (dp). The option redSB forces SINGULAR to work with reduced Gröbner (standard) bases.

```
option(redSB);
ring R = 0, (p01,p02,p03,p12,p13), (dp);
```

The following procedure computes the tangent equation of a sphere. Since the SINGULAR implementation of the wedge function works in a different basis (namely, with regard to our notation $\wedge^2 Q \in \mathbb{R}^{\binom{n}{2},\binom{n}{2}}$, SINGULAR computes $(-1)^{i+j}(\wedge^2 Q)_{ij}$, $1 \le i, j \le \binom{n}{2}$), we compensate these differences in signs by using a modified Plücker vector.

```
proc tangenteq(int c1, int c2, int c3, int rr)
{
  matrix sphereeq[4][4] = c1^2+c2^2+c3^2-rr^2, -c1, -c2, -c3,
                          -c1,                   1,   0,   0,
                          -c2,                   0,   1,   0,
                          -c3,                   0,   0,   1;
  matrix plueckermod[6][1] = p01, -p02, p03, -p12, p13, -1;
  return(transpose(plueckermod) * wedge(sphereeq,2) * plueckermod);
}
```

We consider the four spheres with centers $(0,0,0)^T$, $(1,-2,3)^T$, $(1,0,1)^T$, and $(0,-1,0)^T$ and common radius 1. For these spheres, we define our ideal of common tangent lines, with p_{23} set to 1. We compute a Gröbner (standard) basis of I and compute the dimension and degree (multiplicity) of I. Adapting the convention in [49], we use comment lines starting with // to display the output of a SINGULAR computation.

```
ideal I1 = tangenteq(0,0,0,1);
ideal I2 = tangenteq(1,-2,3,1);
ideal I3 = tangenteq(1,0,1,1);
```

```
ideal I4 = tangenteq(0,-1,0,1);
ideal IPlu = p01*1 - p02*p13 + p03*p12; // Pluecker relation

ideal I = std(I1 + I2 + I3 + I4 + IPlu);
dim(I), mult(I);
// 1 4
```

The variety $\mathcal{V}(I)$ contains a one-dimensional excess component, whose radical ideal is generated by the polynomials in (4.9).

```
// exceptional divisor of I
ideal IE = p01, p02, p03, p12^2 + p13^2 + 1;
```

Let $f_1, \ldots, f_4$ denote these polynomials. Since $f_1, \ldots, f_4$ form a regular sequence, the blow-up ideal is generated by the polynomials

$$v_i f_j - v_j f_i, \quad 1 \le i < j \le 4, \tag{4.11}$$

where $v_1, \ldots, v_4$ denote new variables (see [55, p. 12]; for the non-regular case see [124]). This construction naturally generalizes the blow-up with respect to a single point in Section 4.2.1. The following procedure computes the blow-up for any regular sequence $f_1, \ldots, f_k$ of polynomials. In this procedure, the parameter I denotes the list of polynomials of the excess component, and *NewVars* denotes the corresponding list of new variables.

```
proc computeblowup(ideal I, ideal NewVars)
{
  int i, j;
  ideal A, B;

  for (i = 1; i <= size(I); i++) {
    for (j = 1; j <= size(NewVars); j++) {
      if (i != j) {
        B = I[i] * NewVars[j] - I[j] * NewVars[i];
        A = A + B;
      }
    }
  }
  return(A);
}
```

We extend the polynomial ring R by adjoining new variables t_{01}, t_{02}, t_{03}, q to the ring R. Since we will work in the coordinate patch where $t_{03} \ne 0$, we can set $t_{03} = 1$. We compute the blow-up ideal which has dimension 5 and degree 6.

```
ring S = 0, (p01,p02,p03,p12,p13,t01,t02,q), (dp);
ideal NewVars1 = t01, t02, 1, q;
ideal BlowUp1 = computeblowup(imap(R,IE), NewVars1);
// 5 6
```

Taking the union of the generators of the blow-up ideal and the generators of I_k, we obtain an ideal whose variety corresponds to the one illustrated in Figure 4.4(b). In order to remove the exceptional divisor, we compute the ideal quotient of the ideal in the larger space divided by the exceptional divisor. The resulting ideal J_k is called the *proper transform* of I_k. Here, the proper transform is an ideal in $\mathbb{C}[p_{01}, p_{02}, p_{03}, p_{12}, p_{13}, t_{01}, t_{02}, q]$. We compute the ideal of the proper transforms and see that there is still a one-dimensional excess component of degree 4.

```
// compute equations after the blow-up
ideal J1 = std(quotient(BlowUp1 + imap(R,I1), imap(R,IE)));
ideal J2 = std(quotient(BlowUp1 + imap(R,I2), imap(R,IE)));
ideal J3 = std(quotient(BlowUp1 + imap(R,I3), imap(R,IE)));
ideal J4 = std(quotient(BlowUp1 + imap(R,I4), imap(R,IE)));
ideal JPlu = std(quotient(BlowUp1 + imap(R,IPlu), imap(R,IE)));
ideal J = std(J1 + J2 + J3 + J4 + JPlu);
dim(J), mult(J);
// 1 4
```

In order to explain this observation, we analyze the blow-up by hand. In the coordinate patch $t_{03} \neq 0$, we can set $t_{03} = 1$. Hence, the blow-up equations (4.11) yield $p_{01} = p_{03}t_{01}$, $p_{02} = p_{03}t_{02}$, and $p_{12}^2 + p_{13}^2 + 1 = p_{03}q$. The tangent equation (2.5) after the blow-up results in

$$
\begin{aligned}
0 \;&=\; p^T \wedge^2 Q \; p \\
&=\; p_{03} \cdot \left[(t_{01}, t_{02}, 1) \begin{pmatrix} c_2^2 + c_3^2 - r^2 & -c_1 c_2 & -c_1 c_3 \\ -c_1 c_2 & c_1^2 + c_3^2 - r^2 & -c_2 c_3 \\ -c_1 c_3 & -c_2 c_3 & c_1^2 + c_2^2 - r^2 \end{pmatrix} \begin{pmatrix} p_{01} \\ p_{02} \\ p_{03} \end{pmatrix} + \alpha + q \right]
\end{aligned}
$$

with

$$
\alpha := 2 \, (t_{01}, t_{02}, 1) \begin{pmatrix} c_2 & c_3 & 0 \\ -c_1 & 0 & c_3 \\ 0 & -c_1 & -c_2 \end{pmatrix} \begin{pmatrix} p_{12} \\ p_{13} \\ 1 \end{pmatrix} .
$$

The factor p_{03} describes the exceptional divisor, which we want to remove. Let V_E denote the affine variety satisfying (4.9) as well as $p_{23} = 1$. For elements in $V_E \times \mathbb{R}^4$, the tangent equation after the blow-up simplifies to

$$
\alpha + q \;=\; 0 \,. \tag{4.12}
$$

The equation of the Plücker relation (2.2) after the blow-up results in

$$p_{03} \cdot (t_{01} - t_{02}p_{13} + p_{12}) = 0 .$$

Hence, the proper transform of the Plücker equation is given by

$$t_{01} - t_{02}p_{13} + p_{12} = 0 . \tag{4.13}$$

Now we can state the excess component of the proper transforms.

Lemma 4.3. *Let* $(p_{01}, p_{02}, p_{03}, p_{12}, p_{13}, 1)^T \in V_E$ *and* $(t_{01}, t_{02}, 1, q)^T \in \mathbb{R}^4$. *If* $q = 0$ *and the matrix*

$$\begin{pmatrix} p_{12} & p_{13} & 1 \\ 1 & -t_{02} & t_{01} \end{pmatrix} \tag{4.14}$$

has rank 1 then for any center $c = (c_1, c_2, c_3)^T$ *and any radius* r *the equations* (4.12) *and* (4.13) *are satisfied.*

Proof. First we consider the tangent equation (4.12). Expanding the expression α yields

$$-c_1(p_{12}t_{02} + p_{13}) + c_2(p_{12}t_{01} - 1) + c_3(p_{13}t_{01} + t_{02}) .$$

Hence, if the matrix (4.14) has rank 1 then all its 2×2-subdeterminants vanish, and consequently $\alpha = 0$. In conjunction with $q = 0$, we see that (4.12) is satisfied.

The ideal described by the vanishing of the 2×2-subdeterminants is generated by $g_1 := p_{12}t_{02} + p_{13}$ and $g_2 := p_{12}t_{01} - 1$. To see this, just observe that $g_3 := p_{13}t_{01} + t_{02}$ can be expressed by $g_3 = -t_{01}g_1 + t_{02}g_2$.

In order to see that (4.13) is satisfied, observe that the left-hand side of (4.13) is contained in the ideal generated by g_1, g_2 and q,

$$t_{01} - t_{02}p_{13} + p_{12} = -p_{12}g_2 - p_{13}g_3 + t_{01}q .$$

Hence, if the matrix (4.14) has rank 1 and $q = 0$ then this expression evaluates to zero. $\square$

We implement the second blow-up. The variety of the following radical ideal J_E is the new exceptional divisor.

```
ideal JE = p01, p02, p03, p12^2 + p13^2 + 1, q, p12*t02 + p13,
  p12*t01 - 1;
```

We define a ring extension, creating new variables $u_{01}, u_{02}, u_{03}, u_{04}, v, w_1, w_2$ for the polynomials defining the excess component. One of the new auxiliary variable has to be fixed, since we work locally in one patch. Thus we set $u_{03} = 1$. Since the generators of J_E form a regular sequence, we can use our procedure to compute the blow-up ideal. The dimension of that ideal is 8, and its degree is 26.

```
ring T = 0, (p01,p02,p03,p12,p13,t01,t02,q,u01,u02,u04,v,w1,w2), (dp);

ideal NewVars2 = u01, u02, 1, u04, v, w1, w2;
ideal BlowUp2 = std(computeblowup(imap(S,JE), NewVars2));
dim(BlowUp2), mult(BlowUp2);
// 8 26
```

Now we compute the proper transforms of the second blow-up.

```
ideal K1 = std(quotient(BlowUp2 + imap(S,J1), imap(S,JE)));
ideal K2 = std(quotient(BlowUp2 + imap(S,J2), imap(S,JE)));
ideal K3 = std(quotient(BlowUp2 + imap(S,J3), imap(S,JE)));
ideal K4 = std(quotient(BlowUp2 + imap(S,J4), imap(S,JE)));
ideal KPlu = std(quotient(BlowUp2 + imap(S,JPlu), imap(S,JE)));

ideal K = std(quotient(K1 + K2 + K3 + K4 + KPlu, imap(S,JE)));
dim(K), mult(K);
// 0 12
```

We see that after this second blow-up the ideal has become zero-dimensional. The degree of 12 corresponds to the 12 solutions in Section 3.1.

5. TANGENT PROBLEMS TO QUADRICS IN N-DIMENSIONAL SPACE

We consider the natural (real) enumerative generalization of the tangent problem to spheres and quadrics to n-dimensional space.

In Section 5.1, we discuss the common tangents to $2n-2$ spheres in $\mathbb{R}^n$. The main result of this section can be stated as follows.

Theorem 5.1. *Suppose $n \geq 3$.*

(a) Let $c_1, \ldots, c_{2n-2} \in \mathbb{R}^n$ affinely span $\mathbb{R}^n$, and let $r_1, \ldots, r_{2n-2} > 0$. If the $2n-2$ spheres with centers c_i and radii r_i have only a finite number of common tangent lines in $\mathbb{C}^3$, then that number is bounded by $3 \cdot 2^{n-1}$.

(b) There exists a configuration with $3 \cdot 2^{n-1}$ different real common tangent lines. Moreover, this configuration can be achieved with unit spheres.

We also discuss configurations of spheres whose centers have affine dimension less than n. In particular, we show that there are configurations of such spheres having $3 \cdot 2^{n-1}$ *complex* common tangents; thus, the upper bound of Theorem 5.1 also holds for spheres in this special position.

In Section 5.2 we prove the following result on the lines tangent to $2n-2$ quadrics in $\mathbb{P}^n$.

Theorem 5.2. *Given $2n-2$ general quadratic hypersurfaces in $\mathbb{P}^n$ there are*

$$d_n \ := \ 2^{2n-2} \cdot \frac{1}{n} \binom{2n-2}{n-1}$$

complex lines that are simultaneously tangent to all $2n-2$ hypersurfaces ($n \geq 2$). Furthermore, there is a choice of quadratic hypersurfaces in $\mathbb{R}^n$ for which all the lines are real and lie in affine space $\mathbb{R}^n$.

Table 5.1 exhibits the amazingly large difference between the number of (real) tangent lines for spheres and the number of (real) tangent lines for general quadrics.

We also discuss the case of $2n-2$ quadrics in $\mathbb{P}^n$ when the quadrics all contain the same (smooth) quadric in a given hyperplane.

In Section 5.3, we discuss the problem of finding minimal circumscribing cylinders of a given simplex with vertices $c_1, c_2, \ldots, c_{n+1}$ in $\mathbb{R}^n$. This problem is equivalent to finding

n	3	4	5	6	7	8	9
$3 \cdot 2^{n-1}$	12	24	48	96	192	384	768
d_n	32	320	3584	43008	540672	7028736	93716480

Tab. 5.1: Maximum number of tangents to $2n-2$ spheres in $\mathbb{R}^n$ and to $2n-2$ quadrics in $\mathbb{P}^n$

the smallest radius r such that the spheres $S(c_1, r), \ldots, S(c_{n+1}, r)$ have a real common tangent line. Using the framework of Section 5.1, we provide bounds on the number of local extrema. Moreover, for regular simplices we prove structural results for the direction vectors of any locally extreme circumscribing cylinder.

5.1   Common tangents to $2n-2$ spheres in $\mathbb{R}^n$

In this section we prove Theorem 5.1. First, in Section 5.1.1, we prove part (a) of that Theorem. Then, in Section 5.1.2, we prove part (b) by explicitly describing configurations with $3 \cdot 2^{n-1}$ common real tangents.

In Section 5.1.3, we discuss configurations of spheres whose centers do not affinely span $\mathbb{R}^n$.

5.1.1   Polynomial formulation for centers affinely spanning $\mathbb{R}^n$

Analogous to Section 3.1, we represent a line in $\mathbb{C}^n$ by a point $p \in \mathbb{C}^n$ and a direction vector $v \in \mathbb{P}^{n-1}$. (For notational convenience we typically work with a representative of the direction vector in $\mathbb{C}^n \setminus \{0\}$.) If $v^2 \neq 0$ we can make p unique by requiring that $p \cdot v = 0$.

First note that for $v^2 \neq 0$, the tangent condition (3.1) of a line (p, v) to a sphere with center c and radius r also holds in general dimension n,

$$v^2 p^2 - 2v^2 p \cdot c + v^2 c^2 - (v \cdot c)^2 - r^2 v^2 \; = \; 0 \,. \tag{5.1}$$

To prove part (a) of Theorem 5.1, let $c_1, \ldots, c_{2n-2} \in \mathbb{R}^n$ contain $n+1$ affinely independent points and let $r_1, \ldots, r_{2n-2} > 0$. We can choose c_{2n-2} to be the origin and set $r := r_{2n-2}$. Then the remaining centers span $\mathbb{R}^n$. Subtracting the equation for the sphere centered at the origin from the equations for the spheres $1, \ldots, 2n-3$ gives the system

$$
\begin{aligned}
p \cdot v \; &= \; 0 \,, \\
p^2 \; &= \; r^2 \,, \quad \text{and} \\
2v^2 p \cdot c_i \; &= \; v^2 c_i^2 - (v \cdot c_i)^2 - v^2 (r_i^2 - r^2) \,, \qquad i = 1, 2, \ldots, 2n-3 \,.
\end{aligned}
\tag{5.2}
$$

Remark 5.3. In generalization of Remark 3.3 for the three-dimensional case, this system of equations does not have a solution with $v^2 = 0$. Namely, if we had $v^2 = 0$, then $v \cdot c_i = 0$

for all $i \in \{1, \dots, 2n-3\}$. Since the centers span $\mathbb{R}^n$, this would imply $v = 0$, contradicting $v \in \mathbb{P}^{n-1}$. This validates our assumption that $v^2 \neq 0$ prior to (5.1).

Since $n \geq 3$, the bottom line of (5.2) contains at least n equations. We can assume that $c_1, \dots, c_n$ are linearly independent. Then the matrix $M := (c_1, \dots, c_n)^T$ is invertible, and we can solve the equations with indices $1, \dots, n$ for p:

$$p \;=\; \frac{1}{2v^2} M^{-1} \begin{pmatrix} v^2 c_1^2 - (v \cdot c_1)^2 - v^2(r_1^2 - r^2) \\ \vdots \\ v^2 c_n^2 - (v \cdot c_n)^2 - v^2(r_n^2 - r^2) \end{pmatrix}. \tag{5.3}$$

Now substitute this expression for p into the first and second equation of the system (5.2), as well as into the equations for $i = n+1, \dots, 2n-3$, and then clear the denominators. This gives $n-1$ homogeneous equations in the coordinate v, namely one cubic, one quartic, and $n-3$ quadrics. By Bézout's Theorem, this means that if the system has only finitely many solutions, then the number of solutions is bounded by $3 \cdot 4 \cdot 2^{n-3} = 3 \cdot 2^{n-1}$, for $n \geq 3$. For small values of n, these values are shown in Table 5.1. The values for $n = 4, 5, 6$ were computed experimentally in [129].

We simplify the cubic equation obtained by substituting (5.3) into the equation $p \cdot v = 0$ by expressing it in the basis $c_1, \dots, c_n$. Let the representation of v in the basis $c_1, \dots, c_n$ be

$$v \;=\; \sum_{i=1}^{n} t_i c_i$$

with homogeneous coordinates $t_1, \dots, t_n$. Further, let $c_1', \dots, c_n'$ be a dual basis to $c_1, \dots, c_n$; i.e., let $c_1', \dots, c_n'$ be defined by $c_i' \cdot c_j = \delta_{ij}$, where δ_{ij} denotes Kronecker's delta function. By elementary linear algebra, we have $t_i = c_i' \cdot v$.

When expressing p in this dual basis, $p = \sum p_i' c_i'$, the third equation of (5.2) gives

$$p_i' \;=\; \frac{1}{v^2} \left(v^2 c_i^2 - (v \cdot c_i)^2 - v^2(r_i^2 - r^2) \right).$$

Substituting this representation of p into the equation

$$0 \;=\; 2v^2(p \cdot v) \;=\; 2v^2 \left(\sum_{i=1}^{n} p_i' c_i' \right) \cdot v \;=\; 2v^2 \sum_{i=1}^{n} p_i' t_i \,,$$

we obtain the cubic equation

$$\sum_{i=1}^{n} (v^2 c_i^2 - (v \cdot c_i)^2 - v^2(r_i^2 - r^2)) t_i \;=\; 0 \,.$$

In the case that all radii are equal, expressing v in terms of the t-variables yields

$$\sum_{1 \leq i \neq j \leq n} \alpha_{ij} t_i^2 t_j + \sum_{1 \leq i < j < k \leq n} 2\beta_{ijk} t_i t_j t_k \;=\; 0 \,, \tag{5.4}$$

where

$$
\begin{aligned}
\alpha_{ij} &= \left(\operatorname{vol}_2(c_i, c_j)\right)^2 = \det\begin{pmatrix} c_i \cdot c_i & c_i \cdot c_j \\ c_j \cdot c_i & c_j \cdot c_j \end{pmatrix}, \\
\beta_{ijk} &= \det\begin{pmatrix} c_i \cdot c_j & c_i \cdot c_k \\ c_k \cdot c_j & c_k \cdot c_k \end{pmatrix} + \det\begin{pmatrix} c_i \cdot c_k & c_i \cdot c_j \\ c_j \cdot c_k & c_j \cdot c_j \end{pmatrix} \\
&\quad + \det\begin{pmatrix} c_j \cdot c_k & c_j \cdot c_i \\ c_i \cdot c_k & c_i \cdot c_i \end{pmatrix},
\end{aligned}
$$

and $\operatorname{vol}_2(c_i, c_j)$ denotes the oriented area of the parallelogram spanned by c_i and c_j. In particular, if $0c_1 \ldots c_n$ constitutes a regular simplex in $\mathbb{R}^n$, then we obtain the following characterization.

Theorem 5.4. *Let $n \geq 3$. If $0c_1 \ldots c_n$ is a regular simplex and all spheres have the same radius, then the cubic equation expressed in the basis $c_1, \ldots, c_n$ is equivalent to*

$$
\sum_{1 \leq i \neq j \leq n} t_i^2 t_j + 2 \sum_{1 \leq i < j < k \leq n} t_i t_j t_k = 0. \tag{5.5}
$$

For $n = 3$, this cubic equation factors into three linear terms; for $n \geq 4$ it is irreducible.

Proof. Let e denote the edge length of the regular simplex. Then the form of the cubic equation follows from computing $\alpha_{ij} = e^2(1 \cdot 1 - 1/2 \cdot 1/2) = 3e^2/4$, $\beta_{ijk} = 3e^2(1/2 \cdot 1 - 1/2 \cdot 1/2) = 3e^2/4$.

As discussed in Section 3.2, for $n = 3$ the cubic polynomial factors into $(t_1 + t_2)(t_1 + t_3)(t_2 + t_3)$. For $n \geq 4$, assume that there exists a factorization of the form

$$
\left(t_1 + \sum_{i=2}^{n} \rho_i t_i\right)\left(\sum_{1 \leq i \leq j \leq n} \sigma_{ij} t_i t_j\right)
$$

with $\sigma_{12} = 1$. Since (5.5) does not contain a monomial t_i^3, we have either $\rho_i = 0$ or $\sigma_{ii} = 0$ for $1 \leq i \leq n$.

If there were more than one vanishing coefficient ρ_i, say $\rho_i = \rho_j = 0$, then the monomials $t_i^2 t_j$ could not be generated. So only two cases have to be investigated.

Case 1: $\rho_i \neq 0$ for $2 \leq i \leq n$. Then $\sigma_{ii} = 0$ for $1 \leq i \leq n$. Furthermore, $\sigma_{ij} = 1$ for $i \neq j$ and $\rho_i = 1$ for all i. Hence, the coefficient of the monomial $t_1 t_2 t_3$ is 3, which contradicts (5.5).

Case 2: There exists exactly one coefficient $\rho_i = 0$, say, $\rho_4 = 0$. Then $\sigma_{11} = \sigma_{22} = \sigma_{33} = 0$, $\sigma_{44} = 1$. Further, $\sigma_{ij} = 1$ for $1 \leq i < j \leq 3$ and $\rho_i = 1$ for $1 \leq i \leq 3$. Hence, the coefficient of the monomial $t_1 t_2 t_3$ is 3, which is again a contradiction. $\qquad\square$

5.1.2 Real lines

In Section 5.1.1, we have given the upper bound of $3 \cdot 2^{n-1}$ for the number of complex solutions to the tangent problem. Now we complement this result by providing a class of configurations leading to $3 \cdot 2^{n-1}$ real common tangents. Hence, the upper bound is tight, and is achieved by real tangents.

Our construction is based on the following geometric idea. For four spheres with radius r in $\mathbb{R}^3$ centered at the vertices $(1,1,1)^T$, $(1,-1,-1)^T$, $(-1,1,-1)^T$, $(-1,-1,1)^T$ of a regular tetrahedron, Lemma 3.8 implies that there are

- 3 different real tangents (of multiplicity 4) for radius $r = \sqrt{2}$;

- 12 different real tangents for $\sqrt{2} < r < 3/2$;

- 6 different real tangents (of multiplicity 2) for $r = 3/2$.

Furthermore, from the explicit calculations in Section 3.2.2, it can be easily seen that the symmetry group of the tetrahedron acts transitively on the tangents. By this symmetry argument, all 12 tangents have the same distance d from the origin. In order to construct a configuration of spheres with many common tangents, say, in $\mathbb{R}^4$, we embed the centers via

$$(x_1, x_2, x_3)^T \;\longmapsto\; (x_1, x_2, x_3, 0)^T$$

into $\mathbb{R}^4$ and place additional spheres with radius r at $(0,0,0,a)^T$ and $(0,0,0,-a)^T$ for some appropriate value of a. If a is chosen in such a way that the centers of the two additional spheres have distance r from the above tangents, then, intuitively, all common tangents to the six four-dimensional spheres are located in the hyperplane $x_4 = 0$ and have multiplicity 2 (because of the two different possibilities of signs when perturbing the situation). By perturbing this configuration slightly, the tangents are no longer located in the hyperplane $x_4 = 0$, and therefore the double tangents are forced to split. The idea also generalizes to dimension $n \geq 5$.

Formally, suppose that the $2n-2$ spheres in $\mathbb{R}^n$ all have the same radius, r, and the first four have centers

$$
\begin{aligned}
c_1 &:= (1,1,1,\ 0,\dots,0)^T, \\
c_2 &:= (1,-1,-1,\ 0,\dots,0)^T, \\
c_3 &:= (-1,1,-1,\ 0,\dots,0)^T, \quad \text{and} \\
c_4 &:= (-1,-1,1,\ 0,\dots,0)^T
\end{aligned}
$$

at the vertices of a regular tetrahedron inscribed in the 3-cube $(\pm 1, \pm 1, \pm 1, 0, \dots, 0)^T$. We place the subsequent centers at the points $\pm a e_j$ for $j = 4, 5, \dots, n$, where $e_1, \dots, e_n$ are the standard unit vectors in $\mathbb{R}^n$.

Theorem 5.5. *Let $n \geq 4$, $r > 0$, $a > 0$, and $\gamma := a^2(n-1)/(a^2 + n - 3)$. If*

$$(r^2 - 3)(3 - \gamma)(a^2 - 2)(r^2 - \gamma)\left((3 - \gamma)^2 + 4\gamma - 4r^2\right) \;\neq\; 0\,, \qquad (5.6)$$

then there are exactly $3 \cdot 2^{n-1}$ different lines tangent to the $2n-2$ spheres. If

$$a^2 > 2, \quad \gamma < 3, \quad and \quad \gamma \;<\; r^2 \;<\; \gamma + \tfrac{1}{4}\left(3 - \gamma\right)^2\,, \qquad (5.7)$$

then all these $3 \cdot 2^{n-1}$ lines are real. Furthermore, this system of inequalities defines a nonempty subset of the (a, r)-plane.

Given values of a and r satisfying (5.7), we may scale the centers and parameters by $1/r$ to obtain a configuration with unit spheres, proving Theorem 5.1(b).

Remark 5.6. The set of values of a and r which give all solutions real is nonempty. To show this, we calculate

$$\gamma \;=\; \frac{a^2(n-1)}{a^2 + n - 3} \;=\; (n-1)\left(1 - \frac{n-3}{a^2 + n - 3}\right)\,, \qquad (5.8)$$

which implies that γ is an increasing function of a^2. Similarly, set $\delta := \gamma + (3 - \gamma)^2/4$, the upper bound for r^2. Then

$$\frac{d}{d\gamma}\,\delta \;=\; \frac{d}{d\gamma}\left(\frac{\gamma + (3 - \gamma)^2}{4}\right)p \;=\; 1 + \frac{\gamma - 3}{2}\,,$$

and so δ is an increasing function of γ when $\gamma > 1$. When $a^2 = 2$, we have $\gamma = 2$; so δ is an increasing function of a in the region $a^2 > 2$. Since when $a = \sqrt{2}$, we have $\delta = \frac{9}{4} > \gamma$, the region defined by (5.7) is nonempty.

Moreover, we remark that the region is qualitatively different in the cases $n = 4$ and $n \geq 5$. For $n = 4$, γ satisfies $\gamma < 3$ for any $a > \sqrt{2}$. Hence, $\delta < 3$ and $r < \sqrt{3}$. Thus the maximum value of 24 real lines may be obtained for arbitrarily large a. In particular, we may choose the two spheres with centers $\pm ae_4$ disjoint from the first four spheres. Note, however, that the first four spheres do meet, since we have $\sqrt{2} < r < \sqrt{3}$.

For $n \geq 5$, there is an upper bound to a. The upper and lower bounds for r^2 coincide when $\gamma = 3$; so we always have $r^2 < 3$. Solving $\gamma = 3$ for a^2, we obtain $a^2 < 3(n-3)/(n-4)$. When $n = 5$, Figure 5.1 displays the discriminant locus (defined by (5.6)) and shades the region consisting of values of a and r for which all solutions are real.

Proof of Theorem 5.5. We prove Theorem 5.5 by treating a and r as parameters and explicitly solving the resulting system of polynomials in the coordinates $(p, v) \in \mathbb{C}^n \times \mathbb{P}^{n-1}$ for lines in $\mathbb{C}^n$. This shows that there are $3 \cdot 2^{n-1}$ *complex* lines tangent to the given spheres, for the values of the parameters (a, r) given in Theorem 5.5. The inequalities (5.7) describe the parameters for which all solutions are real.
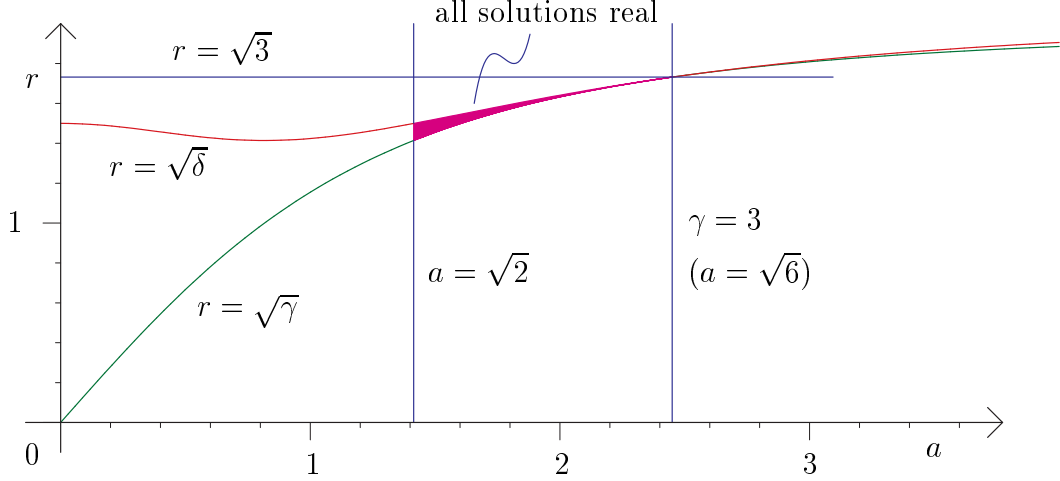
Fig. 5.1: Discriminant locus and values of a, r giving all solutions real

First consider the equations (5.1) for the line to be tangent to the spheres with centers $\pm a e_j$ and radius r:

$$v^2 p^2 - 2av^2 p_j + a^2 v^2 - a^2 v_j^2 - r^2 v^2 \; = \; 0\,,$$
$$v^2 p^2 + 2av^2 p_j + a^2 v^2 - a^2 v_j^2 - r^2 v^2 \; = \; 0\,.$$

Taking their sum and difference (and using $av^2 \neq 0$), we obtain

$$p_j \;=\; 0\,, \qquad\qquad 4 \leq j \leq n\,, \tag{5.9}$$
$$a^2 v_j^2 \;=\; (p^2 + a^2 - r^2)v^2\,, \qquad 4 \leq j \leq n\,. \tag{5.10}$$

Subtracting the equations (5.1) for the centers $c_1, \ldots, c_4$ pairwise gives

$$4v^2(p_2 + p_3) \;=\; -4(v_1 v_3 + v_1 v_2)$$

(for indices 1,2) and analogous equations. Hence,

$$p_1 \;=\; -\frac{v_2 v_3}{v^2}\,, \qquad p_2 \;=\; -\frac{v_1 v_3}{v^2}\,, \qquad p_3 \;=\; -\frac{v_1 v_2}{v^2}\,.$$

Further, $p \cdot v = 0$ implies $v_1 v_2 v_3 = 0$. Thus we have three symmetric cases. We treat one, assuming that $v_1 = 0$. Then we obtain

$$p_1 \;=\; -\frac{v_2 v_3}{v^2}\,, \qquad p_2 = p_3 = 0\,.$$

Hence, the tangent equation (5.1) for the first sphere becomes

$$v^2 p_1^2 - 2v^2 p_1 + 3v^2 - (v_2 + v_3)^2 - r^2 v^2 \;=\; 0\,.$$

Using $0 = v^2 p_1 + v_2 v_3$, we obtain

$$v_2^2 + v_3^2 \;=\; v^2 (p_1^2 + 3 - r^2) \,. \tag{5.11}$$

The case $j = 4$ of (5.10) gives $a^2 v_4^2 = v^2 (p_1^2 + a^2 - r^2)$, since $p_2 = p_3 = 0$. Combining these, we obtain

$$v_2^2 + v_3^2 \;=\; a^2 v_4^2 + v^2 (3 - a^2) \,.$$

Using $v^2 = v_2^2 + v_3^2 + (n-3) v_4^2$ yields

$$(a^2 - 2)(v_2^2 + v_3^2) \;=\; v_4^2 (3(a^2 + n - 3) - a^2 (n - 1)) \,.$$

We obtain

$$(a^2 - 2)(v_2^2 + v_3^2) \;=\; v_4^2 (a^2 + n - 3)(3 - \gamma) \,, \tag{5.12}$$

where $\gamma = a^2 (n-1)/(a^2 + n - 3)$.

Note that $a^2 + n - 3 > 0$ since $n > 3$. If neither $3 - \gamma$ nor $a^2 - 2$ are zero, then we may use this to compute

$$\begin{aligned}
(a^2 + n - 3)(3 - \gamma) v^2 \;&=\; \big((a^2 + n - 3)(3 - \gamma) + (n - 3)(a^2 - 2)\big)\left(v_2^2 + v_3^2\right) \\
&=\; (a^2 + n - 3)(v_2^2 + v_3^2) \,,
\end{aligned}$$

and so

$$(3 - \gamma) v^2 \;=\; v_2^2 + v_3^2 \,. \tag{5.13}$$

Substituting (5.13) into (5.11) and dividing by v^2 gives

$$p_1^2 \;=\; r^2 - \gamma \,. \tag{5.14}$$

Combining this with $v^2 p_1 + v_2 v_3 = 0$, we obtain

$$p_1 (v_2^2 + v_3^2) + (3 - \gamma) v_2 v_3 \;=\; 0 \,. \tag{5.15}$$

Summarizing, we have n linear equations

$$v_1 \;=\; p_2 \;=\; p_3 \;=\; p_4 \;=\; \cdots \;=\; p_n \;=\; 0 \,,$$

and $n - 4$ simple quadratic equations

$$v_4^2 \;=\; v_5^2 \;=\; \cdots \;=\; v_n^2 \,,$$

and the three more complicated quadratic equations, (5.12), (5.14), and (5.15).

We now solve these last three equations. We solve (5.14) for p_1, obtaining

$$p_1 \;=\; \pm \sqrt{r^2 - \gamma} \,.$$

Then we solve (5.15) for v_2 and use (5.14), obtaining

$$v_2 \ = \ -\frac{3 - \gamma \pm \sqrt{(3-\gamma)^2 - 4(r^2 - \gamma)}}{2p_1}\, v_3\,.$$

Finally, (5.12) gives

$$v_4\sqrt{a^2 + n - 3} \ = \ \pm\sqrt{\frac{a^2 - 2}{3 - \gamma}(v_2^2 + v_3^2)}\,.$$

Since $v_3 = 0$ would imply $v = 0$ and hence contradict $v \in \mathbb{P}^{n-1}$, we see that $v_3 \neq 0$. Thus we can conclude that when none of the following expressions

$$r^2 - 3\,, \quad 3 - \gamma\,, \quad a^2 - 2\,, \quad r^2 - \gamma\,, \quad (3 - \gamma)^2 + 4\gamma - 4r^2$$

vanish, there are $8 = 2^3$ different solutions to the last 3 equations. For each of these, the simple quadratic equations give 2^{n-4} solutions; so we see that the case $v_1 = 0$ contributes 2^{n-1} different solutions, each of them satisfying $v_2 \neq 0$, $v_3 \neq 0$. Since there are three symmetric cases, we obtain $3 \cdot 2^{n-1}$ solutions in all, as claimed.

We complete the proof of Theorem 5.5 and determine which values of the parameters a and r give all these lines real. We see that

(1) p_1 is real if $r^2 - \gamma > 0$.

(2) Given that p_1 is real, v_2/v_3 is real if $(3 - \gamma)^2 + 4\gamma - 4r^2 > 0$.

(3) Given this, v_4/v_3 is real if $(a^2 - 2)/(3 - \gamma) > 0$.

Suppose the three inequalities above are satisfied. Then all solutions are real, and (5.13) implies that $3 - \gamma > 0$, and so we also have $a^2 - 2 > 0$. This completes the proof of Theorem 5.5. $\qquad\square$

5.1.3   The lower-dimensional case

In our derivation of the Bézout number $3 \cdot 2^{n-1}$ of common tangents for Theorem 5.1, it was crucial that the centers of the spheres affinely spanned $\mathbb{R}^n$. Also, the construction in Section 5.1.2 of configurations with $3 \cdot 2^{n-1}$ real common tangents had centers affinely spanning $\mathbb{R}^n$. When the centers do not affinely span $\mathbb{R}^n$, we prove the following result.

Theorem 5.7. *For $n \geq 4$, there are $3 \cdot 2^{n-1}$ complex common tangent lines to $2n-2$ spheres whose centers have affine dimension less than n, but otherwise general. There is a choice of unit spheres whose centers have affine dimension less than n and 2^n real common tangent lines.*

Remark 5.8. Theorem 5.7 extends the results of Section 3.2.1, which say that when $n = 3$, there are 12 complex common tangents. Megyesi [93] has shown that there is a configuration of four spheres in $\mathbb{R}^3$ with affinely dependent centers and 12 real common tangents, but that the number of tangents is bounded by 8 for the case of unit spheres.

For $n \geq 4$, we are unable either to find a configuration of unit spheres whose centers do not affinely span $\mathbb{R}^n$ having more than 2^n real common tangents, or to show that the maximum number of real common tangents is less than $3 \cdot 2^{n-1}$. Similar to the case $n = 3$, it might be possible that the case of unit spheres and the case of spheres with general radii might give different maximum numbers. Megyesi [94] showed that there are $2n-2$ spheres whose centers have affine dimension less than n having all $3 \cdot 2^{n-1}$ common tangents real. Furthermore, all but one of the spheres in his construction have equal radii.

By Theorem 5.1, $3 \cdot 2^{n-1}$ is the upper bound for the number of complex common tangents to spheres whose centers do not affinely span $\mathbb{R}^n$. Indeed, if there were a configuration with more common tangents, then—since the system is a complete intersection—perturbing the centers would give a configuration whose centers affinely span $\mathbb{R}^n$ and more common tangent lines than allowed by Theorem 5.1.

By this discussion, to prove Theorem 5.7 it suffices to give $2n-2$ spheres, whose centers have affine dimension less than n, having $3 \cdot 2^{n-1}$ complex common tangents and also such a configuration of $2n-2$ unit spheres with 2^n real common tangents. For this, we use spheres with equal radii whose centers are the vertices of a perturbed cross polytope in a hyperplane. We work with the notation of Sections 5.1.1 and 5.1.2.

Let $a \neq -1$ and suppose we have spheres with equal radii r and centers at the points

$$ae_2, \quad -e_2, \quad \text{and} \quad \pm e_j, \quad \text{for } 3 \leq j \leq n \,.$$

Then we have the equations

$$p \cdot v = 0 \,, \tag{5.16}$$
$$f := v^2(p^2 - 2ap_2 + a^2 - r^2) - a^2v_2^2 = 0 \,, \tag{5.17}$$
$$g := v^2(p^2 + 2p_2 + 1 - r^2) - v_2^2 = 0 \,, \tag{5.18}$$
$$v^2(p^2 \pm 2p_j + 1 - r^2) - v_j^2 = 0 \,, \qquad 3 \leq j \leq n \,. \tag{5.19}$$

As in Section 5.1.2, the sum and difference of the equations (5.19) for the spheres with centers $\pm e_j$ give

$$p_j = 0 \,,$$
$$v^2(p^2 + 1 - r^2) = v_j^2 \,. \qquad 3 \leq j \leq n \,.$$

Thus we have the equations

$$p_3 = p_4 = \cdots = p_n = 0 \,,$$
$$v_3^2 = v_4^2 = \cdots = v_n^2 \,. \tag{5.20}$$

Similarly, we have

$$
\begin{aligned}
f + ag &= (1+a)\left(v^2(p^2 - r^2 + a) - av_2^2\right) = 0\,, \\
f - a^2 g &= (1+a)v^2\left((1-a)(p^2 - r^2) + 2ap_2\right) = 0\,.
\end{aligned}
$$

As before, $v^2 \neq 0$: If $v^2 = 0$, then (5.18) and (5.19) imply that $v_2 = \cdots = v_n = 0$. With $v^2 = 0$, this implies that $v_1 = 0$ and hence $v = 0$, contradicting $v \in \mathbb{P}^{n-1}$. By (5.20), we have $p^2 = p_1^2 + p_2^2$, and so we obtain the system of equations in the variables p_1, p_2, v_1, v_2, v_3:

$$
\begin{aligned}
p_1 v_1 + p_2 v_2 &= 0\,, \\
(1-a)(p_1^2 + p_2^2 - r^2) + 2ap_2 &= 0\,, \\
v^2(p_1^2 + p_2^2 - r^2 + a) - av_2^2 &= 0\,, \\
v^2(p_1^2 + p_2^2 - r^2 + 1) - v_3^2 &= 0\,.
\end{aligned}
\tag{5.21}
$$

(For notational sanity, we do not yet make the substitution $v^2 = v_1^2 + v_2^2 + (n-2)v_3^2$.)

We assume that $a \neq 1$ and will treat the case $a = 1$ at the end of this section. Using the second equation of (5.21) to cancel the terms $v^2(p_1^2 + p_2^2)$ from the third equation and dividing the result by a, we can solve for p_2:

$$
p_2 = \frac{(1-a)(v^2 - v_2^2)}{2v^2}\,.
$$

If we substitute this into the first equation of (5.21), we may solve for p_1:

$$
p_1 = -\frac{(1-a)(v^2 - v_2^2)v_2}{2v^2 v_1}\,.
$$

Substitute these into the second equation of (5.21), clear the denominator $(4v_1^2 v^4)$, and remove the common factor $(1-a)$ to obtain the sextic

$$
(1-a)^2(v_1^2 + v_2^2)(v^2 - v_2^2)^2 - 4r^2 v_1^2 v^4 + 4av_1^2 v^2(v^2 - v_2^2) = 0\,.
\tag{5.22}
$$

Subtracting the third equation of (5.21) from the fourth equation and recalling that $v^2 = v_1^2 + v_2^2 + (n-2)v_3^2$, we obtain the quadratic equation

$$
(1-a)v_1^2 + v_2^2 + \left((n-3) - a(n-2)\right)v_3^2 = 0\,.
\tag{5.23}
$$

Consider the system consisting of the two equations (5.22) and (5.23) in the homogeneous coordinates v_1, v_2, v_3. Any solution to this system gives a solution to the system (5.21), and thus gives 2^{n-3} solutions to the original system (5.16)–(5.19).

These last two equations (5.22) and (5.23) are polynomials in the squares of the variables v_1^2, v_2^2, v_3^2. If we substitute $\alpha = v_1^2, \beta = v_2^2$, and $\gamma = v_3^2$, then we have a cubic and a linear equation, and any solution α, β, γ to these with non-vanishing coordinates gives 4 solutions to the system (5.22) and (5.23): $(v_1, v_2, v_3)^T := (\alpha^{1/2}, \pm\beta^{1/2}, \pm\gamma^{1/2})^T$, as v_1, v_2, v_3 are homogeneous coordinates.

Solving the linear equation in α, β, γ for β and substituting into the cubic equation gives a homogeneous cubic in α and γ whose coefficients are polynomials in a, n, r. The discriminant of this cubic is a polynomial with integral coefficients of degree 16 in the variables a, n, r having 116 terms. Using a computer algebra system, it can be verified that this discriminant is irreducible over the rational numbers. Thus, for any fixed integer $n \geq 3$, the discriminant is a non-zero polynomial in a, r. This implies that the cubic has 3 solutions for general a, r, and any integer n. Since the coefficients of this cubic similarly are non-zero polynomials for any n, the solutions α, β, γ will be non-zero for general a, r, and any n. We conclude:

> For any integer $n \geq 3$ and general a, r, there will be $3 \cdot 2^{n-1}$ complex common tangents to spheres of radius r with centers

$$ae_2, \quad -e_2, \quad \text{and} \quad \pm e_j, \quad \text{for } 3 \leq j \leq n.$$

We return to the case when $a = 1$, i.e., the centers are the vertices of the cross polytope $\pm e_j$ for $j = 2, \ldots, n$. Then our equations (5.20) and (5.21) become

$$
\begin{aligned}
p_2 \;=\; p_3 \;=\; \cdots \;=\; p_n \;&=\; 0\,, \\
v_2^2 \;=\; v_3^2 \;=\; \cdots \;=\; v_n^2\,, & \\
p_1 v_1 \;&=\; 0\,, \\
v^2(p_1^2 - r^2 + 1) - v_2^2 \;&=\; 0\,.
\end{aligned}
\tag{5.24}
$$

As before, $v^2 = v_1^2 + (n-1)v_2^2$. We solve the last two equations. Any solution they have (in $\mathbb{C}^1 \times \mathbb{P}^1$) gives rise to 2^{n-2} solutions, by the second list of equations $v_3^2 = \cdots = v_n^2$. By the penultimate equation $p_1 v_1 = 0$, one of p_1 or v_1 vanishes. If $v_1 = 0$, then the last equation becomes

$$(n-1)v_2^2(p_1^2 - r^2 + 1) \;=\; v_2^2\,.$$

Since $v_2 = 0$ implies $v^2 = 0$, we have $v_2 \neq 0$ and so we may divide by v_2^2 and solve for p_1 to obtain

$$p_1 \;=\; \pm\sqrt{r^2 - 1 + \frac{1}{n-1}}\,.$$

If instead $p_1 = 0$, then we solve the last equation to obtain

$$\frac{v_1}{v_2} \;=\; \pm\sqrt{\frac{1}{1-r^2} + 1 - n}\,.$$

Thus for general r, there will be 2^n common tangents to the spheres with radius r and centers $\pm e_j$ for $j = 2, \ldots, n$. We investigate when these are real.

We will have p_1 real when $r^2 > 1 - 1/(n-1)$. Similarly, v_1/v_2 will be real when $1/(1-r^2) > n-1$. In particular, $1 - r^2 > 0$ and so $1 > r^2$. Using this we get

$$1 - r^2 \;<\; \frac{1}{n-1} \qquad \text{so that} \qquad r^2 \;>\; 1 - \frac{1}{n-1}\,,$$

which we previously obtained.

We conclude that there will be 2^n real common tangents to the spheres with centers $\pm e_j$ for $j = 2, \ldots, n$ and radius r when

$$\sqrt{1 - \frac{1}{n-1}} \;<\; r \;<\; 1\,.$$

This concludes the proof of Theorem 5.7.

5.2 Common tangents to $2n-2$ quadrics in $\mathbb{P}^n$ and $\mathbb{R}^n$

In this section, we study the common tangent lines to $2n-2$ quadrics in $\mathbb{P}^n$ (or $\mathbb{R}^n$, respectively). In Section 5.2.1, we prove Theorem 5.2 stated at the beginning of this chapter on the maximum number of real lines tangent to $2n-2$ quadrics in $\mathbb{P}^n$. Here, we combine recent results in the real Schubert calculus with classical perturbation arguments adapted to the real numbers.

In Section 5.2.2, we put the tangent problem to spheres into the perspective of common tangents to general quadrics. We discuss the excess component at infinity for the problem of spheres. In this setting, Theorem 5.1(a) implies that there will be at most $3 \cdot 2^{n-1}$ isolated common tangents to $2n-2$ quadrics in $\mathbb{P}^n$, when the quadrics all contain the same (smooth) quadric in a given hyperplane. In particular, the problem of the spheres can be seen as the case when the common quadric is at infinity and contains no real points.

5.2.1 Real lines

In Section 4.1, we have given a construction of four real quadrics in $\mathbb{P}^3$ with 32 real common tangent lines. The main idea of that construction was encapsulated by the visually appealing transition from Figure 4.1 to Figure 4.2. Here, we generalize this idea to the n-dimensional case. However, in contrast to the symbolic construction of Section 4.1, the proof of the n-dimensional case is only existential.

Recall that the $(n-1)$-st Catalan number is $C_{n-1} := \frac{1}{n}\binom{2n-2}{n-1}$, which is the number of lines in $\mathbb{P}^n$ simultaneously transversal to $2n-2$ general $(n-2)$-planes [81, 118]. We begin with a configuration of $2n-2$ real $(n-2)$-planes in $\mathbb{R}^n$ having C_{n-1} common real transversal lines. (Such configurations exist, see below.) We then argue that we can replace each of these $(n-2)$-planes by a real quadratic hypersurface such that for each of the original transversal lines, there are 2^{2n-2} nearby real lines tangent to each quadric.

Proposition 5.9. *There exists a configuration of $2n-2$ real $(n-2)$-planes in $\mathbb{R}^n$ having exactly C_{n-1} common real transversals.*

Proof. The corresponding statement for real projective space $\mathbb{P}^n_{\mathbb{R}}$ was proven in [127, Theorem C]. We deduce the affine counterpart above simply by removing a real hyperplane that contains none of the $(n-2)$-planes or any of the transversal lines. $\qquad\square$

Remark 5.10. The purely existential statement in [127] was strongly improved by Eremenko and Gabrielov [52] who gave the following explicit construction of such a collection of $(n-2)$-planes. Let

$$\gamma(s) := (1, s, s^2, \ldots, s^{n-1})^T$$

be the moment curve in $\mathbb{R}^n$. For each $s \in \mathbb{R}$, set $\Lambda(s)$ to be

$$\Lambda(s) := \text{ linear span}\big(\gamma(s), \gamma'(s), \ldots, \gamma^{(n-3)}(s)\big).$$

Geometrically, $\Lambda(s)$ is the kissing, or osculating $(n-2)$-plane to the moment curve at the point $\gamma(s)$. Eremenko and Gabrielov showed that for any distinct numbers $s_1, \ldots, s_{2n-2} \in \mathbb{R}$, the $(n-2)$-planes $\Lambda(s_1), \Lambda(s_2), \ldots, \Lambda(s_{2n-2})$ have exactly C_{n-1} common real transversals.

Definition 5.11. Let $\Lambda \subset \mathbb{R}^n$ be an $(n-2)$-plane and r be a positive real number. Then we define the $(n-2)$-*cylinder* $\text{Cy}(\Lambda, r)$ to be the set of points having Euclidean distance r from Λ. This is a singular quadratic hypersurface in $\mathbb{P}^n$, but smooth in $\mathbb{R}^n$.

A real line ℓ is tangent to $\text{Cy}(\Lambda, r)$ if and only if the Euclidean distance $d(\ell, \Lambda)$ between ℓ and Λ is r. We use the following notation to characterize the Euclidean distance between a line ℓ and an $(n-2)$-plane Λ. For vectors $v_1, \ldots, v_{n-1} \in \mathbb{R}^n$, let $[v_1, \ldots, v_{n-1}] \in \mathbb{R}^n$ denote their n-dimensional vector product (see, e.g., [16, 58]):

$$[v_1, \ldots, v_{n-1}]_j = \sum_{i_1, \ldots, i_{n-1}} \varepsilon_{i_1, \ldots, i_{n-1}, j}\, v_{1, i_1} \cdots v_{n-1, i_{n-1}}, \qquad 1 \le j \le n,$$

where $\varepsilon_{i_1, \ldots, i_n}$ is the Levi-Civita symbol, which is zero unless the indices are distinct, and when they are distinct, it is the sign of the resulting permutation:

$$\varepsilon_{i_1, \ldots, i_n} = \begin{cases} 0 & \text{if at least two of the indices } i_1, \ldots, i_n \text{ are equal,} \\ 1 & \text{if the indices are pairwise different} \\ & \text{and the permutation } i_1, \ldots, i_n \text{ is even,} \\ -1 & \text{if the indices are pairwise different} \\ & \text{and the permutation } i_1, \ldots, i_n \text{ is odd.} \end{cases}$$

The vector $[v_1, \ldots, v_{n-1}]$ is perpendicular to $v_1, \ldots, v_{n-1}$ and its length is the volume of the parallelotope spanned by $v_1, \ldots, v_{n-1}$.

Lemma 5.12. *Let* $\ell = \{a + \lambda b : \lambda \in \mathbb{R}\}$ *with* $a \in \mathbb{R}^n$, $b \in \mathbb{R}^n \setminus \{0\}$ *and*

$$\Lambda = \{p + \sum_{i=1}^{n-2} \mu_i q_i : \mu_1, \ldots, \mu_{n-2} \in \mathbb{R}\}$$

with $p \in \mathbb{R}^n$ *and linearly independent vectors* $q_1, \ldots, q_{n-2} \in \mathbb{R}^n$. *If* $b \notin span\{q_1, \ldots, q_{n-2}\}$ *then the Euclidean distance* $d(\ell, \Lambda)$ *is*

$$d(\ell, \Lambda) = \frac{|[b, q_1, \ldots, q_{n-2}] \cdot (a - p)|}{\|[b, q_1, \ldots, q_{n-2}]\|}.$$

Proof. Since $b \notin \operatorname{span}\{q_1, \ldots, q_{n-2}\}$, the vectors $b, q_1, \ldots, q_{n-2}, [b, q_1, \ldots, q_{n-2}]$ form a basis of $\mathbb{R}^n$. Hence, there exist unique real numbers $\alpha, \beta, \gamma_1, \ldots, \gamma_{n-2}$ such that

$$a - p = \alpha[b, q_1, \ldots, q_{n-2}] + \beta b + \sum_{i=1}^{n-2} \gamma_i q_i.$$

Suppose x and y are points on ℓ and Λ, respectively. Then there exist $\lambda, \mu_1, \ldots, \mu_{n-2}$ such that

$$
\begin{aligned}
x - y &= (a - p) + \lambda b - \sum_{i=1}^{n-2} \mu_i q_i \\
&= \alpha[b, q_1, \ldots, q_{n-2}] + (\beta + \lambda)b + \sum_{i=1}^{n-2} (\gamma_i - \mu_i) q_i.
\end{aligned}
$$

Hence, the distance of ℓ and Λ is $||\alpha[b, q_1, \ldots, q_{n-2}]||$. Since

$$\alpha ||[b, q_1, \ldots, q_{n-2}]||^2 = \alpha[b, q_1, \ldots, q_{n-2}] \cdot [b, q_1, \ldots, q_{n-2}] = [b, q_1, \ldots, q_{n-2}] \cdot (a - p),$$

the lemma follows. $\square$

We record the following useful and basic property of intersection multiplicities [55, p. 1], which we will use.

Proposition 5.13. *Let A be an algebraic curve in complex projective space $\mathbb{P}^n$, and let x be a singular point on A. For any hyperplane $H \subset \mathbb{P}^n$ such that x is an isolated point in $A \cap H$, the intersection multiplicity of A and H in x is greater than 1.*

Theorem 5.14. *Let $\Lambda_1, \Lambda_2, \ldots, \Lambda_{2n-2}$ be $(n-2)$-planes in $\mathbb{R}^n$ having exactly C_{n-1} common real transversals. For each $k = 0, 1, \ldots, 2n-2$, there exist positive real numbers $r_1, \ldots, r_k$ such that there are exactly $2^k C_{n-1}$ real lines that are simultaneously tangent to each of the $(n-2)$-cylinders $\operatorname{Cy}(\Lambda_j, r_j)$, $j = 1, \ldots, k$, and transversal to the $(n-2)$-planes $\Lambda_{k+1}, \ldots, \Lambda_{2n-2}$.*

The case of $k = 2n-2$ implies Theorem 5.2; since the number of real lines will not change under a small perturbation of the cylinders $\operatorname{Cy}(\Lambda_j, r_j)$, we may replace them by quadratic hypersurfaces which are even smooth in $\mathbb{P}^n$, without altering the conclusion of the theorem.

In the proof of Theorem 5.14, we identify the lines we are looking for with the Plücker vectors satisfying the relevant transversal conditions (2.3), tangent conditions (2.5) and the Plücker conditions (2.2).

Proof. We induct on k, with the case of $k = 0$ being the hypothesis of the theorem.

Suppose that $k \leq 2n-2$ and that there exist $r_1, \ldots, r_{k-1} > 0$ and distinct real lines $\ell_1, \ldots, \ell_{2^{k-1}C_n}$ that are simultaneously tangent to $\operatorname{Cy}(\Lambda_j, r_j)$, for each $j = 1, \ldots, k - 1$, and transversal to $\Lambda_k, \ldots, \Lambda_{2n-2}$.

Dropping the condition that the lines meet Λ_k, we obtain a one-dimensional family of lines that are tangent to the cylinders $\mathrm{Cy}(\Lambda_j, r_j)$ for $j = 1, \ldots, k-1$ and that are also transversal to the $(n-2)$-planes $\Lambda_{k+1}, \ldots, \Lambda_{2n-2}$. We consider this one-dimensional family of lines as a curve in Plücker space $\mathbb{G}_{1,n} \subset \mathbb{P}^N$, denoted by A. In particular, the curve A contains the Plücker coordinates of all the lines $\ell_1, \ldots, \ell_{2^{k-1}C_n}$.

Let ℓ be one of the lines $\ell_1, \ldots, \ell_{2^{k-1}C_n}$, and denote its Plücker coordinate by p. Then p is a smooth point on A (the tangent space of A at p is one-dimensional). Namely, otherwise Proposition 5.13 would imply a contradiction to the number of solutions (counting multiplicity) in the induction hypothesis. Consequently, by the complex Implicit Function Theorem (see e.g., [80, Theorem 3.5]), there exist neighborhoods $U \subset \mathbb{C}^n$ of $0 \in \mathbb{C}$, $V \subset \mathbb{P}^N$ of p, and a complex-analytic map $\varphi : U \to \mathbb{G}_{1,n} \subset \mathbb{P}^N$ such that $\varphi(0) = p$ and in V the curve A is given by the parametrization $\varphi(t)$, $t \in U$. By choosing V small enough, we can assume that $A \cap V$ does not contain the Plücker coordinate of another line $\{\ell_1, \ldots, \ell_{2^{k-1}C_n}\} \setminus \{\ell\}$, and that none of the points in $A \cap V$ is the Plücker coordinate of a line at infinity.

Now the crucial point is that the restriction $\varphi_{|\mathbb{R}}$ maps to *real* lines. Namely, assume that the image of any real neighborhood U' of p (or of any other real point $\varphi(t)$ for some real t) contains a non-real point $q \in \mathbb{G}_{1,n} \subset \mathbb{P}^N$. Since $\varphi(U')$ also contains the complex-conjugated point $\overline{q}$, this would imply that p is singular.

Hence, we can assume that $\varphi_{|\mathbb{R}}$ is a function $(-\delta, \delta) \to \mathbb{G}_{1,n} \cap \mathbb{P}^N_{\mathbb{R}}$ for some $\delta > 0$. For a parameter value $t \in (-\delta, \delta)$ let $d(\varphi(t), \Lambda_k)$ be the distance of the real line with Plücker coordinate $\varphi(t)$ from Λ_k. If the direction vector of $\varphi(t)$ is not parallel to Λ_k then d is given by Lemma 5.12. Otherwise, the problem reduces to a lower-dimensional problem. However, $d(\varphi(t), \Lambda_k)$ is a continuous function in t; and we have $d(\varphi(t), \Lambda_k) = 0$ if $t = 0$ and $d(\varphi(t), \Lambda_k) > 0$ if $t \in (-\delta, \delta) \setminus \{0\}$. Let $\rho := \min\{d(\varphi(-\delta/2), \Lambda_k), d(\varphi(\delta/2), \Lambda_k)\}$. Then there are at least two distinct real lines whose Plücker coordinate is contained in $A \cap V$ and whose Euclidean distance to Λ_k is ρ.

We can assume that the $2^{k-1}C_{n-1}$ local parts of A obtained in this way are disjoint. Moreover, let r_k be the minimum value of ρ which has been computed for all the lines $\ell_1, \ldots, \ell_{2^{k-1}C_{n-1}}$. Then there are at least $2^k C_{n-1}$ distinct real lines whose Plücker coordinate is contained in A and whose Euclidean distance to Λ_k is r_k. Since $2^k C_{n-1}$ is the maximum number of lines with this property, there are exactly distinct $2^k C_n$ lines tangent to $\mathrm{Cy}(\Lambda_j, r_j)$ for $j = 1, \ldots, k$ and that are also transversal to the $(n-2)$-planes $\Lambda_{k+1}, \ldots, \Lambda_{2n-2}$. $\qquad\square$

5.2.2   Quadrics versus spheres

In the spirit of Section 4.2 for the three-dimensional case, we can also relate the tangent problem to spheres to the tangent problem to quadrics in n-dimensional space.

Consider a sphere in affine n-space

$$(x_1 - c_1)^2 + (x_2 - c_2)^2 + \cdots + (x_n - c_n)^2 \; = \; r^2 \, .$$

Homogenizing this with respect to the new variable x_0, we obtain

$$(x_1 - c_1 x_0)^2 + (x_2 - c_2 x_0)^2 + \cdots + (x_n - c_n x_0)^2 \;=\; r^2 x_0^2 \,.$$

If we restrict this sphere to the hyperplane at infinity, setting $x_0 = 0$, we obtain

$$x_1^2 + x_2^2 + \cdots + x_n^2 \;=\; 0 \,, \tag{5.25}$$

the equation for an imaginary quadric at infinity. It turns out that every line at infinity tangent to this quadric satisfies the algebraic tangent condition (2.5); we will come back to this in Section 6.1 (see Lemma 6.6). In generalization of (4.9), the resulting excess component in the n-dimensional case is defined by the following equations.

$$
\begin{aligned}
p_{0i} &= 0 \,, & 1 \le i \le n \,, \\
\sum_{1 \le i < j \le n} p_{ij}^2 &= 0 \,, & \\
p_{ij} p_{kl} - p_{ik} p_{jl} + p_{il} p_{jk} &= 0 \,, & 1 \le i < j < k < l \le n \,.
\end{aligned}
$$

It would be interesting to understand the algebraic-geometric and computer-algebraic aspects from Section 4.2 also for general dimension $n > 3$. For example, how many blow-ups are needed to resolve the excess component? From the computer-algebraic point of view, we have not even been able to simulate the multiple blow-up for $n = 4$. Here, the initial excess component is of dimension 3 and is generated by the polynomials

$$p_{01}, p_{02}, p_{03}, p_{04}, p_{12}^2 + p_{13}^2 + p_{14}^2 + p_{23}^2 + p_{24}^2 + p_{34}^2, p_{14} p_{23} - p_{13} p_{24} + p_{12} p_{34} \,.$$

After one blow-up there is still an excess component of dimension 3. However, since every blow-up introduces several new variables, already the computation of the second blow-up exceeds 1 GB of available memory (even when using computer-algebraic standard tricks such as performing the computation over a finite field).

Now let us look at another relationship between tangents to spheres and tangents to general quadrics. Namely, since all smooth quadrics are projectively equivalent, Theorem 5.1 has the following implication for this problem of common tangents to projective quadrics.

Corollary 5.15. *Given $2n-2$ quadrics in $\mathbb{P}^n$ whose intersection with a fixed hyperplane is a given smooth quadric Q, but are otherwise general, there will be at most $3 \cdot 2^{n-1}$ isolated lines in $\mathbb{P}^n$ tangent to each quadric.*

We would like close this section by pointing out some recent results on the following reality question of Corollary 5.15. When all the quadrics are real, how many of the $3 \cdot 2^{n-1}$ common isolated tangents can be real? This question is only partially answered by Theorem 5.1. The point is that projective real quadrics are classified up to real projective transformations by the absolute value of the signature of the quadratic forms on $\mathbb{R}^{n+1}$

defining them. Theorem 5.1 implies that all lines can be real when the shared quadric Q has no real points (signature is $\pm n$).

For $n = 3$, it was shown in [129] that each of the five additional cases concerning nonempty quadrics can have all 12 lines real. For general dimension, the question has largely been answered in [94]. Namely, for any non-zero real numbers $\lambda_3, \dots, \lambda_n$, there are $2n-2$ quadrics of the form

$$(x_1 - c_1)^2 + (x_2 - c_2)^2 + \sum_{j=3}^{n} \lambda_j (x_j - c_j)^2 \;=\; R$$

having all $3 \cdot 2^{n-1}$ tangents real. These all share the same quadric at infinity

$$x_1^2 + x_2^2 + \lambda_3 x_3^2 + \cdots + \lambda_n x_n^2 \;=\; 0\,,$$

and thus the upper bound of Theorem 5.15 is attained, when the shared quadric is this quadric.

5.3   Smallest circumscribing cylinders of simplices in general dimension

In Section 3.4, we have given polynomial formulations with small Bézout number for computing smallest circumscribing cylinders of a tetrahedron in $\mathbb{R}^3$. Based on the characterization in Section 5.1, we generalize these formulations to smallest circumscribing cylinders of a simplex in $\mathbb{R}^n$, $n \geq 3$.

In Section 5.3.1, we deal with general simplices. Then, in Section 5.3.2, we study the regular simplex in detail.

As a byproduct of our computational studies, we discovered a subtle but severe mistake in the paper [148] on the explicit determination of the outer $(n-1)$-radius for a regular simplex in $\mathbb{R}^n$, thus completely invalidating the proof given there. In Section 5.3.3, serving as an appendix to the section, we give a description of that flaw, including some computer-algebraic calculations illustrating it.

5.3.1   General simplices

Let $c_1, \dots, c_{n+1}$ be the affinely independent vertices of the simplex in $\mathbb{R}^n$, and let c_{n+1} be located in the origin.

Using (5.3), we can generalize the optimization formulation (3.41) for the three-dimensional case and obtain the program

$$\min \left(\frac{1}{2} M^{-1} \begin{pmatrix} v^2 c_1^2 - (v \cdot c_1)^2 \\ \vdots \\ v^2 c_n^2 - (v \cdot c_n)^2 \end{pmatrix} \right)^2$$
$$\text{s.t.} \qquad g_1(v_1, \dots, v_n) \;=\; 0\,,$$
$$g_2(v_1, \dots, v_n) := v^2 - 1 \;=\; 0\,. \tag{5.26}$$

Here, $M := (c_1, \ldots, c_n)^T$, and g_1 denotes the cubic equation which results from substituting (5.3) for a common radius into $p \cdot v$ and setting $v^2 = 1$ in the denominator.

In order to show that set of admissible solutions for our optimization problem is nonempty, we record the following result.

Lemma 5.16. *For any simplex in $\mathbb{R}^n$ the $\binom{n+1}{2}$ edge directions of the simplex are direction vectors of circumscribing cylinders.*

Proof. Since the edge directions $c_i - c_j$ have a simple description in the basis $c_1, \ldots, c_n$, we use the representation (5.4) of the cubic equation $g_1(v) = 0$ in that basis. In terms of the t-coordinates, the $\binom{n+1}{2}$ edges of the simplex are $t = e_i$, $1 \leq i \leq n$, and $t = e_i - e_j$, $1 \leq i < j \leq n$, where e_i denotes the i-th standard unit vector. For all these edges, the cubic equation is satisfied. $\qquad\square$

Considering Lagrange multipliers λ_1 and λ_2 yields the following necessary optimality condition.

$$
\begin{aligned}
\operatorname{grad} f &= \lambda_1 \operatorname{grad} g_1 + \lambda_2 \operatorname{grad} g_2 \,, \\
g_1(v_1, \ldots, v_n) &= 0 \,, \\
g_2(v_1, \ldots, v_n) &= 0 \,.
\end{aligned}
\tag{5.27}
$$

Since the Bézout bound of this system is $3^n \cdot 3 \cdot 2 = 2 \cdot 3^{n+1}$, we have:

Lemma 5.17. *For $n \geq 2$, the number of isolated local extrema for the minimal circumscribing cylinder is bounded by $2 \cdot 3^{n+1}$.*

This bound is not tight. Trying to reduce this upper bound of isolated solutions like in the three-dimensional case, we can eliminate the linear occurrences of the Lagrange variables λ_1 and λ_2. Generalizing (3.43), we have to consider the vanishing of all 3×3-subdeterminants of the matrix

$$
\begin{pmatrix}
-\frac{\partial f}{\partial v_1} & \frac{\partial g_1}{\partial v_1} & \frac{\partial g_2}{\partial v_1} \\
-\frac{\partial f}{\partial v_2} & \frac{\partial g_1}{\partial v_2} & \frac{\partial g_2}{\partial v_2} \\
\vdots & \vdots & \vdots \\
-\frac{\partial f}{\partial v_n} & \frac{\partial g_1}{\partial v_n} & \frac{\partial g_2}{\partial v_n}
\end{pmatrix} .
\tag{5.28}
$$

Thus, for $n \geq 4$ we arrive at a non-complete intersection of equations where we have more equations than variables. Hence, we cannot apply our Bézout bound on these systems.

However, for small dimensions we can improve Lemma 5.17 by directly working on the formulation (5.27). In order to provide better bounds, we use well-known characterizations of the number of zeroes of a polynomial equation by the mixed volume of a Minkowski sum of polytopes (for an easily accessible introduction into this topic we refer to [32]). Here, let $\mathbb{C}^* := \mathbb{C} \setminus \{0\}$.

Lemma 5.18. *For $2 \leq n \leq 7$, the number of solutions of the system (5.27) in $(v_1, \ldots, v_n, \lambda_1, \lambda_2) \in (\mathbb{C}^*)^{n+2}$ is bounded by*

$$6 \begin{Bmatrix} n+1 \\ 3 \end{Bmatrix},$$

where $\begin{Bmatrix} n \\ k \end{Bmatrix}$ denotes the Stirling number of the second kind (see, e.g., [60, 134]).

The sequence $6 \begin{Bmatrix} n+1 \\ 3 \end{Bmatrix}$ starts as follows.

n	2	3	4	5	6	7
$6\begin{Bmatrix} n+1 \\ 3 \end{Bmatrix}$	6	36	150	540	1806	5796

Proof. For a polynomial $h = \sum_{\alpha \in \mathbb{N}_0^n} c_\alpha x^\alpha \in \mathbb{C}[x_1, \ldots, x_n]$, let

$$\mathrm{NP}(h) := \mathrm{conv}\{\alpha \in \mathbb{N}_0^n \ : \ c_\alpha \neq 0\}$$

denote the Newton polytope of h (see, e.g., [32, §7.1]). Let $h_1, \ldots, h_n$ be the polynomials of the gradient equation in (5.27). Further let $P_1, \ldots, P_n, Q_1, Q_2$ be the Newton polytopes of $h_1, \ldots, h_n, g_1, g_2$ for generic instances of these equations.

Recall that the mixed volume $\mathrm{MV}(P_1, \ldots, P_n, Q_1, Q_2)$ is the coefficient of the monomial $\lambda_1 \cdot \lambda_2 \cdots \lambda_n \cdot \mu_1 \cdot \mu_2$ in the $(n+2)$-dimensional volume $\mathrm{Vol}_{n+2}(\lambda_1 P_1 + \ldots + \lambda_n P_n + \mu_1 Q_1 + \mu_2 Q_2)$ (which is a polynomial expression in $\lambda_1, \ldots, \lambda_n, \mu_1, \mu_2$). By Bernstein's Theorem, the number of isolated common zeroes in $(\mathbb{C}^*)^{n+2}$ of the set of polynomials $h_1, \ldots, h_n, g_1, g_2$ is bounded above by

$$\mathrm{MV}(P_1, \ldots, P_n, Q_1, Q_2)$$

(see [32, Theorem 5.4 in Chapter 8]). For every given n this volume can be computed using software for computing mixed volumes (see, e.g, [51, 143]). $\qquad \square$

We conjecture that for any $n \geq 2$, the number of isolated solutions in $(\mathbb{C}^*)^{n+2}$ is bounded by $6 \begin{Bmatrix} n+1 \\ 3 \end{Bmatrix}$.

5.3.2   The regular simplex in $\mathbb{R}^n$

Here, we analyze the local extrema of circumscribing cylinders for the regular simplex. Our aim is both to illustrate the algebraic formulations given before and to relate our investigations to classical investigations on the regular simplex in convex geometry. In order to achieve many symmetries in the algebraic formulation, we use a slightly modified coordinate system that is particularly suited for the regular simplex; these coordinates have also been used in [18, 147].

The equation $x_1 + \ldots + x_{n+1} = 1$ defines an n-dimensional affine subspace in $\mathbb{R}^{n+1}$. Now let the regular simplex in this n-dimensional subspace be given by the $n+1$ vertices

$c_i = e_i$, where e_i denotes the i-th standard unit vector, $1 \leq i \leq n+1$. We consider the tangency equation (5.1) for the point c_{n+1},

$$v^2 p^2 - 2v^2 p_{n+1} + v^2 - v_{n+1}^2 - r^2 v^2 \; = \; 0 \, .$$

Subtracting this equation from the equation for c_i, $1 \leq i \leq n$, yields

$$2v^2(p_i - p_{n+1}) \; = \; -(v_i^2 - v_{n+1}^2) \, , \quad 1 \leq i \leq n \, .$$

Moreover, the embedding into the hyperplane $\sum_{i=1}^{n+1} x_i = 1$ implies $\sum_{i=1}^{n+1} p_i = 1$. In order to solve these $n+1$ equations for p, let M be the $(n+1) \times (n+1)$-matrix whose i-th row contains the vector $e_i^T - e_{n+1}^T$ and whose n-th row is $(1, 1, \dots, 1)$. Since M is invertible, we obtain

$$p = \frac{1}{2v^2} M^{-1} \begin{pmatrix} -(v_1^2 - v_{n+1}^2) \\ \vdots \\ -(v_n^2 - v_{n+1}^2) \\ 2v^2 \end{pmatrix} . \tag{5.29}$$

As before, substituting this expression into $p \cdot v = 0$ and setting $v^2 = 1$ in the denominator gives a cubic equation $g_1(v) = 0$. Hence, we obtain the following optimization problem. Here, the objective function f stems from the condition for the vertex c_{n+1}, and the condition $\sum_{i=1}^{n+1} v_i = 0$ comes from the embedding.

$$\begin{aligned} \min \, & p^2 - 2p_{n+1} + 1 - v_{n+1}^2 \\ \text{s.t.} \quad & g_1(v_1, \dots, v_{n+1}) \; = \; 0 \, , \\ & \sum_{i=1}^{n+1} v_i \; = \; 0 \, , \\ & v^2 \; = \; 1 \, . \end{aligned} \tag{5.30}$$

First we record that the functions f and g_1 are symmetric polynomials in the variables $v_1, \dots, v_{n+1}$. In order to show this, let $\sigma_1, \dots, \sigma_{n+1}$ be the elementary symmetric functions in $v_1, \dots, v_{n+1}$,

$$\begin{aligned} \sigma_1 \; &= \; v_1 + \dots + v_{n+1} \, , \\ & \vdots \\ \sigma_k \; &= \; \sum_{1 \leq i_1 < \dots < i_k \leq n+1} v_{i_1} v_{i_2} \cdots v_{i_k} \, , \\ & \vdots \\ \sigma_{n+1} \; &= \; v_1 v_2 \cdots v_{n+1} \end{aligned}$$

(see, e.g., [31, 138]). By providing explicit expressions for f and g_1 as polynomials in the elementary symmetric polynomials $\sigma_1, \dots, \sigma_{n+1}$, the symmetry of f and g_1 follows. More precisely, we obtain:

Lemma 5.19. *The quartic polynomial $f(v_1, \ldots, v_{n+1})$ and the cubic polynomial $g_1(v_1, \ldots, v_{n+1})$ are symmetric polynomials in the variables $v_1, \ldots, v_{n+1}$. In terms of the elementary symmetric functions, f results in*

$$f = \frac{1}{4(n+1)} \left(n\sigma_1^4 - 4n\sigma_1^2\sigma_2 + 2(n-1)\sigma_2^2 - 4\sigma_1^2 + 8\sigma_2 + 4n \right) + \sigma_1\sigma_3 - \sigma_4 \,,$$

and the homogeneous polynomial g_1 results in

$$g_1 = \frac{1}{2(n+1)} \left(-(n-2)\sigma_1^3 + 3(n-1)\sigma_1\sigma_2 \right) - \frac{3}{2}\sigma_3 \,.$$

Since $\sigma_1 = 0$ and $\sum_{i=1}^{n+1} v_i^2 = \sigma_1^2 - 2\sigma_2$, we can also deduce the following formulation of our optimization problem:

Corollary 5.20. *Finding the critical values of the minimization problem (5.30) is equivalent to finding the critical values $(v_1, \ldots, v_{n+1})^T \in \mathbb{R}^{n+1}$ of the maximization problem*

$$
\begin{aligned}
\max \;\; & \sigma_4 \\
\text{s.t.} \;\; \sigma_1 \;\; &= \;\; 0 \,, \\
\sigma_2 \;\; &= \;\; -\frac{1}{2} \,, \\
\sigma_3 \;\; &= \;\; 0 \,,
\end{aligned}
\tag{5.31}
$$

where σ_i are the elementary symmetric functions in $v_1, \ldots, v_{n+1}$.

Theorem 5.21. *The direction vector $(v_1, \ldots, v_{n+1})^T$ of any locally extreme circumscribing cylinder satisfies $|\{v_1, \ldots, v_{n+1}\}| \leq 3$, i.e., for each solution vector the components take at most three distinct values.*

Proof. For $n \leq 2$, the statement is trivial, so we can assume $n \geq 3$. Let v be the direction vector of a locally extreme circumscribing cylinder with $v^2 = 1$. Using Corollary 5.20, let $f(v) := -\sigma_4(v)$, $g_1(v) := \sigma_3(v)$, $g_2(v) := \sigma_2(v) - 1/2$, and $g_3(v) := \sigma_1(v)$. As a necessary condition for a local extremum, for any pairwise different indices $a, b, c, d \in \{1, \ldots, n+1\}$ the determinant

$$
\det \begin{pmatrix}
-\frac{\partial f}{\partial v_a} & \frac{\partial g_1}{\partial v_a} & \frac{\partial g_2}{\partial v_a} & \frac{\partial g_3}{\partial v_a} \\
-\frac{\partial f}{\partial v_b} & \frac{\partial g_1}{\partial v_b} & \frac{\partial g_2}{\partial v_b} & \frac{\partial g_3}{\partial v_b} \\
-\frac{\partial f}{\partial v_c} & \frac{\partial g_1}{\partial v_c} & \frac{\partial g_2}{\partial v_c} & \frac{\partial g_3}{\partial v_c} \\
-\frac{\partial f}{\partial v_d} & \frac{\partial g_1}{\partial v_d} & \frac{\partial g_2}{\partial v_d} & \frac{\partial g_3}{\partial v_d}
\end{pmatrix}
\tag{5.32}
$$

vanishes. Since f, g_1, g_2, and g_3 are symmetric functions in the variables $v_1, \ldots, v_{n+1}$, we can assume without loss of generality $a = 1$, $b = 2$, $c = 3$, and $d = 4$. Setting

$\alpha_n := \sum_{i=5}^{n+1} v_i$ and $\beta_n = \sum_{i=5}^{n+1} v_i^2$, we can write

$$\frac{\partial g_3}{\partial v_i} = 1,$$

$$\frac{\partial g_2}{\partial v_i} = \sum_{\substack{j=1 \\ j \neq i}}^{4} v_j + \alpha_n,$$

$$\frac{\partial g_1}{\partial v_i} = \sum_{\substack{1 \leq j < k \leq 4 \\ j,k \neq i}} v_j v_k + \alpha_n \sum_{\substack{j=1 \\ j \neq i}}^{4} v_j + \frac{1}{2}\left(\alpha_n^2 - \beta_n\right)$$

$(1 \leq i \leq 4)$. Moreover, since $\sigma_3(v) = 0$, we can consider $\sigma_3 + \frac{\partial f}{\partial v_i}$ instead of $\frac{\partial f}{\partial v_i}$. This allows to express the resulting expression easily in terms of α_n and β_n. More precisely, we obtain

$$\sigma_3 + \frac{\partial f}{\partial v_i} = v_i \left(\sum_{\substack{1 \leq j < k \leq 4 \\ j,k \neq i}} v_j v_k + \alpha_n \sum_{\substack{j=1 \\ j \neq i}}^{4} v_j + \frac{1}{2}(\alpha_n^2 - \beta_n) \right).$$

Thus we can consider the determinant (5.32) as a polynomial in $v_1, v_2, v_3, v_4, \alpha_n, \beta_n$. Evaluating this 4×4-determinant Δ shows that it is independent of α_n, β_n and that it factors as

$$\Delta = (v_1 - v_2)(v_1 - v_3)(v_1 - v_4)(v_2 - v_3)(v_2 - v_4)(v_3 - v_4).$$

Hence, $|\{v_1, v_2, v_3, v_4\}| \leq 3$, and this holds true for any quadruple (a, b, c, d) of indices. $\square$

Using this result, we illustrate the occurrence of the Stirling numbers in Lemma 5.18 for the case of a regular simplex. There are $\left\{{n+1 \atop 3}\right\}$ ways to partition the set $V := \{v_1, \dots, v_{n+1}\}$ into three nonempty subsets V_1, V_2, V_3. We assume that $v_i \in V_i$, $1 \leq i \leq 3$, and that all variables within the same set take the same value. Setting $k := |V_1|$ and $l := |V_2|$, the formulation in Corollary 5.20 yields the system of equations

$$
\begin{aligned}
kv_1 + lv_2 + (n+1-k-l)v_3 &= 0, \\
kv_1^2 + lv_2^2 + (n+1-k-l)v_3^2 &= 1, \\
\sum_{\substack{0 \leq i_1 < i_2 < i_3 \leq 3 \\ i_1 + i_2 + i_3 = 3}} \binom{k}{i_1}\binom{l}{i_2}\binom{n+1-k-l}{i_3} v_1^{i_1} v_2^{i_2} v_3^{i_3} &= 0.
\end{aligned}
\tag{5.33}
$$

If one of the indices k, l, or $n+1-k-l$ is zero then this system consists of three equations in two variables, so we do not expect any solutions. For every choice of k, l corresponding to a partition into nonempty subsets, we obtain a system of equations with Bézout number 6. Thus, whenever the values of v_1, v_2, and v_3 in the solutions to (5.33) are distinct, then this reflects the bound in Lemma 5.18.

In particular, in the case $n = 4$ we obtain the following 150 solutions.

$k = 1$, $l = 1$: The six solutions for $(v_1, v_2, v_3)^T$ of the system (5.33) are

$$\left(\frac{1}{\sqrt{2}}, -\frac{1}{\sqrt{2}}, 0 \right)^T, \quad \left(\frac{1}{20}\sqrt{110 - 30i\sqrt{15}}, \frac{1}{20}\sqrt{110 + 30i\sqrt{15}}, -\frac{1}{10}\sqrt{15} \right)^T,$$

and the solutions obtained by permuting the first two components of the first solution and by changing the signs and/or permuting the first two components in the second solution.

For the program (5.31) in the variables $(v_1, \dots, v_5)^T$, this gives $\binom{5}{2}\binom{2}{1} = 20$ critical positions of the form (i.e., up to variable permutations)

$$\left(\frac{1}{\sqrt{2}}, -\frac{1}{\sqrt{2}}, 0, 0, 0 \right)^T,$$

20 complex solutions of the form

$$\left(-\frac{1}{20}\sqrt{110 - 30i\sqrt{15}}, -\frac{1}{20}\sqrt{110 + 30i\sqrt{15}}, \frac{1}{10}\sqrt{15}, \frac{1}{10}\sqrt{15}, \frac{1}{10}\sqrt{15} \right)^T,$$

and 20 complex solutions of the form

$$\left(\frac{1}{20}\sqrt{110 - 30i\sqrt{15}}, \frac{1}{20}\sqrt{110 + 30i\sqrt{15}}, -\frac{1}{10}\sqrt{15}, -\frac{1}{10}\sqrt{15}, -\frac{1}{10}\sqrt{15} \right)^T.$$

$k = 1$, $l = 2$: Here, we obtain 30 solutions of the form

$$\left(0, \frac{1}{2}, \frac{1}{2}, -\frac{1}{2}, -\frac{1}{2} \right)^T,$$

30 solutions of the form

$$\left(\frac{1}{5}\sqrt{10}, \frac{1}{4}\sqrt{2} - \frac{1}{20}\sqrt{10}, \frac{1}{4}\sqrt{2} - \frac{1}{20}\sqrt{10}, -\frac{1}{4}\sqrt{2} - \frac{1}{20}\sqrt{10}, -\frac{1}{4}\sqrt{2} - \frac{1}{20}\sqrt{10} \right)^T,$$

and 30 solutions of the form

$$\left(-\frac{1}{5}\sqrt{10}, \frac{1}{4}\sqrt{2} + \frac{1}{20}\sqrt{10}, \frac{1}{4}\sqrt{2} + \frac{1}{20}\sqrt{10}, -\frac{1}{4}\sqrt{2} + \frac{1}{20}\sqrt{10}, -\frac{1}{4}\sqrt{2} + \frac{1}{20}\sqrt{10} \right)^T.$$

The global minimum is attained for the vector $\left(0, \frac{1}{2}, \frac{1}{2}, -\frac{1}{2}, -\frac{1}{2} \right)^T$, and the objective value of the global optimum is $49/80$. Hence, the radius of the smallest circumscribing cylinder for a regular simplex in $\mathbb{R}^4$ with edge length $\sqrt{2}$ is $\sqrt{49/80} = 7\sqrt{5}/20 \approx 0.7826$.

5.3.3   Appendix: An error in the results of Weißbach

In the course of our investigations, we discovered a subtle but severe mistake in the paper [148] on the explicit determination of the radius of a smallest enclosing cylinder for a regular simplex $S \subset \mathbb{R}^n$. In the notation of Section 2.2.2, this value is the outer $(n-1)$-radius of S. Since this error completely invalidates the proof given there[1], we give a description of that flaw, including some computer-algebraic calculations illustrating it.

In that paper, the computation of the outer $(n-1)$-radius of a regular simplex (with edge length $\sqrt{2}$) is reduced to the analysis of the following optimization problem.

$$
\begin{aligned}
\min \ & \sum_{i=1}^{n+1} u_i^4 \\
\text{s.t.} \quad & \sum_{i=1}^{n+1} u_i^2 \ = \ 1 \,, \\
& \sum_{i=1}^{n+1} u_i \ = \ 0 \,.
\end{aligned}
\tag{5.34}
$$

For any local optimum $(u_1, \ldots, u_{n+1})^T$ there exist Lagrange multipliers λ_1, $\lambda_2 \in \mathbb{R}$ such that

$$
\begin{aligned}
4u_i^3 + 2\lambda_1 u_i + \lambda_2 \ &= \ 0 \,, \qquad 1 \leq i \leq n+1 \,, \\
\sum_{i=1}^{n+1} u_i^2 \ &= \ 1 \,, \\
\sum_{i=1}^{n+1} u_i \ &= \ 0 \,.
\end{aligned}
\tag{5.35}
$$

Erroneously, in [148] it is argued that symmetry arguments imply that $\lambda_2 = 0$ in any solution. The following calculation in the computer algebra system SINGULAR [62] shows that for $n = 3$ this system has 26 solutions (counting multiplicity) over $\mathbb{C}$.

```
ring R = 0, (u1,u2,u3,u4,la1,la2), (dp);

ideal I =
  4*u1^3 + 2*la1*u1 + la2,
  4*u2^3 + 2*la1*u2 + la2,
  4*u3^3 + 2*la1*u3 + la2,
  4*u4^3 + 2*la1*u4 + la2,
  u1^2 + u2^2 + u3^2 + u4^2 - 1,
  u1 + u2 + u3 + u4;

degree(std(I));
```

---

[1] In a personal communication this has been confirmed by B. Weißbach.

This program first defines a polynomial ring in the variables $u_1, \ldots, u_4, \lambda_1, \lambda_2$ over a field of characteristic zero. We then use the `degree` command to compute the dimension and the degree of the ideal defined by our equations. The output of that command is

```
// codimension = 6
// dimension   = 0
// degree      = 26
```

Hence, there are finitely many solutions (since the dimension of the ideal is zero), and the degree of the ideal (the sum of the multiplicities of the solutions) is 26.

18 of these solutions refer to the case $\lambda_2 = 0$ (and those were the ones computed in [148]). Namely, if $\lambda_2 = 0$ then the first row of (5.35) simplifies to

$$u_i(2u_i^2 + \lambda_1) \;=\; 0\,, \qquad 1 \le i \le n+1\,.$$

If we are only interested in the real solutions to this system, then setting $\lambda_1 = -2\lambda^2$ for some $\lambda \ge 0$ gives

$$u_i(u_i^2 - \lambda^2) \;=\; 0\,, \qquad 1 \le i \le n+1\,.$$

Since the vector $(u_1, \ldots, u_{n+1})^T = (0, \ldots, 0)^T$ does not satisfy the second row in (5.35), the solutions with $\lambda_2 = 0$ are

$$
\begin{aligned}
u_i &= \lambda, & i &\in \{i_1, \ldots, i_h\}\,, \\
u_i &= -\lambda, & i &\in \{i_{h+1}, \ldots, i_{2h}\}\,, \\
u_i &= 0\,, & i &\in \{1, \ldots, n+1\} \setminus \{i_1, \ldots, i_{2h}\}
\end{aligned}
$$

for some $h \ge 1$, some set $\{i_1, \ldots, i_{2h}\}$ of pairwise different indices, and $\lambda = (2h)^{-1/2}$. In the case $n = 3$, there are 12 possibilities to choose the indices and the signs for $|h| = 1$ and 6 possibilities to choose the indices and the signs for $|h| = 2$, giving 18 solutions to (5.35).

However, there are 8 additional solutions, which in fact are also real! Namely, these are the solutions

$$
\begin{aligned}
(u_1, \ldots, u_4)^T &= \frac{1}{2\sqrt{3}}(1, -3, 1, 1)^T\,, & \lambda_1 &= -\frac{7}{6}\,, & \lambda_2 &= \frac{1}{\sqrt{3}}\,, \\
(u_1, \ldots, u_4)^T &= \frac{1}{2\sqrt{3}}(-1, 3, -1, -1)^T\,, & \lambda_1 &= -\frac{7}{6}\,, & \lambda_2 &= -\frac{1}{\sqrt{3}}\,,
\end{aligned}
$$

as well as the six distinct solutions obtained from these two by permuting the variables $u_1, \ldots, u_4$. These additional solutions invalidate the subsequent arguments in [148].

The omissions get even worse in the higher-dimensional case. E.g., for $n = 4$, besides the $\binom{5}{2}\binom{2}{1} + \binom{5}{4}\binom{4}{2} = 20 + 30 = 50$ solutions described in [148], we obtain the following

solutions:

$$
\begin{aligned}
(u_1, \ldots, u_5)^T &= \frac{1}{\sqrt{30}}(-2, -2, -2, 3, 3)^T, \quad \lambda_1 = -\frac{7}{15}, \quad \lambda_2 = -\frac{2}{75}\sqrt{30}, \\
(u_1, \ldots, u_5)^T &= \frac{1}{\sqrt{30}}(2, 2, 2, -3, -3)^T, \quad \lambda_1 = -\frac{7}{15}, \quad \lambda_2 = \frac{2}{75}\sqrt{30}, \\
(u_1, \ldots, u_5)^T &= \frac{1}{2\sqrt{5}}(1, -4, 1, 1, 1)^T, \quad \lambda_1 = -\frac{13}{10}, \quad \lambda_2 = \frac{6}{25}\sqrt{5}, \\
(u_1, \ldots, u_5)^T &= \frac{1}{2\sqrt{5}}(-1, 4, -1, -1, -1)^T, \quad \lambda_1 = -\frac{13}{10}, \quad \lambda_2 = -\frac{6}{25}\sqrt{5},
\end{aligned}
$$

as well as those solutions obtained by permuting the variables. Altogether, we have $10 + 10 + 5 + 5 = 30$ solutions with $\lambda_2 \neq 0$, and thus a total number of 80 solutions.

Finally, we remark that the paper [147], which computes the outer $(n-1)$-radius of a regular simplex in *odd* dimension n, is correct.

6. COMMON TRANSVERSALS AND TANGENTS

We study the lines simultaneously tangent to k given spheres and transversal to $4-k$ given lines, $k \in \{0, \dots, 4\}$. In Section 6.1, we prove the following result.

Theorem 6.1. *Given $4-k$ lines and k spheres in $\mathbb{R}^3$, $0 \leq k \leq 4$. If there exist only finitely many lines in $\mathbb{R}^3$ simultaneously tangent to the spheres and transversal to the lines then the number of these lines is bounded by*

$$
\begin{cases}
2 & \text{if } k = 0 \,, \\
4 & \text{if } k = 1 \,, \\
8 & \text{if } k = 2 \,, \\
12 & \text{if } k \in \{3, 4\} \,.
\end{cases}
$$

These bounds are tight, i.e., for each k there exists a configuration where the number of distinct real solutions matches the stated number. The bounds are tight even if the spheres are unit spheres.

Table 6.1 summarizes the results. Even if we are primarily interested in the real solutions, the upper bounds are in fact complex bounds in $\mathbb{C}^3$, which are given in the first main column. The second column contains the matching numbers of real solutions in our constructions. The last column shows that in some cases, we are able to explicitly characterize the configurations with an infinite number of real common tangents. In the entries with a "–" we do not know such a characterization (cf. the discussion in Section 3.3.5).

For $k \in \{1, 2\}$, the upper bounds immediately follow from Bézout's Theorem. Whereas for $k = 1$ it is easy to give a construction matching this bound, the construction for $k = 2$ is quite involved. In particular, for $k = 2$ we use a computation of intersection multiplicities based on standard bases in local rings to prove correctness of the construction. For $k = 3$, the Bézout bound in the Plücker formulation is 16 instead of 12. Here, it turns out that there are two solutions with multiplicity at least two in the plane at infinity.

Besides the tight upper bounds, we characterize the configurations with infinitely many common tangents for $k = 1$ and $k = 2$. For three lines and one sphere, our proof is based on classical line-geometric techniques. In order to characterize the situations where two lines and two spheres have infinitely many real common tangent lines, we study the fascinating geometry behind that degree 8 problem in Section 6.2. A second purpose of this section is to develop a variety of computer-algebraic techniques for tackling problems

	upper bound # solutions		# real solutions of our construction		characterization of degenerate instances	
4 lines	2	(well-known)	2	(well-known)	yes	(well-known)
3 lines, 1 sphere	4		4		yes	
2 lines, 2 spheres	8		8		yes	
1 line, 3 spheres	12		12		–	
4 unit spheres	12	(see Chapter 3)	12	(see Chapter 3)	yes	(see Chapter 3)
4 spheres	12	(see Chapter 3)	12	(see Chapter 3)	–	

Tab. 6.1: Summary of results

of this kind. For that reason, we first deal with the more general problem where we replace the spheres in $\mathbb{R}^3$ by general quadrics in $\mathbb{P}^3$. In order to study the geometry of this problem, we fix two lines and a quadric in general position, and describe the set of (second) quadrics for which there are infinitely many common transversals/tangents in terms of an algebraic curve. It turns out that this set is an algebraic curve of degree 24 in the space $\mathbb{P}^9$ of quadrics. Factoring the ideal of this curve shows that it is remarkably reducible:

Theorem 6.2. *Fix two skew lines ℓ_1 and ℓ_2 and a general quadric Q in $\mathbb{P}^3$. The closure of the set of quadrics Q' for which there are infinitely many lines simultaneously transversal to ℓ_1 and ℓ_2 and tangent to both Q and to Q' is a curve of degree 24 in the $\mathbb{P}^9$ of quadrics. This curve consists of 12 plane conics.*

We prove this theorem by investigating the ideal defining the algebraic curve describing the set of (second) quadrics. Based on this, we prove the theorem with the aid of a computer calculation in the computer algebra system SINGULAR. As explained in Section 6.2.3, the success of that computation depends crucially on the preceding analysis of the curve. Quite interestingly, there are real lines ℓ_1 and ℓ_2 and real quadrics Q such that all 12 components of the curve of second quadrics are real. In general, given real lines ℓ_1, ℓ_2, and a real quadric Q, not all of the 12 components are defined over the real numbers.

Based on the discussion of lines and general quadrics, we give a complete characterization of configurations of two lines and two spheres having infinitely many lines transversal to the lines and tangent to the spheres.

6.1   Enumerative results

We show Theorem 6.1. For brevity, we denote the maximum numbers of lines in $\mathbb{R}^3$ simultaneously tangent to $4-k$ lines and k spheres (in the finite case) by N_k, $k \in \{0, \dots, 4\}$.
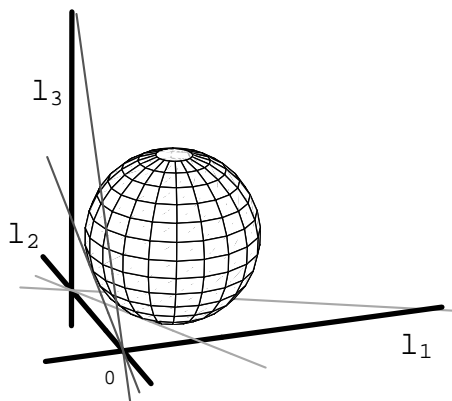
Fig. 6.1: The figure shows a configuration with three lines ℓ_1, ℓ_2, ℓ_3, and one sphere of radius 11/10, leading to 4 common tangent lines. The two tangent lines in the x_1x_2-plane are drawn in light grey, whereas the two tangent lines in the x_2x_3-plane are drawn in dark grey.

6.1.1 Proofs and constructions

Note that the upper bounds $N_0 \le 2$, $N_1 \le 4$, $N_2 \le 8$ immediately follow from Bézout's Theorem. Namely, since the common tangent lines to three lines and one sphere can be formulated by three linear equations of the form (2.4), one equation of the form (2.5) as well as the Plücker relation (2.2) in the six homogeneous variables $p_{01}, \dots, p_{23}$, we obtain $N_1 \le 4$. Analogously, we obtain $N_0 \le 2$, $N_2 \le 8$.

As mentioned earlier, the common transversals to four given lines in 3-dimensional space are a well-studied problem in enumerative geometry, and it is well-known that the upper bound of 2 can be actually achieved in real space $\mathbb{R}^3$ (see, e.g., [75, §XIV.7]); hence $N_0 = 2$. The number of common transversals is finite if and only if the Plücker vectors of the four given lines are linearly independent.

Lemma 6.3. $N_1 = 4$.

Proof. Since $N_1 \le 4$, it suffices to give a construction with 3 lines and 1 sphere, leading to 4 common tangents. Denoting the three coordinate axes in $\mathbb{R}^3$ by x_1, x_2, and x_3, let ℓ_1 be the x_1-axis, ℓ_2 be the x_2-axis, and ℓ_3 be parallel to the x_3-axis and passing through $(0,2,0)^T$ (see Figure 6.1); hence $\ell_1 \cap \ell_2 = \{(0,0,0)^T\}$ and $\ell_2 \cap \ell_3 = \{(0,2,0)^T\}$.

Each line intersecting the three lines ℓ_1, ℓ_2, and ℓ_3 is located in the x_1x_2-plane (in which case it passes through $(0,2,0)^T$) or is located in the x_2x_3-plane (in which case it passes through the origin). For $1 < r < \sqrt{2}$ the sphere $S((1,1,1)^T, r)$ intersects both the x_1x_2-plane and the x_2x_3-plane, but does not intersect with any of the lines ℓ_1, ℓ_2, ℓ_3. Hence, since there are two tangents to the sphere passing through the origin and lying in

the x_1x_2-plane, and since there are two tangents to the sphere passing through $(0, 2, 0)^T$ and lying in the x_1x_3-plane, there are 4 common tangents altogether. Figure 6.1 shows a configuration with $1 < r = 11/10 < \sqrt{2}$. We remark that by appropriate scaling, the sphere can be transformed into a unit sphere. Furthermore, by slightly perturbing the configuration, the lines can be made pairwise skew. $\qquad\square$

To complete the entries for 3 lines and 1 sphere in Table 6.1, it remains to characterize the configurations with infinitely many real solutions. If the three lines are not pairwise skew, then all real common transversals lie in the same plane or pass through a point of intersection. Since the resulting characterization can be easily established, we can assume that the three lines are pairwise skew.

It is well-known that the common transversals of three pairwise skew lines define a hyperboloid of one sheet (see, e.g., [11]). By applying a translation and a rotation, the hyperboloid can be transformed into

$$\frac{x_1^2}{\alpha^2} + \frac{x_2^2}{\beta^2} - \frac{x_3^2}{\gamma^2} = 1 \qquad \text{with } \alpha, \beta, \gamma > 0 \,. \tag{6.1}$$

This transformation changes the center of the sphere into some new center $c = (c_1, c_2, c_3)^T \in \mathbb{R}^3$. Now the characterization of infinitely many solutions is given by the following statement.

Theorem 6.4. *Let ℓ_1, ℓ_2, ℓ_3 be three pairwise skew lines whose common transversals generate a hyperboloid of the form (6.1), and let S_4 be a sphere with center $c \in \mathbb{R}^3$ and radius $r > 0$. Then there exist infinitely many lines simultaneously transversal to ℓ_1, ℓ_2, ℓ_3 and tangent to S_4 if and only if $c_1 = c_2 = 0$, $\alpha = \beta$, and in the x_1x_3-plane the circle $x_1^2 + (x_3 - c_3)^2 = r^2$ is a tangent circle to both branches of the hyperbola $x_1^2/\alpha^2 - x_3^2/\gamma^2 = 1$.*

Proof. The hyperboloid (6.1) can be parametrized by one of the two sets of generating lines. In particular, this hyperboloid is generated by the set of lines

$$\left\{ (x_1, x_2, 0)^T + \lambda \left(-\frac{\alpha}{\beta\gamma} x_2, \frac{\beta}{\alpha\gamma} x_1, 1 \right)^T : \lambda \in \mathbb{R} \right\}, \quad \text{where } \frac{x_1^2}{\alpha^2} + \frac{x_2^2}{\beta^2} = 1 \tag{6.2}$$

(see, e.g., [82]). By the upper bound of 4 in Lemma 6.3, we see that either this parametrization contains at most 4 tangents to the sphere or *all* lines in the parametrization are tangent to the sphere.

First assume that there are infinitely many lines transversal to the three lines and tangent to the sphere; thus all lines in the parametrization are tangents. Specifically, we

consider the following lines in the parametrization:

$$
\begin{aligned}
g_1 &= \left\{ \left(\alpha, \lambda\frac{\beta}{\gamma}, \lambda \right)^T : \lambda \in \mathbb{R} \right\} \quad (i.e., (x_1, x_2) = (\alpha, 0)) \,, \\[2mm]
g_2 &= \left\{ \left(-\alpha, -\lambda\frac{\beta}{\gamma}, \lambda \right)^T : \lambda \in \mathbb{R} \right\} \quad (i.e., (x_1, x_2) = (-\alpha, 0)) \,, \\[2mm]
g_3 &= \left\{ \left(-\lambda\frac{\alpha}{\gamma}, \beta, \lambda \right)^T : \lambda \in \mathbb{R} \right\} \quad (i.e., (x_1, x_2) = (0, \beta)) \,, \\[2mm]
g_4 &= \left\{ \left(\lambda\frac{\alpha}{\gamma}, -\beta, \lambda \right)^T : \lambda \in \mathbb{R} \right\} \quad (i.e., (x_1, x_2) = (0, -\beta)) \,.
\end{aligned}
$$

The condition that the center c must have the same distance from g_1 and g_2 gives the equation

$$
\alpha(\beta^2 + \gamma^2)c_1 + \beta\gamma c_2 c_3 = 0 \,,
$$

and the equality of distances from g_3 and g_4 gives the distances

$$
\beta(\alpha^2 + \gamma^2)c_2 - \alpha\gamma c_1 c_3 = 0 \,.
$$

Since $\alpha, \beta, \gamma > 0$, the common solutions of these equations have $c_1 = c_2 = 0$. Using this information, the equality of the distances from the first and third lines gives $\alpha = \beta$, or $c_3 = \pm\sqrt{(\alpha^2 + \gamma^2)(\beta^2 + \gamma^2)}/\gamma$. To eliminate this second possibility, consider two more lines in the ruling of the hyperboloid

$$
\begin{aligned}
g_5 &= \left\{ \left(\frac{\alpha}{\sqrt{2}}\left(1 - \frac{\lambda}{\gamma}\right), \frac{\beta}{\sqrt{2}}\left(1 + \frac{\lambda}{\gamma}\right), \lambda \right)^T : \lambda \in \mathbb{R} \right\} \left(i.e., (x_1, x_2) = \left(\frac{\alpha}{\sqrt{2}}, \frac{\beta}{\sqrt{2}} \right) \right), \\[2mm]
g_6 &= \left\{ \left(\frac{\alpha}{\sqrt{2}}\left(1 + \frac{\lambda}{\gamma}\right), \frac{\beta}{\sqrt{2}}\left(-1 + \frac{\lambda}{\gamma}\right), \lambda \right)^T : \lambda \in \mathbb{R} \right\} \left(i.e., (x_1, x_2) = \left(\frac{\alpha}{\sqrt{2}}, \frac{-\beta}{\sqrt{2}} \right) \right).
\end{aligned}
$$

The equality of distances from these two lines together with $c_1 = c_2 = 0$ gives $\alpha = \beta$ or $c_3 = 0$. Therefore the only case when c can be at the same distance from all lines in the ruling (6.2) is when $\alpha = \beta$. Hence, since $c_1 = c_2 = 0$ and $\alpha = \beta$, both the hyperboloid and the sphere are rotational symmetric with respect to the x_3-axis, and it suffices to consider the section through the $x_1 x_3$-plane. In this section, the circle $x_1^2 + (x_3 - c_3)^2 = r^2$ must be a tangent circle to both branches of the hyperbola $x_1^2/\alpha^2 - x_3^2/\gamma^2 = 1$.

If, conversely, $c_1 = c_2 = 0$, $\alpha = \beta$, and in the $x_1 x_3$-plane, the circle $x_1^2 + (x_3 - c_3)^2 = r^2$ is a tangent circle to the hyperbola $x_1^2/\alpha^2 - x_3^2/\gamma^2 = 1$, then the rotational symmetry implies that every line in the hyperboloid $x_1^2/\alpha^2 + x_2^2/\beta^2 - x_3^2/\gamma^2 = 1$ is tangent to the sphere S_4. Hence, there are infinitely many common tangents. $\qquad\square$
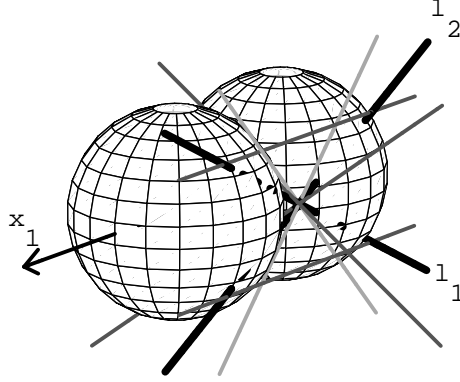
Fig. 6.2: The figure shows a construction with 2 lines and 2 spheres, leading to 6 distinct solutions. The two tangents lying in the plane $x_2 = \beta$ and passing through $(0, \beta, 0)^T$ are drawn in light grey. The other four tangents are drawn in dark grey.

Lemma 6.5. $N_2 = 8$.

Proof. Since $N_2 \leq 8$, it suffices to give a construction with 2 lines and 2 spheres of the same radius, leading to 8 solutions. We start from the following configuration with 6 distinct solutions. The two spheres are symmetrically located on the x_1-axis: $c_3 = (\gamma, 0, 0)^T$, $c_4 = (-\gamma, 0, 0)^T$; the radius r will be specified below. The lines ℓ_1 and ℓ_2 are chosen in a plane $x_2 = \beta$ for some $\beta > 0$ such that the lines intersect in $(0, \beta, 0)^T$. Hence, every common transversal of the two lines either lies in the plane $x_2 = \beta$ or passes through the point $(0, \beta, 0)^T$. If the two spheres intersect with each other, and $\beta < r$, and $(0, \beta, 0)^T$ is not contained in the union of the spheres $S(c_3, r)$, $S(c_4, r)$, then there are exactly 6 distinct lines which are tangents to the spheres and transversal to the given lines and tangent to the given spheres (see Figure 6.2): two tangents pass through $(0, \beta, 0)^T$ and lie in the plane $x_1 = 0$; two tangents lie in the plane $x_2 = \beta$ and are parallel to the x_1-axis; and two tangents lie in the plane $x_2 = \beta$ and pass through $(0, \beta, 0)^T$. For the following considerations it is quite useful to have a succinct description of the last two tangents and also to work with integer coefficients for β, γ, and r. In particular, we will force the two tangents in the plane $x_2 = \beta$ and passing through $(0, \beta, 0)^T$ to be of the form $(0, \beta, 0)^T + \lambda(1, 0, \pm 1)^T$. In order to obtain these tangents, β, γ and r have to satisfy $\beta^2 + \gamma^2/2 = r^2$ and $r > \gamma$. An appropriate choice is $\beta = 7$, $\gamma = 8$, and $r = 9$, so that the tangents of the last type are

$$t_1 := \left\{ (0, 7, 0)^T + \lambda(1, 0, 1)^T \; : \; \lambda \in \mathbb{R} \right\} \quad \text{and} \quad t_2 := \left\{ (0, 7, 0)^T + \lambda(1, 0, -1)^T \; : \; \lambda \in \mathbb{R} \right\} .$$

Now the key observation is that these two tangents have multiplicity 2. In order to prove this we consider the system of equations in Plücker coordinates stemming from (2.4)

and (2.6). Independent of the specific choice of lines ℓ_1, ℓ_2 with the above properties, the common transversals of ℓ_1 and ℓ_2 are given by the common zeroes of the two linear, homogeneous polynomials

$$
\begin{aligned}
f_1 &= -7p_{03} + p_{23}, \\
f_2 &= 7p_{01} + p_{12}.
\end{aligned}
$$

The quadratic equations resulting from the spheres $S(c_3, r)$ and $S(c_4, r)$ are

$$
\begin{aligned}
f_3 &= -81p_{01}^2 - 17p_{02}^2 - 17p_{03}^2 - 16p_{02}p_{12} + p_{12}^2 - 16p_{03}p_{13} + p_{13}^2 + p_{23}^2, \\
f_4 &= -81p_{01}^2 - 17p_{02}^2 - 17p_{03}^2 + 16p_{02}p_{12} + p_{12}^2 + 16p_{03}p_{13} + p_{13}^2 + p_{23}^2.
\end{aligned}
$$

Furthermore let $f_5 = p_{01}p_{23} - p_{02}p_{13} + p_{03}p_{12}$ be the polynomial of the Plücker relation (2.2).

The tangent t_1 has Plücker coordinate $(1, 0, 1, -7, 0, 7)^T$. In order to compute the multiplicity of this solution, we follow the method and the notation in [32, §4.4]. First we pass to an affine version of the polynomials by adding the polynomial $f_6 = p_{01} - 1$; this forces $p_{01} = 1$ in any common zero of the system. Then we move the point t_1 to the origin by applying the linear variable transformation

$$
(p_{01}, p_{02}, p_{03}, p_{12}, p_{13}, p_{23})^T = (q_{01}, q_{02}, q_{03}, q_{12}, q_{13}, q_{23})^T + (1, 0, 1, -7, 0, 7)^T.
$$

The local intersection multiplicity μ can be computed as the vector space dimension of the quotient ring

$$
\mu = \dim R_l / I_l,
$$

where $R_l := \mathbb{C}[q_{01}, \ldots, q_{23}]_{\langle q_{01}, \ldots, q_{23} \rangle}$ is the local ring whose elements are the rational functions in $q_{01}, \ldots, q_{23}$ with non-vanishing denominator at 0. I_l is the ideal defined by $f_1, \ldots, f_6$ in the local ring R_l.

In order to compute μ, we use the fact that in case of finite dimension

$$
\dim R_l / I_l = \dim R_l / \langle \mathrm{LT}(I_l) \rangle,
$$

where $\langle \mathrm{LT}(I_l) \rangle$ denotes the ideal generated by the leading terms of I_l (see, e.g., [32, Corollary 4.5 in Chapter 4]). This dimension can be easily extracted from a standard basis of I_l (For the convenience of the reader, a short review of standard bases can be found in Section 6.1.2). Since by our choice of β, γ, and r, all coefficients are integers, we can apply a computer algebra package (such as SINGULAR [62]), to compute a standard basis $\{h_1, \ldots, h_6\}$ of the ideal I_l with respect to anti-graded reverse lexicographical order:

$$
\begin{aligned}
h_1 &= q_{01}, \\
h_2 &= 112q_{02} + 34q_{03} + 14q_{12} - 16q_{13}, \\
h_3 &= 14q_{03} + q_{12}, \\
h_4 &= q_{12}, \\
h_5 &= 64q_{23}, \\
h_6 &= 112q_{13}^2.
\end{aligned}
$$
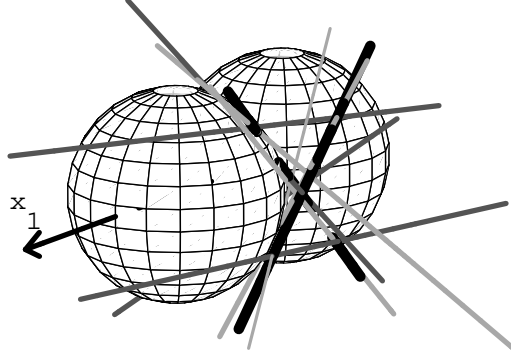
Fig. 6.3: Construction with 2 lines and 2 spheres, leading to 8 distinct solutions

Hence, the leading monomials of $h_1, \ldots, h_6$ with respect to anti-graded reverse lexicographical order are q_{01}, q_{02}, q_{03}, q_{12}, q_{23}, q_{13}^2. The desired multiplicity μ is the cardinality of the set of cosets $\{1 + I_l, q_{13} + I_l\}$, which implies $\mu = 2$. By symmetry, the tangent t_2 has multiplicity 2 as well.

Now we choose one particular configuration of the presented class, namely the one with $\ell_1 := t_1$ and $\ell_2 := t_2$. By perturbing this configuration, the two double solutions will split into four distinct solutions: first, we slightly increase the x_2-coordinate of the line ℓ_2, so that the resulting line ℓ_2' becomes $(0, \beta', 0)^T + \lambda(1, 0, -1)^T$ for some $\beta' > \beta$. In this process, the double tangent t_1 splits into two tangents t_1^a and t_1^b intersecting ℓ_1 and ℓ_2' in different orders; i.e., one of the tangents t_1^a, t_1^b touches ℓ_1, ℓ_2, S_3, and S_4 in the order $(S_3, \ell_1, \ell_2, S_4)$, and one of them in the order $(S_3, \ell_2, \ell_1, S_4)$. However, the tangent t_2 is still a double zero of the system of polynomials, since the parallel lines t_2 and ℓ_2' intersect in the plane at infinity of $\mathbb{P}_{\mathbb{R}}^3$.

Similarly, we can make the double tangent t_2 split into two tangents by slightly decreasing the x_2-coordinate of the line ℓ_1; denote the resulting line by ℓ_1'. Figure 6.3 shows the configuration for ℓ_1' passing through the points $(0, 6.5, 0)^T$, $(2, 6.5, 2)^T$, and ℓ_2' passing through the points $(0, 7.5, 0)^T$, $(2, 7.5, -2)^T$. □

For N_3 the situation is more involved. The Bézout bound gives 16, but in fact, the number of solutions in $\mathbb{C}^3$ is bounded by 12. As in the discussion of the common tangents to four spheres in Section 4.2, the remaining solutions are located in the plane at infinity. Specifically, we will show that there are always two solutions at infinity with multiplicity at least 2.

Let us recall the framework from Section 4.2. The sphere with center $(c_1, c_2, c_3)^T \in \mathbb{R}^3$ and radius r has the homogeneous equation in $\mathbb{P}^3$:

$$(x_1 - c_1 x_0)^2 + (x_2 - c_2 x_0)^2 + (x_3 - c_3 x_0)^2 = r^2 x_0^2.$$

In the plane at infinity $x_0 = 0$, this gives the equation

$$x_1^2 + x_2^2 + x_3^2 = 0,$$

which is independent of the center and the radius. Let ω denote this conic section in the plane at infinity. Later in the proof, we will work in the space of lines in $\mathbb{P}^3$. In that situation, we will have to consider those tangents through any point $z \in \omega$ in the plane at infinity rather than z itself. For this reason, we provide a characterization of these tangents:

Lemma 6.6. *Let $z = (0, z_1, z_2, z_3)^T \in \omega$. The tangent to the conic ω at z which lies in the plane at infinity has Plücker coordinate*

$$(p_{01}, p_{02}, p_{03}, p_{12}, p_{13}, p_{23})^T = (0, 0, 0, z_3, -z_2, z_1)^T.$$

In particular, the tangent contains the points $(0, -z_2, z_1, 0)^T$, $(0, z_3, 0, -z_1)^T$, and $(0, 0, -z_3, z_2)^T$.

Proof. Since $z_0 = 0$ we can compute in projective plane $\mathbb{P}^2$; so let $\overline{z} = (z_1, z_2, z_3)^T$. The conic section

$$x^T A x = 0 \qquad \text{with } A = \begin{pmatrix} 1 & 0 & 0 \\ 0 & 1 & 0 \\ 0 & 0 & 1 \end{pmatrix}$$

is regular in $\overline{z}$ with tangent $\{y = (y_1, y_2, y_3)^T \in \mathbb{P}^2 : \overline{z}^T A y = 0\}$. In particular, $(-z_2, z_1, 0)^T$, $(z_3, 0, -z_1)^T$, $(0, -z_3, z_2)^T$, and $\overline{z}$ itself lie on this tangent. Now any two of these points can be used to compute the Plücker coordinate of the tangent line. $\square$

Consider a configuration with a line ℓ_1 and three spheres in $\mathbb{R}^3$. Since we consider the spheres as quadrics, we denote them by Q_2, Q_3, and Q_4. The idea to prove the double solutions at infinity is to transfer the geometry of ω to the space of lines in $\mathbb{P}^3$. More precisely, let t be a tangent to ω at z in the plane at infinity. Since the quadrics $\wedge^2 Q_2, \wedge^2 Q_3, \wedge^2 Q_4 \in \mathbb{P}^5$ characterize the tangents to Q_2, Q_3, Q_4, the Plücker vector p_t of t is contained in $\wedge^2 Q_2$, $\wedge^2 Q_3$, and $\wedge^2 Q_4$. Let Ω denote the quadric in $\mathbb{P}^5$ defined by the Plücker equation (2.2). Since t is a line in $\mathbb{P}^3$, t is also contained in Ω. We will show that the tangent hyperplanes to the quadrics $\wedge^2 Q_2$, $\wedge^2 Q_3$, $\wedge^2 Q_4$, Ω at p_t contain a common subspace of dimension 2. In connection with the linear form defined by the transversals of the line ℓ_1, this will prove the multiplicity of at least 2.

Let us investigate the spheres Q_2, Q_3, Q_4 first. For $i \in \{2, 3, 4\}$, we are looking for lines whose Plücker vectors lie in the tangent hyperplane of $\wedge^2 Q_i$ at p_t. The geometric concept behind this relation is *polarity*. Recall that the polar plane of a point $a \in \mathbb{P}^n$ with respect to an arbitrary quadric Q is defined by

$$\{y \in \mathbb{P}^n : a^T Q y = 0\}.$$

If $a \in Q$ then the polar hyperplane is a tangent hyperplane. The polar line of a line $\ell \in \mathbb{P}^3$ is defined by

$$\{y \in \mathbb{P}^3 \ : \ a^T Q y = 0 \text{ for all } a \in \ell\} \, .$$

The following lemma establishes a connection between the tangent hyperplanes to $\wedge^2 Q$ and the concept of polarity for a quadric Q.

Lemma 6.7. *Let t be a tangent line to a quadric $Q \subset \mathbb{P}^3$, and let the point $a \in \mathbb{P}^3$ be contained in the polar line of t. Then, for any line ℓ containing a, the Plücker vector p_ℓ of ℓ is contained in the tangent hyperplane to $\wedge^2 Q$ at p_t, i.e., $p_t^T (\wedge^2 Q) p_\ell = 0$.*

Proof. Let T be a representation of t by a 4×2-matrix as described in the Section 2.3. Further let b be a point on ℓ with $b \neq a$, and let $L = (a, b)$ be a representation of ℓ by a 4×2-matrix. Since a is contained in the polar line of t, we have $T^T Q a = (0, 0)^T$. Hence, by reasoning as in Lemma 2.11, we can conclude

$$p_t^T (\wedge^2 Q) p_\ell = \det(T^T Q L) = 0 \, . \qquad \square$$

In particular, the following version of a well-known relationship (see, e.g., [100]) shows that the precondition of Lemma 6.7 is satisfied if $a = t \cap Q$.

Lemma 6.8. *If t is tangent to a quadric Q at some point a, then a is contained in the polar line of t.*

Proof. Let $y \neq a$ be a point on t. Since t lies on the polar plane (namely, the tangent plane) of a with respect to Q, we have $a^T Q y = 0$. Since also $a^T Q a = 0$, a lies on the polar line of t with respect to Q. $\qquad \square$

Finally, we are ready to prove the upper bound for N_3.

Lemma 6.9. $N_3 \leq 12$.

Proof. Let L_1 be the hyperplane (2.4) in $\mathbb{P}^5$ characterizing the transversals of the line ℓ_1, that is, any point on L_1 which satisfies the Plücker relation is the Plücker coordinate of a transversal to ℓ_1. Let $\wedge^2 Q_2, \wedge^2 Q_3, \wedge^2 Q_4$ be the quadrics (2.6) characterizing the tangents to the three spheres. Further let $z = (0, z_1, z_2, z_3)^T \in \omega$, and let $\pi \subset \Omega \subset \mathbb{P}^5$ be the set of Plücker vectors whose corresponding lines in $\mathbb{P}^3$ pass through z. π can be written as the image of the projective mapping $h : \mathbb{P}^3 \to \Omega \subset \mathbb{P}^5$,

$$h(y_0, y_1, y_2, y_3) = \wedge^2 \begin{pmatrix} 0 & y_0 \\ z_1 & y_1 \\ z_2 & y_2 \\ z_3 & y_3 \end{pmatrix} \, .$$

Since h is linear, it follows that π is a two-dimensional plane in $\mathbb{P}^5$ with $\pi \subset \Omega$.

Let t be the tangent to ω at z in the plane at infinity. By Lemmas 6.8 and 6.7, π is contained in the tangent hyperplane to $\wedge^2 Q_i$ at p_t, $2 \le i \le 4$.

In order to show that π is also contained in the tangent hyperplane to Ω at p_t, let y be a point different from z, and let ℓ be a line through z and y. Then, by Lemma 6.6, the Plücker vectors p_t and p_ℓ satisfy

$$
\begin{aligned}
p_t^T \Omega p_\ell &= (0,0,0,z_3,-z_2,z_1) \cdot \frac{1}{2} \begin{pmatrix} 0 & 0 & 0 & 0 & 0 & 1 \\ 0 & 0 & 0 & 0 & -1 & 0 \\ 0 & 0 & 0 & 1 & 0 & 0 \\ 0 & 0 & 1 & 0 & 0 & 0 \\ 0 & -1 & 0 & 0 & 0 & 0 \\ 1 & 0 & 0 & 0 & 0 & 0 \end{pmatrix} \cdot \begin{pmatrix} -z_1 y_0 \\ -z_2 y_0 \\ -z_3 y_0 \\ z_1 y_2 - z_2 y_1 \\ z_1 y_3 - z_3 y_1 \\ z_2 y_3 - z_3 y_2 \end{pmatrix} \\
&= -\frac{1}{2} y_0 (z_1^2 + z_2^2 + z_3^2) \\
&= 0 \,.
\end{aligned}
$$

Hence, the four tangent hyperplanes of $\wedge^2 Q_2$, $\wedge^2 Q_3$, $\wedge^2 Q_4$, Ω at p_t contain a common subspace of dimension at least 2. By Lemma 6.6, the tangents to the conic ω lie on a conic $\overline{\omega}$, namely on

$$
p_{12}^2 + p_{13}^2 + p_{23}^2 = 0 \,,
$$

in the two-dimensional subspace of $\mathbb{P}^5$ given by $p_{01} = p_{02} = p_{03} = 0$. The restriction of the hyperplane L_1 to the subspace $p_{01} = p_{02} = p_{03} = 0$ defines a one-dimensional subspace $\overline{L_1}$. Since $\overline{L_1}$ is one-dimensional, it intersects with $\overline{\omega}$ at two points $b_1, b_2 \in \mathbb{P}^5$ in the plane $p_{01} = p_{02} = p_{03} = 0$. Further, since b_1 and b_2 satisfy the Plücker relation, they are Plücker vectors of some tangents t_1 and t_2 to ω. Altogether, the five tangent hyperplanes of $\wedge^2 Q_2$, $\wedge^2 Q_3$, $\wedge^2 Q_4$, Ω, L_1 at b_1 and b_2 contain a common subspace of dimension at least 1. Hence, the tangent hyperplanes are not independent, which implies that the multiplicity of intersection in b_1 and b_2 is at least 2 (see, e.g., [97, p. 115]). $\square$

In order to show that $N_3 = 12$ it remains to give a construction with one line ℓ_1 and three spheres S_2, S_3, S_4 of the same radius r, leading to 12 real solutions. Let ℓ_1 be the x_3-axis, and let the centers c_2, c_3, c_4 of the spheres constitute an equilateral triangle with edge length 1 in the $x_1 x_2$-plane, say $c_2 = (\sqrt{3}/3, 0, 0)^T$, $c_3 = (-\sqrt{3}/6, 1/2, 0)^T$, $c_4 = (-\sqrt{3}/6, -1/2, 0)^T$ (see Figure 6.4). For $1/2 < r < \sqrt{3}/3$, the spheres are non-disjoint, and none of them contains the origin.

Let t be a line which intersects ℓ_1, and let H be the plane containing t and ℓ_1. The three cuts $H \cap \operatorname{conv}(S_1)$, $H \cap \operatorname{conv}(S_2)$, and $H \cap \operatorname{conv}(S_3)$ are discs (maybe degenerated to single points or empty sets). Unless H is equidistant to two of the centers, one of these discs is strictly contained in one of the other two. Hence, any line transversal to the line and tangent to the spheres lies in one of the three planes which contain the x_3-axis and which are equidistant to two of the centers.
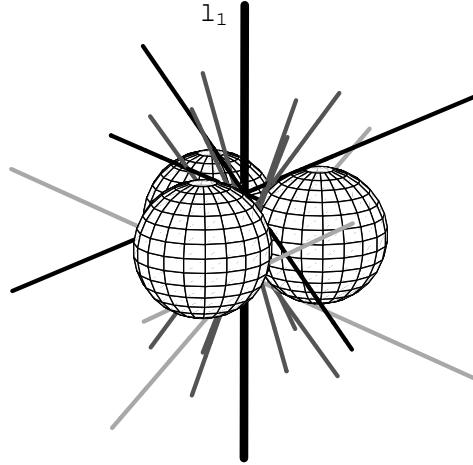
Fig. 6.4: Construction with one line and 3 spheres, leading to 12 solutions

For example, one of these planes is the $x_1 x_3$-plane, which is equidistant to c_2 and c_3. The section through this plane contains two disjoint discs: one representing the (identical) intersections of the plane with $\text{conv}(S_2)$ and $\text{conv}(S_3)$, and the second one because of $\text{conv}(B_1)$. These two discs are separated by the line ℓ_1. Hence, in this plane there are 4 common tangents. Altogether, since there are three planes of this kind, we have 12 common tangents.

6.1.2 Appendix: Standard bases

In Section 6.1.1, we have applied standard bases in local rings. In this appendix to that section, we review the definitions of a standard basis, starting from Gröbner basis theory (see [32]). The theory of Gröbner bases provides computational methods to find "nice" generators for an ideal I in a polynomial ring $\mathbb{C}[x_1, \dots, x_n]$. The theory of *standard bases* extends this theory for ideals in local rings. More precisely, let $R_l := \mathbb{C}[x_1, \dots, x_n]_{\langle x_1, \dots, x_n \rangle}$ be the set of rational functions f/g in $x_1, \dots, x_n$ with $g(0, \dots, 0) \neq 0$. R_l defines a *local* ring, i.e., it contains exactly one maximal ideal. Since the algebraic-geometric definitions of intersection multiplicities are related to the concept of local rings, standard bases provide a powerful tool to effectively compute intersection multiplicities.

From the various possible term orders, we restrict ourselves to consider the *anti-graded reverse lexicographical order* (arevlex). For $\alpha, \beta \in \mathbb{N}_0^n$, We have $x^\alpha >_{arevlex} x^\beta$ if and only if

$$\sum_{i=1}^n \alpha_i < \sum_{i=1}^n \beta_i,$$

or

$$\sum_{i=1}^{n} \alpha_i = \sum_{i=1}^{n} \beta_i \quad \text{and} \quad x^\alpha >_{revlex} x^\beta,$$

where $>_{revlex}$ denotes the reverse lexicographical order of Gröbner basis theory. For any polynomial f, the leading term of f, denoted $\mathrm{LT}(f)$, is the maximal term of f with regard to the arevlex-order.

For an ideal I in R_l, the *set of leading terms of I*, abbreviated $\mathrm{LT}(I)$, is the set of leading terms of elements of I.

A *standard basis* of I is a set $\{g_1, \ldots, g_t\} \subset I$ such that $\langle \mathrm{LT}(I) \rangle = \langle \mathrm{LT}(g_1), \ldots, \mathrm{LT}(g_t) \rangle$. Given a set of polynomial generators of I, a standard basis of I can be effectively computed by variants of the Buchberger algorithm.

6.2 Two lines and two quadrics

Here, we prove Theorem 6.2 and provide the characterization of two lines and two spheres with infinitely many real common tangent lines.

The section is structured as follows. In Section 6.2.1, we characterize the set of lines transversal to two skew lines and tangent to a quadric in terms of algebraic curves; we study and classify these so-called $(2,2)$-*curves*. In Section 6.2.2, we discuss a normal form for the subclass of generic curves, which we call asymmetric smooth $(2,2)$-curves. Then, in Section 6.2.3, we study the set of quadrics which (for prescribed lines ℓ_1 and ℓ_2) lead to most $(2,2)$-curves. This includes computer-algebraic calculations, based on which we establish the proof of Theorem 6.2. In Section 6.2.4, we give some detailed examples illustrating the geometry described by Theorem 6.2, and complete its proof. Finally, in Section 6.2.5, we solve the original question of spheres and give the complete characterization of configurations of two lines and two spheres having infinitely many lines transversal to the lines and tangent to the spheres. For a precise statement of that characterization see Theorems 6.21 and 6.25. Section 6.2.6 serves an appendix to the current section and contains annotated computer code used in the proof of Theorem 6.2.

6.2.1 Lines in $\mathbb{P}^3$ meeting 2 lines and tangent to a quadric

We work here over the ground field $\mathbb{C}$. First suppose that ℓ_1 and ℓ_2 are lines in $\mathbb{P}^3$ that meet at a point p and thus span a plane Π. Then the common transversals to ℓ_1 and ℓ_2 either contain p or they lie in the plane Π. This reduces any problem involving common transversals to ℓ_1 and ℓ_2 to a planar problem in $\mathbb{P}^2$ (or $\mathbb{R}^2$), and so we shall always assume that ℓ_1 and ℓ_2 are skew. Such lines have the form

$$
\begin{aligned}
\ell_1 &= \{wa + xb \,:\, [w, x] \in \mathbb{P}^1\}, \\
\ell_2 &= \{yc + zd \,:\, [y, z] \in \mathbb{P}^1\}
\end{aligned}
\tag{6.3}
$$

where the points $a, b, c, d \in \mathbb{P}^3$ are affinely independent. We describe the set of lines meeting ℓ_1 and ℓ_2 that are also tangent to a smooth quadric Q. We will refer to this set as the *envelope* of common transversals and tangents, or (when ℓ_1 and ℓ_2 are understood) simply as the envelope of Q.

The parametrization of (6.3) allows us to identify each of ℓ_1 and ℓ_2 with $\mathbb{P}^1$; the point $wa + xb \in \ell_1$ is identified with the parameter value $[w, x] \in \mathbb{P}^1$, and the same for ℓ_2. We will use these identifications throughout this section. In this way, any line meeting ℓ_1 and ℓ_2 can be identified with the pair $([w, x], [y, z]) \in \mathbb{P}^1 \times \mathbb{P}^1$ corresponding to its intersections with ℓ_1 and ℓ_2. By (2.4), the Plücker coordinates $p_\ell = p_\ell(w, x, y, z)$ of the transversal ℓ passing through the points $wa + xb$ and $yc + zd$ are separately homogeneous of degree 1 in each set of variables $\{w, x\}$ and $\{y, z\}$, called *bihomogeneous* of *bidegree* (1,1) (see, e.g., [31, §8.5]).

By Lemma 2.11, the envelope of common transversals to ℓ_1 and ℓ_2 that are also tangent to Q is given by the common transversals ℓ of ℓ_1 and ℓ_2 whose Plücker coordinates p_ℓ additionally satisfy $p_\ell(\wedge^2 Q)p_\ell = 0$. This yields a homogeneous equation

$$F(w, x, y, z) := p_\ell(w, x, y, z)^T(\wedge^2 Q)p_\ell(w, x, y, z) = 0 \tag{6.4}$$

of degree four in the variables w, x, y, z. More precisely, F has the form

$$F(w, x, y, z) = \sum_{i,j=0}^{2} c_{ij} w^i x^{2-i} y^j z^{2-j} \tag{6.5}$$

with coefficients c_{ij}, that is F is bihomogeneous with bidegree $(2, 2)$. The zero set of a (non-zero) bihomogeneous polynomial defines an algebraic curve in $\mathbb{P}^1 \times \mathbb{P}^1$ (see the treatment of projective elimination theory in [31, §8.5]). In correspondence with its bidegree, the curve defined by F is called a $(2, 2)$-*curve*. The nine coefficients of this polynomial identify the set of $(2, 2)$-curves with $\mathbb{P}^8$.

It is well-known that the Cartesian product $\mathbb{P}^1 \times \mathbb{P}^1$ is isomorphic to a smooth quadric surface in $\mathbb{P}^3$ [31, Proposition 10 in § 8.6]. Thus the set of lines meeting ℓ_1 and ℓ_2 and tangent to the quadric Q is described as the intersection of two quadrics in a projective 3-space. When it is smooth, this set is a genus 1 curve [71, Exer. I.7.2(d) and Exer. II.8.4(g)]. This set of lines cannot be parametrized by polynomials—only genus 0 curves (also called rational curves) admit such parametrizations (see, e.g., [123, Corollary 2 on p.268]). This observation is the starting point for our study of common transversals and tangents.

Let C be a $(2, 2)$-curve in $\mathbb{P}^1 \times \mathbb{P}^1$ defined by a bihomogeneous polynomial F of bidegree 2. The components of C correspond to the irreducible factors of F, which are bihomogeneous of bidegree at most $(2, 2)$. Thus any factors of F must have bidegree one of $(2, 2)$, $(2, 1)$, $(1, 1)$, $(1, 0)$, or $(0, 1)$. (Since we are working over $\mathbb{C}$, a homogeneous quadratic of bidegree $(2, 0)$ factors into two linear factors of bidegree $(1, 0)$.) Recall (for example, [31]) a point $([w_0, x_0], [y_0, z_0]) \in C \subset \mathbb{P}^1 \times \mathbb{P}^1$ is *singular* if the gradient ∇F vanishes at that point, $\nabla F([w_0, x_0], [y_0, z_0]) = 0$. The curve C is *smooth* if it does not contain a singular point; otherwise C is *singular*. We classify $(2, 2)$-curves, up to change

of coordinates on $\ell_1 \times \ell_2$, and interchange of ℓ_1 and ℓ_2. Note that an (a, b)-curve and a (c, d)-curve meet if either $ad \neq 0$ or $bc \neq 0$, and the intersection points are singular on the union of the two curves.

Lemma 6.10. *Let C be a $(2, 2)$-curve on $\mathbb{P}^1 \times \mathbb{P}^1$. Then, up to interchanging the factors of $\mathbb{P}^1 \times \mathbb{P}^1$, C is either*

1. *smooth and irreducible,*

2. *singular and irreducible,*

3. *the union of a $(1, 0)$-curve and an irreducible $(1, 2)$-curve,*

4. *the union of two distinct irreducible $(1, 1)$-curves,*

5. *a single irreducible $(1, 1)$-curve, of multiplicity two,*

6. *the union of one irreducible $(1, 1)$-curve, one $(1, 0)$-curve, and one $(0, 1)$-curve,*

7. *the union of two distinct $(1, 0)$-curves, and two distinct $(0, 1)$-curves,*

8. *the union of two distinct $(1, 0)$-curves, and one $(0, 1)$-curve of multiplicity two,*

9. *the union of one $(1, 0)$-curve, and one $(0, 1)$-curve, both of multiplicity two.*

In particular, when C is smooth it is also irreducible.

When the polynomial F has repeated factors, we are in cases (5), (8), or (9). We study the form F when the quadric is reducible, that is either when Q has rank 1, so that it defines a double plane, or when Q has rank 2 so that it defines the union of two planes.

Lemma 6.11. *Suppose Q is a reducible quadric.*

(1) If Q has rank 1, then $\wedge^2 Q = 0$, and so the form F in (6.4) is identically zero.

(2) Suppose Q has rank 2, so that it defines the union of two planes meeting in a line ℓ. If ℓ is one of ℓ_1 or ℓ_2, then the form F in (6.4) is identically zero. Otherwise the form F is the square of a $(1, 1)$-form, and hence we are in cases (5) or (9) of Lemma 6.10.

Proof. The first statement is immediate. For the second, let ℓ' be a line in $\mathbb{P}^3$ with Plücker coordinates $p_{\ell'}$. From the algebraic characterization of tangency of Lemma 2.11, $p_{\ell'}^T (\wedge^2 Q) p_{\ell'} = 0$ implies that the restriction of the quadratic form to ℓ' either has a zero of multiplicity two, or it vanishes identically. In either case, this implies that ℓ' meets the line ℓ common to the two planes. Conversely, if ℓ' meets the line ℓ, then $p_{\ell'}^T (\wedge^2 Q) p_{\ell'} = 0$.

Thus if ℓ equals one of ℓ_1 or ℓ_2, then $p_{\ell'}^T (\wedge^2 Q) p_{\ell'} = 0$ for every common transversal ℓ' to ℓ_1 and ℓ_2, and so the form F is identically zero. Suppose that ℓ is distinct from both ℓ_1 and ℓ_2. We observed earlier that the set of lines transversal to ℓ_1 and ℓ_2 that also meet ℓ is defined by a $(1, 1)$-form G. Since the $(2, 2)$-form F defines the same set as does the $(1, 1)$-form G, we must have that $F = G^2$, up to a constant factor. $\square$

As above, let C be defined by the polynomial F. For a fixed point $[w, x]$, the restriction of the polynomial F to $[w, x] \times \mathbb{P}^1$ is a homogeneous quadratic polynomial in y, z. A line passing through $[w, x] \in \ell_1$ and the point of ℓ_2 corresponding to any zero of this restriction is tangent to Q. This construction gives all lines tangent to Q that contain the point $[w, x]$. We call the zeroes of this restriction the *fiber over* $[w, x]$ of the projection of C to ℓ_1.

We investigate these fibers. Consider the polynomial F as a polynomial in the variables y, z with coefficients polynomials in w, x. The resulting quadratic polynomial in y, z has discriminant

$$\left(\sum_{i=0}^{2} c_{i1} w^i x^{2-i} \right)^2 \ - \ 4 \left(\sum_{i=0}^{2} c_{i0} w^i x^{2-i} \right) \left(\sum_{i=0}^{2} c_{i2} w^i x^{2-i} \right) \ . \tag{6.6}$$

Lemma 6.12. *If this discriminant vanishes identically, then the polynomial F has a repeated factor.*

Proof. Let α, β, γ be the coefficients of y^2, yz, z^2 in the polynomial F, respectively. Then we have $\beta^2 = 4\alpha\gamma$, as the discriminant vanishes. Since the ring of polynomials in w, x is a unique factorization domain, either α differs from γ by a constant factor, or else both α and γ are squares. If α and γ differ by a constant factor, then so do α and β. Writing $\beta = 2d\alpha$ for some $d \in \mathbb{C}$, we have

$$F \ = \ \alpha y^2 + 2d\alpha yz + d^2 \alpha z^2 \ = \ \alpha(y + dz)^2 \ .$$

If we have $\alpha = \delta^2$ and $\gamma = \sigma^2$ for some linear polynomials δ and σ, then

$$F \ = \ \delta^2 y \pm 2\delta\sigma yz + \sigma^2 z^2 \ = \ (\delta y \pm \sigma z)^2 \ .$$

$\square$

When F does not have repeated factors, the discriminant does not vanish identically. Then the fiber of C over the point $[w, x]$ of ℓ_1 consists of two distinct points exactly when the discriminant does not vanish at $[w, x]$. Since the discriminant has degree 4, there are at most four fibers of C consisting of a double point rather than two distinct points. We call the points $[w, x]$ of ℓ_1 whose fibers consist of such double points *ramification* points of the projection from C to ℓ_1.

This discussion shows how we may parametrize the curve C, at least locally. Suppose that we have a point $[w, x] \in \mathbb{P}^1$ where the discriminant (6.6) does not vanish. Then we may solve for $[y, z]$ in the polynomial F in terms of $[w, x]$. The different branches of the square root function give local parametrizations of the curve C.

6.2.2 *A normal form for asymmetric smooth $(2, 2)$-curves*

Recall that for any distinct points $a_1, a_2, a_3 \in \mathbb{P}^1$ and any distinct points $b_1, b_2, b_3 \in \mathbb{P}^1$, there exists a projective linear transformation (given by a regular 2×2-matrix) which maps a_i to b_i, $1 \leq i \leq 3$ [31, 106].

Lemma 6.13. *If the $(2,2)$-curve is smooth then the projection of C to ℓ_1 has four different ramification points.*

Proof. Changing coordinates on ℓ_1 and ℓ_2 by a projective linear transformation if necessary, we may assume that this projection to ℓ_1 is ramified over $[w,x] = [1,0]$, and the double root of the fiber is at $[y,z] = [1,0]$. Restricting the polynomial F (6.5) to the fiber over $[w,x] = [1,0]$ gives the equation

$$c_{22}y^2 + c_{21}yz + c_{20}z^2 \; = \; 0 \,.$$

Since we assumed that this has a double root at $[y,z] = [1,0]$, we have $c_{21} = c_{22} = 0$.

Suppose now that the projection from C to ℓ_1 is ramified at fewer than four points. We may assume that $[w,x] = [1,0]$ is a double root of the discriminant (6.6), which implies that the coefficients of w^4 and w^3x in (6.6) vanish. The previously derived condition $c_{21} = c_{22} = 0$ implies that the coefficient of w^4 vanishes and the coefficient of w^3x becomes $-4c_{20}c_{12}$. If $c_{20} = 0$, then every non-vanishing term of (6.5) depends on x; hence, x divides F, and so C is reducible, and hence not smooth. If $c_{12} = 0$ then the gradient ∇F vanishes at the point $([1,0],[1,0])$, and so C is not smooth. $\qquad\square$

Suppose that C is a smooth $(2,2)$-curve. Then its projection to ℓ_1 is ramified at four different points. We further assume that the double points in the ramified fibers project to at least 3 distinct points in ℓ_2. We call such a smooth $(2,2)$-curve *asymmetric*. The choice of this terminology will become clear in Section 6.2.4. We will give a normal form for such asymmetric smooth curves.

Hence, we may assume that three of the ramification points are $[w,x] = [0,1]$, $[1,0]$, and $[1,1]$, and the double points in these ramification fibers occur at $[y,z] = [0,1]$, $[1,0]$, and $[1,1]$, respectively. As in the proof of Lemma 6.13, the double point at $[y,z] = [1,0]$ in the fiber over $[w,x] = [1,0]$ implies that $c_{21} = c_{22} = 0$. Similarly, the double point at $[y,z] = [0,1]$ in the fiber over $[w,x] = [0,1]$ implies that $c_{00} = c_{01} = 0$. Thus the polynomial F (6.5) becomes

$$c_{20}w^2z^2 + c_{10}wxz^2 + c_{11}wxyz + c_{12}wxy^2 + c_{02}x^2y^2$$

Restricting F to the fiber of $[w,x] = [1,1]$ gives

$$c_{10}z^2 + c_{20}z^2 \; + \; c_{11}yz \; + \; c_{02}y^2 + c_{12}y^2 \,.$$

Since this has a double root at $[y,z] = [1,1]$, we must have

$$-\frac{1}{2}c_{11} \; = \; c_{10} + c_{20} \; = \; c_{02} + c_{12} \,.$$

Dehomogenizing (setting $c_{11} = -2$) and letting $c_{20} := s$ and $c_{02} := t$ for some $s,t \in \mathbb{C}$, we obtain the following theorem.

Theorem 6.14. *After projective linear transformations in ℓ_1 and ℓ_2, an asymmetric smooth $(2,2)$-curve is the zero set of a polynomial*

$$sw^2z^2 \;+\; (1{-}s)wxz^2 \;-\; 2wxyz \;+\; (1{-}t)wxy^2 \;+\; tx^2y^2\,, \tag{6.7}$$

for some $(s,t) \in \mathbb{C}^2$ satisfying

$$st(s{-}1)(t{-}1)(s{-}t) \;\neq\; 0\,. \tag{6.8}$$

We complete the proof of Theorem 6.14. The discriminant (6.6) of the polynomial (6.7) is

$$4wx(w{-}x)\,(s(t{-}1)w \;-\; t(s{-}1)x)\,,$$

which has roots at $[w,x] = [0,1], [1,0], [1,1]$, and $\alpha = [t(s{-}1),\, s(t{-}1)]$. Since we assumed that these are distinct, the fourth point α must differ from the first three, which implies that (s,t) satisfies (6.8). The double point in the fiber over α occurs at $[y,z] = [s{-}1, t{-}1]$. This equals a double point in another ramification fiber only for values of the parameters not allowed by (6.8).

Remark 6.15. These calculations show that smooth $(2,2)$-curves exhibit the following dichotomy. Either the double points in the ramification fibers project to four distinct points in ℓ_2 or to two distinct points. They must project to at least two points, as there are at most two points in each fiber of the projection to ℓ_2. We showed that if they project to at least three, then they project to four.

We compute the parameters s and t from the intrinsic geometry of the curve C. Recall the following definition of the cross ratio (see, for example [106, §1.1.4]).

Definition 6.16. *For four points $a_1, \ldots, a_4 \in \mathbb{P}^1$ with $a_i = [\alpha_i, \beta_i]$, the cross ratio of $a_1, \ldots, a_4$ is the point of $\mathbb{P}^1$ defined by*

$$\left[\frac{\det \begin{pmatrix} \alpha_1 & \alpha_4 \\ \beta_1 & \beta_4 \end{pmatrix}}{\det \begin{pmatrix} \alpha_1 & \alpha_3 \\ \beta_1 & \beta_3 \end{pmatrix}}\,,\; \frac{\det \begin{pmatrix} \alpha_2 & \alpha_4 \\ \beta_2 & \beta_4 \end{pmatrix}}{\det \begin{pmatrix} \alpha_2 & \alpha_3 \\ \beta_2 & \beta_3 \end{pmatrix}} \right]\,.$$

If the points are of the form $a_i = [1, \beta_i]$, this simplifies to

$$\left[\frac{\beta_4 - \beta_1}{\beta_3 - \beta_1}\,,\; \frac{\beta_4 - \beta_2}{\beta_3 - \beta_2} \right]\,.$$

The cross ratio of four points $a_1, a_2, a_3, a_4 \in \mathbb{P}^1$ remains invariant under any projective linear transformation.

The projection of C to ℓ_1 is ramified over the points $[w, x] = [0, 1], [1, 0], [1, 1]$ and $\alpha = [t(s-1), s(t-1)]$. The cross ratio of these four (ordered) ramification points is $[t(s-1), s(t-1)]$. Similarly, the cross ratio of the four (ordered) double points in the ramification fibers is $[s-1, t-1]$.

This computation of cross ratios allows us to compute the normal form of an asymmetric smooth $(2, 2)$-curve. Namely, let a_1, a_2, a_3, and a_4 be the four ramification points of the projection of C to ℓ_1 and b_1, b_2, b_3, and b_4 be the images in ℓ_2 of the corresponding double points. Let γ_1 be the cross ratio of the four points a_1, a_2, a_3, and a_4 (this is well-defined, as cross ratios are invariant under projective linear transformation). Similarly, let γ_2 be the cross ratio of the points b_1, b_2, b_3, and b_4. For four distinct points, the cross ratio is an element of $\mathbb{C} \setminus \{0, 1\}$, so we express γ_1, γ_2 as complex numbers. The invariance of the cross ratios yields the conditions on s and t

$$\frac{s(t-1)}{t(s-1)} = \gamma_1 \quad \text{and} \quad \frac{t-1}{s-1} = \gamma_2 \, .$$

Again, since $\gamma_1, \gamma_2 \in \mathbb{C} \setminus \{0, 1\}$, these two equations have the unique solution

$$s = \frac{\gamma_1(\gamma_2 - 1)}{\gamma_2(\gamma_1 - 1)} \quad \text{and} \quad t = \frac{\gamma_2 - 1}{\gamma_1 - 1} \, .$$

6.2.3 Proof of the 12 families of conics

We characterize the quadrics Q which generate the same envelope of tangents as a given quadric. A symmetric 4×4 matrix has 10 independent entries which identifies the space of quadrics with $\mathbb{P}^9$. Central to our analysis is a map φ defined for almost all quadrics Q. For a quadric Q (considered as a point in $\mathbb{P}^9$) whose associated $(2, 2)$-form (6.4) is *not* identically zero, we let $\varphi(Q)$ be this $(2, 2)$-form, considered as a point in $\mathbb{P}^8$. With this definition, we see that the Theorem 6.2 is concerned with the fiber $\varphi^{-1}(C)$, where C is the $(2, 2)$-curve associated to a general quadric Q. Since the domain of φ is 9-dimensional while its range is 8-dimensional, we expect each fiber to be 1-dimensional.

We will show that every smooth $(2, 2)$ curve arises as $\varphi(Q)$ for some quadric Q. It is these quadrics that we meant by general quadrics in the statement of Theorem 6.2. This implies that Theorem 6.2 is a consequence of the following theorem.

Theorem 6.17. *Let $C \in \mathbb{P}^8$ be a smooth $(2, 2)$-curve. Then the closure $\overline{\varphi^{-1}(C)}$ in $\mathbb{P}^9$ of the fiber of φ is a curve of degree 24 that is the union of 12 plane conics.*

We prove Theorem 6.17 by computing the ideal J of the fiber $\varphi^{-1}(C)$. Then we factor J into several ideals, which corresponds to decomposing the curve of degree 24 into the union of several curves. Finally, we analyze the output of these computations by hand to prove the desired result.

Our initial formulation of the problem gives an ideal I that not only defines the fiber of φ, but also the subset of $\mathbb{P}^9$ where φ is not defined. We identify and remove this subset

from I in several costly auxiliary computations that are performed in the computer algebra system SINGULAR [62]. It is only after removing the excess components that we obtain the ideal J of the fiber $\varphi^{-1}(C)$.

Since we want to analyze this decomposition for *every* smooth $(2,2)$-curve, we must treat the representation of C as symbolic parameters. This leads to additional difficulties, which we circumvent. It is quite remarkable that the computer-algebraic calculation succeeds and that it is still possible to analyze its result.

In the following, we denote the coordinates in $\mathbb{R}^3$ and $\mathbb{C}^3 (\subset \mathbb{P}^3)$ by x, y, z and assume that ℓ_1 is the x-axis. Furthermore, we may apply a projective linear transformation and assume without loss of generality that ℓ_2 is the yz-line at infinity. Thus we have

$$\begin{aligned}
\ell_1 &= \left\{ (w, x, 0, 0)^T \in \mathbb{P}^3 \ : \ [w, x] \in \mathbb{P}^1 \right\}, \\
\ell_2 &= \left\{ (0, 0, y, z)^T \in \mathbb{P}^3 \ : \ [y, z] \in \mathbb{P}^1 \right\}.
\end{aligned}$$

Hence, in Plücker coordinates, the lines intersecting ℓ_1 and ℓ_2 are given by

$$\left\{ (0, wy, wz, xy, xz, 0)^T \in \mathbb{P}^5 \ : \ [w, x], [y, z] \in \mathbb{P}^1 \right\}. \tag{6.9}$$

By Lemma 2.11, the envelope of common transversals to ℓ_1 and ℓ_2 that are also tangent to Q is given by those lines in (6.9) which additionally satisfy

$$(0, wy, wz, xy, xz, 0) \left(\wedge^2 Q \right) (0, wy, wz, xy, xz, 0)^T = 0. \tag{6.10}$$

A quadric Q in $\mathbb{P}^3$ is given by the quadratic form associated to a symmetric 4×4-matrix

$$Q := \begin{pmatrix} a & b & c & d \\ b & e & f & g \\ c & f & h & k \\ d & g & k & l \end{pmatrix}. \tag{6.11}$$

In a straightforward approach the ideal I of quadrics giving a general $(2,2)$-curve C is obtained by first expanding the left hand side of (6.10) into

$$\begin{aligned}
(el-g^2)x^2z^2 &+ 2(bl-dg)wxz^2 + (al-d^2)w^2z^2 \\
+ 2(ek-gf)x^2yz &+ 2(2bk-cg-df)wxyz + 2(ak-dc)w^2yz \\
+ (eh-f^2)x^2y^2 &+ 2(bh-cf)wxy^2 + (ah-c^2)w^2y^2.
\end{aligned} \tag{6.12}$$

We equate this $(2,2)$-form with the general $(2,2)$-form (6.5), as points in $\mathbb{P}^8$. This is accomplished by requiring that they are proportional, or rather that the 2×9 matrix of their coefficients

$$\begin{pmatrix} c_{00} & c_{10} & c_{20} & c_{01} & c_{11} & \ldots & c_{22} \\ el - g^2 & 2(bl - dg) & al - d^2 & 2(ek - gf) & 2(2bk - cg - df) & \ldots & ah - c^2 \end{pmatrix}$$

has rank 1. Thus the ideal I is generated by the $\binom{9}{2}$ minors of this coefficient matrix.

With this formulation, the ideal I will define the fiber $\varphi^{-1}(C)$ as well as additional, excess components that we wish to exclude. For example, the variety in $\mathbb{P}^9$ defined by the vanishing of the entries in the second row of this matrix will lie in the variety I, but these points are not those that we seek. Geometrically, these excess components are precisely where the map φ is not defined. By Lemma 6.11, we can identify three of these excess components, those points of $\mathbb{P}^9$ corresponding to rank 1 quadrics, and those corresponding to rank 2 quadrics consisting of the union of two planes meeting in either ℓ_1 or in ℓ_2. The rank one quadrics have ideal E_1 generated by the entries of the matrix $\wedge^2 Q$, the rank 2 quadrics whose planes meet in ℓ_1 have ideal E_2 generated by a, b, c, d, e, f, g, and those whose plane meets in ℓ_2 have ideal E_3 generated by c, d, f, g, h, k, l.

We remove these excess components from our ideal I to obtain an ideal J whose set of zeroes contain the fiber $\varphi^{-1}(C)$. After factoring J into its irreducible components, we will observe that φ does not vanish identically on any component of J, completing the proof that J is the ideal of $\varphi^{-1}(C)$, and also the proof of Theorem 6.17.

Since $c_{00}, c_{10}, \ldots, c_{22}$ have to be treated as parameters, the computation should be carried out over the function field $\mathbb{Q}(c_{00}, c_{10}, \ldots, c_{22})$. That computation is infeasible. Even the initial computation of a Gröbner basis for the ideal I (a necessary prerequisite) did not terminate in two days. In contrast, the computation we finally describe terminates in 7 minutes on the same computer. This is because the original computation in $\mathbb{Q}(c_{00}, c_{10}, \ldots, c_{22})[a, b, \ldots, l]$ involved too many parameters.

We instead use the 2-parameter normal form (6.7) for asymmetric smooth $(2, 2)$-curves. This will prove Theorem 6.17 in the case when C is an asymmetric smooth $(2, 2)$-curve. We treat the remaining cases of symmetric smooth $(2, 2)$-curves in Section 6.2.4. As described in Section 6.2.2, by changing the coordinates on ℓ_1 and ℓ_2, every asymmetric smooth $(2, 2)$-curve can be transformed into one defined by a polynomial in the family (6.7). Equating the $(2, 2)$-form (6.12) with the form (6.7) gives the ideal I generated by the following polynomials:

$$el - g^2, \ ek - gf, \ ak - dc, \ ah - c^2, \tag{6.13}$$

and the ten 2×2 minors of the coefficient matrix:

$$M := \begin{pmatrix} s & 1-s & -2 & 1-t & t \\ al - d^2 & 2(bl - dg) & 2(2bk - cg - df) & 2(bh - cf) & eh - f^2 \end{pmatrix}. \tag{6.14}$$

This ideal I defines the same three excess components as before, and we must remove them to obtain the desired ideal J. Although the ideal I should be treated in the ring $S := \mathbb{Q}(s, t)[a, b, c, d, e, f, g, h, k, l]$, the necessary calculations are infeasible even in this ring, and we instead work in subring $R := \mathbb{Q}[a, b, c, d, e, f, g, h, k, l][s, t]$. In the ring R, the ideal I is homogeneous in the set of variables $a, b, \ldots, l$, thus defining a subvariety of $\mathbb{P}^9 \times \mathbb{C}^2$. The ideals E_1, E_2, and E_3 describing the excess components satisfy $E_j \supset I$, $1 \leq j \leq 3$.

A SINGULAR computation shows that I is a five-dimensional subvariety of $\mathbb{P}^9 \times \mathbb{C}^2$ (see Section 6.2.6 for details). Moreover, the dimensions of the three excess components are 5, 4, and 4, respectively. In fact, it is quite easy to see that dim $E_2 =$ dim $E_3 = 4$ as both ideals are defined by 7 independent linear equations.

We are faced with a geometric situation of the following form. We have an ideal I whose variety contains an excess component defined by an ideal E and we want to compute the ideal of the difference

$$\mathcal{V}(I) - \mathcal{V}(E) \,,$$

here, $\mathcal{V}(K)$ is the variety of an ideal K. Computational algebraic geometry gives us an effective method to accomplish this, namely saturation. The elementary notion is that of the ideal quotient $(I : E)$, which is defined by

$$(I : E) \ := \ \{f \in R \mid fg \in I \text{ for all } g \in E\} \,.$$

Then the saturation of I with respect to E is

$$(I : E^\infty) \ := \ \bigcup_{n=1}^\infty (I : E^n) \,.$$

The least number n such that $(I : E^\infty) = (I : E^n)$ is called the saturation exponent.

Proposition 6.18. ([31, §4.4] or [48, §15.10] or the reference manual for SINGULAR). *Over an algebraically closed field,*

$$\mathcal{V}(I : E^\infty) \ = \ \overline{\mathcal{V}(I) - \mathcal{V}(E)} \,.$$

A SINGULAR computation shows that the saturation exponent of the first excess ideal E_1 in I is 1, and so the ideal quotient suffices to remove the excess component $\mathcal{V}(E_1)$ from $\mathcal{V}(I)$. Set $I' := (I : E_1)$, an ideal of dimension 4. The excess ideals E_2 and E_3 each have saturation exponent 4 in I_1, and so we saturate I' with respect to each to obtain an ideal $J := (\,(I' : E_2^\infty) : E_3^\infty)$, which has dimension 3 in $\mathbb{P}^9 \times \mathbb{C}^2$.

To study the components of $\mathcal{V}(J)$, we first apply the factorization Gröbner basis algorithm to J, as implemented in the SINGULAR command `facstd` (see [98] or the reference manual of SINGULAR). This algorithm takes two arguments, an ideal I and a list $L = f_1, \ldots, f_n$ of polynomials. It proceeds as in the usual Buchberger algorithm to compute a Gröbner basis for I, except that whenever it computes a Gröbner basis element G that it can factor, it splits the calculation into subcalculations, one for each factor of G that is not in the list L, adding that factor to the Gröbner basis for the corresponding subcalculation. The output of `facstd` is a list $I_1, I_2, \ldots, I_m$ of ideals with the property that

$$\overline{\bigcup_{j=1}^m \mathcal{V}(I_j)} \ - \mathcal{V}(f_1 \cdots f_n) \ = \ \overline{\mathcal{V}(I) - \mathcal{V}(f_1 \cdots f_n)} \,.$$

Thus, the zero set of I coincides with the union of zero sets of the factors I_j, in the region where none of the polynomials in the list L vanish. In terms of saturation, this is

$$\mathrm{rad}(I_1 \cdots I_m : (f_1 f_2 \cdots f_n)^\infty) \;=\; \mathrm{rad}(I : (f_1 f_2 \cdots f_n)^\infty) \tag{6.15}$$

where $\mathrm{rad}(K)$ denotes the radical of an ideal K. Some of the ideals I_j may be spurious in that $\mathcal{V}(I_j)$ is already contained in the union of the other $\mathcal{V}(I_i)$.

We run `facstd` on the ideal J with the list of polynomials s, t, $s-1$, $t-1$, and $s-t$, and obtain seven components $J_0, J_1, \dots, J_6$. The components $J_1, \dots, J_6$ each have dimension 3, while the component J_0 has dimension 2. Since $\mathcal{V}(J_0)$ is contained in the union of the $\mathcal{V}(J_1), \dots, \mathcal{V}(J_6)$, it is spurious and so we disregard it.

We now, finally, change from the base ring R to the base ring S, and compute with the parameters s, t. There, J defines an ideal of dimension 1 and degree 24 in the 9-dimensional projective space over the field $\mathbb{Q}(s,t)$. As we remarked before, we have that $\mathcal{V}(J) \supset \varphi^{-1}(C)$. The factorization of J into $J_1, \dots, J_6$ remains valid over S. The reason we did not compute the factorization over S is that `facstd` and the saturations were infeasible over S, and the arguments from computational algebraic geometry we have given show that it suffices to compute without parameters, as long as care is taken when interpreting the output.

Each of the factors J_i has dimension 1 and degree 4. Moreover, each ideal contains a homogeneous quadratic polynomial in the variables k, l which must factor over some field extension of $\mathbb{Q}(s,t)$. In fact, these six quadratic polynomials all factor over the field $\mathbb{Q}(\sqrt{s}, \sqrt{t})$. For example, two of the J_i contain the polynomial $(s-1)k^2 - 2kl - l^2$, which is the product

$$\left((\sqrt{s}+1)k \;+\; l \right) \left((\sqrt{s}-1)k \;-\; l \right) \;.$$

For each ideal J_i, the factorization of the quadratic polynomial induces a factorization of J_i into two ideals J_{i1} and J_{i2}. Inspecting a Gröbner basis for each ideal shows that each defines a plane conic in $\mathbb{P}^9$. Thus, over the field $\mathbb{Q}(\sqrt{s}, \sqrt{t})$, J defines 12 plane conics.

Theorem 6.17 is a consequence of the following two observations.

(1) The factorization of J gives 12 distinct components for all values of the parameters s, t satisfying (6.8).

(2) The map φ does not vanish identically on any of the components $\mathcal{V}(J_{ij})$ for values of the parameters s, t satisfying (6.8).

By (1), no component of J is empty for any s, t satisfying (6.8) and thus, for every asymmetric $(2,2)$-curve C, there is a quadric Q with $\varphi(Q) = C$. Also by (1), J has exactly 12 components with each a plane conic, for any s, t satisfying (6.8), and by (2), $\mathcal{V}(J) = \overline{\varphi^{-1}(C)}$.

6.2.4   Symmetric smooth $(2,2)$-curves

We investigate smooth curves C whose double points in the ramified fibers over ℓ_1 have *only* two distinct projections to ℓ_2. Assume that the ramification is at the points $[w,x] = [1,1],[1,-1],[1,s]$, and at $[1,-s]$, for some $s \in \mathbb{C} \setminus \{0,\pm 1\}$ with the double points in the fibers at $[y,z] = [1,0]$ for the first two and at $[0,1]$ for the second two. Since the points $[1,1],[1,-1],[1,s]$, and $[1,-s]$ have cross ratio

$$\left[\frac{1+s}{1-s}, \frac{1-s}{1+s} \right] \;=\; \left[1, \frac{(1-s)^2}{(1+s)^2} \right] ,$$

we see that all cross ratios in $\mathbb{P}^1 \setminus \{[1,0],[0,1],[1,1]\}$ are obtained for some $s \in \mathbb{C} \setminus \{0,\pm 1\}$. Thus our choice of ramification results in no loss of generality.

As in Section 6.2.1, these conditions give equations on the coefficients c_{ij} of the general $(2,2)$-curve (6.5):

$$\begin{aligned}
c_{00} + c_{10} + c_{20} &= 0, & c_{01} + c_{11} + c_{21} &= 0, & c_{00} - c_{10} + c_{20} &= 0, \\
c_{01} - c_{11} + c_{21} &= 0, & c_{02} + c_{12}s + c_{22}s^2 &= 0, & c_{01} + c_{11}s + c_{21}s^2 &= 0, \\
c_{02} - c_{12}s + c_{22}s^2 &= 0, & c_{01} - c_{11}s + c_{21}s^2 &= 0.
\end{aligned}$$

These equations have the following consequences

$$0 \;=\; c_{21} \;=\; c_{01} \;=\; c_{12} \;=\; c_{11} \;=\; c_{10} \;=\; c_{02} + c_{22}s^2 \;=\; c_{00} + c_{20} .$$

Hence after normalizing by setting $c_{20} = 1$, the $(2,2)$-form (6.5) becomes

$$(x^2 - w^2)y^2 + c_{22}(x^2 - s^2 w^2)z^2 .$$

While the choice of ramification points $[1,1],[1,-1],[1,s],[1,-s]$ fixes the parametrization of ℓ_1, the double points in the fibers of $[1,0]$ and $[0,1]$ do not fix the parametrization of ℓ_2. Thus we are still free to scale the z-coordinate. We normalize this equation setting $c_{22} = \pm 1$. We do not simply set $c_{22} = 1$ because that misses an important real form of the polynomial. This normalization gives

$$(x^2 - w^2)y^2 \;\pm\; (x^2 - s^2 w^2)z^2 \;\;=\;\; (y^2 \pm z^2)x^2 - (y^2 \pm s^2 z^2)w^2 . \qquad (6.16)$$

This shows the equation to be symmetric under the involution $[w,x] \leftrightarrow [\sqrt{\mp 1}z, y]$. This symmetry is the source of our terminology for the two classes of $(2,2)$-curves. Also, if $s \notin \{\pm 1, 0\}$, then this is the equation of a smooth $(2,2)$-curve. With the choice of sign $(-)$, which we call the curve $C(s)$.

Note that (6.16) is real if s either is real or is purely imaginary ($s \in \mathbb{R}\sqrt{-1}$). We complete the proof of Theorem 6.2 with the following result for symmetric $(2,2)$-curves.

Theorem 6.19. *For each $s \in \mathbb{C} \setminus \{\pm 1, 0\}$, the closure of the fiber $\varphi^{-1}(C(s))$ consists of 12 distinct plane conics. When $s \in \mathbb{R}$ or $s \in \mathbb{R}\sqrt{-1}$ and we use the real form of (6.16) with the plus sign $(+)$, then exactly 4 of these 12 components will be real. If we use the real form of (6.16) with the minus sign $(-)$, then if $s \in \mathbb{R}$, all 12 components will be real, but if $s \in \mathbb{R}\sqrt{-1}$, then exactly 4 of these 12 components will be real.*

Proof. Our proof follows the proof of Theorem 6.17 almost exactly, but with significant simplifications and a case analysis. The outline is as before, except that we work over the ring of parameters $\mathbb{Q}(s)$, and find no extraneous components when we factor the ideal into components. We formulate this as a system of equations, remove the same three excess components, and then factor the resulting ideal. We do this calculation four times, once for each choice of sign $(\pm)$ in (6.16), and for $s \in \mathbb{R}$ and $s \in \mathbb{R}\sqrt{-1}$. Using SINGULAR computations similar to (but substantially simpler than) the one explained in detail in Section 6.2.6, we can actually carry out these computations. Examining the output proves the result. $\qquad\square$

We consider in some detail four cases of the geometry studied in Section 6.2.1, which correspond to the four real cases of Theorem 6.19. As in Section 6.2.1, let ℓ_1 be the x-axis and ℓ_2 be the yz-line at infinity. Viewed in $\mathbb{R}^3$, lines transversal to ℓ_1 and ℓ_2 are the set of lines perpendicular to the x-axis. For a transversal line ℓ, the coordinates $[y, z]$ of the point $\ell \cap \ell_2$ can be interpreted as the slope of ℓ in the two-dimensional plane orthogonal to the x-axis.

Consider real quadrics given by an equation of the form

$$x^2 + (y - y_0)^2 \pm z^2 \ = \ 1 \, . \tag{6.17}$$

The quadrics with the plus $(+)$ sign are spheres with center $(0, y_0, 0)^T$ and radius 1, and those with the minus $(-)$ sign are hyperboloids of one sheet. When $|y_0| > 1$ the quadric does not meet the x-axis. We look at four families of such quadrics: spheres and hyperboloids that meet and do not meet the x-axis. We remark that quadrics which are tangent to the x-axis give singular $(2, 2)$-curves.

First, consider the resulting $(2, 2)$-curve

$$(x^2 - w^2)y^2 \pm (x^2 - (1 - y_0^2)w^2)z^2 \, .$$

Thus we see that these correspond to the case $s = \sqrt{1 - y_0^2}$ in the parametrization of symmetric $(2, 2)$-curves given above (6.16), while in (6.17) and (6.16) the signs $(\pm)$ correspond.

Figures 6.5 and 6.6 display pictures of these four quadrics, together with the x-axis, some tangents perpendicular to the x-axis, and the curve on the quadric where the lines are tangent.

Remark 6.20. For each of the spheres, there is another sphere of radius r which leads to the same envelope, namely the one with center $(0, -y_0, 0)^T$.
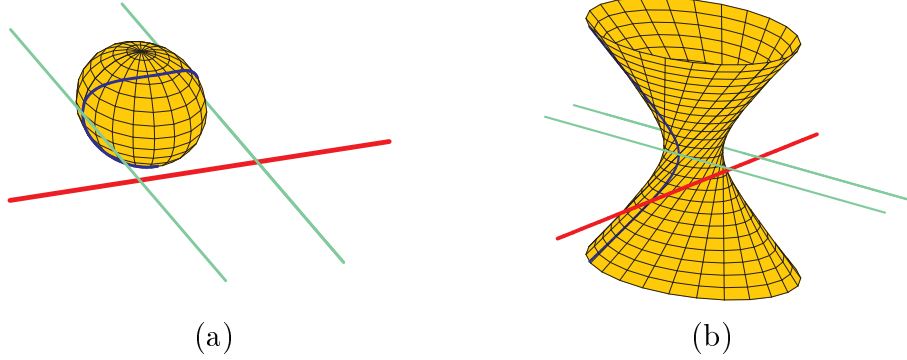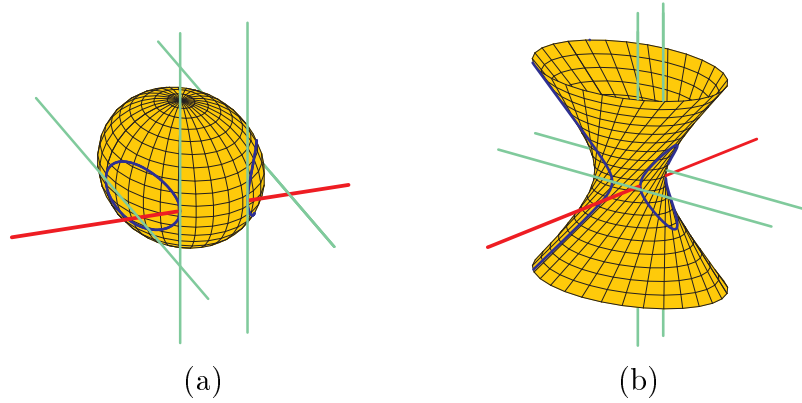
Fig. 6.5: Real quadrics not meeting the x-axis.

Fig. 6.6: Real quadrics meeting the x-axis.

The ramification of the $(2, 2)$-curve of tangents perpendicular to the x-axis is evident from Figures 6.5 and 6.6. When $x = \pm 1$, there is a single tangent line; this line has slope $[y, z] = [1, 0]$, i.e., it is a horizontal line. When $x = \pm\sqrt{1 - y_0^2}$, there is a single tangent line, which is vertical (i.e., which has slope $[y, z] = [0, 1]$). Figures 6.5 and 6.6 depict these lines in case they are real. In Figure 6.5 we have $|y_0| > 1$, and hence the vertical tangent lines are complex. All other values of x give two lines perpendicular to the x-axis and tangent to the quadric, but some have imaginary slope.

The difference in the number of real components of the fiber $\varphi^{-1}(C(s))$ noted in Theorem 6.19 is evident in these examples. The spheres and hyperboloid displayed together are isomorphic under the change of coordinates $z \mapsto \sqrt{-1} \cdot z$, which interchanges the transversal tangents of purely imaginary slope for one quadric with the real transversal tangents of the other and corresponds to the different signs $\pm$ in (6.17) and (6.16).

For the sphere of Figure 6.5, only 4 of the 12 families are real. One consists of ellipsoids, including the original sphere, one of hyperboloids of two sheets, and two of hyperboloids of one sheet. Since a hyperboloid of two sheets can be seen as an ellipsoid meeting the plane at infinity in a conic, we see there are two families of ellipsoids and two of hyperboloids.

In Figure 6.7, we display one quadric from each family (except the family of the sphere), together with the original sphere, the x-axis, and the curve on the quadric where the lines perpendicular to the x-axis are tangent to the quadric.
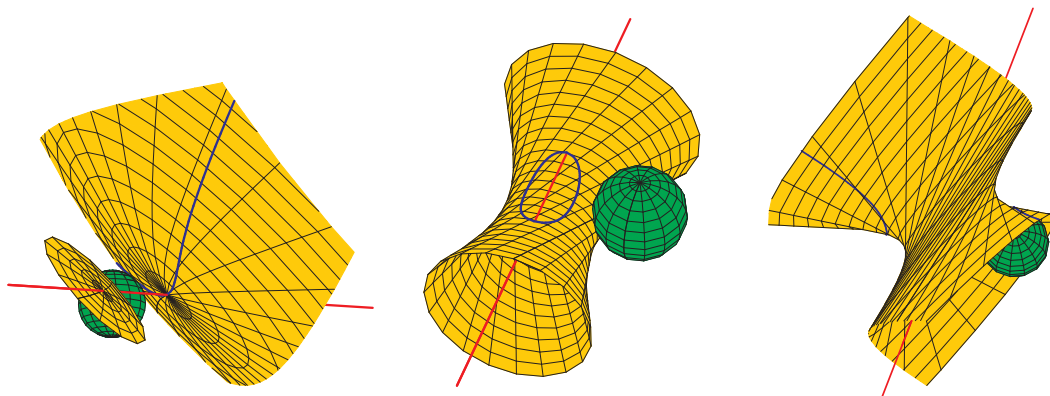

Fig. 6.7: The other three families.

Similarly, the hyperboloid of Figure 6.5 has only 4 of its 12 families real with two families of ellipsoids and two of hyperboloids. The sphere of Figure 6.6 has only 4 of its 12 families real, and all 4 contain ellipsoids. In contrast, the hyperboloid of Figure 6.6 has all 12 of its families real, and they contain only hyperboloids of one sheet.

6.2.5 Transversals to two lines and tangents to two spheres

We solve the original question of configurations of two lines and two spheres for which there are infinitely many real transversals to the two lines that are also tangent to both spheres. While general quadrics are naturally studied in projective space $\mathbb{P}^3$, spheres naturally live in (the slightly more restricted) affine space $\mathbb{R}^3$. As noted in Section 6.2.1, we treat only skew lines. There are two cases to consider. Either the two lines are in $\mathbb{R}^3$ or one lies in the plane at infinity. We work throughout over the real numbers.

Lines in affine space $\mathbb{R}^3$.

The complete geometric characterization of configurations where the lines lie in $\mathbb{R}^3$ is stated in the following theorem and illustrated in Figure 6.8.

Theorem 6.21. *Let S_1 and S_2 be two distinct spheres and let ℓ_1 and ℓ_2 be two skew lines in $\mathbb{R}^3$. There are infinitely many lines in $\mathbb{R}^3$ that meet ℓ_1 and ℓ_2 and are tangent to S_1 and S_2 in* exactly *the following cases.*

(1) The spheres S_1 and S_2 are tangent to each other at a point p which lies on one line, and the second line lies in the common tangent plane to the spheres at the point p. The pencil of lines through p that also meet the second line is exactly the set of common transversals to ℓ_1 and ℓ_2 that are also tangent to S_1 and S_2.

(2) *The lines ℓ_1 and ℓ_2 are each tangent to both S_1 and S_2, and they are images of each other under a rotation about the line connecting the centers of S_1 and S_2. If we rotate ℓ_1 about the line connecting the centers of the spheres, it sweeps out a hyperboloid of one sheet. One of its rulings contains ℓ_1 and ℓ_2, and the lines in the other ruling are tangent to S_1 and S_2 and meet ℓ_1 and ℓ_2, except for those that are parallel to one of them.*

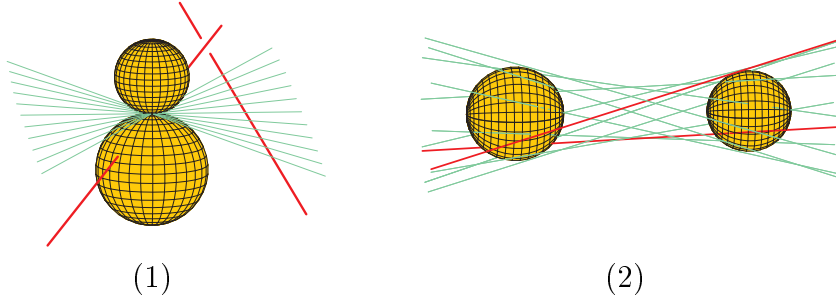(1)   (2)

Fig. 6.8: Examples from Theorem 6.21.

Let ℓ_1 and ℓ_2 be two skew lines. The class of spheres is not invariant under the set of projective linear transformations, but rather under the group generated by rotations, translations, and scaling the coordinates. Thus we can assume that

$$\ell_1 = \left\{ \begin{pmatrix} 0 \\ 0 \\ 1 \end{pmatrix} + x \begin{pmatrix} 1 \\ \delta \\ 0 \end{pmatrix} \ : \ x \in \mathbb{R} \right\}, \qquad \ell_2 = \left\{ \begin{pmatrix} 0 \\ 0 \\ -1 \end{pmatrix} + z \begin{pmatrix} -1 \\ -\delta \\ 0 \end{pmatrix} \ : \ z \in \mathbb{R} \right\}$$

for some $\delta \in \mathbb{R} \setminus \{0\}$. As before, there is a one-to-one correspondence between lines meeting ℓ_1 and ℓ_2 and pairs $(x, z) \in \mathbb{R}^2$. The transversal corresponding to a pair (x, z) passes through the points $(x, \delta x, 1)^T$ and $(z, -\delta z, -1)^T$, and has Plücker coordinates

$$(z - x, -\delta(x + z), -2, -2\delta xz, -(x + z), \delta(z - x))^T .$$

Let S_1 have center $(a, b, c)^T$ and radius r. By Lemma 2.11 and (2.6), the transversals tangent to S_1 are parametrized by a curve C_1 of degree 4 with equation

$$\begin{aligned} 0 \ = \ & 4\delta^2 x^2 z^2 \ + \ 4\delta(b - a\delta)x^2 z \ + \ \big((b - a\delta)^2 + (1 + \delta^2)((1 + c)^2 - r^2)\big)x^2 \\ & - 4\delta(b + a\delta)xz^2 \ + \ 2\big((r^2 - c^2)(1 - \delta^2) + (1 - b^2) + \delta^2(a^2 - 1)\big)xz \qquad (6.18) \\ & - 4(1 + c)(a + b\delta)x \ + \ \big((b + a\delta)^2 + (1 + \delta^2)((1 - c)^2 - r^2)\big)z^2 \\ & + 4(c - 1)(a - b\delta)z \ + \ 4(a^2 + b^2 - r^2) . \end{aligned}$$

This is a dehomogenized version of the bihomogeneous equation (6.5) of bidegree $(2, 2)$. Note also that the curve C_1 is defined over our ground field $\mathbb{R}$. The transversals to ℓ_1 and ℓ_2 tangent to S_2 are parametrized by a similar curve C_2. There are infinitely many

lines which meet ℓ_1 and ℓ_2 and are tangent to S_1 and S_2 if and only if the curves C_1 and C_2 have a common component. That is, if and only if the associated polynomials share a common factor. We first rule out the case when the curves are irreducible.

Lemma 6.22. *The curve C_1 in* (6.18) *determines the sphere S_1 uniquely.*

Proof. Given the curve (6.18), we can rescale the equation such that the coefficient of x^2z^2 is $4\delta^2$. From the coefficients of x^2z and xz^2 we can determine a and b, and then from the coefficients of x^2 and z^2 we can determine c and r. $\square$

Remark 6.23. By Remark 6.20, Lemma 6.22 does not hold if the lines are allowed to live in projective space $\mathbb{P}^3_{\mathbb{R}}$. We come back to this in Section 6.2.5.

By Lemma 6.22, there can be infinitely many common transversals to ℓ_1 and ℓ_2 that are tangent to two spheres only if the curves C_1 and C_2 are reducible. In particular, this rules out cases (1) and (2) of Lemma 6.10. Our classification of factors of $(2,2)$-forms in Lemma 6.10 gives the following possibilities for the common irreducible factors (over $\mathbb{R}$) of C_1 and C_2, up to interchanging x and z. Either the factor is a cubic (the dehomogenization of a $(2,1)$-form), or it is linear in x and z (the dehomogenization of a $(1,1)$-form), or it is linear in x alone (the dehomogenization of a $(1,0)$-form). There is the possibility that the common factor will be an irreducible (over $\mathbb{R}$) quadratic polynomial in x (coming from a $(2,0)$-form), but then this component will have no real points, and thus contributes no common real tangents.

We rule out the possibility of a common cubic factor, showing that if C_1 factors as $x - x_0$ and a cubic, then the cubic still determines S_1. The vector $(-\delta, -1, \delta x_0)^T$ is perpendicular to the plane through $(x_0, \delta x_0, 1)^T$ and ℓ_2, so the center of S_1 will be $(x_0, \delta x_0, 1)^T + \lambda(-\delta, -1, \delta x_0)^T$ for some non-zero $\lambda \in \mathbb{R}$. Thus $r^2 = \lambda^2(1 + \delta^2 + \delta^2 x_0^2)$. Substituting this into (6.18) and dividing by $(x - x_0)$ we obtain the equation of the cubic:

$$
\begin{aligned}
0 \;=\;& \delta^2 xz^2 \;+\; \delta(\delta^2 - 1)\lambda xz \;+\; (1 + \delta^2(1 - \lambda^2) + \delta\lambda(1 + \delta^2)x_0)x \\
& + \delta(\lambda(1 + \delta^2) - \delta x_0)z^2 \;+\; \delta(\delta^2 - 1)\lambda x_0 z \;+\; 4\delta\lambda + (\delta^2\lambda^2 - \delta^2 - 1)x_0 \,.
\end{aligned}
\tag{6.19}
$$

Given only this curve, we can rescale its equation so that the coefficient of xz^2 is δ^2, then if $\delta \neq \pm 1$, we can uniquely determine λ, x_0 and therefore S_1, too, from the coefficients of xz and x.

The uniqueness is still true if $\delta = \pm 1$. Assume that $\delta = 1$. Then (6.19) reduces to

$$
xz^2 \;+\; (2\lambda - x_0)z^2 \;+\; (2 - \lambda^2 + 2\lambda x_0)x \;+\; 4\lambda + (\lambda^2 - 2)x_0 \;=\; 0 \,.
$$

Set $\alpha := 2\lambda - x_0$, $\beta := 2 - \lambda^2 + 2\lambda x_0$, and $\gamma := 4\lambda + (\lambda^2 - 2)x_0$. We can solve for λ and x_0 in terms of α and β,

$$
\lambda \;=\; \frac{\alpha \pm \sqrt{\alpha^2 + 3\beta - 6}}{3}, \qquad x_0 \;=\; \frac{-\alpha \pm 2\sqrt{\alpha^2 + 3\beta - 6}}{3} \,.
$$

(We take the same sign of the square root in both cases). If we substitute these values into the formula for γ, we see that the two possible values of γ coincide if and only if $\alpha^2 + 3\beta - 6 = 0$, in which case there is only one solution for λ and x_0, so α, β, and γ always determine λ and x_0 uniquely and hence S_1 uniquely. The case $\delta = -1$ is similar.

We now are left only with the cases when C_1 and C_2 contain a common factor of the form $x - x_0$ or $xz + sx + tz + u$. Suppose the common factor is $x - x_0$. Then any line through $p := (x_0, \delta x_0, 1)^T$ and a point of ℓ_2 is tangent to S_1. This is only possible if the sphere S_1 is tangent to the plane through p and ℓ_2 at the point p. We conclude that if C_1 and C_2 have the common factor $x - x_0$, then the spheres S_1 and S_2 are tangent to each other at the point $p = (x_0, \delta x_0, 1)^T$ lying on ℓ_1 and ℓ_2 lies in the common tangent plane to the spheres at the point p. This is case (1) of Theorem 6.21.

Suppose now that C_1 and C_2 have a common irreducible factor $xz + sx + tz + u$. We can solve the equation $xz + sx + tz + u = 0$ uniquely for z in terms of x for general values of x, or for x in terms of z for general values of z, this gives rise to an isomorphism ϕ between the projectivizations of ℓ_1 and ℓ_2. The lines connecting q and $\phi(q)$ as q runs through the points of ℓ_1 sweep out a hyperboloid of one sheet. The lines ℓ_1 and ℓ_2 are contained in one ruling, and the lines meeting both of them and tangent to S_1 are the lines in the other ruling.

We need the following geometric statement, which is an immediate consequence of Theorem 6.4.

Corollary 6.24. *Let $H \subset \mathbb{R}^3$ be a hyperboloid of one sheet. If all lines in one of its rulings are tangent to a sphere S, then H is a hyperboloid of revolution, the center of the sphere S is on the axis of rotation and S is tangent to H.*

By this corollary, the hyperboloid swept out by the lines meeting ℓ_1 and ℓ_2 and tangent to S_1 is a hyperboloid of revolution with the center of S_1 on the axis of rotation. Furthermore, ℓ_1 and ℓ_2 are lines in one the rulings of the hyperboloid, therefore they are images of each other under suitable rotation about the axis, the images of ℓ_1 sweep out the whole hyperboloid, and ℓ_1, ℓ_2 are both tangent to S_1. Applying the lemma to S_2 shows that the center of S_2 is also on the axis of rotation and ℓ_1, ℓ_2 are both tangent to S_2. We cannot have S_1 and S_2 concentric, therefore the axis of rotation is the line through their centers. This is exactly case (2) of Theorem 6.21, and we have completed its proof.

<div align="center">*Lines in projective space.*</div>

We give the complete geometric characterization of configurations in real projective space where the line ℓ_2 lies in the plane at infinity.

Theorem 6.25. *Let S_1 and S_2 be two distinct spheres and let ℓ_1 lie in $\mathbb{R}^3$ with ℓ_2 a line at infinity skew to ℓ_1. There are infinitely many lines that meet ℓ_1 and ℓ_2 and are tangent to S_1 and S_2 in exactly the following cases.*

(1) *The spheres S_1 and S_2 are tangent to each other at a point p which lies on ℓ_1, and ℓ_2 is the line at infinity in the common tangent plane to the spheres at the point p. The pencil of lines through p that lie in this tangent plane are exactly the common transversals to ℓ_1 and ℓ_2 that are also tangent to S_1 and S_2.*

(2) *Any line meeting ℓ_1 and ℓ_2 is perpendicular to ℓ_1 and S_1 and S_2 are related to each other by multiplication by -1 in the directions perpendicular to ℓ_1. Thus we are in exactly the situation of Remark 6.20 of Section 6.2.4 as shown in Figures 6.5(a) and 6.6(a).*

Proof. Let Π be any plane passing through a point of ℓ_1 and containing ℓ_2. Then common transversals to ℓ_1 and ℓ_2 are lines meeting ℓ_1 that are parallel to Π. Choose a Cartesian coordinate system in $\mathbb{R}^3$ such that ℓ_1 is the x-axis. Suppose that S_1 has center $(a, b, c)^T$ and radius r. Let $u = (u_1, u_2, 0)^T$ and $v = (v_1, 0, v_3)^T$ be vectors with $u_2 \neq 0$ and $v_3 \neq 0$ parallel to Π. Such vectors exist as ℓ_1 and ℓ_2 are skew. A common transversal to ℓ_1 and ℓ_2 is determined by the intersection point $(x, 0, 0)^T$ with ℓ_1 and a direction vector corresponding to the intersection point with ℓ_2, which can be written as $u + zv$ for some $z \in \mathbb{R}$, unless it is parallel to v. Since S_1 has at most two tangent lines which meet ℓ_1 that are parallel to v, so by omitting these we are not losing an infinite family of common transversals/tangents.

The transversals that are tangent to S_1 are parametrized by a curve C_1 in the xz-plane with equation

$$
\begin{aligned}
0 \;=\; & v_3^2 x^2 z^2 + u_2^2 x^2 + 2v_3(cv_1 - av_3)xz^2 + 2(bu_2v_1 + cu_1v_3)xz \\
& + 2u_2(bu_1 - au_2)x + ((b^2 + c^2 - r^2)v_1^2 - 2acv_1v_3 + (a^2 + b^2 - r^2)v_3^2)z^2 \quad (6.20) \\
& + 2((b^2 + c^2 - r^2)u_1v_1 - acu_1v_3 - bu_2(av_1 + cv_3))z \\
& + ((b^2 + c^2 - r^2)u_1^2 - 2abu_1u_2 + (a^2 + c^2 - r^2)u_2^2)
\end{aligned}
$$

The transversals tangent to S_2 are parametrized by a similar curve C_2. There are infinitely many lines that meet ℓ_1 and ℓ_2 and are tangent to S_1 and S_2 if and only if C_1 and C_2 have a common nonempty real component.

It is easy to see from the coefficients of xz^2, xz and x and the constant term that if $u_1 \neq 0$ or $v_1 \neq 0$, then C_1 determines a, b, c and r^2 and therefore S_1 uniquely, so if C_1 is irreducible and $u_1 \neq 0$ or $v_1 \neq 0$, then there cannot be infinitely many common transversals that are tangent to S_1 and S_2.

Assume now that $u_1 = v_1 = 0$, this is equivalent to the plane Π being perpendicular to ℓ_1. From the coefficient of x we can determine a, and then from the coefficients of z^2, z, and the constant term we can calculate the quantities $\alpha = c^2 - r^2$, $\beta = bc$, and $\gamma = b^2 - r^2$. The equation $(\alpha + r^2)(\gamma + r^2) - \beta^2 = 0$ is a quadratic equation for r^2 with solutions

$$
r^2 \;=\; \frac{1}{2}\left(-\alpha - \gamma \pm \sqrt{(\alpha - \gamma)^2 + 4\beta^2}\right).
$$

Only the larger root is feasible, even when both are positive, since both $\alpha + r^2 = c^2$ and $\gamma + r^2 = b^2$ must be non-negative. Hence r^2, and thus b^2 and c^2 are uniquely determined.

The values of b^2, bc, and c^2 determine two possible pairs (b, c) which are negatives of each other. This is exactly case (2) of the theorem. In fact, this case is illustrated by Figures 6.5(a) and 6.6(b).

Let us now consider the cases when C_1 is reducible. As in the proof of Theorem 6.21, we need only consider cubics and factors of the form $xz + sx + tz + u$, $x - x_0$, and $z - z_0$.

Assume that C_1 has a component with equation $xz + sx + tz + u$. As described in the proof of Theorem 6.21, this establishes an isomorphism between the projectivizations of ℓ_1 and ℓ_2. The lines connecting the corresponding points of the projectivizations of ℓ_1 and ℓ_2 sweep out a hyperbolic paraboloid. However, the lines in one ruling of the hyperbolic paraboloid cannot all be tangent to a sphere, therefore this case cannot occur.

Likewise, the factor $z - z_0$ cannot appear, since it would mean that all the lines through a point of ℓ_1 parallel to a certain direction are tangent to S_1, which is clearly impossible.

Consider the case where the equation of C_1 has a factor of $x - x_0$. As we saw in the proof of Theorem 6.21, ℓ_1 meets the sphere S_1 at the point $p := (x_0, 0, 0)^T$, and ℓ_2 lies in the tangent plane to S_1 at p, and so this tangent plane is parallel to Π.

If $x - x_0$ is a factor of C_2, too, then C_2 passes through p and its tangent plane there is also parallel to Π, so we have case (1) of the theorem.

To finish the proof we investigate what happens if the common component of C_1 and C_2 is the cubic obtained from C_1 after removing the line $x - x_0 = 0$.

The center of S_1 has coordinates $(x_0 + \mu u_2 v_3, -\mu u_1 v_3, -\mu u_2 v_1)^T$ for some $\mu \in \mathbb{R}$, since S_1 passes through $(x_0, 0, 0)^T$ and its tangent plane there is parallel to Π, and we have $r^2 = \mu^2(u_1^2 v_3^2 + u_2^2 v_1^2 + u_2^2 v_3^2)$. Substituting this into (6.20) we obtain the equation of the remaining cubic,

$$v_3^2 x z^2 + u_2^2 x - v_3(x_0 v_3 + 2\mu u_2(v_1^2 + v_3^2))z^2$$
$$-4\mu u_1 u_2 v_1 v_3 z - u_2(x_0 u_2 + 2\mu v_3(u_1^2 + u_2^2)) = 0.$$

If $u_1 \neq 0$ or $v_1 \neq 0$ then from the coefficients of this curve we can determine x_0 and μ, hence S_1 uniquely, so C_1 and C_2 cannot have a common cubic component. If $u_1 = v_1 = 0$ then the above equation factorizes as

$$(x - (2\mu u_2 v_3 + x_0))(v_3^2 z^2 + u_2^2) = 0,$$

so if C_2 contains the curve defined by this equation, then the line $x - (2\mu u_2 v_3 + x_0) = 0$ is a common component of both C_1 and C_2, which is a case we have already dealt with. $\quad\square$

6.2.6   *Appendix: Calculations from Section 6.2.3*

We describe the computation of Section 6.2.3 in much more detail, giving a commentary on the SINGULAR file that accomplishes the computation and displaying its output. In our description of the SINGULAR computation, we follow Section 4.2.2. The library `primdec.lib` contains the function `sat` for saturating ideals.

```
LIB "primdec.lib";
option(redSB);
```

We initialize our ring.

```
ring R = 0, (s,t,a,b,c,d,e,f,g,h,k,l), (dp(2), dp(10));
```

The underlying coefficient field has characteristic 0 (so it is $\mathbb{Q}$) and variables $s, t, a, \dots, k, l$, with a product term order chosen to simplify our analysis of the projection to $\mathbb{C}^2$, the space of parameters.

We consider the ideal generated by (6.13)

```
ideal I = el-g^2, ek-gf, ak-dc, ah-c^2;
```

and by the 2×2 minors of the coefficient matrix (6.14).

```
matrix M[2][5] =     s   ,    1-s   ,       -2      ,    1-t  ,   t   ,
                  al-d^2, 2*(bl-dg), 2*(2bk-cg-df), 2*(bh-cf), eh-f^2;
I = I + minor(M,2);
```

We check the dimension and degree of the variety $\mathcal{V}(I)$, first computing a Gröbner basis for I.

```
I = std(I);  dim(I), mult(I);
//   6  8
```

SINGULAR gives the dimension of $\mathcal{V}(I)$ in affine space $\mathbb{C}^{12}$. Since I is homogeneous in the variables $a, b, \dots, h, k, l$, we consider $\mathcal{V}(I)$ to be a subvariety of $\mathbb{P}^9 \times \mathbb{C}^2$. Its dimension is one less than that of the corresponding affine variety. Thus $\mathcal{V}(I)$ has dimension 5 and degree 8.

In Section 6.2.3, we identified three spurious components of $\mathcal{V}(I)$ which we remove. The first and largest is the ideal of rank 1 quadrics, given by the 2×2-minors of the 4×4-symmetric matrix (6.11).

```
matrix Q[4][4] =  a , b , c , d ,
                  b , e , f , g ,
                  c , f , h , k ,
                  d , g , k , l ;
ideal E1 = std(minor(Q,2));
```

We remove this spurious component, computing the quotient ideal $(I : E_1)$.

```
I = std(quotient(I,E1));  dim(I), mult(I);
//   5  20
```

The other two spurious components describe rank 2 quadrics which are unions of two planes with intersection line ℓ_1 or ℓ_2.

```
ideal E2 = g, f, e, d, c, b, a;   // intersection line l1
ideal E3 = l, k, h, g, f, d, c;   // intersection line l2
```

The corresponding components are not reduced; rather than take ideal quotients, we saturate the ideal I with respect to these spurious ideals. The SINGULAR command `sat` for saturation returns a pair whose first component is a Gröbner basis of the saturation and the second is the saturation exponent. Here, both saturations have exponent 4. We saturate I with respect to E_2,

```
I = sat(I,E2)[1];  dim(I), mult(I);
//   5  10
```

and then with respect to E_3.

```
ideal J = sat(I,E3)[1];  dim(J), mult(J);
//   4  120
```

Thus we now have a variety $\mathcal{V}(J)$ of dimension 3 in $\mathbb{P}^9 \times \mathbb{C}^2$. We check that it projects onto the space $\mathbb{C}^2$ of parameters by eliminating the variables $a, b, \ldots, h, k, l$ from J.

```
eliminate(J, abcdefghkl);
//   _[1]=0
```

Since we obtain the zero ideal, the image of $\mathcal{V}(J)$ is Zariski dense in $\mathbb{C}^2$ [31, Chapter 4, §4]. However, the projection $\mathbb{P}^9 \times \mathbb{C}^2 \twoheadrightarrow \mathbb{C}^2$ is a closed map, so the image of $\mathcal{V}(J)$ is $\mathbb{C}^2$. Thus, for every smooth $(2,2)$-curve C defined by (6.7), there is a quadric whose transversal tangents are described by the curve C.

We now apply the factorization Gröbner basis algorithm `facstd` to J. The second argument of `facstd` is the list of non-zero constraints which are given by Theorem 6.14.

```
ideal L = s, t, t-1, s-1, s-t;
list F = facstd(J,L);
```

SINGULAR computes seven factors

```
size(F);
//   7
```

Since J and the seven factors $L_1, \ldots, L_7$ are radical ideals, this factorization can be verified by checking that that the following ideals V_1 and V_2 coincide.

```
int i;
ideal FF = 1;
for (i = 1; i <= 7; i++) { FF = intersect(FF,F[i]); }
ideal V1, V2;
V1 = std(sat(sat(sat(sat(sat(FF,t)[1],s)[1],t-1)[1],s-1)[1],s-t)[1]);
V2 = std(sat(sat(sat(sat(sat(J ,t)[1],s)[1],t-1)[1],s-1)[1],s-t)[1]);
```

Note, in particular, that for any given explicit values of s, t satisfying the non-zero conditions, the parametric factorization (in s, t) produced by `facstd` can be specialized to an explicit factorization.

We examine the ideals in the list F, working over the ring with parameters.

```
ring S = (0,s,t), (a,b,c,d,e,f,g,h,k,l), lp; short = 0;
```

First, the ideal J has dimension 1 and degree 24 over this ring, as claimed.

```
ideal JS = std(imap(R,J));   dim(JS), mult(JS);
//   2  24
```

The first ideal in the list L has dimension 0.

```
setring R; FR = F[1]; setring S;
FS = std(imap(R,FR));  dim(FS), mult(FS);
//   1  4
```

This ideal is a spurious component from the factorization. It is contained in the spurious ideal E_2.

```
FS[5], FS[6], FS[7], FS[8], FS[9], FS[10], FS[11];
//   g f e d c b a
```

The other six components each have dimension 1 and degree 4, and each contains a homogeneous quadratic polynomial in the variables x and y.

```
for (i = 2; i <= 7; i++) {
  setring R;  FR = F[i];  setring S;
  FS = std(imap(R,FR));  dim(FS), mult(FS);
  FS[1];
  print("-------------------------------");
}
//   2  4
//   (-s^2+2*s-1)*k^2+(2*s-2)*k*l+(s*t-1)*l^2
//   -------------------------------
//   2 4
//   (s-1)*k^2-2*k*l-l^2
//   -------------------------------
//   2 4
//   (s^2-2*s+1)*k^2+(-2*s+2)*k*l+(-t+1)*l^2
//   -------------------------------
//   2 4
//   (s^2-2*s+1)*k^2+(-2*s+2)*k*l+(-t+1)*l^2
//   -------------------------------
```

```
//   2 4
//   (s-1)*k^2-2*k*l-l^2
//   ------------------------------
//   2 4
//   (-s^2+2*s-1)*k^2+(2*s-2)*k*l+(s*t-1)*l^2
//   ------------------------------
```

The whole computation takes 7 minutes CPU time on an 800 Mhz Pentium III processor, and 3 minutes of that time are spent on the `facstd` operation.

Each of these homogeneous quadratic polynomials factors over $\mathbb{Q}(\sqrt{s}, \sqrt{t})$, and induces a factorization of the corresponding ideal. We describe this factorization—which is carried out by hand—in detail for the second component F_2. We start from the Gröbner basis of the ideal F_2 computed in the program above,

$$(s-1)k^2 - 2kl - l^2, \ (s-1)h + (2t-2)k + (t-1)l, \ fl - gk,$$
$$el - g^2, \ d + f + g, \ c, \ 2b + e, \ a, \tag{6.21}$$
$$(s-1)fk - 2gk - gl, \ (s-1)f^2 - 2fg - g^2, \ ek - fg.$$

Over $\mathbb{Q}(\sqrt{s}, \sqrt{t})$, the first polynomial factors into

$$\left((\sqrt{s} + 1)k + l\right)\left((\sqrt{s} - 1)k - l\right) .$$

We consider the first factor; the second one can be treated similarly. Substituting $l = -(\sqrt{s} + 1)k$ into the generator $fl - gk$, that one factors into

$$-k\left((\sqrt{s} + 1)f + g\right) .$$

Since any zero of F_2 with $k = 0$ would imply $a = c = d = f = g = h = k = l = 0$ and thus be contained in $\mathcal{V}(E_3)$, we can divide by k and obtain a linear polynomial. Altogether, the first two rows of (6.21) become a set of seven independent linear polynomials and one quadratic polynomial $el - g^2$. For any pair (s, t) satisfying (6.8) they define a plane conic. It can be verified that the three polynomials in the third row are contained in the ideal generated by the first two rows.

In order to show that for none of the parameters s, t satisfying (6.8) the map φ vanishes identically on this conic, consider the following point p on it:

$$(0, \ -(\sqrt{s} + 1)(s - 1), \ 0, \ -2\sqrt{s}(s - 1), \ 2(\sqrt{s} + 1)(s - 1), \ -2(s - 1),$$
$$2(\sqrt{s} + 1)(s - 1), \ 4(t - 1) - 2(t - 1)(\sqrt{s} + 1), \ -2(s - 1), \ 2(\sqrt{s} + 1)(s - 1))^2 .$$

The coefficient of $w^2 z^2$ in $\varphi(C)$ is

$$-4s(\sqrt{s} - 1)^2(\sqrt{s} + 1)^2 ,$$

so $\varphi(C)$ does not not vanish identically.

In order to show that for all parameters s, t satisfying (6.8) the 12 conics are distinct, consider the quadratic polynomials in k and l in the SINGULAR output above. In the factorization over $\mathbb{Q}(\sqrt{s}, \sqrt{t})$, the ideal of each of the 12 conics contains a generator which is linear in k and l and independent of $a, \dots, h$. To show the distinctness of two conics, we distinguish two cases.

If these linear homogeneous polynomials are distinct (over $\mathbb{Q}(s,t)$), then it can be checked that for every given pair (s,t) they define subspaces whose restrictions to $(k,l) \neq (0,0)$ are disjoint.

In case that the linear homogeneous polynomials coincide then it can be explicitly checked that both conics are distinct. For example, both F_2 and F_5 contain the factor $(\sqrt{s} + 1)k + l$ in the first polynomial. As seen above, the corresponding conic of F_2 is contained in the subspace $a = c = 0$. Similarly, the corresponding conic of F_5 is contained in $e = g = 0$. Assuming that the two conics are equal for some pair (s,t), the equations of the ideals can be used to show further $a = b = c = \dots = h = 0$. However, due to the saturation with the excess component E_2 this is not possible, and hence the two conics are distinct.

The same calculations can be carried out for the other components.

7. ALGORITHMIC COMPLEXITY OF VISIBILITY COMPUTATIONS WITH MOVING VIEWPOINTS

We investigate the computational complexity of visibility problems with moving viewpoints. The results complement our results from the previous sections on the underlying algebraic complexity of these algorithmic problems.

Before stating our main results precisely, we review the necessary complexity-theoretical framework in Section 7.1. After formally introducing the complexity-theoretical problems in Section 7.2, we state our main results in Section 7.3.

In Section 7.4, we determine the computational complexity of the considered visibility problems for variable dimension. Then, in Section 7.5, we use the real algebraic-geometric technique of real quantifier elimination to establish polynomial solvability results for fixed dimension. In Section 7.6, we establish connections between our complexity-theoretical results and the algebraic-geometric results from the earlier sections. Finally, in Section 7.7, we discuss the relationship between our hardness results and the number-theoretical view obstruction problem.

7.1 Geometric objects and the model of computation

The geometric objects relevant for the complexity-theoretical investigations are convex bodies as introduced in Section 2.1.1. Whereas in earlier sections, we used well-known classical geometric frameworks, for our current complexity-theoretical investigations we would like to recall the underlying geometric computation models.

Our model of computation is the binary Turing machine: all relevant convex bodies can be presented by certain rational numbers, and the size of the input is defined as the length of the binary encoding of the input data (see, e.g., [57, 65, 67]).

Specifically, a $\mathcal{B}$-*presentation* of a 'rational' ball B is a triple $(n; c, \rho)$ with $n \in \mathbb{N}$, $c \in \mathbb{Q}^n$, and $\rho \in (0, \infty) \cap \mathbb{Q}$. B and $(n; c, \rho)$ are then related via $B = \{x \in \mathbb{R}^n : ||x - c||^2 \leq \rho\}$. Let $\mathcal{B}_2^n$ denote the class of all $\mathcal{B}$-balls in $\mathbb{R}^n$, and set $\mathcal{B}_2 = \bigcup_{n \in \mathbb{N}} \mathcal{B}_2^n$.

Remark 7.1. In a more restrictive model of balls we might require that the radius itself is rational. Although we will not discuss that model further, we remark that our complexity results hold in that model in the same way.

For rational polytopes we distinguish between $\mathcal{H}$- and $\mathcal{V}$-presentations [65]. A $\mathcal{V}$-*polytope* is a polytope P that is represented by integers n, k, and points $v_1, \dots, v_k \in \mathbb{Q}^n$

such that $P = \text{conv}(\{v_1, \ldots, v_k\})$, i.e., P is the convex hull of $v_1, \ldots, v_k$. An $\mathcal{H}$-*polytope* is a polytope P that is represented by integers n, k, a rational $k \times n$-matrix A, and a vector $b \in \mathbb{Q}^k$ such that $P = \{x \in \mathbb{R}^n : Ax \leq b\}$.

Let $\mathcal{P}_\mathcal{H}^n$ and $\mathcal{P}_\mathcal{V}^n$ denote the classes of $\mathcal{H}$- and $\mathcal{V}$-polytopes in $\mathbb{R}^n$, respectively, and set $\mathcal{P}_\mathcal{H} = \bigcup_{n \in \mathbb{N}} \mathcal{P}_\mathcal{H}^n$, $\mathcal{P}_\mathcal{V} = \bigcup_{n \in \mathbb{N}} \mathcal{P}_\mathcal{V}^n$. For fixed dimension $\mathcal{H}$- and $\mathcal{V}$-presentations of a polytope can be converted into each other in polynomial time. If, however, the dimension is part of the input then the size of one presentation may be exponential in the size of the other [92].

In some problems under consideration, we will consider single points instead of balls or polytopes. In this case we speak of a *degenerated body*.

7.2   Partial visibility and quadrant visibility

We consider the fundamental visibility problem with moving viewpoints as introduced in Section 2.2.1. Here, we consider a scene in n-dimensional space consisting of $m + 1$ convex bodies $B_0, B_1, \ldots, B_m$ from a class $\mathcal{X}$, where $\mathcal{X} \in \{\mathcal{B}_2, \mathcal{P}_\mathcal{H}, \mathcal{P}_\mathcal{V}\}$.

For the complexity-theoretical investigations it is quite crucial which information is part of the input of the problem. Thus let us recall the formal definition of the main problem PARTIAL VISIBILITY with respect to a given body class $\mathcal{X}$. Note that the dimension is part of the input.

Problem PARTIAL VISIBILITY$_\mathcal{X}$:

Instance: m, n, bodies $B_0, B_1, \ldots, B_m \subset \mathbb{R}^n$ from the class $\mathcal{X}$.
Question: Decide whether B_0 is partially visible with respect to $B_1, \ldots, B_m$.

Our hardness results for this problem will exploit the property that in the definition of partial visibility every viewpoint outside of $\text{conv}(\bigcup_{i=1}^m B_i)$ is allowed. In order to show that similar hardness results also hold for visibility problems with more restricted viewpoint regions we also investigate the following problem QUADRANT VISIBILITY.

We call B_0 *partially visible from the positive orthant* (with respect to $B_1, \ldots, B_m$) if there exists a viewpoint $v \in (0, \infty)^n \setminus \text{conv}(\cup_{i=1}^m B_i)$ such that B_0 is partially visible from v.

Problem QUADRANT VISIBILITY$_\mathcal{X}$:

Instance: m, n, bodies $B_0, B_1, \ldots, B_m \subset \mathbb{R}^n$ from the class $\mathcal{X}$.
Question: Decide whether B_0 is partially visible from the positive orthant with respect to $B_1, \ldots, B_m$.

We add the index $\emptyset$ if the input bodies $B_0, \ldots, B_m$ are required to be disjoint. Furthermore we add the index $\odot$ if B_0 is a degenerated body that consists of a single point in the origin (e.g., PARTIAL VISIBILITY$_{\mathcal{B}_2, \odot, \emptyset}$). If $\mathcal{X} = \mathcal{P}_\mathcal{H}$ or $\mathcal{X} = \mathcal{P}_\mathcal{V}$, we will usually denote the bodies by $P_0, \ldots, P_m$.

Ray sets. In the next sections, the following notation will be convenient. A ray which issues from the origin is called a *central ray*. For a set $A \subset \mathbb{R}^n$ let pos $A = \{\sum_{i=1}^{k} \lambda_i x_i : \{x_1, \ldots, x_k\} \subset A, \lambda_1, \ldots, \lambda_k \geq 0, k \in \mathbb{N}\}$ denote the *positive hull* of A. For a set $A \subset \mathbb{R}^n \setminus \{0\}$ let the *central ray set* of A be the set of central rays defined by the elements of A. A central ray set R *covers* a set $B \subset \mathbb{R}^n \setminus \{0\}$ if the central ray set of B is contained in R.

7.3   Main complexity results

We analyze the binary Turing machine complexity of the visibility problems for the case of variable dimension. Our main intractability results are summarized in the following theorem.

Theorem 7.2. *(a) For $\mathcal{X} \in \{\mathcal{B}_2, \mathcal{P}_\mathcal{H}, \mathcal{P}_\mathcal{V}\}$ the problems* PARTIAL VISIBILITY$_\mathcal{X}$ *and* QUADRANT VISIBILITY$_\mathcal{X}$ *are* $\mathbb{NP}$-*hard. This statement remains true if the bodies are disjoint and/or if B_0 (or P_0, respectively) is a single point located in the origin.*

(b) For $\mathcal{X} \in \{\mathcal{P}_\mathcal{H}, \mathcal{P}_\mathcal{V}\}$ the problems PARTIAL VISIBILITY$_{\mathcal{X},\odot}$ *and* QUADRANT VISIBILITY$_\mathcal{X}$ *are* $\mathbb{NP}$-*complete.*

These hardness results are contrasted by the following positive results for *fixed* dimension.

Theorem 7.3. *Let the dimension n be a fixed constant. For $\mathcal{X} \in \{\mathcal{B}_2, \mathcal{P}_\mathcal{H}, \mathcal{P}_\mathcal{V}\}$, the problems* PARTIAL VISIBILITY$_\mathcal{X}$ *and* QUADRANT VISIBILITY$_\mathcal{X}$ *can be solved in polynomial time.*

7.4   Complexity results for variable dimension

7.4.1   Idea of the hardness proofs

Let us consider the case where the body B_0 is a degenerated body located in the origin.

In order to show $\mathbb{NP}$-hardness, we provide reductions from the well-known NP-complete 3-satisfiability (3-SAT) problem [57]. Let $\mathcal{C} = \mathcal{C}_1 \wedge \ldots \wedge \mathcal{C}_k$ denote a 3-SAT formula with clauses $\mathcal{C}_1, \ldots, \mathcal{C}_k$ in the variables $y_1, \ldots, y_n$. Further, let $\overline{y_i}$ denote the complement of a variable y_i, and let the literals y_i^1 and y_i^0 be defined by $y_i^1 = y_i$, $y_i^0 = \overline{y_i}$. Let the clause $\mathcal{C}_i$ be of the form

$$\mathcal{C}_i = y_{i_1}^{e_{i_1}} \vee y_{i_2}^{e_{i_2}} \vee y_{i_3}^{e_{i_3}}, \tag{7.1}$$

where $e_{i_1}, e_{i_2}, e_{i_3} \in \{0, 1\}$ and $1 \leq i_1, i_2, i_3 \leq n$ are pairwise different indices.

Each of the reductions consists of two ingredients. First we enforce that any central visibility ray has a direction which is close to a direction in the set $\{-1, 1\}^n$. For this purpose, consider the cube $[-1, 1]^n$. For each of the $2n$ facets of the cube we construct
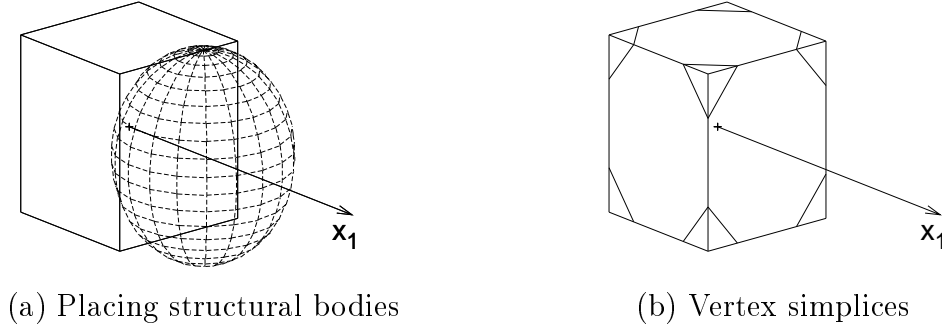
(a) Placing structural bodies   (b) Vertex simplices

Fig. 7.1: Imposing discrete structure

a suitable body (a ball or a polytope) whose positive hull covers the whole facet with the exception of "regions near the vertices". We call these bodies *structural bodies*. Figure 7.1(a) shows the situation for the 3-dimensional case of a ball. Any central visibility ray can then be naturally associated with a central ray in one of the directions $\{-1, 1\}^n$; this imposes a discrete structure on the problem. The $2n$ structural bodies are always part of the construction, independent of the specific 3-SAT formula. The positions of each of these $2n$ bodies will depend linearly on some positive parameter γ. In fact, all bodies can be moved radially and their size be appropriately adjusted so that the crucial covering properties persist. The parameters will be used later to make the bodies disjoint. In order to define the "region near a vertex" we consider Figure 7.1(b). For every vertex v of $[-1, 1]^n$ let the *vertex simplex of* v be defined as the convex hull of v and those n points which result by dividing exactly one component of v by 2. The construction will be such that any point in the boundary of $[-1, 1]^n$ that is not covered by the central ray set of a structural body will be contained in some vertex simplex.

In the second step, we relate satisfying assignments of a clause (7.1) to certain central visibility rays. Let $t : \{\text{TRUE}, \text{FALSE}\} \rightarrow \{-1, 1\}$ be defined by $t(\text{TRUE}) = 1$ and $t(\text{FALSE}) = -1$. Then, more precisely, we establish a correspondence between a truth assignment $a = (a_1, \ldots, a_n)^T \in \{\text{TRUE}, \text{FALSE}\}^n$ to the variables $y_1, \ldots, y_n$ and the central ray with direction $(t(a_1), \ldots, t(a_n))^T$.

For this purpose, let us consider the clause (7.1), and without loss of generality let $e_{i_1} = 0$, $e_{i_2} = 1$, $e_{i_3} = 0$. Then we want to ensure that neither one of the 2^{n-3} central rays in $\{x \in \{-1, 1\}^n : x_{i_1} = 1, x_{i_2} = -1, x_{i_3} = 1\}$ nor a ray defined by the corresponding vertex simplex can be a visibility ray. Hence, we construct a body whose central ray set completely covers an $(n-3)$-dimensional face of the cube $[-1, 1]^n$ but which does not cover any vertex not belonging to this face. Similar to the structural bodies, the positions of each body depends linearly on some positive parameter δ. Again, the parameters will be specified later so as to achieve disjointness of the bodies. The bodies which represent the clauses are called *clause bodies*.

The construction will guarantee that a truth assignment a is a satisfying assignment

for the 3-SAT formula $\mathcal{C}$ if and only there exists a visibility ray for B_0.

7.4.2 The case of balls

For $p \in \mathbb{R}^n$, $q \in \mathbb{R}^n \setminus \{0\}$, let $d(p, [0, \infty)q)$ denote the Euclidean distance of $p \in \mathbb{R}^n$ from the central ray $[0, \infty)q$. In the first lemma we compute some distances needed within the construction.

Lemma 7.4. *(a) Let $n \geq 3$, $\gamma > 0$, $0 \leq \phi \leq 1$, $p = \gamma \cdot (1, 0, \dots, 0)^T$, and $q = (1, \dots, 1, \phi)^T \in \mathbb{R}^n$. Then*

$$d(p, [0, \infty)q)^2 = \gamma^2 \left(1 - \frac{1}{n - 1 + \phi^2} \right).$$

(b) Let $n \geq 4$, $\delta > 0$, $-1 \leq \phi \leq 1$, $p = \delta \cdot (1, -1, 1, 0, \dots, 0)^T$, and $q = (1, -1, \phi, 1, \dots, 1)^T \in \mathbb{R}^n$. Then

$$d(p, [0, \infty)q)^2 = \delta^2 \left(3 - \frac{(2 + \phi)^2}{n - 1 + \phi^2} \right).$$

Proof. (a) For $\lambda \in \mathbb{R}$, let $q_\lambda := \lambda \cdot q$. The parameter λ for which the minimum distance of $\mathbb{R}q$ to p is attained satisfies $q_\lambda \cdot (p - q_\lambda) = 0$. Hence,

$$\lambda(\gamma - \lambda) - (n - 2)\lambda^2 - \lambda^2 \phi^2 = 0,$$

whose nontrivial solution is $\lambda = \gamma/(n - 1 + \phi^2) > 0$. For this value of λ we obtain

$$
\begin{aligned}
d(p, [0, \infty)q)^2 &= \gamma^2 \left(\left(\frac{1}{n - 1 + \phi^2} - 1 \right)^2 + (n - 2) \left(\frac{1}{n - 1 + \phi^2} \right)^2 + \left(\frac{\phi}{n - 1 + \phi^2} \right)^2 \right) \\
&= \gamma^2 \left(1 - \frac{1}{n - 1 + \phi^2} \right).
\end{aligned}
$$

(b) Here,

$$2\lambda(\lambda - \delta) + \lambda\phi(\lambda\phi - \delta) + (n - 3)\lambda^2 = 0$$

has the nontrivial solution $\lambda = \delta(2 + \phi)/(n - 1 + \phi^2) > 0$. Hence,

$$
\begin{aligned}
&d(p, [0, \infty)q)^2 \\
&= \delta^2 \left(2 \left(\frac{2 + \phi}{n - 1 + \phi^2} - 1 \right)^2 + \left(\frac{(2 + \phi)\phi}{n - 1 + \phi^2} - 1 \right)^2 + (n - 3) \left(\frac{2 + \phi}{n - 1 + \phi^2} \right)^2 \right) \\
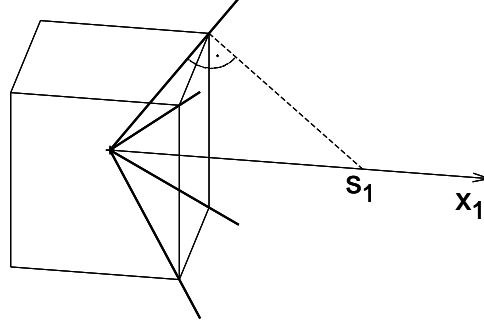&= \delta^2 \left(3 - \frac{(2 + \phi)^2}{n - 1 + \phi^2} \right).
\end{aligned}
$$

$\square$

Fig. 7.2: Computing the distance from the diagonal rays

Lemma 7.5. PARTIAL VISIBILITY$_{\mathcal{B}_2,\odot,\emptyset}$ *is* $\mathbb{NP}$*-hard.*

Proof. We complete the construction outlined so as to provide a polynomial time reduction from 3-SAT to PARTIAL VISIBILITY$_{\mathcal{B}_2,\odot,\emptyset}$. Without loss of generality let $n \geq 4$.

Let us consider the $2n$ structural balls $S_i(\gamma_i) = (n; s_i(\gamma_i), \sigma_i(\gamma_i))$, $1 \leq i \leq 2n$, where $s_i(\gamma_i) \in \mathbb{R}^n$ and $\sigma_i(\gamma_i) > 0$ are the center and the square of the radius of S_i, and γ_i is the scaling parameter of S_i as described above. Naturally, we place these balls symmetrically so that so that their centers lie on coordinate axes, i.e., let

$$s_i(\gamma_i) = \gamma_i e_i \quad \text{and} \quad s_{n+i}(\gamma_{n+i}) = -\gamma_{n+i}e_i \,,$$

where e_i denotes the i-th standard unit vector, $1 \leq i \leq n$.

In order to specify the squares of the radii $\sigma_i(\gamma_i)$ of the structural balls, let us consider $S_1(\gamma_1)$. For convenience of notation, we omit to state the index 1 and the dependence on $\gamma = \gamma_1$, and shortly write $S = (n; s, \sigma)$. See also Figure 7.1(a). The construction of the other balls is done analogously.

In order to impose the discrete structure we will satisfy the following two conditions. Firstly, $\mathrm{pos}(S)$ must not contain the vertices $\{1\} \times \{-1, 1\}^n$. Secondly, $\mathrm{pos}(S)$ must cover those points which result from the vertices of the facet $\{1\} \times [-1, 1]^{n-1}$ after dividing exactly one of the last $n - 1$ components by 2. The two conditions will yield an upper and a lower bound for σ.

We start with the first condition. Since any of the central rays $\{1\} \times \{-1, 1\}^{n-1}$ has the same distance from the center s, it suffices to consider $q = (1, 1, \ldots, 1)^T$ (see Figure 7.2). Hence, by choosing $\phi = 1$ in Lemma 7.4(a),

$$d(s, [0, \infty)q)^2 = \gamma^2 \frac{n - 1}{n} \,.$$

Consequently, we have to choose $\sigma < \gamma^2(n - 1)/n$. For the second condition, consider the point $q = (1, \ldots, 1, 1/2)^T$. Then, choosing $\phi = 1/2$ in Lemma 7.4(a) yields

$$d(s, [0, \infty)q)^2 = \gamma^2 \frac{4n - 7}{4n - 3} \,.$$

Therefore, a ball centered in s with square of the radius σ satisfying

$$\gamma^2 \frac{4n-7}{4n-3} \; < \; \sigma \; < \; \gamma^2 \frac{n-1}{n}$$

guarantees the two conditions. The construction of structural balls for all $2n$ facets guarantees that any point in a facet of $[-1,1]^n$ that is not covered by the central ray set of a structural ball is contained in a facet of some vertex simplex.

Now we can turn towards constructing the balls $C_i(\delta_i) = (c_i(\delta_i), \rho_i(\delta_i))$, $1 \le i \le k$, representing the k clauses. For notational convenience we assume that the clause is given by $y_1^0 \vee y_2^1 \vee y_3^0$, and abbreviate the ball for this clause by $C = (n; c, \rho)$ (assuming implicitly the dependence on the parameter $\delta := \delta_i$ in this notation). By setting $c = \delta(1, -1, 1, 0, \dots, 0)^T$, all the Boolean variables $y_4, \dots, y_n$ are treated in a uniform way. The rotation axis of the resulting central ray set is the central ray spanned by $(1, -1, 1, 0, \dots, 0)^T$.

In order to represent the given clause by the ball C we guarantee the following two properties. First, none of the vectors in $\{-1,1\}^n \backslash (1,-1,1) \times \{-1,1\}^{n-3}$ must be covered by the central ray set of the ball. Among this set of vectors, the vector $q = (1, -1, -1, 1, \dots, 1)^T$ leads to the smallest distance. Choosing $\phi = -1$ in Lemma 7.4(b) implies

$$d(c, [0, \infty)q)^2 = \delta^2 \frac{3n-1}{n}$$

which yields the condition $\rho < \delta^2 (3n-1)/n$.

Moreover, we guarantee the following second property. The central ray set of C must cover all the points in $(1, -1, 1) \times \{-1,1\}^{n-3}$ as well as their vertex simplices. Among all these points and among the vertices of the vertex simplices, the vector $q = (1, -1, 1/2, 1, \dots, 1)^T$ has largest distance from c. Lemma 7.4(b) with $\phi = 1/2$ implies

$$d(c, [0, \infty)q)^2 = \delta^2 \frac{12n-34}{4n-3} \; .$$

Hence, a ball centered in c with square of the radius ρ satisfying

$$\delta^2 \frac{12n-34}{4n-3} \; < \; \rho \; < \; \delta^2 \frac{3n-1}{n}$$

guarantees the two conditions for the clause ball. Note that the upper bound implies that the origin is not contained in the ball.

As yet, the definitions of the $2n$ structural balls and the k clause balls depend on the positive parameters $\gamma_1, \dots, \gamma_{2n}$ and $\delta_1, \dots, \delta_k$, respectively. Finally, by choosing these parameters appropriately, we make the balls disjoint. Since $\sigma_i < \gamma_i^2 (n-1)/n$ for the structural balls, we choose the parameter γ_i of the i-th structural ball successively so that

$$\gamma_i - \gamma_i \sqrt{\frac{n-1}{n}} > \gamma_{i-1} + \gamma_{i-1} \sqrt{\frac{n-1}{n}} \; .$$

Setting $\gamma_0 = 1$, this leads to

$$
\begin{aligned}
\gamma_i \;>\;& \left(\frac{1 + \sqrt{\frac{n-1}{n}}}{1 - \sqrt{\frac{n-1}{n}}} \right)^i \\
=\;& \left(2n - 1 + 2\sqrt{n \cdot (n-1)} \right)^i .
\end{aligned}
$$

Hence, choosing $\gamma_i = (4n - 1)^i$ for $1 \leq i \leq 2n$ guarantees that the structural balls are pairwise disjoint. The binary logarithm of these numbers grows only polynomially in the number of balls. Hence, inductively, we can choose the centers and the squares of the radii of the structural balls as rational numbers of polynomial size. The same method applies to the parameters $\delta_1, \dots, \delta_k$ of the clause balls. In particular, when also choosing δ_1 sufficiently large, then the clause balls are disjoint from the structural balls.

Now we show that the given 3-SAT formula $\mathcal{C}$ can be satisfied if and only if B_0 is partially visible. Let $a = (a_1, \dots, a_n)^T$ be a satisfying assignment of $\mathcal{C}$. Then there does not exist any ball B in the construction whose central ray set intersects with the central ray in direction $(t(a_1), \dots, t(a_n))^T$. Hence, B_0 is partially visible. Conversely, let b be a visibility ray for B_0. Due to the structural balls the ray b intersects with the vertex simplex of some vector $v \in \{-1, 1\}^n$. Consequently, the truth assignment $(t^{-1}(v_1), \dots, t^{-1}(v_n))^T$ is a satisfying assignment because otherwise the central ray set of some clause ball would contain the vertex simplex of v. Hence, $\mathcal{C}$ can be satisfied. $\qquad\square$

Corollary 7.6. PARTIAL VISIBILITY$_{\mathcal{B}_2, \emptyset}$ *is* $\mathbb{NP}$-*hard.*

Proof. The proof for the case that B_0 is a single point generalizes to the case of a non-degenerated ball centered in 0 with some square of the radius $\sigma_0 > 0$ by the following consideration. Let $0 < \sigma_0 < \min\{\sigma_1, \dots, \sigma_{2n}, \rho_1, \dots \rho_k\}$, where $S_i = (n; s_i, \sigma_i)$ and $C_j = (n; c_j, \rho_j)$ are the structural balls and the clause balls in the proof of Lemma 7.5. Further, let $B_0' = (n; 0, \sigma_0)$. If b is a visibility ray for B_0 then b is in particular a visibility ray for B_0'. Conversely, consider the situation where all the squares of the radii σ_i of the structural balls S_i, $1 \leq i \leq 2n$, and all the squares of the radii ρ_j of the clause balls C_j, $1 \leq j \leq k$, in the proof of Lemma 7.5 are decreased by σ_0. If b' is a visibility ray for B_0' in the new situation, then there exists a visibility ray b parallel to b' for the single point B_0. Hence, if the given inequalities in the proofs of Lemma 7.5 hold for both σ_i, ρ_j and for $\sigma_i' := \sigma_i - \sigma_0$, $\rho_j' := \rho_j - \sigma_0$, $1 \leq i \leq 2n$, $1 \leq j \leq k$, then the reduction from 3-SAT also holds for the non-degenerated ball B_0'. The given bounds show that it is possible to choose σ_0 both in polynomial size and at the same time sufficiently small in its value. $\qquad\square$

7.4.3   The case of $\mathcal{V}$-polytopes

Lemma 7.7. PARTIAL VISIBILITY$_{\mathcal{P}_\mathcal{V}, \odot, \emptyset}$ *is* $\mathbb{NP}$-*hard. This result persists if the instances are restricted to those consisting of cross polytopes.*
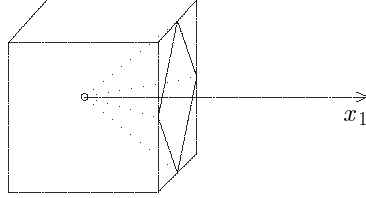
Fig. 7.3: Imposing discrete structure with cross polytopes

Proof. We establish a polynomial time reduction from 3-SAT to the problem PARTIAL VISIBILITY$_{\mathcal{P}_\mathcal{V}, \odot, \emptyset}$ based on the framework in Section 7.4.1.

This time, we choose the $2n$ structural bodies as cross polytopes of the form $S_i(\gamma_i) = \text{conv}(\{s_i(\gamma_i) + \sigma_{ij}(\gamma_i)e_j \ : \ 1 \leq j \leq n\})$ with rational coefficients $s_i(\gamma_i)$, $\sigma_{ij}(\gamma_i)$ depending on the scaling parameter γ_i. The centers of the cross polytopes are defined by

$$s_i(\gamma_i) = \gamma_i e_i \ \text{ and } \ s_{n+i}(\gamma_{n+i}) = -\gamma_{n+i}e_i \, , \quad 1 \leq i \leq 2n \, .$$

Now we specify the coefficients σ_{ij}. By symmetry, similar to the proof of Lemma 7.5, it suffices to consider the cross polytope $S_1(\gamma_1)$ which we abbreviate by $S = \text{conv}(\{s + \sigma_j e_j \ : \ 1 \leq j \leq n\})$ implicitly assuming the dependence on $\gamma := \gamma_1$; see Figure 7.3.

For any choice of the parameters $\sigma_2, \ldots, \sigma_n > 0$, the $(n-1)$-dimensional cross polytope $S' = \text{conv}(\{s + \sigma_j e_j \ : \ 2 \leq j \leq n\})$ is contained in the hyperplane $x_1 = \gamma$. Similar to the case of the balls, two conditions are imposed on the choice of $\sigma_2, \ldots, \sigma_n$. Firstly, the central ray set of S' must not contain the vertices $\{1\} \times \{-1, 1\}^n$. Secondly, the central ray set of S' must cover those points resulting from the vertices of the facet $\{1\} \times [-1, 1]^{n-1}$ by dividing exactly one of the last $n - 1$ components by 2.

We choose $\sigma_2 = \ldots = \sigma_n$. The necessary upper and lower bounds for σ_2 result as follows. Without loss of generality we consider the central ray $(1, \ldots, 1)^T$. The vertex $\gamma(1, \ldots, 1)^T$ of $\gamma[-1, 1]^n$ is contained in a facet of the $(n - 1)$-dimensional cross polytope $\text{conv}(\{s \pm \gamma(n - 1)e_j \ : \ 2 \leq j \leq n\})$. On the other hand, the point $\gamma(1, 1, 1, \ldots, 1, 1/2)^T$ is contained in a facet of the $(n - 1)$-dimensional cross polytope with vertices $\text{conv}(\{s \pm \gamma(n - 3/2)e_j\})$, $2 \leq j \leq n$. Hence, if σ_2 satisfies

$$\gamma \left(n - \frac{3}{2} \right) < \sigma_2 < \gamma \left(n - 1 \right)$$

then the two conditions enforcing the discrete structure are satisfied.

In order to make the $(n - 1)$-dimensional polytope S' full-dimensional we consider some ε with $0 < \varepsilon < \gamma$. Then $s - \varepsilon e_1 \in \text{pos } S'$. Hence, by adding the vertices $s \pm \varepsilon e_1$ we obtain an n-dimensional cross polytope S having the same central ray set as S'.

Now we show how to represent a clause by a cross polytope. Once more, we assume that the clause is given by $y_1^1 \vee y_2^0 \vee y_3^1$. Let C be the cross polytope $C = \text{conv}(\{c \pm \rho_j e_j \ :$

$2 \leq j \leq n\}$) with $c = \delta(1, -1, 1, 0, \ldots, 0)^T$ and coefficients ρ_j (also depending on the parameter δ) as defined in the following.

For any choice of parameters $\rho_4, \ldots, \rho_n > 0$, the $(n-3)$-dimensional cross polytope $C' = \mathrm{conv}(\{c \pm \rho_j e_j : 2 \leq j \leq n\})$ is contained in the $(n-3)$-dimensional plane $x_1 = \delta$, $x_2 = -\delta$, $x_3 = \delta$. We choose $\rho_4 = \ldots = \rho_n$. Moreover, we make the $(n-3)$-dimensional cross polytope C' full-dimensional by adding the vertices $c \pm \varepsilon e_j$, $1 \leq j \leq 3$, for some parameter $0 < \varepsilon < \delta$. If $\rho_4 = 2(n-3)$ then the point $\delta(1, -1, 1/2, 1, \ldots, 1)^T$ is contained in the n-dimensional cross polytope. Hence, by choosing $\rho_4 > 2(n-3)$ the central ray set of C covers all the points in $(1, -1, 1) \times \{-1, 1\}^{n-3}$ as well as their vertex simplices. Moreover, since the whole central ray set of the cross polytope is located in the orthant defined by $x_1 \geq 0$, $x_2 \leq 0$, $x_3 \geq 0$, none of the vectors in $\{-1, 1\}^n \setminus (1, -1, 1) \times \{-1, 1\}^{n-3}$ is covered by the central ray set of the ball.

Similar to the proof of Lemma 7.5, we can choose the parameters $\gamma_1, \ldots, \gamma_{2n}, \delta_1, \ldots, \delta_k$, and ε (for making the bodies n-dimensional) in such a way that the bodies are pairwise disjoint and that their encoding lengths remain polynomially bounded. Hence, the polynomial time reduction from 3-SAT follows in the same way as in the proof of Theorem 7.5. $\qquad \square$

Using an inclusion technique like in Lemma 7.6 we obtain the following corollary.

Corollary 7.8. PARTIAL VISIBILITY$_{\mathcal{P}_\mathcal{V}, \emptyset}$ *is* $\mathbb{NP}$-*hard. This result remains true if the instances are restricted to those consisting of cross polytopes.*

Lemma 7.9. PARTIAL VISIBILITY$_{\mathcal{P}_\mathcal{V}, \odot}$ *is contained in* $\mathbb{NP}$.

Proof. Let $(m; n; P_0, \ldots, P_m)$ be an instance of PARTIAL VISIBILITY$_{\mathcal{P}_\mathcal{V}, \odot}$ with $P_0 = \{0\}$ and $\mathcal{V}$-polytopes $P_1, \ldots, P_m$, and let $\mathcal{F}_{n-2}(P_i)$ denote the set of all $(n-2)$-dimensional faces of P_i, $1 \leq i \leq m$. Further let $\mathrm{lin}\, F$ denote the linear hull of a set F. The set of all linear subspaces $\mathrm{lin}\, F$, $F \in \mathcal{F}_{n-2}(P_i)$, naturally decomposes the unit sphere $\mathbb{S}^{n-1} := \{x \in \mathbb{R}^n : \|x\| = 1\}$ into $(n-1)$-dimensional sectors. For two central rays belonging to the same sector either both of them are visibility rays or none of them.

We show: if the single point P_0 is partially visible then there exists a certificate of polynomial size. Let $[0, \infty)q$ be a visibility ray for P_0 spanned by some vector $q \in \mathbb{R}^n \setminus \{0\}$. By the decomposition of $\mathbb{S}^{n-1}$ into equivalence classes we can assume that the linear subspace $\mathbb{R}q$ is the intersection of (at most) $n-1$ linear subspaces $\mathrm{lin}\, F_1, \ldots, \mathrm{lin}\, F_{n-1}$ with $F_1, \ldots, F_{n-1} \in \bigcup_{i=1}^m \mathcal{F}_{n-2}(P_i)$.

Of course, the number of combinatorial choices for $F_1, \ldots, F_{n-1}$ might grow exponentially in the input size. However, the following considerations show that the witness vector q can be represented in polynomial size nevertheless. For any subspace $\mathrm{lin}\, F_i$ the $\mathcal{V}$-presentation of F_i immediately gives a generating system of polynomial size. Since $\mathbb{R}q$ is the intersection of at most $n-1$ of these subspaces, we can find a witness vector of polynomial size.

It remains to show: one can verify in polynomial time that a given witness ray does not intersect with *the interior of* any of the polytopes P_i. Since the number of polytopes
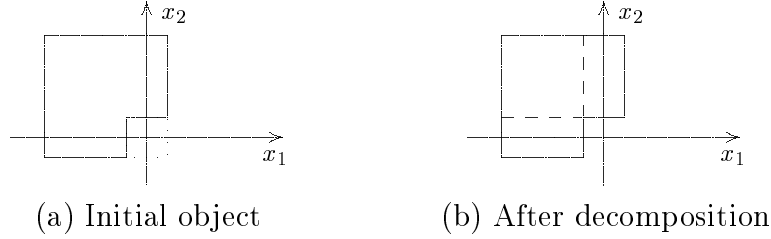
(a) Initial object (b) After decomposition

Fig. 7.4: Representing a 2-clause

is bounded by the input length of the instance, it suffices to explain this polynomial verification method for a single polytope $P \in \{P_1, \ldots, P_m\}$. Let the $\mathcal{V}$-presentation of P be $P = \text{conv}(\{v_1, \ldots, v_k\})$ with vectors $v_1, \ldots, v_k \in \mathbb{R}^n$. P does not intersect with the ray $[0, \infty)q$ if and only if the system

$$
\begin{aligned}
\sum_{i=1}^{k} \mu_i v_i &= \lambda q, \\
\sum_{i=1}^{k} \mu_i &= 1, \\
\mu_i &\geq 0, \quad 1 \leq i \leq k, \\
\lambda &\geq 0
\end{aligned}
$$

does not have a solution. This can be checked in polynomial time by linear programming. However, if $P \cap [0, \infty)q \neq \emptyset$ then we still have to check whether $\text{int}(P) \cap [0, \infty)q \neq \emptyset$. Let $\lambda_1 := \min \lambda$ and $\lambda_2 := \max \lambda$ under the linear constraints stated before. Obviously, $\text{int}(P) \cap [0, \infty)q \neq \emptyset$ if and only if the point $p := \frac{1}{2}(\lambda_1 + \lambda_2)q$ is contained in $\text{int}(P)$. By considering the k linear programs

$$
\begin{aligned}
\max \mu_j & \\
\sum_{i=1}^{k} \mu_i v_i &= p, \\
\sum_{i=1}^{k} \mu_i &= 1, \\
\mu_i &\geq 0, \quad 1 \leq i \leq k,
\end{aligned}
$$

$(1 \leq j \leq k)$ we can compute which of the vectors v_j occurs with non-zero coefficient in *some* convex combination $p = \sum_{i=1}^{k} \mu_i v_i$. Now $p \in \text{int}(P)$ if and only if this set of vectors has affine dimension n. Altogether, verification of a witness ray can be done in polynomial time. □

7.4.4 The case of $\mathcal{H}$-polytopes

Lemma 7.10. PARTIAL VISIBILITY$_{\mathcal{P}_{\mathcal{H}}, \emptyset}$ *is* $\mathbb{NP}$-*hard. This statement persists if we restrict the polytopes to be n-dimensional boxes.*

Proof. We give a polynomial time reduction from 3-SAT. This time the proof differs from the given framework. We begin with the case where P_0 is a single point located in the origin.

For notational convenience, consider the clause $y_1^1 \vee y_2^0 \vee y_3^1$. We construct a set of polytopes ensuring that central rays spanned by some vector $b \in \mathbb{R}^n$ with $b_1 \geq 0$, $b_2 \leq 0$, $b_3 \geq 0$ cannot be visibility rays. Figure 7.4 depicts the idea of the construction for two variables y_1, y_2, and the 2-clause $y_1^1 \vee y_2^0$: the polytopes will originate from a "big" n-dimensional box in which a small n-dimensional cube is cut off (see Figure 7.4(a)) and which is then decomposed to re-establish boxes (see Figure 7.4(b))

When representing the clause, we have to take care that in the visibility problem only the interior points of the boxes $P_1, \dots, P_m$ are considered. As a consequence, we have to extend the boxes blocking P_0 slightly across the coordinate hyperplanes. For some parameters ε, δ with $0 < \varepsilon < \delta$ we define the box Q by

$$-\delta \leq x_1 \leq \varepsilon, \quad -\varepsilon \leq x_2 \leq \delta, \quad -\delta \leq x_3 \leq \varepsilon, \quad -\delta \leq x_j \leq \delta, \qquad 4 \leq j \leq n. \quad (7.2)$$

Since Q contains the origin, we consider $Q \backslash [-\varepsilon, \varepsilon]^n$ instead. In order to re-establish convex bodies, we decompose $Q \setminus [-\varepsilon, \varepsilon]$ into smaller boxes $Q_1, \dots, Q_r$. This decomposition will satisfy the following conditions.

(a) $\operatorname{int}(Q_1), \dots, \operatorname{int}(Q_r)$ are disjoint and do not contain the origin.

(b) For any vector $a \in \{\text{TRUE}, \text{FALSE}\}^n$ one of the boxes $Q_1, \dots, Q_r$ intersects the central ray in direction $(t(a_1), \dots, t(a_n))^T$ if and only if $t(a_1) = -1$, $t(a_2) = 1$, $t(a_3) = -1$.

Let $E = \{(x_1, x_2, x_3)^T : -\delta \leq x_1 \leq \varepsilon, -\varepsilon \leq x_2 \leq \delta, -\delta \leq x_3 \leq \varepsilon\}$. For $1 \leq i \leq n-3$, define the boxes Q_{2i-1}, Q_{2i} by the following conditions.

$$
\begin{aligned}
Q_{2i-1}: \quad & (x_1, x_2, x_3)^T \in E \,; \\
& -\delta \leq x_j \leq \delta, \quad 4 \leq j < n-i+1 \,; \\
& -\delta \leq x_{n-i+1} \leq -\varepsilon \,; \\
& -\varepsilon \leq x_j \leq \varepsilon, \quad n-i+1 < j \leq n \,; \\
Q_{2i}: \quad & (x_1, x_2, x_3)^T \in E \,; \\
& -\delta \leq x_j \leq \delta, \quad 4 \leq j < n-i+1 \,; \\
& \varepsilon \leq x_{n-i+1} \leq \delta \,; \\
& -\varepsilon \leq x_j \leq \varepsilon, \quad n-i+1 < j \leq n \,.
\end{aligned}
$$

These boxes successively cut off parts of Q. In particular, $Q \setminus \bigcup_{i=1}^{k} (Q_{2i-1} \cup Q_{2i})$, $1 \leq k \leq n-3$, results in the subset of $\mathbb{R}^n$ satisfying

$$
\begin{aligned}
& (x_1, x_2, x_3)^T \in E \,; \\
& -\delta \leq x_j \leq \delta, \quad 4 \leq j < n-k+1 \,; \\
& -\varepsilon \leq x_j \leq \varepsilon, \quad n-k+1 \leq j \leq n \,.
\end{aligned}
$$

Further let Q_{2n-5}, Q_{2n-4}, Q_{2n-3} serve to cut off the parts referring to the variables x_1, x_2, x_3:

$$Q_{2n-5}: \quad -\delta \leq x_1 \leq \varepsilon\,; \quad -\varepsilon \leq x_2 \leq \delta\,; \quad -\delta \leq x_3 \leq -\varepsilon\,;$$
$$-\varepsilon \leq x_j \leq \varepsilon\,, \quad 4 < j \leq n\,;$$
$$Q_{2n-4}: \quad -\delta \leq x_1 \leq \varepsilon\,; \quad \varepsilon \leq x_2 \leq \delta\,; \quad -\varepsilon \leq x_3 \leq \varepsilon\,;$$
$$-\varepsilon \leq x_j \leq \varepsilon\,, \quad 4 < j \leq n\,;$$
$$Q_{2n-3}: \quad -\delta \leq x_1 \leq -\varepsilon\,; \quad -\varepsilon \leq x_2 \leq \varepsilon\,; \quad -\varepsilon \leq x_3 \leq \varepsilon\,;$$
$$-\varepsilon \leq x_j \leq \varepsilon\,, \quad 4 < j \leq n\,.$$

Then $Q \setminus \bigcup_{i=1}^{2n-3} Q_i$ results to

$$-\varepsilon \leq x_j \leq \varepsilon\,, \quad 1 \leq j \leq n\,.$$

In other words: the union of $Q_1, \ldots, Q_{2n-3}$ results to Q with the exception of a small cube containing the origin. Note that the interior parts of $Q_1, \ldots, Q_{2n-3}$ are pairwise disjoint.

Now we show that condition (b) is satisfied. First let $a \in \{\text{TRUE}, \text{FALSE}\}^n$ with $t(a_1) = -1$, $t(a_2) = 1$, $t(a_3) = -1$. Since $Q \setminus \bigcup_{i=1}^{2n-3} Q_i = [-\varepsilon, \varepsilon]^n$ and by (7.2), one of the open boxes $\text{int}(Q_i)$ intersects with the central ray spanned by $(t(a_1), \ldots, t(a_n))^T$. Namely, the points $\tau(t(a_1), \ldots, t(a_n))^T$ with $\tau \in (\varepsilon, \delta)$ are contained in Q but not in $[-\varepsilon, \varepsilon]$. Conversely, let $a \in \{\text{TRUE}, \text{FALSE}\}^n$ and for some $j \in \{1, \ldots, 2n-3\}$ let $\text{int}(Q_j)$ intersect with the central ray spanned by $(t(a_1), \ldots, t(a_n))^T$. Since all entries of this vector are of absolute value 1, there exists some $\tau \in (\varepsilon, \delta)$ such that $\tau(t(a_1), \ldots, t(a_n))^T \in \text{int}(Q_j)$. Hence, the definitions of $Q, Q_1, \ldots, Q_{2n-3}$ imply $t(a_1) = -1$, $t(a_2) = 1$, $t(a_3) = -1$.

The essential reason why it suffices to consider the *interior parts* of Q_j, $1 \leq j \leq 2n-3$, for the intersections is that none of their facets is contained in one of the coordinate hyperplanes $x_i = 0$. For exactly the same reason it is possible to make every box slightly smaller and therefore properly disjoint.

For different clauses $\mathcal{C}_i$ and $\mathcal{C}_j$, $i < j$, of the 3-SAT formula $\mathcal{C}$ we have to ensure that the resulting cubes are all disjoint. This can be achieved by suitably setting ε_i, δ_i and ε_j, δ_j for the clauses $\mathcal{C}_i$ and $\mathcal{C}_j$. If $\varepsilon_j > \delta_i$ then the boxes of $\mathcal{C}_i$ and $\mathcal{C}_j$ do not intersect with each other.

Finally, we show that the 3-SAT formula $\mathcal{C}$ is satisfiable if and only if B_0 is partially visible. First let $a \in \{\text{TRUE}, \text{FALSE}\}^n$ be a satisfying assignment for $\mathcal{C}$. Since a is a satisfying assignment for every 3-clause $\mathcal{C}_j$, condition (b) guarantees that $(t(a_1), \ldots, t(a_n))^T$ is a visibility ray for B_0. Conversely, let $[0, \infty)b$ be a visibility ray for B_0 spanned by some vector $b \in \mathbb{R}^n$. Define the modified sign function $\text{sg} : \mathbb{R} \to \{-1, 1\}$ by

$$\text{sg}(x) = \begin{cases} 1 & \text{if } x \geq 0\,, \\ -1 & \text{if } x < 0\,. \end{cases}$$

Hence, by definition of the boxes, the vector $(\text{sg}(b_1), \ldots, \text{sg}(b_n))^T$ is a visibility ray. By condition (b), $a := (t^{-1}(\text{sg}(b_1)), \ldots, t^{-1}(\text{sg}(b_n)))^T$ satisfies every 3-clause $\mathcal{C}_j$. Consequently, $\mathcal{C}$ is satisfiable.

Finally, we remark that the single point P_0 can be replaced by a sufficiently small cube, since none of the facets of the boxes lies in a hyperplane containing the origin. $\square$

Lemma 7.11. PARTIAL VISIBILITY$_{\mathcal{P}_{\mathcal{H}}, \odot}$ *is contained in* $\mathbb{NP}$.

Proof. Similar to the proof of Lemma 7.9 we show: if the single point P_0 is partially visible then there exists a certificate of polynomial size. Once more, it suffices to consider the rays $[0, \infty)b$ resulting from the intersection of at most $n - 1$ subspaces $\lim F_1, \dots, \lim F_{n-1}$ with $F_1, \dots, F_{n-1} \in \cup_{i=1}^{m} \mathcal{F}_{n-2}(P_i)$. The $\mathcal{H}$-presentations of $F_1, \dots, F_{n-1}$ immediately give an $\mathcal{H}$-presentation of the one-dimensional subspace $\mathbb{R}b$. Hence, there exists a witness vector b of polynomial size. Finally, it can be checked in polynomial time, whether a given witness ray $[0, \infty)b$ intersects with the interior of at least one of the $\mathcal{H}$-polytopes $P_1, \dots, P_m$. $\square$

7.4.5   Quadrant visibility

In Sections 7.4.1–7.4.4 our hardness results for PARTIAL VISIBILITY were based on reductions from 3-SAT in which any assignment $a \in \{\text{TRUE}, \text{FALSE}\}^n$ was identified with one of the 2^n quadrants in $\mathbb{R}^n$. For that reason, the question arises whether the hardness results still hold for more restricted viewpoint areas, say, for those viewpoint areas which are contained in a single quadrant.

In the following we prove the part of Theorem 7.2 which says that the hardness results also hold QUADRANT VISIBILITY.

Lemma 7.12. QUADRANT VISIBILITY$_{\mathcal{B}_2, \odot, \emptyset}$ *is* $\mathbb{NP}$-*hard.*

Proof. Once more, we provide a reduction from 3-SAT, and therefore consider a 3-SAT formula in the variables $y_1, \dots, y_n$. The essential idea of the reduction is to construct an instance of QUADRANT VISIBILITY in $(n + 1)$-dimensional space $\mathbb{R}^{n+1}$. The central ray with direction $v := (1, \dots, 1)^T$ is contained in the positive orthant Q of $\mathbb{R}^{n+1}$. By considering a hyperplane which is orthogonal to v and which intersects $(0, \infty)v$, we transfer the proof ideas of PARTIAL VISIBILITY to QUADRANT VISIBILITY.

In order to simplify notation, we apply an orthogonal transformation to transform the diagonal ray $[0, \infty)v$ into $[0, \infty)e_{n+1}$, the non-negative part of the x_{n+1}-axis. By this operation, Q is transformed into a cone Q'. Similar to the proof of Lemma 7.5, we impose a discrete structure on the visibility problem. Namely, for some positive parameter $\tau > 0$ specified below, we associate the 2^n truth assignments $\{\text{TRUE}, \text{FALSE}\}^n$ with the central rays spanned by the vectors $\{-\tau, \tau\}^n \times \{1\}$. Note that the set $[-\tau, \tau]^n \times \{1\}$ is an n-dimensional cube in $\mathbb{R}^{n+1}$.

In order to achieve this discrete structure, we place $2n + 1$ structural balls $S_i(\gamma_i, \tau) = (n; s_i(\gamma_i, \tau), \sigma_i(\gamma_i, \tau))$, $0 \leq i \leq 2n$, at the centers $c_0 = \gamma_0 e_{n+1}$, $c_i = \gamma_i(e_{n+1} + \tau e_i)$, $c_{n+i} = \gamma_{n+i}(e_{n+1} - \tau e_i)$, $1 \leq i \leq n$. In contrast to the proofs for PARTIAL VISIBILITY, the centers of the structural balls do not only depend on positive parameters γ_i, but also on the global positive parameter τ. Figure 7.5 shows this situation for the case $n = 2$. The parameter τ is chosen such that the n-dimensional cube $[-\tau, \tau]^n \times \{1\}$ is contained in Q'.
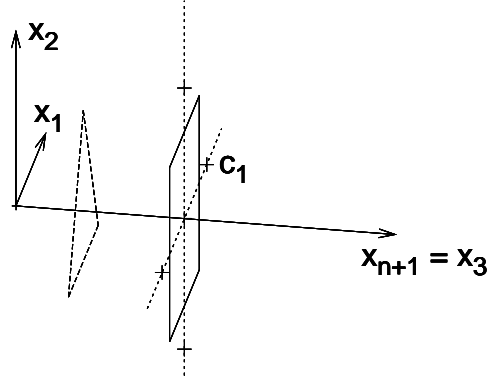
Fig. 7.5: Imposing discrete structure on QUADRANT VISIBILITY in case $n = 2$ and $\gamma_0 = \ldots = \gamma_{2n} =: \gamma$ (so all the centers of the structural balls are contained in the hyperplane $x_{n+1} = \gamma$). The positive hull of the triangle represents Q', the positive orthant after the orthogonal transformation.

The squares of the radii $s_i(\gamma_i, \tau)$, $1 \le i \le n$, of the structural balls can be chosen such that any visibility ray must be close to a vertex of the n-dimensional cube; this establishes the discrete structure. In a second step, the parameters γ_i can be used to scale the balls in order to make them disjoint.

Then, similar to the proof of Lemma 7.6, we can construct balls representing the clauses of the 3-SAT formula in order to complete the desired polynomial time reduction. $\qquad\square$

Similar to proof of Lemma 7.6, we can extend this result to the case QUADRANT VISIBILITY$_{\mathcal{B}_2, \emptyset}$, where B_0 is a proper ball. Moreover, by combining the proofs of Lemmas and Corollaries 7.7–7.11 with a lifting into $\mathbb{R}^{n+1}$, the hardness results can also be established for the case of $\mathcal{V}$- and $\mathcal{H}$-polytopes. Note that the proof technique of Lemma 7.12 can also be generalized to establish hardness results for other classes of viewpoint areas.

7.5 Polynomial solvability results for fixed dimension

In order to prove the polynomial solvability results for fixed dimension, we use the fact that for fixed dimension the theory of real closed fields can be decided in polynomial time [7, 29]. More precisely, for rational polynomials $p_1(x_1, \ldots, x_n), \ldots, p_l(x_1, \ldots, x_n)$ in the variables $x_1, \ldots, x_n$, a *Boolean formula over* $p_1, \ldots, p_l$ is defined as a Boolean combination (allowing the operators $\wedge$, $\vee$, NOT) of polynomial equations and inequalities of the type $p_i(x_1, \ldots, x_n) = 0$ or $p_i(x_1, \ldots, x_n) \le 0$. We consider the following decision problem for quantified Boolean formulas over the real numbers.

Problem REAL QUANTIFIER ELIMINATION:

Instance: n, l, rational polynomials $p_1(x_1, \dots, x_n), \dots, p_l(x_1, \dots, x_n)$, a Boolean formula $\varphi(x_1, \dots, x_n)$ over $p_1, \dots, p_l$, and quantifiers $Q_1, \dots, Q_n \in \{\forall, \exists\}$.

Question: Decide the truth of the statement

$$Q_1(x_1 \in \mathbb{R}) \ \dots \ Q_n(x_n \in \mathbb{R}) \quad \varphi(x_1, \dots, x_n) \,.$$

In [7, 29] it was shown:

Proposition 7.13. *For fixed dimension n, REAL QUANTIFIER ELIMINATION can be decided in polynomial time.*

Remark 7.14. In spite of this polynomial solvability result for fixed dimension, current implementations are only capable of dealing with very small dimensions. Generally, there are two approaches towards practical solutions of decision problems over the reals. One is based on Collins' cylindrical algebraic decomposition (CAD) [29], and the other is the critical point method ([61]; for the state of the art see [5]).

In order to prove polynomial solvability of PARTIAL VISIBILITY$_{\mathcal{B}_2}$ for fixed dimension, we formulate the problem algebraically. We represent a ray $p + [0, \infty)q$ by its initial vector $p \in \mathbb{R}^n$ and a direction vector $q \in \mathbb{R}^n$ with $||q|| = 1$. B_0 is partially visible with respect to $B_0 = (n; c_0, \rho_0), \dots, B_m = (n; c_m, \rho_m)$ if and only if there exist $p, q \in \mathbb{R}^n$ such that for all $\lambda \in \mathbb{R}$ the following formula holds:

$$
\begin{aligned}
&&||q||^2 &= 1 \,, \\
\text{and} && ||p - c_0||^2 &\leq \rho_0 \,, \\
\text{and} && (\lambda < 0 \ \vee \ ||p + \lambda q - c_i||^2 &\geq \rho_i) \,, && 1 \leq i \leq m \,.
\end{aligned}
$$

Hence, we have to decide the truth of the following statement:

$$\exists p \in \mathbb{R}^n \quad \exists q \in \mathbb{R}^n \quad \forall \lambda \in \mathbb{R}$$
$$||q||^2 = 1 \ \wedge \ ||p - c_0||^2 \leq \rho_0 \ \wedge \ \big((\lambda < 0 \ \vee \ ||p + \lambda q - c_i||^2 \geq \rho_i), \quad 1 \leq i \leq m\big) \,.$$

After expanding the Euclidean norm and applying some trivial transformations (such as establishing the mentioned normal form $p_i(x_1, \dots, x_n) \leq 0$ for the polynomial inequalities), this is a quantified Boolean formula of the required form. Hence, Proposition 7.13 implies the following statement.

Lemma 7.15. *For fixed dimension n, PARTIAL VISIBILITY$_{\mathcal{B}_2}$ can be solved in polynomial time.*

For the case of $\mathcal{H}$-polytopes, let $P_i = \left\{ x \in \mathbb{R}^n \,:\, A_i x \leq b_i \right\}$ with $A_i \in \mathbb{Q}^{k_i \times n}$, $b_i \in \mathbb{Q}^{k_i}$, $0 \leq i \leq m$. P_0 is partially visible if and only if there exist $p, q \in \mathbb{R}^n$ such that for all $\lambda \in \mathbb{R}$ we have

$$
\begin{array}{rrcl}
& ||q||^2 & = & 1 \,, \\
\text{and} & A_0 p & \leq & b_0 \,, \\
\text{and} & (\lambda < 0 \ \vee \ \mathrm{NOT}(\, A_i(p + \lambda q) & < & b_i \,))\,, \quad 1 \leq i \leq m \,.
\end{array}
$$

Applying Proposition 7.13 on this formulation we can conclude:

Lemma 7.16. *For fixed dimension n, PARTIAL VISIBILITY$_{\mathcal{P}_\mathcal{H}}$ can be solved in polynomial time.*

Since for fixed dimension n, a $\mathcal{V}$-polytope can be transformed into a $\mathcal{H}$-polytope in polynomial time [44], this also implies

Corollary 7.17. *For fixed dimension n, PARTIAL VISIBILITY$_{\mathcal{P}_\mathcal{V}}$ can be solved in polynomial time.*

Similarly, by small modifications of the proofs, the polynomial time solvability results for PARTIAL VISIBILITY can also be transferred to QUADRANT VISIBILITY.

7.6   *On the frontiers of Theorems 7.2 and 7.3*

Theorems 7.2 and 7.3 do not guarantee membership of PARTIAL VISIBILITY$_{\mathcal{B}_2}$ or PARTIAL VISIBILITY$_{\mathcal{B}_2, \odot}$ in $\mathbb{NP}$. Let us illuminate this situation from the algebraic point of view. First note that even though quantifier elimination methods can decide PARTIAL VISIBILITY$_{\mathcal{B}_2}$ for fixed dimension in polynomial time (see Lemma 7.15), it is not known how to compute a short witness of a positive solution with these methods (see [7]).

Combining the algorithmic, the algebraic, and the complexity-theoretical viewpoint, the situation looks as follows. For PARTIAL VISIBILITY$_{\mathcal{B}_2}$ or PARTIAL VISIBILITY$_{\mathcal{B}_2, \odot}$, we can construct instances in $\mathbb{R}^n$ which have exactly a single visibility ray. This visibility ray can be seen as a common tangent line to several spheres. Hence, the question of membership in $\mathbb{NP}$ is tightly connected to the algebraic characterization of the common tangent lines to a given set of spheres in $\mathbb{R}^n$ from Section 5.1.

Similarly, Theorems 7.2 and 7.3 do not guarantee membership of PARTIAL VISIBILITY$_{\mathcal{P}_\mathcal{H}}$ or PARTIAL VISIBILITY$_{\mathcal{P}_\mathcal{V}}$ in $\mathbb{NP}$. These questions are tightly connected to the common transversals to $2n-2$ given $(n-2)$-dimensional planes in $\mathbb{R}^n$. For algebraic characterizations of this problem see Section 5.2.1.

In both cases (balls and polytopes), the algebraic degree statements in the oracle model are reflected by our hardness results in the Turing machine model. However, we do not know in how far the algebraic characterizations for balls or polytopes can be exploited for proving a short witness visibility ray.

Concerning $\mathbb{NP}$-hardness, Theorem 7.2 does not include a statement for PARTIAL VISIBILITY$_{\mathcal{B}_2,\emptyset}$ or PARTIAL VISIBILITY$_{\mathcal{B}_2,\odot,\emptyset}$ if the balls are restricted to be unit balls. However, the following statement shows that in "Yes"-instances of PARTIAL VISIBILITY$_{\mathcal{B}_2,\emptyset}$ the number of balls necessarily grows exponentially in the input dimension n. Even if this does not rule out the existence of a polynomial time algorithm (since the running time of the algorithm is not measured in terms of the dimension n but in the overall length of the input size), it might give a useful sufficient criterion for large input dimensions.

Lemma 7.18. *Let $n \geq 6$, $m \in \mathbb{N}$, and let $B_0, B_1, \ldots, B_m$ be a set of $n + 1$ disjoint unit balls in $\mathbb{R}^n$. If $m < \sqrt{3n}\, e^{\frac{3}{8}(n-1)}$ then B_0 is partially visible with respect to $B_1, \ldots, B_m$.*

Proof. Without loss of generality we can assume that B_0 is the unit ball centered in the origin. Let $0 < r < 1$ and H be a hyperplane in $\mathbb{R}^n$ at distance r from the origin. Then the set of points on the unit sphere separated from the origin by H is called an *r-cap*. Since any ball B_i, $1 \leq i \leq m$, is disjoint from B_0, an elementary geometric inspection shows that $\mathrm{pos}(B_i)$ intersects the unit sphere in an r-cap with $\sqrt{3}/2 < r < 1$. A necessary condition for B_0 being not partially visible is that these r-caps cover the unit sphere. Let $\tau(n, r)$ denote the minimum number of r-caps covering the unit sphere. By Lemma 5.2 in [20], for $r > 2/\sqrt{n}$ we have

$$\tau(n, r) \geq 2r\sqrt{n}\, e^{r^2(n-1)/2} \,.$$

Substituting the value $r = \sqrt{3}/2$ into this formula implies the desired estimation. $\qquad\square$

7.7   *Partial visibility and view obstruction*

Throughout this thesis, we have investigated the hardness of visibility computations with moving viewpoints with regard to the underlying algebraic complexity and with regard to computational complexity. In this final section, we would like to mention a related number-theoretical aspect.

In 1968, Wills investigated the following problem of diophantine approximation [150]. Let $||x||_I$ denote the distance of a real number x to the nearest integer. For any $n \in \mathbb{N}$ and $v_1, \ldots, v_n \in \mathbb{N}$, let

$$d(v_1, \ldots, v_n) = \sup_{\tau \in [0,1]} \min_{1 \leq i \leq n} ||\tau v_i||_I \,,$$

and

$$\kappa(n) \;=\; \inf_{v_1, \ldots, v_n \in \mathbb{N}} d(v_1, \ldots, v_n)$$
$$=\; \inf_{v_1, \ldots, v_n \in \mathbb{N}} \sup_{\tau \in [0,1]} \min_{1 \leq i \leq n} ||\tau v_i||_I \,.$$
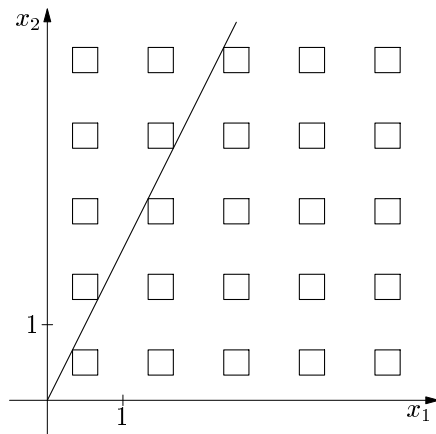
Fig. 7.6: The picture shows the situation of the view obstruction problem in $\mathbb{R}^2$. In particular, $\lambda(2) = \frac{1}{3}$.

Based on the pigeonhole principle, Wills showed $\frac{1}{2n} \leq \kappa(n) \leq \frac{1}{n+1}$ and conjectured $\kappa(n) = \frac{1}{n+1}$. This conjecture was later restated by Cusick [34] who interpreted it as a visibility problem called *view obstruction*. Let $C = [-\frac{1}{2}, \frac{1}{2}]^n$. For some factor $\alpha > 0$, consider the infinite set of cubes

$$\left\{ \left(\gamma_1 + \frac{1}{2}, \ldots, \gamma_n + \frac{1}{2} \right)^T + \alpha C \ : \ \gamma_1, \ldots, \gamma_n \in \mathbb{N}_0 \right\}. \tag{7.3}$$

Now the problem is to determine the supremum of $\alpha > 0$ such that there exists a visibility ray in the strictly positive orthant (see Figure 7.6). This supremum, called $\lambda(n)$, can be written as

$$\lambda(n) = 2 \sup_{\omega_1, \ldots, \omega_n \in (0, \infty)} \inf_{x \in (0, \infty)} \max_{1 \leq i \leq n} ||\omega_i x - \frac{1}{2}||_I.$$

The following statement from [34, 150] establishes the connection between Wills' problem and the view obstruction problem.

Proposition 7.19. *For $n \geq 2$ we have $\lambda(n) = 1 - 2\kappa(n)$.*

Yet another approach to the same core problem called *lonely runner* has been given in [12]. In spite of many research efforts during the last 30 years, the exact value of $\kappa(n)$ is known only for values up to 5 ([13]). For $n \geq 6$, only upper and lower bounds have been determined. If one considers balls instead of cubes [35], then the exact values for the view obstruction problem are also known up to dimension 5 ([39]).

Let us close the present thesis by discussing some tight connections between our complexity results and the view obstruction problem. First of all, the number-theoretical

papers do not give any real evidence why determining $\kappa(n)$ is hard. Although, of course, the view obstruction problem involves an infinite number of bodies, our complexity results for finite instances can be seen as a certain complexity-theoretical indication for the hardness of this evaluation. Namely, by Theorem 7.3, for fixed dimension PARTIAL VISIBILITY or QUADRANT VISIBILITY can be solved in polynomial time. However, if the dimension is part of the input, then the problem becomes $\mathbb{NP}$-hard by Theorem 7.2. In a non-rigorous sense, this can be seen as a quantification of the strong influence of the dimension compared to the other input parameters.

Another connection which we would like to point out refers to characterizing some easy instances of PARTIAL VISIBILITY or QUADRANT VISIBILITY. Namely, consider the view obstruction problem in $\mathbb{R}^n$. If the edge length α of the cubes in (7.3) satisfies $\alpha \leq \lambda(n)$ then there exists a visibility ray $[0, \infty)q$ in the strictly positive orthant for this visibility problem with infinitely many cubes. Fix this ray, and consider now the following class of n-dimensional instances of QUADRANT VISIBILITY. The bodies are cubes whose centers are contained in the grid $(\frac{1}{2}, \dots, \frac{1}{2})^T + \mathbb{N}_0^n$, and every cube has an edge length at most $\lambda(n)$. Additionally, let there be bodies which do not intersect the ray $[0, \infty)q$ and which guarantee that there cannot be a visibility ray which has a direction "quite close" to one of the coordinate hyperplanes. By the definition of $\lambda(n)$ we know that in this instance the answer is "VISIBLE". So the characterization of that class might be seen as a sufficient criterion for QUADRANT VISIBILITY (or similarly for PARTIAL VISIBILITY), and progress on the evaluation of $\lambda(n)$ might – at least theoretically – improve the characterization of that class.

BIBLIOGRAPHY

[1] P. Aluffi and W. Fulton. Lines tangent to four surfaces containing a curve. In preparation.

[2] P.K. Agarwal, B. Aronov, and M. Sharir. Computing envelopes in four dimensions with applications. *SIAM J. Computing* 26:1714–1732, 1997.

[3] P.K. Agarwal, B. Aronov, and M. Sharir. Line transversals of balls and smallest enclosing cylinders in three dimensions. *Discrete Comput. Geom.* 21:373–388, 1999.

[4] P. Angelier and M. Pocchiola. A sum of squares theorem for visibility complexes. *ACM Proc. Symposium on Computational Geometry (Medford, MA)*, 302–311, 2001.

[5] Ph. Aubry, F. Rouillier, and M. Safey El Din. Real solving for positive dimensional systems. *J. Symb. Comp.* 34:543–560, 2002.

[6] H.F. Baker. *Principles of Geometry*, vol. 4 (Higher Geometry). Cambridge University Press, 1925.

[7] M. Ben-Or, D. Kozen, and J. Reif. The complexity of elementary algebra and geometry. *J. Comp. Syst. Sci.* 32:251–264, 1986.

[8] M. de Berg. *Ray Shooting, Depth Orders and Hidden Surface Removal*. Lecture Notes in Computer Science, vol. 703, Springer-Verlag, Berlin, 1993.

[9] M. de Berg, M. van Krefeld, M. Overmars, and O. Schwarzkopf. *Computational Geometry. Algorithms and Applications*. 2nd ed., Springer-Verlag, Berlin, 2000.

[10] M. Bern, D. Dobkin, D. Eppstein, and R. Grossman. Visibility with a moving point of view. *Algorithmica* 11:360–378, 1994.

[11] A. Beutelspacher and U. Rosenbaum. *Projective Geometry: From Foundations to Applications*. Cambridge University Press, 1998.

[12] W. Bienia, L. Goddyn, P. Gvozdjak, A. Sebö, and M. Tarsi. Flows, view obstructions, and the lonely runner. *J. Comb. Theory, Ser. B* 72:1–9, 1998.

[13] T. Bohman, R. Holzman, and D. Kleitman. Six lonely runners. *Electronic Journal of Combinatorics* 8(2):R3, 2001.

[14] T. Bonnesen and W. Fenchel. *Theorie der konvexen Körper.* Springer-Verlag, Berlin, 1934.

[15] O. Bottema and G.R. Veldkamp. On the lines in space with equal distances to n given points. *Geom. Dedicata* 6:121–129, 1977.

[16] R.M. Bowen and C.-C. Wang. *Introduction to Vectors and Tensors*, vol. 1. Plenum Press, New York, 1976.

[17] R. Brandenberg. *Radii of Convex Polytopes.* Ph.D. thesis, Dept. of Mathematics, Technische Universität München, 2002.

[18] R. Brandenberg. Radii of regular polytopes. Preprint, 2002.

[19] R. Brandenberg and T. Theobald. Algebraic methods for computing smallest enclosing and circumscribing cylinders of simplices. Preprint, 2002. `math.OC/0211344` .

[20] A. Brieden, P. Gritzmann, R. Kannan, V. Klee, L. Lovász, and M. Simonovits. Approximation of diameters: Randomization doesn't help. *Proc. 39th Annual Symposium on Foundations of Computer Science (Palo Alto, CA)*, 244–251, 1998.

[21] H. Brönnimann, O. Devillers, V. Dujmović, H. Everett, M. Glisse, X. Gaoac, S. Lazard, H.-S. Na, S. Whitesides. On the number of lines tangent to four convex polyhedra. *Proc. 14th Canadian Conference on Computational Geometry (Lethbridge)*, 113–117, 2002.

[22] J. Canny. *The Complexity of Robot Motion Planning.* ACM Doctoral Dissertation Awards. MIT Press, Cambridge, MA, 1988.

[23] S.E. Cappell, J.E. Goodman, J. Pach, R. Pollack, M. Sharir, and R. Wenger. Common tangents and common transversals. *Adv. Math.* 106:198–215, 1994.

[24] T.M. Chan. Approximating the diameter, width, smallest enclosing cylinder, and minimum-width annulus. *Internat. J. of Comp. Geom. and Applications* 12:67–85, 2002.

[25] M. Chasles. Construction des coniques qui satisfont à cinque conditions. *C. R. Acad. Sci. Paris* 58:297–308, 1864.

[26] B. Chazelle, H. Edelsbrunner, L.J. Guibas, M. Sharir, and J. Stolfi. Lines in space: Combinatorics and algorithms. *Algorithmica* 15:428–447, 1996.

[27] Y.-G. Chen and T.W. Cusick. The view-obstruction problem for n-dimensional cubes. *J. Number Theory* 74:126–133, 1999.

[28] R. Cole and M. Sharir. Visibility problems for polyhedral terrains. *J. Symb. Comp.* 7:11–30, 1989.

[29] G.E. Collins. Quantifier eliminations for real closed fields by cylindrical algebraic decomposition. *Proc. Automated Theory and Formal Languages*, Lecture Notes in Computer Science, vol. 33, 134–183, Springer-Verlag, Berlin, 1975.

[30] Computational Geometry Impact Task Force (B. Chazelle et. al., 37 coauthors altogether). Application Challenges to Computational Geometry. In *Advances in Discrete and Computational Geometry*, 1996, Contemporary Mathematics, vol. 223, 407–463, AMS, Providence, RI, 1999. Also Technical report TR-521-96, Dept. of Computer Science, Princeton University, 1996.

[31] D. Cox, J. Little, and D. O'Shea. *Ideals, Varieties, and Algorithms*. UTM, 2nd ed., Springer-Verlag, New York, 1996.

[32] D. Cox, J. Little, and D. O'Shea. *Using Algebraic Geometry. Graduate Texts in Mathematics*, vol. 185, Springer-Verlag, New York, 1998.

[33] H.S.M. Coxeter. *Introduction to Geometry*. John Wiley & Sons, 1961.

[34] T.W. Cusick. View-obstruction problems. *Aequationes Math.* 9:165–170, 1973.

[35] T.W. Cusick and J. Pomerance. View-obstruction problems III. *J. Number Theory* 19:131–139, 1984.

[36] O. Devillers, V. Dujmovic, H. Everett, X. Gaoac, S. Lazard, H.S. Na, and S. Petitjean. The expected number of 3D visibility events is linear. Technical report, INRIA, no. 4671, 2002.

[37] O. Devillers, B. Mourrain, F.P. Preparata, and Ph. Trébuchet. On circular cylinders by four or five points in space. Technical report, INRIA, no. 4195, 2001. To appear in *Discrete and Computational Geometry*.

[38] G. Dos Reis, B. Mourrain, F. Rouillier, and Ph. Trébuchet. SYNAPS: An environment for symbolic and numeric computation, 2002.
`http://www-sop.inria.fr/galaad/logiciels/synaps/` .

[39] V.C. Dumir, R.J. Hans-Gill, and J.B. Wilker. The view-obstruction problem for spheres in $\mathbb{R}^n$. *Monatshefte Math.* 122:21–34, 1996.

[40] C. Durand. *Symbolic and Numerical Techniques for Constraint Solving*. Ph.D. thesis, Purdue University, 1998.

[41] F. Durand. *3D Visibility: Analytical Study and Applications*. Ph.D. thesis, Université Joseph Fourier, Grenoble, 1999.

[42] F. Durand, G. Drettakis, and C. Puech. The 3D visibility complex: a unified data structure for global visibility of scenes of polygons and smooth objects. *Proc. 9th Canadian Conference on Computational Geometry (Kingston)*, 153–158, 1997.

[43] F. Durand, G. Drettakis, and C. Puech. The 3D visibility complex. To appear in *ACM Trans. Graph.*

[44] M.E. Dyer. The complexity of vertex enumeration methods. *Math. Oper. Res.* 8:381–402, 1983.

[45] H. Edelsbrunner. *Algorithms in Combinatorial Geometry.* Springer-Verlag, Berlin, 1987.

[46] H. Edelsbrunner and E.P. Mücke. Simulation of simplicity: A technique to cope with degeneracy. *ACM Trans. Graph.* 9:43–72, 1990.

[47] H. Edelsbrunner and M. Sharir. The maximum number of ways to stab n convex nonintersecting sets in the plane is $2n - 2$. *Discrete Comput. Geom.* 5:35–42, 1990.

[48] D. Eisenbud. *Commutative Algebra with a View Towards Algebraic Geometry.* Graduate Texts in Mathematics, vol. 150, Springer-Verlag, New York, 1995.

[49] D. Eisenbud, D. Grayson, M. Stillman, and B. Sturmfels (eds.). *Computations in Algebraic Geometry with Macaulay* 2. Algorithms and Computations in Mathematics, vol. 8, Springer-Verlag, Berlin, 2001.

[50] D. Eisenbud and J. Harris. *The Geometry of Schemes.* Graduate Texts in Mathematics, vol. 197, Springer-Verlag, New York, 2000.

[51] I. Emiris and J. Canny. Efficient incremental algorithms for the sparse resultant and the mixed volume. *J. Symb. Comp.* 20:117–149, 1995.

[52] A. Eremenko and A. Gabrielov. Rational functions with real critical points and the B. and M. Shapiro conjecture in real enumerative geometry. *Ann. Math.* 155:131–156, 2002.

[53] U. Faigle, W. Kern, and M. Streng. Note on the computational complexity of j-radii of polytopes in $\mathbb{R}^n$. *Math. Program.* 73A:1–5, 1996.

[54] G. Fischer and J. Piontkowski. *Ruled Varieties.* Vieweg, Braunschweig, 2001.

[55] W. Fulton. *Introduction to Intersection Theory in Algebraic Geometry.* CBMS regional conference series in mathematics, vol. 54, 2nd ed., AMS, Providence, RI, 1996.

[56] W. Fulton. *Intersection Theory.* Ergebnisse der Mathematik, vol. 2, 2nd ed., Springer-Verlag, New York, 1998.

[57] M.R. Garey and D.S. Johnson. *Computers and Intractability: A Guide to the Theory of NP–Completeness.* Freeman, 1979.

[58] S. Golab. *Tensor Calculus.* Elsevier, Amsterdam, 1974.

[59] J.E. Goodman and J. O'Rourke (eds.). *Handbook of Discrete and Computational Geometry*. CRC Press, Boca Raton, 1997.

[60] R.L. Graham, D.E. Knuth, and O. Patashnik. *Concrete Mathematics*. Addison-Wesley, 1989.

[61] D.Y. Grigor'ev and N.N. Vorobjov, Jr. Solving systems of polynomial inequalities in subexponential time. *J. Symb. Comp.* 5:37–64, 1988.

[62] G.-M. Greuel, G. Pfister, and H. Schönemann. Singular 2.0. A computer algebra system for polynomial computations. Centre for Computer Algebra, University of Kaiserslautern, 2001. http://www.singular.uni-kl.de .

[63] P. Gritzmann and V. Klee. Inner and outer *j*-radii of convex bodies in finite-dimensional normed spaces. *Discrete Comput. Geom.* 7:255-280, 1992.

[64] P. Gritzmann and V. Klee. Computational complexity of inner and outer *j*-radii of polytopes in finite-dimensional normed spaces. *Math. Program.* 59A:163-213, 1993.

[65] P. Gritzmann and V. Klee. On the complexity of some basic problems in computational convexity I: Containment problems. *Discrete Math.* 136:129–174, 1994.

[66] P. Gritzmann and V. Klee. Computational convexity. In [59], pp. 491–515, 1997.

[67] M. Grötschel, L. Lovász, and A. Schrijver. *Geometric Algorithms and Combinatorial Optimization*. Algorithms and Combinatorics, vol. 2. Springer-Verlag, Berlin, 1993.

[68] M. de Guzmán. An extension of the Wallace-Simson Theorem: Projecting in arbitrary directions. *Amer. Math. Monthly* 106:574–580, 1999.

[69] J. Harris. Galois groups of enumerative problems. *Duke Math. J.* 46:685–724, 1979.

[70] J. Harris. *Algebraic Geometry*. Graduate Texts in Mathematics, vol. 133, Springer-Verlag, New York, 1992.

[71] R. Hartshorne. *Algebraic Geometry*. Graduate Texts in Mathematics, vol. 52, Springer-Verlag, New York, 1977.

[72] A. Henderson. *The Twenty–Seven Lines upon the Cubic Surface*. Cambridge Tracts, vol. 13, 1911.

[73] D. Hilbert and S. Cohn-Vossen. *Anschauliche Geometrie*. Springer-Verlag, Berlin, 1932. Translation: Geometry and the Imagination, Chelsea Publ., New York, 1952.

[74] W. Hodge and D. Pedoe. *Methods of Algebraic Geometry*, volume 1. Cambridge University Press, 1947.

[75] W. Hodge and D. Pedoe. *Methods of Algebraic Geometry*, volume 2. Cambridge University Press, 1952.

[76] C.M. Hoffmann and B. Yuan. On spatial constraint solving approaches. *Proc. 3rd Workshop on Automated Deduction in Geometry 2000 (Zürich)*, Lecture Notes in Computer Science, vol. 2061, 1–15, Springer-Verlag, Berlin, 2001.

[77] F. Hohenberg. Das Apollonische Problem im $\mathbb{R}^n$. *Deutsche Mathematik* 7:78–81, 1942.

[78] M. Husty and H. Sachs. Abstandsprobleme zu windschiefen Geraden. *Sitzungsber., Abt. II, Österr. Akad. Wiss.*, vol. 203, 31–55, 1985.

[79] A. Karger. Classical geometry and computers. *J. Geom. Graph.* 2:7–15, 1998.

[80] K. Kendig. *Elementary Algebraic Geometry*. Graduate Texts in Mathematics, vol. 44, Springer-Verlag, New York, 1977.

[81] S.L. Kleiman and D. Laksov. Schubert calculus. *Amer. Math. Monthly* 79:1061–1082, 1972.

[82] H. Knörrer. *Geometrie*. Vieweg, 1996.

[83] U. Kortenkamp and J. Richter-Gebert. Dynamic geometry I: The problem of continuity. *Proc. European Workshop Comput. Geom. 1999 (Sophia-Antiopolis)*, 51–53.

[84] D. Kotzor. *Homotopieverfahren bei der Visualisierung dreidimensionaler Tangentenprobleme*. Diplomarbeit, Dept. of Mathematics, Technische Universität München, 2002.

[85] D. Kotzor and T. Theobald. Homotopy methods for real-time visualization of geometric tangent problems. Video presentation, *ACM Symposium on Computational Geometry 2002 (Barcelona)*. Accompanying article in the proceedings, pp. 275–276, 2002.

[86] Y.S. Kupitz and H. Martini. Equifacial tetrahedra and a famous location problem. *Math. Gazette* 83:464–467, 1999.

[87] D. Larman. Problem posed in the Problem Session of the DIMACS Workshop on Arrangements, Rutgers University, New Brunswick, NJ, 1990.

[88] H.-P. Lenhof and M. Smid. Maintaining the visibility map of spheres while moving the viewpoint on a circle at infinity. *Algorithmica* 13:301–312, 1995.

[89] T. Lewis, B. von Hohenbalken, and V. Klee. Common supports as fixed points. *Geom. Dedicata* 60:277–281, 1996.

[90] I.G. Macdonald, J. Pach, and T. Theobald. Common tangents to four unit balls in $\mathbb{R}^3$. *Discrete Comput. Geom.* 26:1–17, 2001.

[91] M. Marcus. *Finite Dimensional Multilinear Algebra, Part I.* Dekker, New York, 1973.

[92] P. McMullen. The maximum numbers of faces of a convex polytope. *Mathematika* 17:179–184, 1970.

[93] G. Megyesi. Lines tangent to four unit spheres with coplanar centres. *Discrete Comput. Geom.* 26:493–497, 2001.

[94] G. Megyesi. Configurations of $2n-2$ quadrics in $\mathbb{R}^n$ with $3 \cdot 2^{n-1}$ common tangent lines. *Discrete Comput. Geom.* 28:405–409, 2002.

[95] G. Megyesi. Personal communication.

[96] G. Megyesi, F. Sottile, and T. Theobald. Common transversals and tangents to two lines and two quadrics in $\mathbb{P}^3$. Preprint, 2002. `math.AG/0206044` .

[97] J. Milnor. *Singular Points of Complex Hypersurfaces.* Annals of mathematics studies, vol. 61. Princeton Univ. Press, 1968.

[98] H.M. Möller, H. Melenk, and W. Neun. Symbolic solution of large stationary chemical kinetics problems. *Impact of Computing in Science and Engineering* 1:138–167, 1989.

[99] J. O'Rourke. Visibility. In [59], pp. 467–479, 1997.

[100] D. Pedoe. *A Course of Geometry for Colleges and Universities.* Cambridge University Press, 1970.

[101] D. Pedoe. The missing seventh circle. *Elem. Math.* 25:14–15, 1970.

[102] M. Pellegrini. Ray shooting and lines in spaces. In [59], pp. 599–614, 1997.

[103] M. Pellegrini and P.W. Shor. Finding stabbing lines in 3-space. *Discrete Comput. Geom.* 8:191–208, 1992.

[104] M. Penna and R. Patterson. *Projective Geometry and its Applications to Computer Graphics.* Prentice-Hall, 1986.

[105] M. Pocchiola and G. Vegter. Topologically sweeping visibility complexes via pseudotriangulations. *Discrete Comput. Geom.* 16:419–453, 1996.

[106] H. Pottmann and J. Wallner. *Computational Line Geometry.* Springer-Verlag, Berlin, 2001.

[107] M. Reid. *Undergraduate Algebraic Geometry.* London Mathematical Society Student Texts, vol. 12. Cambridge University Press, Cambridge, 1988.

[108] J. Richter-Gebert and U.H. Kortenkamp. *The interactive geometry software Cinderella.* Springer-Verlag, Berlin, 1999.

[109] A. Robson. *An Introduction to Analytical Geometry,* vol. 1. Cambridge University Press, 1940.

[110] F. Ronga, A. Tognoli, and T. Vust. The number of conics tangent to 5 given conics: the real case. *Rev. Mat. Univ. Complut. Madrid* 10:391–421, 1997.

[111] G. Salmon. *A Treatise on the Analytic Geometry of Three Dimensions,* vol. 1. Longmans and Green, London, 7th edition, 1928. Reprinted by Chelsea Publishing Company, New York, 1958.

[112] H. Schaal. Ein geometrisches Problem der metrischen Getriebesynthese. *Sitzungsber., Abt. II, Österr. Akad. Wiss.,* vol. 194, 39–53, 1985.

[113] L. Schläfli. On the distributions of surfaces of the third order into species, in reference to the absence of presence of singular points, and the reality of their lines. *Phil. Trans. Royal Society of London* 153:193–241, 1863.

[114] E. Schömer, J. Sellen, M. Teichmann, and C. Yap. Smallest enclosing cylinders. *Algorithmica* 27:170–186, 2000.

[115] Martin Schönert et al. GAP – Groups, Algorithms, and Programming. Lehrstuhl D für Mathematik, Rheinisch Westfälische Technische Hochschule, Aachen, 1995.

[116] H. Schubert. Eine geometrische Eigenschaft der 16 Kugeln, welche 4 beliebig gegebene Kugeln berühren. *Zeitschrift für Mathematik und Physik* 14:506–513, 1869.

[117] H. Schubert. *Kalkül der abzählenden Geometrie.* Springer-Verlag, Berlin, 1879. Reprinted by Springer-Verlag, Berlin (1979).

[118] H. Schubert. Anzahlbestimmungen für lineare Räume beliebiger Dimension. *Acta Math.* 8:97-118, 1886.

[119] J.T. Schwartz and M. Sharir. On the "piano movers'" problem. I. The case of a two-dimensional rigid polygonal body moving amidst polygonal barriers. *Comm. Pure Appl. Math.* 36:345–398, 1983.

[120] J.T. Schwartz and M. Sharir: On the "piano movers" problem. II. General techniques for computing topological properties of real algebraic manifolds. *Adv. in Appl. Math.* 4:298–351, 1983.

[121] B. Segre. *The Non-Singular Cubic Surfaces.* Oxford University Press, 1942.

[122] J. M. Selig. *Geometrical Methods in Robotics.* Springer-Verlag, New York, 1996.

[123] J.G. Semple and G.T. Kneebone. *Algebraic Curves*. Oxford University Press, 1959.

[124] G.G. Smith and B. Sturmfels. Teaching the geometry of schemes. In [49], pp. 55–70, 2001.

[125] K.E. Smith, L. Kahanpää, P. Kekäläinen, and W. Traves. *An Invitation to Algebraic Geometry*. Springer-Verlag, New York, 2000.

[126] F. Sottile. Enumerative geometry for real varieties. In *Proc. Algebraic Geometry 1995*, Santa Cruz (J. Kollár, R. Lazarsfeld, and D. Morrison, eds.), Proc. Sympos. Pure Math., vol. 62, Part 1, 435–447, AMS, Providence, RI, 1997.

[127] F. Sottile. Enumerative geometry for the real Grassmannian of lines in projective space. *Duke Math. J.* 87:59–85, 1997.

[128] F. Sottile. The special Schubert calculus is real. *Electronic Research Announcements of the AMS* 5:35–39, 1999.

[129] F. Sottile. From enumerative geometry to solving systems of equations. In [49], pp. 101–129, 2001.

[130] F. Sottile. Enumerative real algebraic geometry. To appear in Proc. DIMACS Workshop on Algorithmic and Quantitative Aspects of Real Algebraic Geometry in Mathematics and Computer Science, 2001 (S. Basu and L. Gonzalez-Vega, eds.), DIMACS series, AMS.

[131] F. Sottile and T. Theobald. Lines tangent to $2n-2$ spheres in $\mathbb{R}^n$. *Trans. Amer. Math. Soc.* 354:4815–4829, 2002.

[132] F. Sottile and T. Theobald. Real lines tangent to $2n-2$ quadrics in $\mathbb{R}^n$. Preprint, 2002. `math.AG/0206099` .

[133] H. Stachel. Unendlich viele Kugeln durch vier Tangenten. *Math. Pannonica*, 6:55–66, 1995.

[134] R.P. Stanley. *Enumerative Combinatorics*. Cambridge University Press, 1997.

[135] J. Steiner. Elementare Lösung einer geometrischen Aufgabe und über einige damit in Beziehung stehende Eigenschaften der Kegelschnitte. *J. Reine Angew. Math.* 37:161–192, 1848.

[136] J. Stolfi. *Oriented Projective Geometry*. Academic Press, 1991.

[137] B. Sturmfels. *Solving Systems of Polynomial Equations*. CBMS series, vol. 97, AMS, Providence, RI, 2002.

[138] B. Sturmfels. *Algorithms in Invariant Theory.* RISC Series in Symbolic Computation, Springer-Verlag, Wien, 1993.

[139] D.F. Swayne, D. Cook, and A. Buja. XGobi. Interactive dynamic data visualization in the X window system. *J. Comput. Graphical Statistics* 7:113–130, 1998.

[140] T. Theobald. An enumerative geometry framework for algorithmic line problems in $\mathbb{R}^3$. *SIAM J. Computing* 31:1212–1228, 2002.

[141] T. Theobald. How to realize a given number of tangents to four given balls in $\mathbb{R}^3$. To appear in *Mathematika*.

[142] T. Theobald. Visibility computations: From discrete algorithms to real algebraic geometry. To appear in Proc. DIMACS Workshop on Algorithmic and Quantitative Aspects of Real Algebraic Geometry in Mathematics and Computer Science, 2001 (S. Basu and L. Gonzalez-Vega, eds.), DIMACS series, AMS.

[143] J. Verschelde. PHCpack: A general-purpose solver for polynomial systems by homotopy continuation. *ACM Trans. Math. Software* 25:251–276, 1999.

[144] J. Verschelde. Polynomial homotopies for dense, sparse and determinantal systems. MSRI Preprint 1999-041, 1999.

[145] G. Walker. *Algebraic Curves.* Princeton University Press, 1950. Reprinted by Springer-Verlag, New York (1979).

[146] C.A. Wang and B. Zhu. Three-dimensional weak visibility: Complexity and applications. *Theor. Comp. Sci.* 234:219–232, 2000.

[147] B. Weißbach. Über die senkrechten Projektionen regulärer Simplexe. *Beitr. Algebra Geom.* 15:35–41, 1983.

[148] B. Weißbach. Über Umkugeln von Projektionen regulärer Simplexe. *Beitr. Algebra Geom.* 16:127–137, 1983.

[149] J. Wernecke. *The Inventor Mentor: Programming Object-Oriented 3D Graphics with Open Inventor.* Addison-Wesley, Reading, MA, 1994.

[150] J.M. Wills. Zur simultanen homogenen diophantischen Approximation I. *Monatshefte Math.* 72:254–263, 1968.

DEUTSCHSPRACHIGE ZUSAMMENFASSUNG

New algebraic methods in computational geometry –
Neue algebraische Methoden in der algorithmischen Geometrie

Gegenstand der Arbeit sind fundamentale algebraisch-geometrische Probleme in der nichtlinearen algorithmischen Geometrie, die beispielsweise bei Sichtbarkeitsproblemen mit bewegten Kamerapunkten oder der Berechnung minimal einschließender Kreiszylinder von Punktmengen im $\mathbb{R}^n (n \geq 3)$ auftreten.

Im dreidimensionalen Fall führen die algorithmischen Probleme auf Anzahl- und Endlichkeitsfragen der Form: Wie viele Geraden gibt es (im Endlichkeitsfall) im $\mathbb{R}^3$, die gleichzeitig Transversale zu k vorgegebenen Geraden und Tangente an $4-k$ vorgegebene Sphären im $\mathbb{R}^3$ sind $(0 \leq k \leq 3)$? Unter welchen Bedingungen gibt es unendlich viele solcher Geraden? Bereits für den Fall von Einheitssphären stellte die Anzahlfrage ein von D. Larman im Jahr 1990 aufgeworfenes offenes Problem dar.

Vom algebraischen Standpunkt sind hierzu die reellen Lösungen polynomialer Gleichungssysteme zu studieren. Ausgehend von Fragen des obigen Typs werden in der Arbeit algebraische Methoden zur Lösung dieser reell-enumerativen Fragen für wichtige Klassen geometrischer Tangentenprobleme im dreidimensionalen sowie n-dimensionalen Raum entwickelt.

In Kapitel 2 der Arbeit werden die zugrundeliegenden geometrischen und algorithmischen Grundlagen zusammengestellt. Insbesondere wird ein sweep-basierter Algorithmus zur Lösung des zweidimensionalen Sichtbarkeitproblems vorgestellt sowie gezeigt, wie im dreidimensionalen Fall die algorithmischen Probleme auf die algebraisch-geometrischen Kernprobleme zurückgeführt werden können. Ferner werden Tangentialbedingungen in liniengeometrischen Plückerkoordinaten formuliert, die in den weiteren Kapiteln von grundlegender Bedeutung sind.

In Kapitel 3 wird das Problem der gemeinsamen Tangenten an vier Sphären studiert. Für den Fall affin unabhängiger Mittelpunkte wird eine Formulierung des Problems als Schnittpunkte einer kubischen sowie einer quartischen Kurve in der projektiven Ebene $\mathbb{P}^2$ angegeben. Anschließend wird der Fall von Einheitssphären betrachtet. Es wird folgender Satz gezeigt, der das Problem von D. Larman vollständig löst:

Satz. Vier Einheitssphären im $\mathbb{R}^3$ mit nicht-kollinearen Mittelpunkten haben höchstens 12 gemeinsame Tangenten im $\mathbb{R}^3$. Diese Schranke ist scharf.

Die Tatsache, daß für das algebraische Problem vom Grad 12 eine *exakte* Charakterisierung der Fälle mit unendlich vielen gemeinsamen Tangenten angegeben werden kann, ist besonders bemerkenswert.

Der Beweis der Aussage unterscheidet zwischen mehreren Fällen. Für den Fall affin unabhängiger Mittelpunkte sowie einer irreduziblen, kubischen Kurve werden die sechs Kantenrichtungen des Grundtetraeders untersucht, die sechs ausgezeichnete Punkte auf der kubischen Kurve definieren. Eine genaue Analyse dieser Punkte zeigt, daß die kubische Kurve nicht in der quartischen Kurve enthalten sein kann. Ist die kubische Kurve reduzibel, dann liefern die algebraischen Zerfallsbedingungen geometrische Bedingungen an das Grundtetraeder, auf deren Grundlage in jedem der zu untersuchenden Unterfälle ein Endlichkeitsbeweis gelingt. Der Beweis für den Fall affin abhängiger Mittelpunkte beruht auf einer direkten Betrachtung der Ellipsen mit vorgegebener kleinerer Halbachse durch die vier gegebenen Mittelpunkte.

Hinsichtlich der Realisierbarkeit von Konfigurationen wird gezeigt, daß für alle Zahlen $k \in \{0, \dots, 12\}$ eine Konfiguration von vier Einheitssphären existiert, die auf k verschiedene, relle, gemeinsame Tangentialgeraden führt.

Ferner wird die Berechnung des minimal umschreibenden Kreiszylinders eines vorgegebenen (nicht notwendigerweise regulären) Tetraeders im $\mathbb{R}^3$ untersucht. Für diese Optimierungsvariante des Tangentenproblems haben Devillers, Mourrain, Preparata und Trébuchet polynomiale Formulierungen mit Bézout-Zahl 60 angegeben. Die Gleichungen enthalten einige zusätzliche Lösungen mit Vielfachheit 4, und als Folge dieser Vielfachheiten sind die Rechenzeiten (mittels aktueller numerischer Löser polynomialer Gleichungssysteme) um etwa einen Faktor 100 größer als die Rechenzeiten für vergleichbare Probleme, in denen nur einfache Lösungen auftreten. Wir verbessern diese Ergebnisse, indem wir eine polynomiale Formulierung für die lokal extremen Zylinder mit Bézout-Zahl 36 angeben, bei der jede Lösung generisch die Vielfachheit 1 hat. Darüber hinaus werden Teilklassen von Tetraedern studiert, in denen die Grade der algebraischen Formulierungen weiter verringert werden können.

Wir schließen Kapitel 3 mit einer kurzen Diskussion dynamischer Visualisierungsaspekte des Tangentenproblems.

Vom algebraisch-geometrischen Standpunkt ist das Tangentenproblem an Sphären aus folgendem Grund von besonderem Interesse. Die Formulierung des Problems in liniengeometrischen Plückerkoordinaten ergibt fünf quadratische Gleichungen im reellen projektiven Raum $\mathbb{P}^5_{\mathbb{R}}$, deren gemeinsame Lösungen im komplexen projektiven Raum $\mathbb{P}^5$ eine gemeinsame Komponente im Unendlichen enthalten (die für die „fehlenden" $2^5 - 12 = 20$ Lösungen zählt). Diese gemeinsame Komponente kann nicht durch einen einzigen Blow-up aufgelöst werden.

In Kapitel 4 wird das Problem der gemeinsamen Tangenten an vier allgemeine Quadriken im $\mathbb{R}^3$ und $\mathbb{P}^3$ studiert. Zunächst wird gezeigt, daß vier reelle Quadriken im dreidimensionalen Raum 32 reelle gemeinsame Tangenten haben können. Hierzu wird für dieses Problem vom Grad 32 konstruktiv eine Familie von Konfigurationen angegeben, deren Symmetrien die explizite Untersuchung der rellen Lösungen ermöglicht.

Darüber hinaus werden computeralgebraische Methoden entwickelt, um den doppelten Blow-up des Tangentenproblems an Sphären zu studieren. Hierzu beschreiben wir das Ideal der eindimensionalen Komponente. Durch Erweiterung des Polynomrings sowie Hinzufügen geeigneter Polynome simulieren wir den Blow-up im Computeralgebra-System SINGULAR und studieren das resultierende Ideal sowie den zweiten Blow-up.

In Kapitel 5 werden die verallgemeinerten Probleme der gemeinsamen Tangenten an $2n-2$ Sphären bzw. allgemeine Quadriken im $\mathbb{R}^n$ studiert, insbesondere unter Gesichtspunkten der reellen, abzählenden Geometrie. In den algorithmischen Anwendungen treten diese Probleme etwa beim Berechnen minimal einschließender Zylinder im $\mathbb{R}^n$ auf. Für den Fall der Sphären wird folgende Aussage gezeigt:

Satz. Sei $n \geq 3$.

(a) Seien $c_1, \dots, c_{2n-2} \in \mathbb{R}^n$ von der affinen Dimension n, und seien $r_1, \dots, r_{2n-2} > 0$. Haben die $2n-2$ Sphären mit Mittelpunkten c_i und Radien r_i nur eine endliche Anzahl gemeinsamer Tangentialgeraden in $\mathbb{C}^n$, dann ist diese Anzahl höchstens $3 \cdot 2^{n-1}$.

(b) Es existiert eine Konfigurationen mit $3 \cdot 2^{n-1}$ verschiedenen, reellen, gemeinsamen Tangentialgeraden. Darüber hinaus können solche Konfigurationen mit Einheitssphären erzielt werden.

Ferner werden Konfiguration von Sphären studiert, deren Mittelpunkte eine affine Dimension kleiner als n haben.

Für die gemeinsamen Tangenten an $2n-2$ Quadriken in $\mathbb{P}^n$ wird gezeigt:

Satz. Zu $2n-2$ allgemeinen quadratischen Hyperflächen im $\mathbb{P}^n$ gibt es

$$d_n := 2^{2n-2} \cdot \frac{1}{n} \binom{2n-2}{n-1}$$

komplexe gemeinsame Tangentialgeraden an die $2n-2$ Hyperflächen ($n \geq 2$). Darüber hinaus gibt es eine Konfiguration von quadratischen Hyperflächen im $\mathbb{R}^n$, für die alle diese Tangentialgeraden reell sind und im affinen Raum $\mathbb{R}^n$ liegen.

Der Beweis dieser Aussage beruht auf der Kombination sehr junger Resultate des reellen Schubert-Kalküls und auf die reelle Situation angepaßten, klassischen Perturbationstechniken. Im Gegensatz zum dreidimensionalen Fall ist der Beweis im n-dimensionalen Fall lediglich existentiell.

Die folgende Tabelle veranschaulicht die große Differenz zwischen der maximalen Anzahl der (reellen) Tangentialgeraden für Sphären und für allgemeine Quadriken.

n	3	4	5	6	7	8	9
$3 \cdot 2^{n-1}$	12	24	48	96	192	384	768
d_n	32	320	3584	43008	540672	7028736	93716480

Darüber hinaus wird der Fall von $2n-2$ Quadriken in $\mathbb{P}^n$ betrachtet, die alle die gleiche glatte Quadrik in einer vorgegeben Hyperebene enthalten.

Mit Hilfe der Charakterisierungen der Tangenten an $2n-2$ Sphären werden zudem effiziente polynomiale Formulierungen zur Berechnung minimal umschreibender Zylinder von Simplexen im $\mathbb{R}^n$ vorgestellt und analysiert. Die Bézout-Zahlen dieser Formulierungen liefern obere Schranken für die Anzahl lokal extremer Zylinder. Da diese Schranken nicht scharf sind, werden für kleine Dimensionen bessere Schranken auf der Grundlage gemischter Volumina und dem Satz von Bernstein bestimmt. Für den Fall regulärer Simplexe wird mittels elementarer Invariantentheorie gezeigt, daß in einem geeigneten Koordinatensystem der Richtungsvektor jedes lokal extremen umschreibenden Zylinders höchstens drei verschiedene Einträge enthält.

Kapitel 6 behandelt die Geraden, die gleichzeitig tangential an k Sphären und transversal zu $4-k$ Geraden im $\mathbb{R}^3$ sind, $k \in \{0, \ldots, 4\}$. Vom algorithmischen Standpunkt treten diese Probleme in den genannten Anwendungen auf, wenn die Klasse der zulässigen Körpern aus Kugeln und Polytopen besteht. Es werden die scharfen oberen Schranken für die Anzahl der gesuchten Geraden (im Endlichkeitsfall) im $\mathbb{R}^3$ bestimmt. Zum Nachweis der Korrektheit der angegebenen Konstruktionen mit der Maximalzahl an reellen Geraden werden teilweise computeralgebraische Methoden (Standardbasen in lokalen Ringen) verwendet. Die Anzahlergebnisse sind in der nachstehenden Tabelle zusammengefaßt.

	Scharfe obere Schranke	Charakterisierung der ∞-Konfigurationen
4 Geraden	2 (wohlbekannt)	ja (wohlbekannt)
3 Geraden, 1 Sphäre	4	ja
2 Geraden, 2 Sphären	8	ja
1 Gerade, 3 Sphären	12	–
4 Einheitssphären	12	ja
4 Sphären	12	–

Wie in der Tabelle angegeben, können für den Fall von drei Geraden und einer Sphäre sowie zwei Geraden und zwei Sphären die Fälle mit unendlich vielen reellen gemeinsamen Tangenten exakt charakterisiert werden. In den Einträgen mit einem „–" sind diese Charakterisierungen offene Probleme.

Die Charakterisierung der degenerierten Situationen im Fall dreier Geraden und einer Sphäre erfolgt mittels klassischer Methoden der Geometrie.

Für den Fall zweier Geraden und zweier Sphären sind die degenerierten Situationen von algebraischen Problemen achten Grades zu untersuchen. Zur Untersuchung der Geometrie dieser Probleme werden computeralgebraische Methoden entwickelt und mit klassischen Methoden der Klassifikation algebraischer Kurven kombiniert. Zunächst wird das allgemeinere Problem behandelt, bei dem die Sphären im $\mathbb{R}^3$ durch allgemeine Quadriken in $\mathbb{P}^3$ ersetzt werden. Um die Geometrie dieses Problem zu studieren, werden zwei Geraden und eine Quadrik in allgemeiner Lage fixiert, und die Menge der (zweiten) Quadriken,

für die es unendlich viele gemeinsame Transversalen/Tangenten gibt, durch eine algebraische Kurve beschrieben. Diese Kurve ist vom Grad 24 im Raum $\mathbb{P}^9$ der Quadriken. Das Faktorisieren des Ideals dieser Kurve zeigt, daß sie erstaunlich reduzibel ist:

Satz. Gegeben seien zwei windschiefe Geraden ℓ_1 und ℓ_2 sowie eine allgemeine Quadrik Q in $\mathbb{P}^3$. Der Abschluß der Menge der Quadriken Q', für welche es unendlich viele Geraden gibt, die transversal zu ℓ_1 und ℓ_2 sowie Tangente an Q und Q' sind, ist eine Kurve vom Grad 24 im Raum $\mathbb{P}^9$ der Quadriken. Diese Kurve besteht aus 12 ebenen Kegelschnitten.

Der Beweis dieser Aussage erfolgt durch eine genaue Analyse des Ideals, das die algebraische Kurve der (zweiten) Quadriken definiert. Darauf aufbauend wird der Satz mit Hilfe einer Computerberechnung im Computeralgebra-System SINGULAR ausgeführt. Der Erfolg der Berechnung hängt maßgeblich von der vorangehenden Klassifikation der Kurve sowie der Überführung in Normalformen ab. Ferner wird gezeigt, daß es reelle Geraden ℓ_1 und ℓ_2 und eine Quadrik Q gibt, für die alle 12 Komponenten der Kurve der zweiten Quadriken reell sind.

Aufbauend auf diesen strukturgeometrischen Untersuchungen wird die folgende Charakterisierung der gemeinsamen Transversalen/Tangenten an zwei Geraden und zwei Sphären bewiesen.

Satz. Seien $S_1 \neq S_2$ Sphären, und seien ℓ_1 und ℓ_2 windschiefe Geraden im $\mathbb{R}^3$. Es gibt unendlich viele reelle transversale Tangenten zu ℓ_1, ℓ_2, S_1 und S_2 in *genau* den folgenden Fällen:

(1) Die Sphären S_1 und S_2 berühren sich an einem Punkt p, der auf einer der Geraden liegt, und die zweite Gerade liegt in der gemeinsamen Tangentialebene der Sphären am Punkt p.

(2) ℓ_1 und ℓ_2 sind beide Tangenten sowohl von S_1 als auch von S_2, und sie gehen durch eine Rotation um eine die Mittelpunkte von S_1 und S_2 verbindende Gerade hervor.

In Kapitel 7 werden die algebraischen Ergebnisse durch komplexitätstheoretische Untersuchungen von Sichtbarkeitsproblemen mit bewegten Kamerapunkten reflektiert. Es wird die Turingmaschinen-Komplexität dieser Sichtbarkeitsprobleme in Räumen variabler und fester Dimension untersucht. Die hierbei betrachteten Klassen geometrischer Körper sind die Klasse der Kugeln, der als konvexe Hülle endlich vieler Punkte dargestellten Polytope („$\mathcal{V}$-Polytope") sowie der als Durchschnitt endlich vieler Halbräume dargestellten Polytope („$\mathcal{H}$-Polytope").

Es werden die folgenden Resultate gezeigt, die die komplexitätstheoretische Grenzlinie zwischen effizient lösbaren und schwierigen Problemen charakterisiert. Falls die Dimension des Raumes Teil der Eingabe ist, dann ist das Überprüfen der partiellen Sichtbarkeit eines gegebenen Körpers $\mathbb{NP}$-schwer. Falls die Dimension fest ist, dann wird das Sichtbarkeitsproblem für alle drei Klassen in polynomialer Zeit lösbar. Der Nachweis der $\mathbb{NP}$-Schwierigkeitsresultate beruht auf geometrischen Konstruktionen, durch die den Sichtbarkeitsproblemen eine kombinatorische Struktur induziert wird. In einem zweiten Schritt

werden diese Probleme auf das aussagenlogische 3-SAT-Problem reduziert. Einige der Polynomialitätsaussagen beruhen auf der algebraisch-geometrischen Technik der reellen Quantorenelimination.

Schließlich wird eine Verbindung zwischen den Komplexitätsresultaten und dem „view obstruction" Problem aus der diophantischen Approximation hergestellt.